DISSERTATION

INVESTIGATION AND APPLICATIONS OF CURRENT AND NOVEL SUSTAINABILITY SCIENCES

Submitted by

Katherine K. DeRose

Department of Mechanical Engineering

In partial fulfillment of the requirements

For the Degree of Doctor of Philosophy

Colorado State University

Fort Collins, Colorado

Summer 2020

Doctoral Committee:

Advisor: Jason C. Quinn

Anthony J. Marchese
Shantanu Jathar
Christie Peebles

ABSTRACT

INVESTIGATION AND APPLICATIONS OF CURRENT AND NOVEL SUSTAINABILITY SCIENCES

Engineering-based sustainable solutions are required to ensure continued access to energy, food and clean water for a growing population. Techno-economic analysis and life cycle assessment provide a means of evaluating emerging technologies to determine if they can economically and sustainably provide solutions to current and future resource demands. Concurrently, performance targets can be identified to help drive technology forward in a sustainable fashion. A major advantage of sustainability analyses is the ability to perform early-stage technology evaluation prior to intensive research investment. The application of these techniques can be applied to a variety of technologies including renewable bio-based fuels. It is also necessary to understand the limitations of these sustainability sciences to properly interpret analysis results. This work focuses on the applications of sustainability sciences to multiple technologies including foundational investigation of the methodology behind assessments. The first technology evaluation showcases the iterative nature and relationship between sustainability sciences and research for a novel biofuel conversion process using algae as a feedstock. The second technology evaluation seeks to improve sustainability metrics of the widespread corn-ethanol process; and is also used as a case study to identify limitations in current sustainability sciences. The final technology evaluation is a novel application of sustainability sciences to identify technology solutions for environmental disruptions.

Microalgae has been a feedstock of interest for renewable fuels production, but the technology remains impeded due to high growth costs. Most research has been focused on increasing biomass productivity and lipid content and/or reducing capital and operation costs associated with traditional growth systems. An alternative approach is to consider an entirely new growth method; attached-

growth systems. Sustainability modeling was used to identify the optimal processing opportunities for the production of renewable fuels from algae grown in this method through the use of economic and environmental analyses. Results indicated that ash reduction, energy intensive processing and high growth costs needed to be addressed to improve economic viability. A secondary effort focused on advancing the research and modelling to further refine results based on this focus. Results show minimum fuel selling prices ranging between $9.13 to $31.22 per gallon of gasoline equivalent, dependent on scenario and process assumptions.

Sustainability analyses can also be applied to improve current technologies. Corn ethanol represents a mature technology with a long production history as a first-generation alternative fuel but has been widely criticized for high production costs and only marginal sustainability improvements over traditional petroleum-based fuels. One approach for improving these metrics is to focus on increased utilization of co-products through additional processing. Sustainability analysis results indicate an additional co-product fermentation process may be considered as a value-add for refiners but is dependent on economic and product market assumptions. This process was also used as a case study to explore how life cycle methodology affects environmental impact results. Life cycle assessment (LCA) results have a broad variability with well-to-pump results ranging between 42 to 210 g $CO_{2\text{-}eq}$ MJ $fuel^{-1}$, dependent on co-product allocation methodology. This variability within the results can affect a product's ability to meet environmental standards, such as the Renewable Fuel Standard, and represents a critical area for improved methodological guidance.

In addition to technology, sustainability sciences can also be applied to identify economically viable solutions for environmental disruptions such as harmful algae blooms (HAB's). HAB's affect both fresh and saltwater bodies around the world, causing a variety of environmental and economic damages to surrounding ecosystems and communities. The primary driver of HAB's is eutrophication, or excess nutrients in the water, and the principal approach to mitigating HAB's is reducing nutrients before they

collect *en masse* downstream. Technology solutions can be employed to remove nutrients from waterways, but feasibility of technology deployment is dependent on the economic viability. Applications of sustainability sciences allows researchers to identify potential solutions to reduce HAB events which are both effective and economically viable. Results show that on average, Lake Erie communities lose $142 M (± $29M) year^{-1} from HAB's without mitigation. Use of attached-algae systems show an average savings of $12-42M per year from HAB mitigation and represent the most promising technology investigated. Attached-algae systems are the only nutrient reduction technology to show net-positive cash flow when compared with traditional nutrient removal systems.

This research dissertation outlines tasks associated with the different applications of sustainability sciences. First, sustainability analyses are used to identify current research roadblocks associated with a technology and are used to identify optimal processing options and provide feedback to researchers to improve these metrics. Next, the tool set was adapted to a novel biorefining process and used to evaluate a value-add proposition for a current technology and showcase current limitations of LCA methodology. And finally, they were leveraged to create a framework for evaluating costs and benefits of technology adoption for pro-active mitigation of environmental disruptions.

ACKNOWLEDGMENTS

I would like to recognize and thank everyone who has helped and supported me during my time at Colorado State University. I would especially like to thank my advisor, Jason Quinn. Jason, thank you so much for this opportunity. Thank you for encouraging my research interests, thank you for helping me develop as a writer and communicator, thank you for your patience as we struggled through my first manuscript, thank you helping me grow as leader. I have truly loved and appreciated the opportunity to work with you and everyone in the group.

I would also like to thank everyone in the Quinn Research group, both past and present. You have all been amazing to work with and I especially thank you for all the wonderful feedback you have provided over the years and all the fun times we've had together. I would especially like to thank Hailey Summers, Evan Sproul and Peter Chen for all your help and feedback over the years. Thank you for always being open to sharing your knowledge and expertise with me and everyone else in the group. I am lucky to have been able to work with you all.

Thank you to all my collaborators at Sandia National Laboratories, especially Ryan W. Davis and Eric Monroe. Thank you for all your experimental support and creative ideas.

And a very special thank you my wonderful partner, Karl Semelis. Thank you for always supporting, believing and encouraging me. Thank you for always listening to my presentations and reading my manuscripts, even though you are probably tired of hearing about algae. I truly could not have done this without you.

Funding support for this work was provided by DOE-EERE BioEnergy Technologies Office (BETO) under agreement numbers 26336 and 27375. Sandia National Laboratories is a multi-mission laboratory managed and operated by National Technology and Engineering Solutions of Sandia, LLC., a wholly owned subsidiary of Honeywell International, Inc., for the U.S. Department of Energy's National Nuclear

Security Administration under contract DE-NA0003525. Chapter 3 of this work was part of the DOE Joint BioEnergy Institute (http://www.jbei.org) supported by the U.S. Department of Energy, Office of Science, Office of Biological and Environmental Research, through contract DE-AC02- 05CH11231 between Lawrence Berkeley National Laboratory and the U. S. Department of Energy.

TABLE OF CONTENTS

CHAPTER 1: INTRODUCTION AND MOTIVATION

Today is going to be a great day, you say, as you pack your car for a trip to the beach. After pulling out of your driveway, you notice the fuel gauge is precariously close to empty and pull into the next gas station you see. As you pump gas into your vehicle, you stare across the road and see a field of tall grass. Switch grass, you think it's called. The term tickles the back of your brain. Hadn't you heard of the possibility of making gasoline from grass? Wasn't that like 10 years ago? *How come I am not filling my car up with switchgrass gas?* you ponder as you settle back into the driver's seat. Before taking off, you pull a granola bar from your beach bag. "Green-ola" it reads, "the most sustainable granola bar on the market today!" *But how do they know that? How can they prove their granola bar is better for the environment than another bar?* you wonder, pulling back onto the road. Soon, you pull into the local beach parking lot. It seems a little less busy today than you'd expect. You open the car door and a distinct musty odor assaults your nose. *Oh no*. A better glance at the water confirms your suspicions; instead of crystal blue waters, it looks as though someone has spilled green paint. The annual harmful algae bloom has started earlier than usual this year. You remember hearing about the causes of these blooms a few years ago. *If they know what is causing this problem, why haven't we done something to prevent them?* you ask yourself as you pull away and head home. These questions form the backbone of sustainability sciences.

As the population and affluence of world's population continues to grow, it becomes ever more imperative to employ creative and sustainable solutions to continue to supply food, clean water, energy, housing and health care for current and future generations [1–3]. Sustainable solutions are those which "allow humanity to meet the needs of the present without compromising the ability of future generations to meet their own needs" including "meeting the basic needs of all and extending to all the opportunity to fulfil their aspirations for a better life" [4].

It is not enough to simply provide a solution for these issues. The solution must also be cost effective and environmentally and socially responsible[5,6]. These facts make up the backbone of sustainability sciences. Applications of sustainability sciences allow us to answer the questions of "is this solution economically viable" and "is this solution environmentally responsible?". A sustainable solution cannot be implemented without meeting both criteria. For instance, lignocellulosic (e.g. switchgrass, agriculture residue, corn stover) fuels have high conversion costs, above $5 gallon of gasoline equivalent^{-1} (GGE^{-1}) for lignocellulose fuels, which prevent them from being competitive with traditional petroleum fuels which currently sit at less than $3 $gallon^{-1}$. In addition, the process must also be sustainable from an environmental standpoint. Ideally, a new process would reduce all environmental burdens. In reality, a process may reduce greenhouse gas (GHG) emissions but may increase eutrophication (nutrient impacts on the environment). Or a bioenergy process may seem to reduce GHG emissions by utilizing a biobased feedstock, but additional processing, energy requirements or land-use change may increase life cycle GHG emissions. These costs and benefits must be included in the evaluation of adopting any new process to preserve long-term environmental health.

Two well-known tools of sustainability scientists are techno-economic assessment (TEA) and life cycle assessment (LCA). TEA allows researchers to understand the economic costs of a solution while it is still in the early phases of research and development. When applied to processes, such as renewable fuel production or "green" chemical production, researchers incorporate laboratory or pilot scale data into an engineering process model. These models can then be leveraged to understand the capital investment requirements, annual production costs and how much a product or service would need to be sold for to produce adequate profits for investors. If the outcomes of the analysis are favorable, i.e. production costs are lower than current market prices for the item or service, researchers can confidently continue research knowing their process, product or service can be cost competitive with existing solutions. Alternatively, if the results are unfavorable, TEA work can be leveraged to target high

impact areas for future research to reduce the costs of the process, product or service. TEA has been heavily employed in both bioenergy and bioproducts based research[7–12].

LCA also utilizes the engineering process model, but instead evaluates the environmental impact associated with the product or service. Many LCA's focus on quantifying the GHG emissions, but the analysis may be expanded to include other environmental impacts such as eutrophication, acidification, water stress and ozone layer depletion, among many other impact categories[13–16]. In the renewable fuels arena, LCA is used to evaluate if renewable fuels meet mandates such as the Renewable Fuel Standard (RFS). The RFS calls for a 50% reduction of GHG emissions when compared to traditional fuels, on a well–to-wheel system boundary[17]; some states, however, may impose more strict regulations. Similar to TEA, LCA results can help direct future research in areas to reduce the environmental impact of a production pathway.

While TEA and LCA are both well-known and well used tools in the sustainable science community, both systems have their limitations. Results of TEA analysis are highly dependent on the foundational assumptions of the economic modelling. For instance, comparing studies with different loan terms, internal rates of return (IRR) and depreciation schemes is similar to comparing apples to oranges since their foundations are dissimilar. Are the improved results in study X due to a better process or more optimistic economic assumptions compared to study Y? In an effort to reduce this uncertainty across studies, the Department of Energy's (DOE) Bioenergy Technologies Office (BETO) has standardized a set of economic inputs for TEA assessments called "*N*-th plant" assumptions, shown in Appendix A 1 [10–12,18]. One major assumption behind these inputs is that the technology is "mature" or well known. Newer, or first-of-a-kind processes (FOAK), typically have longer start-up times, unoptimized production, increased capital equipment costs and higher IRR's which will increase the required production cost per unit, Figure 1[19,20]. By assuming a technology is mature, the TEA can focus on identifying areas for long-term process improvement without being skewed by complications

associated with FOAK challenges. However, as a process nears feasibility and potential adoption, more focus should be shifted to understanding the requirements associated with a FOAK facility.

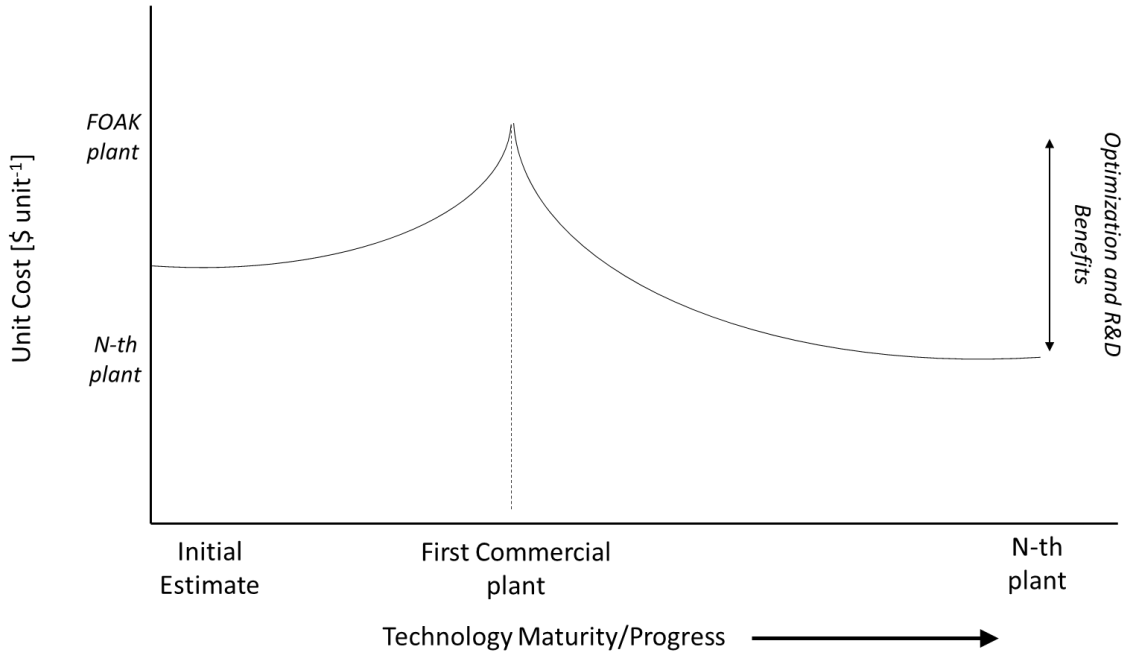

Figure 1: Production cost per unit produced as the technology progresses and matures[19]*. FOAK plants have higher unit production costs which are reduced over time as the technology matures through process optimization and additional research and development (R&D).* N*-th plant TEA's typically include benefits from additional R&D and process optimization.*

When applying LCA methodology, a lot of discretion is left to the LCA practitioner on how to best set system boundaries. System boundary decisions are especially important when considering inputs that are the products from different systems; for example, ethylene from a refinery being used as a feedstock for polymer production. In these instances, the International Organization for Standardization (ISO) recommends in their 14040:2006 Standard to always expand the system the boundary, such as shown in Figure 2, to account for all possible environmental outputs [21].

A)

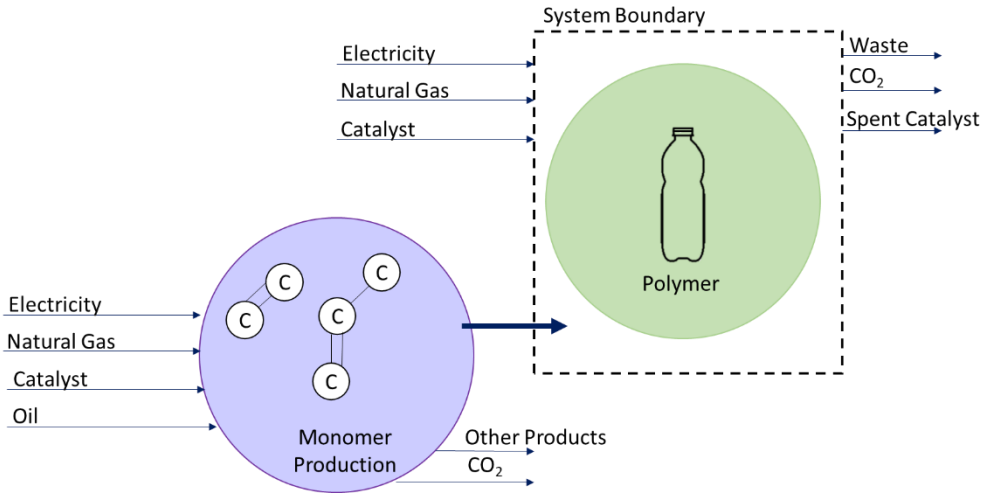

B)

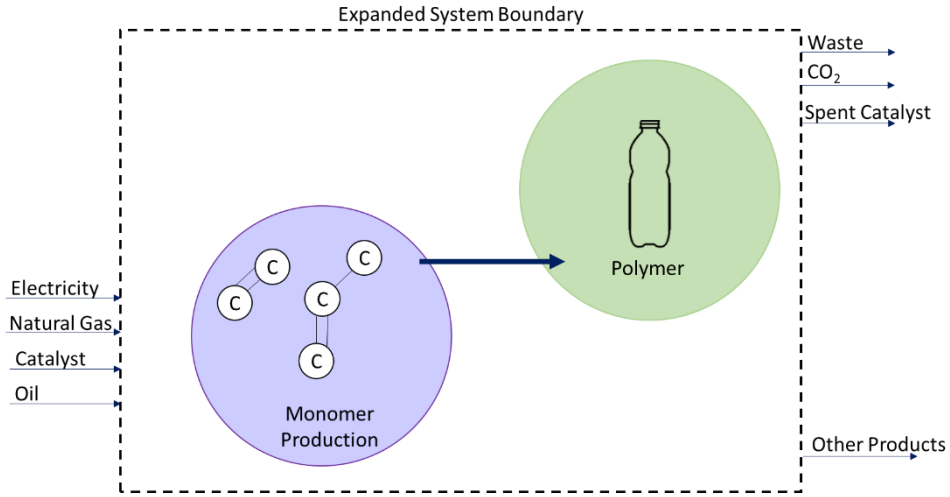

Figure 2: A) Contracted and B) expanded system boundaries for an LCA for a polymer production system. In the expanded system boundary (B), inputs for all processes included in the upstream monomer production process are considered.

However, this type of boundary expansion may not always be possible or practical. Additionally, a process may produce many products and it may be desirable to understand the emissions associated with only one product. One workaround is applying an allocation method, which allocate some portion of the upstream process environmental burdens to input/product of interest. Three well-established allocation methods delineate environmental burdens based on the products' relative mass ("mass

allocation"), its relative economic value ("economic allocation") or its relative energy value ("energy allocation")[21], Figure 3. Application of the different allocation methods is left to the discretion of the practitioner but can drastically impact results.

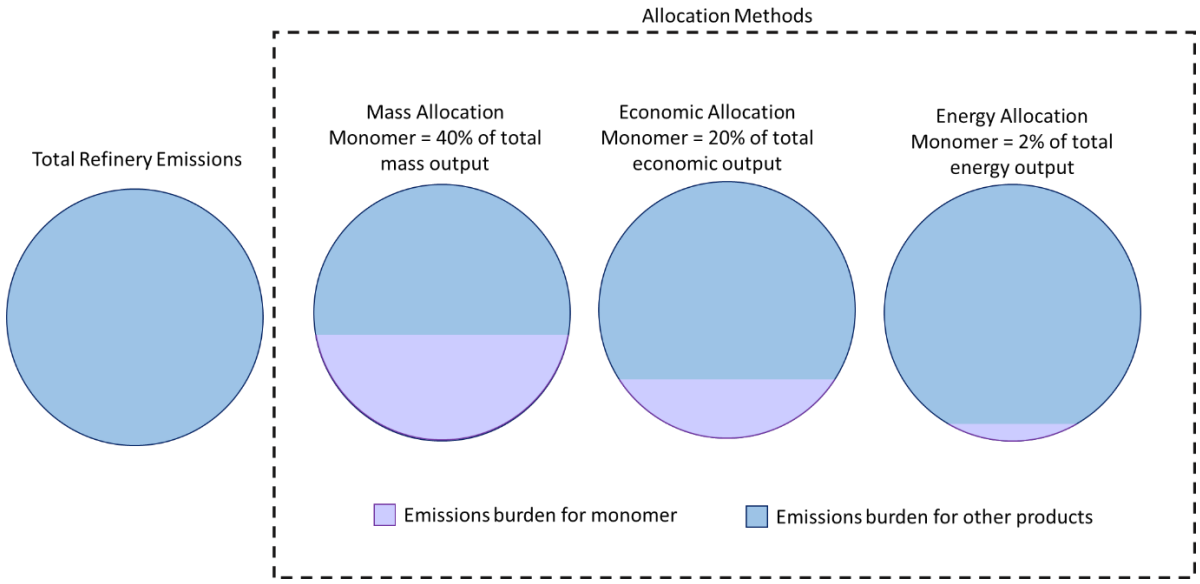

Figure 3: Examples of different allocation methods used to find the emissions burden associated with monomer production at the refinery. Values shown here are not meant to be representative of all refineries.

Another option for system boundary discretion is utilizing a displacement method. In this method, all process emissions are assigned to the product of interest and a "credit", or emissions reduction, is given for the co-products "displacing" another product. A well-known example of this is corn-ethanol production. The corn ethanol process also creates distiller's grains with solubles (DGS) which is sold as animal feed. By generating animal feed with DGS, the process is assumed to "displace" some amount of animal feed, i.e. animal feed that no longer needs to be created by traditional methods. The corn-ethanol process has therefore "saved" those emissions from traditional animal feed production by avoiding their production in the first place, Figure 4. With so many system boundary and emissions accounting options available, it is imperative to understand if and how applying these different options can affect LCA results.

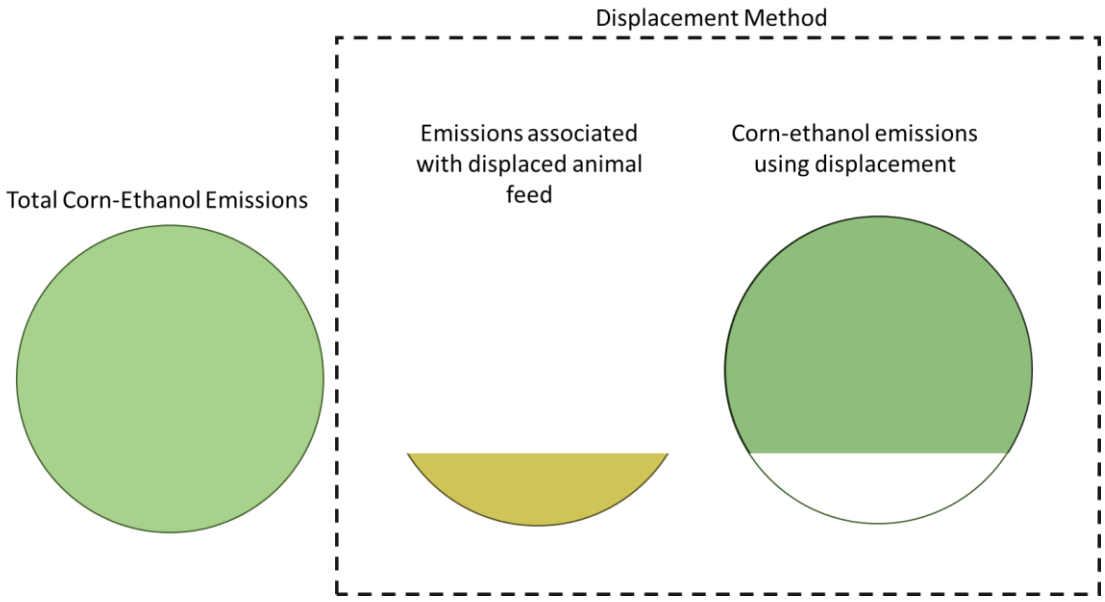

Figure 4: Example of the LCA displacement method. Total emissions are reduced by taking a credit for the displacing emissions through co-products

In this work, three novel contributions to the field of sustainable sciences are presented. Chapter 2 presents the application of current TEA and LCA methodology to a novel algae growth system and fuel conversion process. Chapter 3 explores current limitations of LCA methodology using a secondary processing opportunity for distiller's grains with solubles (DGS) as a case study. This process seeks to improve the economic and environmental metrics associated with corn-ethanol production by extracting additional value from the primary co-product, DGS. This case study also explores the impact of the current TEA methodology assumptions of "mature technology" compared to a FOAK on process economics. Chapter 4 focuses on creating a framework for identifying cost-effective technologies for proactive environmental disaster prevention and mitigation. This framework was created specifically for harmful algae bloom (HAB's) in Lake Erie, but the underlying principles could be adapted to any geographic area or annual environmental phenomena. The foundation of this framework is estimating current economic damages caused by the environmental problem and quantifying the costs and benefits of adopting technologies to prevent or mitigate that disaster. Each chapter includes an introduction and research motivation, detailed methodology, research results, an in-depth discussion of the results,

implications and opportunities for future work. Lastly, a conclusion section and future work section details next steps.

CHAPTER 2: INTEGRATED TEA AND LCA OF THE GROWTH OF HIGH PRODUCTIVITY, LOW LIPID ALGAE AND CONVERSION INTO RENEWABLE FUELS[1]

2.1 Introduction

One of the top priorities for sustainable development and energy security is access to renewable yet affordable energy. Wind, solar, geothermal, and hydrothermal systems can help produce electricity to meet stationary energy needs, such as homes and businesses, and will most likely be used to meet most transportation needs in the future as the vehicle fleets move towards electrification. However, during this transition period most transportation relies on a portable fuel source, such as gasoline or diesel, and aviation will most likely always rely on a portable, energy dense fuel due to weight concerns. To meet these needs, researchers have turned their interest toward bio-based renewable fuels. Bio-based renewable fuels are liquid fuels, either alcohols (e.g. ethanol), biodiesel (methyl-esters) or renewable diesel, made from a bio-based feedstock such as corn, soybeans, or switchgrass. As renewable fuel demands increase, it is imperative to utilize alternative feedstocks which reduce water, land and fertilizer inputs and do not compete with food crops.

For these reasons, algae continues to be a feedstock of interest due to its high productivity, integration with waste streams, cultivation with non-potable or contaminated water and the ability to be grown in non-arable land [9,14,22–24]. As this interest continues to grow, a number of economic analysis have been performed on algal systems to determine the viability of algal derived renewable biofuels, with the main conclusions that the cost of the feedstock has the greatest impact on the overall economics [11,12,25,26]. The majority of these analysis are performed on biorefineries utilizing algae from

[1] This chapter was published as a manuscript and is reprinted (adapted) with permission *from Integrated techno economic and life cycle assessment of the conversion of high productivity, low lipid algae to renewable fuels*. DeRose, K.; DeMill, C.; Davis, R. W.; Quinn, J. C. *Algal Research* **2019** *38*. Copyright Elsevier 2019.

open raceway ponds (ORP)[27–30]. The cost of this feedstock varies from analysis to analysis and can range anywhere from $445 to $3711 per ash-free dry weight (AFDW) mt [18,25,31,32]. Additionally, there are also a number of challenges when considering growing large volumes of algae for biofuels production using ORP systems, including significant resources requirements (e.g. water, nutrients and carbon dioxide), which typically are expensive to supply [33–36]. Considering the high economic and resources costs associated with ORP systems, it is imperative to consider alternative growth strategies for algae biomass.

Alternatives to ORP's include photobioreactors (PBR) and attached-algae growth (AAG) systems. PBR's represent a robustly studied system, which can decrease water requirements by limiting evaporation losses and potentially improve productivity by increasing the availability of sunlight and limiting outside contamination. These systems, however, also represent a capitally intensive growth scheme, for which the economic assessments have conclusively shown represent a significant challenge for fuel production pathways [32,37,38]. Conversely, AAG systems have received minimal investigation [25,39]. In the AAG systems, nutrient-rich surface waters are pumped down long flow ways which are covered in a substrate, Figure 5. Native periphyton attach to the substrate and propagate. In this system, the surface waters provide required nutrients, such as nitrogen, phosphorus and trace metals, and carbon which reduces external input requirements for algal growth. Since the water's own contaminants are nutrients for the algae, the AAG system synergistically produces biomass while providing an environmental service through water remediation. Additionally, since the algae is grown on an attached turf, traditional farming equipment, such as tractors with mounted scrappers[40], may be used for harvesting instead of other more energy intensive methods such as centrifugation or filtration, which are typically used in ORP and PBR production systems[24,41–43]. AAG systems also tend to produce a polyculture which is more robust than the carefully crafted monocultures in ORP or PBR systems,

reducing the overall occurrence of culture crashes. All of these advantages combine to reduce the cost of the biomass [39].

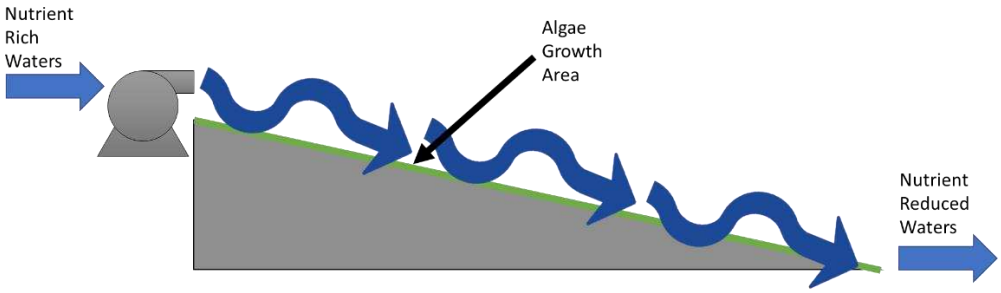

Figure 5: Diagram of the AAG system; nutrient rich surface waters are pumped down a long flow way. Native periphyton attached to a substrate on the flow way and grow, removing nutrients from the water. Algae is the harvested from the flow way and the process is allowed to repeat. Water leaving the system has reduced nutrients. The typical grade of the system is very low with the figure used to illustrate the concept and is not drawn to scale.

There are some complications when considering using algae from AAG systems for biofuels production. First, AAG systems have notoriously high ash content which can have negative effects on downstream processing. This high ash content is a function of the total suspended solids (TSS) of the source waters and proclivity for the system to harbor diatomaceous alga. Biogenic ash has been found to contribute between 30-65% of the total ash in the harvested material, with the remainder primarily arising from entrainment of inorganic solids in the biomass. Correspondingly, the system has been demonstrated to achieve high efficiency reduction of TSS and volatile dissolved solids from compromised surface waters. Second, this algae tends to have a very low lipid content, 5 wt% AFDW compared ≥25 wt % AFDW for traditional monoculture systems[18,27,29,30,44]. Since the majority of algal biofuel processing options rely upon a lipid extraction and conversion process to create biofuels, the low lipid content of the AAG algae makes this processing option unfavorable[11,27,29,45]. As illustrated with previous experimental work and sustainability assessments, the downstream conversion needs to be tailored to the feedstock composition[11,27,29,45].

This analysis seeks to investigate the sustainability of a novel conversion pathway formulated for low lipid algae grown using an AAG and converted to renewable fuels via a carbohydrate and protein targeted fermentation. This research was conducted in two phases. In Phase One, two conversion pathways were considered; a novel fermentation followed by hydrothermal liquefaction (HTL) and whole algal HTL. HTL is a high temperature, high pressure reaction used to convert biomass into a biocrude which can then be upgraded to a drop in transportation fuel[12]. A modular engineering process model was developed and validated with experimental data. Foundational sustainability sciences were used to understand the performance of these pathways based on the metrics of economic viability using TEA and environmental impact using LCA. Results from Phase One were used to direct further research and a second round of sustainability analysis. Discussion focuses on identifying the requirements to produce economically and environmentally viable renewable products from AAG algae based on both research phases.

2.2 Phase One

Phase One was based on initial experimental work performed by our partners at Sandia National Laboratories. Two conversion processes were considered for the conversion of AAG system algae into renewable fuels; a novel protein-targeted fermentation process followed by HTL ("biochemical pathway") and whole algal HTL ("thermal-chemical pathway"). A block flow diagram (BFD) for these two conversion pathways is shown in Figure 6.

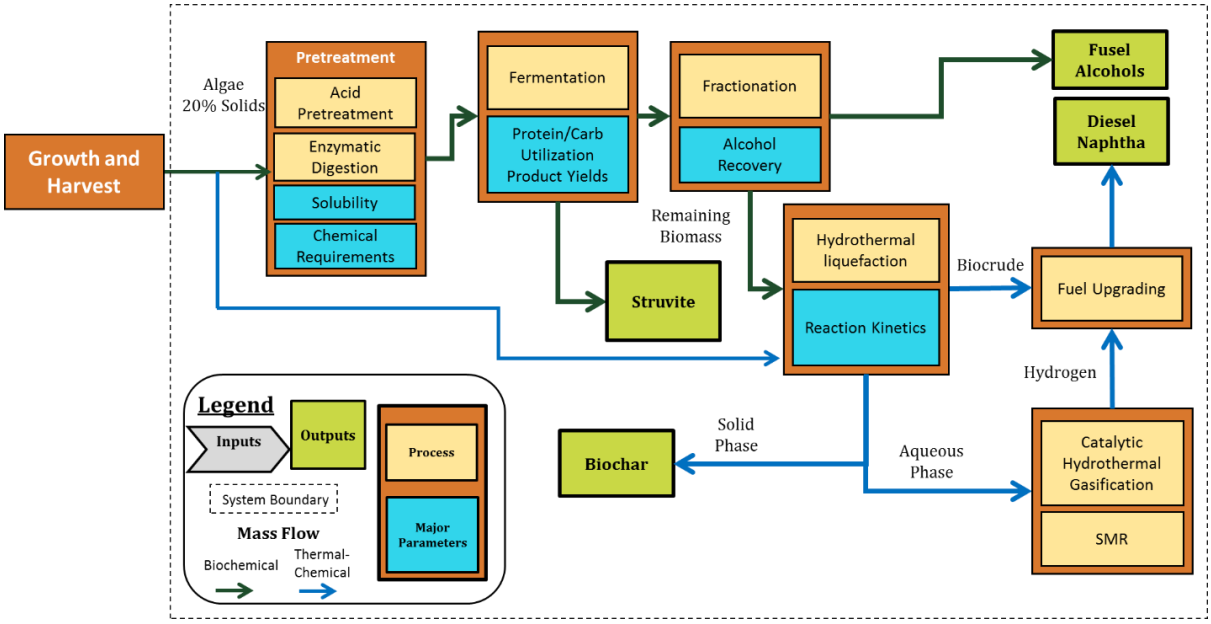

Figure 6: BFD for the two conversion cases; Biochemical and Thermal-chemical. The biochemical process includes an up-front fermentation and fractionation process to remove alcohol products, followed by hydrothermal liquefaction of the remaining biomass. The Thermal-chemical process consists of hydrothermal liquefaction of the whole algae. Process steps for the hydrothermal liquefaction process are the same for both pathways.

2.2.1 Phase One – Methods

A modular engineering process model was developed for the biochemical and thermal-chemical pathways and validated with experimental data; this model was then used as the foundation for the sustainability analyses, TEA and LCA. These processes were modeled in Aspen Plus, a process simulation software, based off experimentally validated inputs provided by researchers at Sandia National Laboratories for the fermentation process and inputs from literature for the HTL [46]. For this analysis, the system boundary was defined to include all required processes in the biorefinery, with biomass being purchased from a co-located AAG system for $515 ash free dry weight (AFDW) metric ton $(mt)^{-1}$, Figure 6.

Since it is the nature of ATS algae to be different combinations of diatoms, green and red algae depending on which type ends up growing on the turf between harvests, the resulting biomass may have different AFDW compositions and ash content for each harvest [47]. Sandia National Laboratories

took samples over a year at their Salton Sea Algal Turf facility to provide an average algal AFDW composition and ash content for this model. This average algal composition was reported to be 30% protein, 50% carbohydrates, 5% lipids and 15% other organics, on an AFDW basis. The ash content was reported to be 75% [g ash g harvested material^{-1}], which is consistent with results from other AAG system[43]. This composition and ash content were used as the basis for the feedstock for biorefinery model, Table 1.

Table 1: Biorefinery model inputs for Phase One

Model Inputs		
Feed Conditions		
Feed Rate	56,500	kg day^{-1}
Feed Temperature	20	°C
Feed Pressure	1	atm
Slurry Concentration	20%	wt%
Ash Concentration	75%	wt%
Biomass Cost	$515	$ metric ton^{-1}
Composition (AFDW)		
Carbohydrates	30%	wt%
Protein	50%	wt%
Lipids	5%	wt%
Other Organics	15%	wt%

Ash was modeled as silica dioxide (SiO_2) and was treated as an inert mass flowing through the system with no adverse or beneficial effects on conversions or unit process equipment. However, it has been shown that ash may adversely affect some process equipment; for example, scaling on boiler tubes, pitting or catalyst deactivation. Alternatively, the ash could serve as a catalyst in thermochemical processing, but the improved performance is expected to be minimal. The effects of ash were already significant before accounting for increased maintenance or equipment replacement. Therefore, it was deemed unnecessary to further quantify the effects of ash at this time.

2.2.1.1 Fermentation Process

The process flow diagram (PFD) for the fermentation process is presented in Figure 7. The first step of the process was an acid pretreatment step, which solubilizes the carbohydrates and proteins in the feed. This process works by breaking the long-chain carbohydrates and protein molecules down to their monomer sugar and amino acid building blocks. The monomer sugars and amino acids are then available for fermentation. The process was done using a strong acid to lower the pH to approximately 6. The insoluble fraction was then separated and subjected to a second acid treatment. The treated fraction was then cooled and neutralized using a strong base in a stirred tank reactor, before blending back with the soluble fraction from the first acid pretreatment. Total solubility for the carbohydrates, proteins and lipids increased to 90%, 70% and approximately 100% [g soluble after pretreatment g total mass^{-1}], respectively. After acid pretreatment, an enzyme pretreatment step was performed. In this step, an enzyme was used to further solubilize the proteins before fermentation. The slurry was treated with 1-gram protease enzyme per liter of total slurry. Experimental work showed that the total protein solubility increased to 90% [g soluble protein g total protein^{-1}] from this procedure. Complete model inputs for the pretreatment process are available in Table 3.

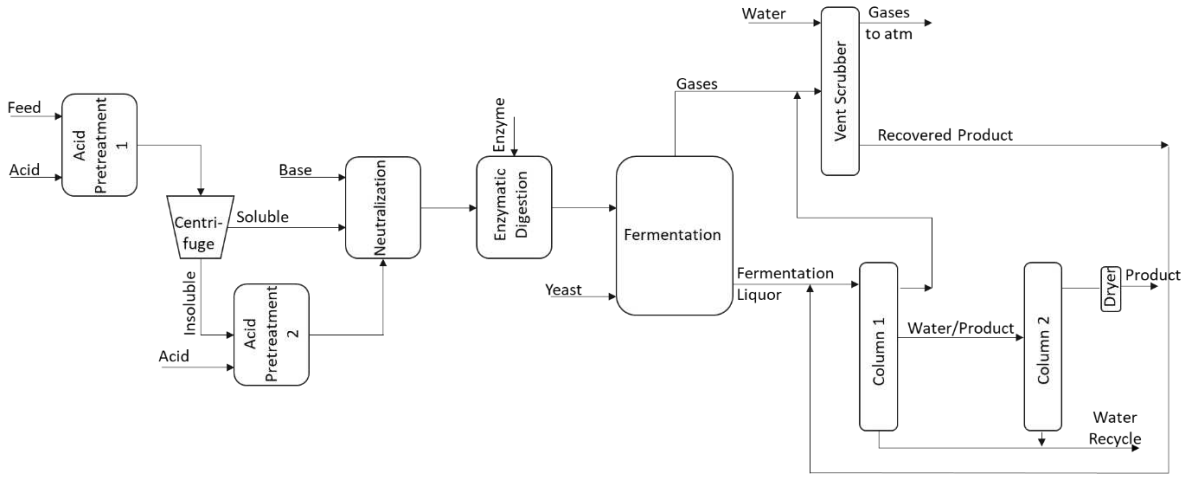

Figure 7: Process flow diagram (PFD) for the fermentation process, including pretreatment through product recovery.

The fermentation step has been optimized for the AAG algae with the inclusion of protein fermentation in combination with carbohydrate fermentation. Fermentation was done using a proprietary blend of yeasts to produce a fusel alcohol blend, mostly C4 and C5 alcohols, Table 2[48]. Initial experimentation performed at Sandia National Laboratories shows utilization of 31% and 90% of the solubilized proteins and fermentable carbohydrates, respectively. For the AAG system algae, fermentable sugars (glucose/xylose/arabinose) made up 26% of the carbohydrate hydrolysates, Appendix A 7. However, these hydrolysates contained a high fraction of mannitol, a sugar alcohol, which has been shown to be preferentially consumed by E. coli over C5 sugars such as xylose and arabinose[49]. Assuming that 90% of fermentable sugars and mannitol would be consumed, as seen in previous experimental work, a total of 76% of the carbohydrate hydrolysate would be used in fermentation. Protein hydrolysate (amino acid) consumption was found the be ambivalent to amino acid composition, with 31% of the amino acids being consumed for a multiple feedstocks; therefore this same consumption of protein hydrolysates was assumed in this model[48]. Experiment should be conducted to verify these assumptions. For modeling purposes, carbohydrates were modeled as $C_6H_{13.3}O_6$ based on the average fermentable carbohydrate composition while proteins were modeled as $C_4H_8O_{2.3}N$ based on the amino acid profiles. Both profiles were provided by Sandia National Labs and are available in Appendix A 7 and Appendix A 8 for the carbohydrates and amino acids, respectively. Overall fermentation yields were reduced to 95% of laboratory values to estimate industrial scale production[50]. Total conversion yields for this biomass were calculated to be 14.3 g fusel alcohols per 100 g algal biomass and leveraged as model inputs, Table 3. Fermentation products were limited to fusel alcohols ($C_4H_{9.8}O$), carbon dioxide (CO_2), ammonia (NH_3), ammonium (NH_4^+), water and hydrogen ions (H^+). Gas phase fermentation products were captured in the head space of the reactors and sent to a vent scrubber to recover any low boiling products. The recovered products were then sent back to the product recovery step and the remaining gases are vented to atmosphere, Figure 7.

Table 2: Fusel alcohol composition and energy density of the products from the fermentation process. Energy densities for the individual components were taken from Aspen Plus

Fusel Alcohol Composition			
Component	**Chemical Formula**	**wt%**	**Energy Density [MJ kg^{-1}]**
Ethanol	C_2H_6O	18%	30.0
Isobutanol	$C_4H_{10}O$	64%	36.2
2-methyl-butanol	$C_5H_{12}O$	3%	38.6
3-methyl-butanol	$C_5H_{12}O$	8%	38.7
Phenyl-ethanol	$C_8H_{10}O$	7%	35.8
Weighted Average	$C_4H_{9.8}O$		

Additionally, this fermentation step produced struvite precipitate as a byproduct of a side reaction. Struvite may be used a fertilizer replacement or for nutrient recycle purposes, and was sold as a co-product valued at \$455 mt^{-1} [39]. Experimentation showed that nitrogen is released in the form of NH_3 during fermentation and that phosphorus was released and re-mineralized to phosphate during acid pretreatment [51]. These nitrogen and phosphorus containing compounds then react with extracellular magnesium to form struvite ($NH_4MgPO_4 \cdot 6H_2O$)[51]. Experimentation from Sandia National Laboratories with AAG system algae showed approximately 1% of the AFDW biomass is phosphorus and 80% of the phosphorus is recaptured as struvite, with struvite formation being limited by phosphorous availability.

The fusel alcohols were recovered using two distillation columns, Figure 7. This first column was for bulk water and CO_2 removal, in the column bottoms and distillate, respectively. Some of the alcohol products do not separate from water in the bulk distillation column and recovery of these products in another distillation column was found to be uneconomical. Therefore, these products were assumed to be lost. A fusel alcohol/water mix was pulled from a side stream of the bulk distillation and sent to a rectification column which produced a concentrated fusel alcohol blend in the distillate. Distillation in the rectification column was set to recovery >99.5% of fusel alcohol products. The alcohol blend was then dried in a molecular sieve dryer before being sent to storage. The distillation process was modeled in Aspen Plus to determine mass recovery rates, and heating and cooling requirements. After the fusel

alcohol product was recovered, the remaining algal slurry was sent to hydrothermal liquefaction. The mass composition of the remaining biomass entering the secondary processing step on AFDW basis is 55% protein, 16% carbohydrates, 8% lipids and 21% other organics. Complete model inputs for the fermentation section of the fermentation process are shown in Table 3.

Table 3: Model inputs and outputs for the fermentation conversion process, includes pretreatment, fermentation, and product recovery for phase one

Model Inputs		
Treatment Times		
Acid Pretreatment	0.75	hours
2nd Acid Pretreatment	6	hours
Neutralization	5	hours
Digestion	16	hours
Fermentation	54	hours
Material Loadings		
Acid Pretreatment	2	%vol vol^{-1}
Enzyme	0.01	g L^{-1}
Yeast	1	%vol vol^{-1}
Pretreatment		
Solubility after Acid Pretreatment		
Carbohydrates	90	wt%
Protein	70	wt%
Lipids	100	wt%
Solubility after Enzymatic Digestion		
Protein	90	wt%
Fermentation Reaction		
Carbohydrate Utilization	72	% of carb hydrolysates
Protein Utilization	31.3	% of protein hydrolysates
Fusel Alcohol Yield	14.3	g FA (100 g biomass)$^{-1}$
Struvite Yield	0.05	g struvite (100 g biomass)$^{-1}$
Product Recovery		
Production recovery	99.5	% by mass
Product purity after Drying	99.5	% by mass
Model Outputs		
Fusel Alcohols	15.6	GGE $year^{-1}$
Struvite	6	tons $year^{-1}$

2.2.1.2 Hydrothermal Liquefaction

The HTL process was based on the process proposed by Pacific Northwest National Laboratory (PNNL), and a block flow diagram of the process is shown in Figure 8[12]. The HTL reaction produced three

different phases, a biocrude phase, an aqueous phase, and a biogas. The proportion of each phase was based on the biomass composition, with higher biocrude fraction driven by higher lipid content [52,53]. Due to the low lipid content of the AAG system biomass, it was necessary to create a model for the HTL reaction to estimate reaction products instead of relying on yields estimated by PNNL in HTL their report. This model was created by a member of the Quinn Research Group, Chen, and was based off experimental data generated and modeled in MatLab [52,53]. Outputs from this kinetic model showed biocrude fractions between 35-38 wt%, compared to the approximately 60 wt% reported by PNNL[12]. Results used for model inputs for the two different pathways are shown in Table 4.

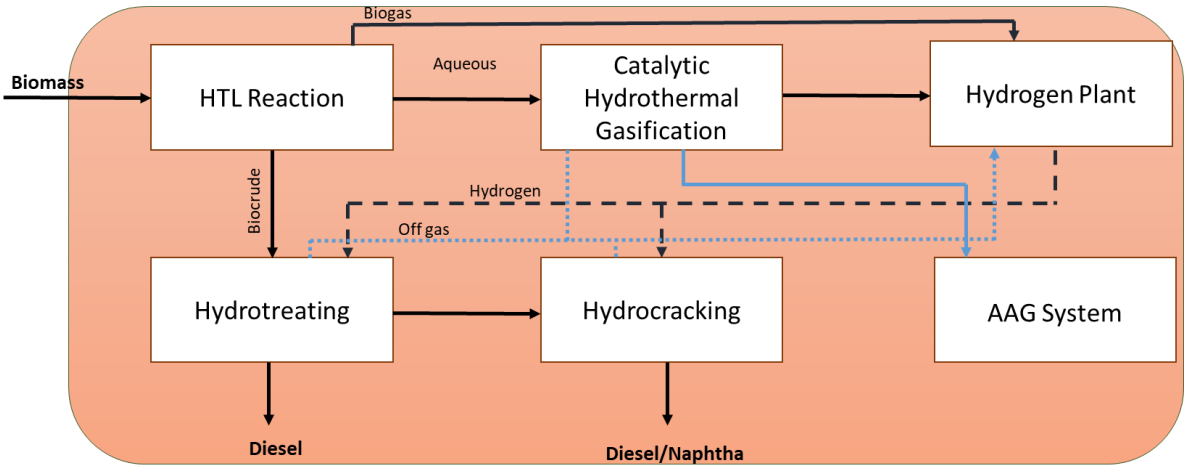

Figure 8: Block flow diagram of the HTL process

The HTL process also included several distillation columns for product recovery and hydrogen for hydrotreating and hydrocracking. Heat requirements for these processes were based on the PNNL report, scaled on a per kg of biocrude [12]. Energy requirements for the product recovery columns were estimated by taking the total energy requirements, as reported by Jones, et al. [12] and subtracting the heating and cooling requirements of discreet heat exchangers and power requirements of discreet pumps. The remaining energy requirements were then assumed to be used within product recovery. Product recovery energy was normalized on a per kg of biocrude basis, as it was assumed that energy requirements were a function of biocrude product rates. This method resulted in energy requirements

of 6 kJ-kg biocrude^{-1} of electricity, 2.9 MJ-kg biocrude^{-1} of heat and 0.9 MJ-kg biocrude^{-1} for cooling. Product recovery was based on the model by Jones, et al. [12], which predicts that on a mass basis 65.2% of the biocrude will upgraded to diesel, 12.8% will be upgraded to naphtha and the remainder being lost as off-gas which is recycled to the Steam-Methane Reformer (SMR) [12].

The aqueous phase was treated in a Catalytic Hydrothermal Gasifier (CHG) to create a gas. This gas was combined with the biogas from HTL reactor and off gas from processing and was used in the SMR to create the necessary hydrogen for the hydrocracker and hydrotreater. Off gas was treated in an ammonia scrubber to remove nitrogen compounds before being used in the SMR. The remaining water was then recycled to the AAG system to remove any remaining nutrients before being discharged.

Make up H_2 requirements for hydrotreating and hydrocracking were found to be 5 kg H_2 per 100 kg biocrude and 2 kg H_2 per 100 kg heavy oil, respectively[12]. Hydrogen was created on site in the SMR. In this process, methane and steam react over a catalyst to produce a mixture of carbon monoxide and hydrogen with 84% of the methane converted to carbon monoxide[12]. The SMR reaction was followed by a Water Gas Shift (WGS) reaction; $CO + H_2O \leftrightarrow CO_2 + H_2$, which converted 95% of the CO to CO_2 [12]. These reactions showed sufficient H_2 production for the hydrotreater and hydrocracker.

Heat from the SMR was recovered in the steam drum, which made high pressure steam for process heat for the facility. The steam drum heated enough steam to recover all excess heat from the SMR. Any steam created in excess of the process heat needs were used in a steam turbine to produce electricity. Excess electricity was then sold to the grid. Model inputs and outputs for the HTL model for the Biochemical and Thermal-Chemical pathways are shown in Table 4.

Table 4: List of model inputs and outputs for the HTL model for the Bio-chemical and Thermal Chemical pathways used in Phase One.

Model Inputs

Feed Inputs			
	Biochemical	Thermal-Chemical	
Biomass Feed Rate	37,365	56,500	kg day^{-1}
Feed Temperature	20	20	°C
Feed Pressure	1	1	atm
Slurry Concentration	18%	20%	wt%
Ash Concentration	82%	75%	wt%
Composition (AFDW)			
Carbohydrates	55%	50%	wt%
Protein	16%	30%	wt%
Lipids	8%	5%	wt%
Other Organics	21%	15%	wt%
HTL Reaction Yields			
Biocrude	38%	35%	g biocrude (g algae) $^{-1}$
Aqueous	60%	63%	g aqueous (g algae) $^{-1}$
Gas	2%	2%	g gas (g algae) $^{-1}$
Product Recovery Energy Use			
Electricity Usage	6		kJ kg $biocrude^{-1}$
Heat	2.90		MJ kg $biocrude^{-1}$
Cooling	0.90		MJ kg $biocrude^{-1}$
Product Recovery			
Diesel	65.2%		% mass
Naphtha	12.8%		% mass
Hydrogen Requirements			
Hydrotreating	5		kg H_2 (kg $biocrude)^{-1}$
Hydrocracking	2		kg H_2 (kg heavy $oil)^{-1}$

Model Outputs

	Biochemical	Thermal-Chemical	
Products			
Fusel Alcohols	15.6		GGE $year^{-1}$
Struvite	6.0		tons $year^{-1}$
Diesel	26.1	34	GGE $year^{-1}$

Naphtha	4.2	10	GGE year $^{-1}$
Electricity	1.7	2.6	MW

2.2.1.3 Techno-economic analysis

The process models described above were integrated into a modular engineering process model and leveraged as the foundation for TEA. The basis of the TEA is a 30-year discounted cash flowrate of return (DCFROR) model which accounts for all capital expenditures, depreciation, manufacturing costs, taxes and product sales for the 30-year lifetime of the biorefinery. The DCFROR used *N*-th plant assumptions, as defined by BETO. A list of these economic assumptions is available Appendix A 1. *N*-th plant assumptions correspond with the mature technology; this means the bio-refinery herein was not a first- or second-of-its-kind, representing a more secure and reliable investment. By studying the bio-refinery using these *N*-th plant assumption, a direct comparison of the technology to existing commercial biofuel plants is realistic. Further, this type of analysis enabled results from sustainability work to directly focus future research and development through the identification of performance targets to meet sustainable production goals. A FOAK analysis, while potentially a better indicator of performance in short term, does not accurately represent the long-term large-scale economics of the system.

The DCFROR model was used to estimate the minimum fuel selling price (MFSP) of the energy products; fusel alcohols, diesel and naphtha. The MFSP was calculated as the price required to sell one a gallon of gasoline equivalent (GGE) in order to provide a net present value of zero at the end of the biorefinery life time, while also supplying a 10% Internal Rate of Return (IRR) for investors after taxes[54]. The stated IRR is a standard for bio-refinery based TEA's, as specified by BETO. A GGE is the amount of fuel required to provide as much energy as a gallon of traditional petroleum-based gasoline, 120 MJ.

The capital and operational costs were estimated from the resulting mass and energy balances. For this analysis it was assumed that all capital equipment would be new, and not retrofitted from a retired refinery, even though it could be possible to repurpose a refinery in this way[55]. This assumption was adopted to allow for a direct comparison of results with other biomass-to-fuels processes, which require the purchase of new equipment [9,11,12,25,45,56]. Capital equipment costs were based on quotes for similar equipment in literature scaled to this system using Equation [1]. These quotes were sourced from Davis, et al. for the fermentation/alcohol recovery process and utilities and from Jones, et al. for the HTL equipment[11,12]. Any additional equipment was priced based off either the capital cost estimator within Aspen Plus or using estimation equations from Towler et al [57].

$$New\ Cost = (Base\ Cost)\left(\frac{New\ Size}{Base\ Size}\right)^{n} \quad [1]$$

Where *Base Cost* is the original equipment quote price, *Base Size* is the original equipment sizing variable value (ex. mass flow rate, heat exchanger duty), *New Size* is the new equipment sizing variable value and *n* is the sizing exponent (values typically range between 0.5-0.9).

Additional direct and indirect capital costs were found using information from Table 5. All costs were scaled to 2011 dollars using Equation [2]. 2011 was chosen as the base year to allow for easy comparisons with other high impact algae biorefinery TEA's in literature[11,12]. Capital and labor costs were scaled using the Chemical Engineering Plant Cost Index and Engineering News Reports Skilled Labor Index, respectively. Complete capital costs for each pathway is available in Appendix A 2 and Appendix A 3

$$2011\ Cost = (Base\ Cost)\left(\frac{2011\ Index}{Base\ index}\right) \quad [2]$$

Table 5: Inputs used to calculate the additional direct and indirect capital costs. Inside battery limits (ISBL) was all conversion process equipment excepting storage and utilities.

Model Inputs		
Additional direct costs[10–12]		
Warehouse	4%	of ISBL
Site Development	9%	of ISBL
Additional Piping	4.5%	of ISBL
Indirect costs[10–12]		
Prorate-able expenses	10%	of Total Direct Capital (TDC)
Field expenses	10%	of TDC
Home office	20%	of TDC
Project Contingency	10%	of TDC
Other Costs	20%	of TDC

Operational costs included the purchase of electricity and natural gas, consumable materials (i.e. acid used for pretreatment), catalysts, fuel, maintenance and labor. Table 6 shows variable operational costs and co-product selling prices. A complete set of operational costs are shown in Appendix A 4 and Appendix A 5.

Table 6: Utility and consumable costs and co-products selling prices from the different conversion cases

Consumable	**Conversion Process**	**Cost**	**Units**
Electricity	Ferm and HTL	0.067	$ kWh^{-1} [58]
Natural Gas	Ferm and HTL	5.13	$ $(1000\ scf)^{-1}$ [59]
Biomass	Ferm and HTL	515	$ mt^{-1} [39]
Ash Disposal	Ferm and HTL	28.86	$ mt^{-1} [10]
Acid	Fermentation	110	$ mt^{-1} [10]
Base	Fermentation	244	$ mt^{-1} [10]
Enzyme	Fermentation	1050	$ mt^{-1} [60]
Yeast	Fermentation	50	$ mt^{-1} [60]
Catalyst - CHG	HTL	132	$ kg $catalyst^{-1}$ [12]
Catalyst – Hydrotreater	HTL	34	$ kg $catalyst^{-1}$ [12]
Catalyst – Hydrocracker	HTL	34	$ kg $catalyst^{-1}$ [12]
Catalyst - SMR	HTL	3.6	$ 1000 scf H_2^{-1} [12]
Co-Product	**Conversion Process**	**Selling Price**	**Units**
Struvite	Fermentation	455	$ mt^{-1}
Electricity	HTL	0.067	$ kWh^{-1}

2.2.2 Phase One – Results and Discussion

Phase one focuses on the economic viability of the Biochemical and Thermal-Chemical process pathways. TEA results show a MFSP of \$14.61 GGE^{-1} for the Biochemical pathway and \$11.24 GGE^{-1} for the Thermal-Chemical pathway. Figure 9 shows the MFSP broken down for each discrete cost including but not limited to capital expenditures, feed stock costs, utilities expenses, and taxes for each pathway. The TEA indicates that there are number of factors contributing to the high costs associated with these pathways. While biomass feedstock plays a large role in the current MFSP results, high capital and operational costs driven by high ash content and low biocrude yields from HTL also play significant roles in the system economics.

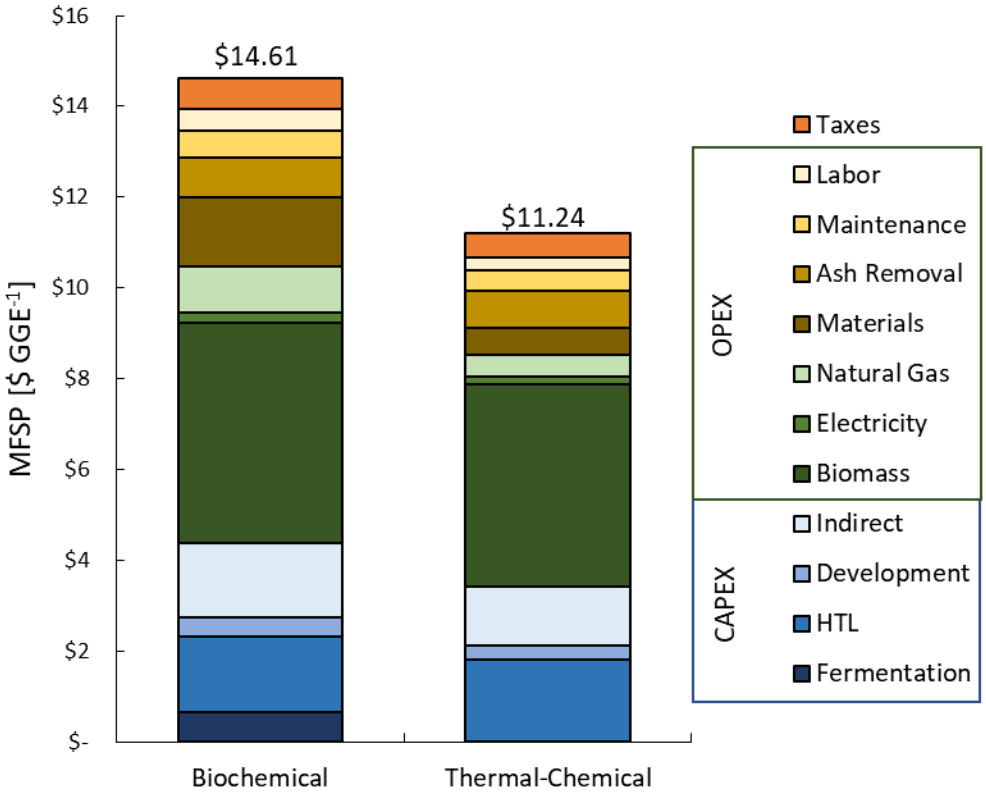

Figure 9: Breakdown of the major economic constituents (capital and operational) for both processing pathways. Each constituent is then further broken down into its major cost drivers to identify significant contributors.

The main cost contributor for both pathways is the biomass feedstock cost, accounting for 33% and 40% of the MFSP for the biochemical and thermal-chemical pathways, respectively. As with other algae-based conversion processes, biomass costs continue to dominate the process economics[9,11,12]. This analysis considered algae grown using AAG system, which should represent and low cost biomass[22,25,39,61], yet biomass costs still have significant impacts on process economics. These results highlight the importance of continuing to decrease biomass production costs for algal biofuels to be competitive in current fuels markets. However, with the system boundary drawn around the bio-refinery itself, it is impossible to understand what is driving the biomass production costs. Understanding the causes high biomass production costs is imperative for recommending solutions to reduce these costs. These results suggest the importance of adding a growth system model to identify high impact cost-drivers within the growth system.

There exists a lot of uncertainty concerning algae biomass selling prices in sustainability work. Some studies consider the current state of technology, while others use more optimistic assumptions. This study uses a biomass price of \$515 AFDW mt^{-1}, which is higher than ORP biomass prices used in studies by Davis et al (2014) and Jones et al (biomass price of \$430 AFDW mt^{-1})[11,12]. The ORP biomass price used in these studies is based on DOE targets and may not be representative of current technology without significant process improvements. More recent sustainability work from Davis et al. (2016) shows a minimum biomass selling price of \$491 AFDW mt^{-1} [22]. The AAG system analysis currently does not utilize these more optimistic assumptions as seen in ORP-based studies. This implies that there may be more opportunity to improve system performance for AAG studies if more research was focused on these systems.

The second largest cost driver for both production pathways was the capital cost, accounting for a similar proportion of the overall MFSP as the biomass costs. This result is unsurprising, as the algae contains a large percentage of ash, 75 wt%. Since the ash is not removed either upstream during

harvesting or within the fuels conversion process, the result is a dramatic increase in capital equipment sizing. The size of the facility must not only be increased to accommodate the ash content but also the water that must accompany the ash. The slurry is fed at 20 wt% solids, thus for every kg of ash or algae entering the system there is an additional 4 kg of water, which leads to significant water requirements. This increase feed capacity does not correlate to an increase in fuel production as the ash and accompanying water are, in essence, inert masses flowing through the system. The ash primarily impacts the capital but also has an impact on the operational costs, requiring more pumping and mixing energy, increased material (ex. acid for pretreatment) consumption and increased heating and cooling loads. These impacts of ash, the inorganic fraction of the biomass, are very significant even before accounting for other potential negative impacts of ash such as equipment damage. Ash can either originate from suspended solids in the surface waters which settles and collects with the biomass (e.g. sand) or from metals absorbed into the biomass. Therefore, future work should focus on reducing ash content, specifically reducing the suspended solids-based ash, to mitigate these issues.

Energy requirements also have a large impact on overall economics. The biochemical pathway uses distillation to separate and purify the fusel alcohol products, which is shown to be very energy intensive due to the high volumes of water in the system. In total, the biochemical pathway requires 2.7 TWh for heating which is 175% higher than the Thermal-Chemical pathway. Most of the extra heat (80%) is required the distillation system. Heating requirements effect operational costs, boiler capital costs and potential revenue from electricity generation. It is therefore desirable to reduce heating requirements for the system. Distillation is not the only separation method available to process engineers. Solvent extraction represents a lower-energy alternative separation method and may be economically favorable than distillation and should be explored as a part of future work.

The HTL system as part of the Biochemical pathway may not be the most cost-effective method for utilizing the remaining biomass. This system is both capitally and operationally expensive, accounting

for 67% of the total capital costs and 50% of the operational energy costs. HTL is notorious for its high capital costs, and a low-cost process such as anaerobic digestion (AD) may be a better alternative for utilizing the unfermented biomass.

2.3 Phase Two

There were four main conclusions from Phase One; the need to reduce ash content, the need to understand the cost drivers of the AAG system, reducing energy requirements for fusel alcohol recovery and considering alternative secondary process options after fermentation. These conclusions drove the research into Phase Two. In Phase Two, the model system boundary was expanded to include an upstream growth and harvest system. This expanded system boundary was called the "Integrated System Boundary", Figure 10, and is used for both the TEA and LCA. The system boundary is consistent with a well-to-wheels system boundary for conventional fuels, and considers all economics and emissions from growth, conversion, distribution and end use for the LCA work.

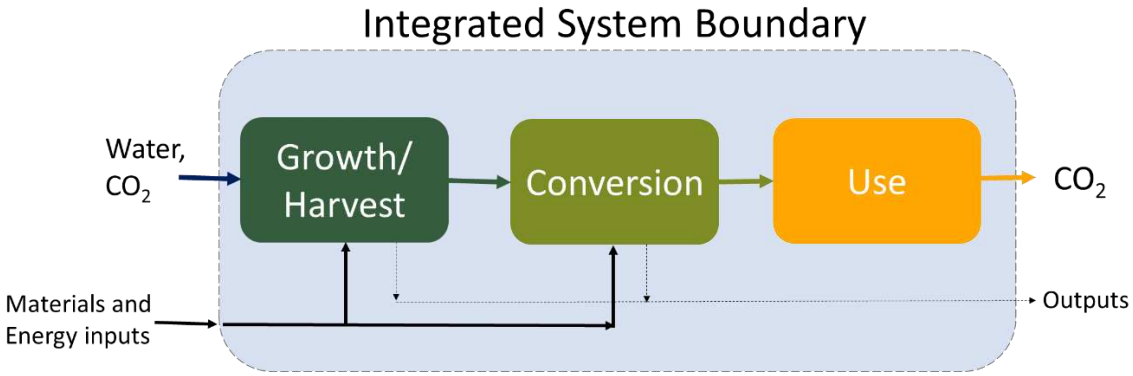

Figure 10: System boundary for integrated process model. The process model includes the growth and harvest of algae biomass from an AAG system, conversion to renewable fuels using one of four conversion pathways (Fermentation Only, Fermentation + AD, Fermentation + HTL or HTL Only) and final use of the renewable fuels product. This system boundary is consistent with a well-to-wheels system for conventional fuels.

In addition to the growth system, an optional ash removal system was added to the process model. This ash removal model was based on experimental work conducted as Sandia National Laboratories. In Phase Two, fusel alcohols were recovered using solvent extraction, a low energy separations process. This phase also considered four different processing options; fermentation (Ferm

Only), fermentation and AD (Ferm + AD), fermentation and HTL (Ferm + HTL)and whole algal HTL (HTL Only), Figure 11.

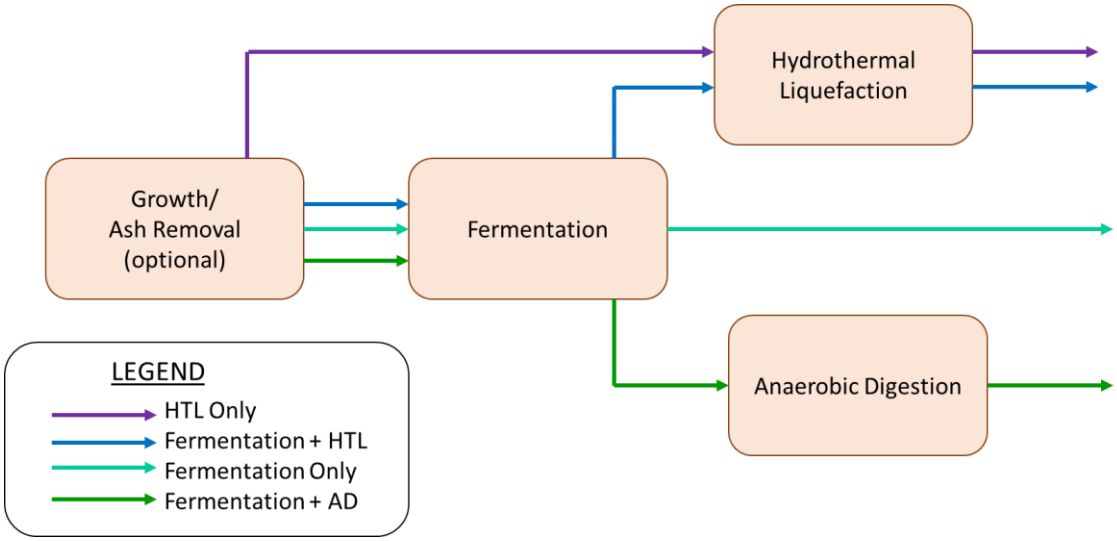

Figure 11: Block flow diagram of the different downstream processing options evaluated in this study. Three options included fermentation: fermentation Only, Fermentation + AD and Fermentation + HTL, and one option considered only HTL. Each conversion process was considered for biomass that had received an ash removal treatment and for biomass that had not undergone ash removal.

2.3.1 Phase Two – Methods

Most of the foundational process model inputs from Phase One were leveraged as a part of Phase Two. The modular processing model was then updated to include the AAG system model, ash removal, solvent recovery and AD. Each new module within the process model is explained in more detail in the following sections.

2.3.1.1 Attached-Algae Growth System Model

The AAG system growth model was based on a small-scale attached growth systems seen in literature and pilot scale data provided by Sandia National Laboratories [39,40,47,62,63]. Figure 12 shows a BFD for the process model including process inputs and outputs.

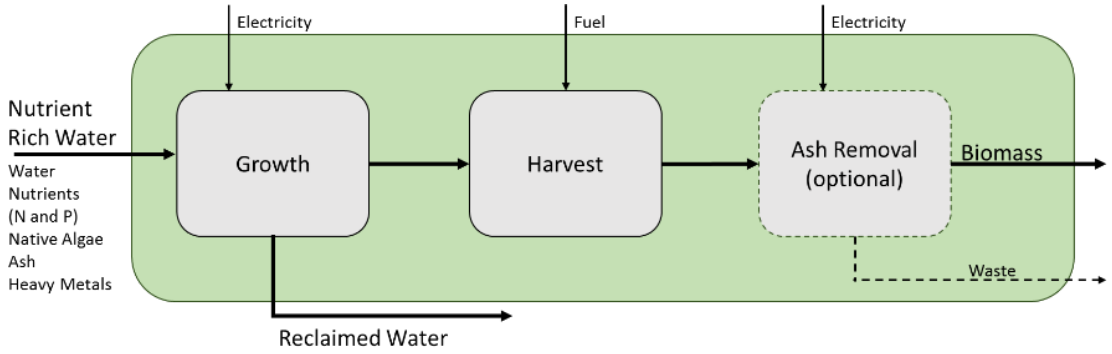

Figure 12: BFD of the AAG system including an optional ash removal system. Nutrient rich surface waters enter the growth system, where native periphyton attached to growth system substrate and remove nutrient, heavy metals and ash from the waters. Algae biomass was then harvested from the growth system and ash can be removed. The biomass can then be used as the feedstock for the bio-refinery.

The growth system was sized to produce 1215 AFDW mt of algae biomass per day (50,625 AFDW kg hr^{-1}) which is consistent with other algal biorefinery feed rates [11,12]. Using an average biomass productivity of 20 g m^{-2} day^{-1}, the AAG system required an area of 13500 acres[39]. Capital costs for the growth system include civil works, such as land grading and interconnecting piping, complete lining of the raceways with a geomembrane liner, and pumps. Capital and operational costs were calculated on a per acre basis based on economic assessments of AAG systems in literature [22,39,62,64]. A survey of these studies is available in Appendix C 4. Model inputs and outputs for the growth system are shown in Table 7. Model outputs include the capital investment (CAPEX) and annual operational costs (OPEX).

Table 7: List of model inputs and outputs for the AAG growth system model.

Model Inputs		
Growth Conditions		
Growth Rate	20	g AFDW m^{-2} day^{-1}
Algae Production	1215	AFDW metric tons day^{-1}
Runway Length	500	ft
Hydraulic Loading Rate	20	gal min^{-1} linear ft^{-1}
Growth Area	13500	acres
Capital Investment		
Land [65]	3,610	\$ $acre^{-1}$
Peripheral Land	20%	of total growth area
Civil Works	13,765	\$ $acre^{-1}$
Geomembrane	18,093	\$ $acre^{-1}$
Pumps	2,831	\$ $acre^{-1}$
Electrical	1,067	\$ $acre^{-1}$
Piping	5,784	\$ $acre^{-1}$
Auto-siphon	470	\$ $acre^{-1}$
Harvest System	5,390	\$ $acre^{-1}$
Operational Costs		
Electricity	0.068	\$ kWh^{-1}
Diesel	4	\$ gal^{-1}
Maintenance	1.60%	of capital costs
Growth OPEX		
Pump electricity usage	0.006	kw gpm^{-1}
Additional energy costs	10%	of pump elec
Harvest OPEX		
Harvest Costs	627	\$ $acre^{-1}$
Labors Costs	1400	\$ $acre^{-1}$
Additional direct costs[18]		
Warehouse	1.20%	of installed costs
Site Development Additional Piping	included in project estimates	
Indirect costs[18]		
Prorate-able expenses	4	% of TDC
Field expenses	4.5%	% of TDC
Home office	10.3%	% of TDC
Project Contingency	10%	% of TDC
Other Costs	2.6%	% of TDC

2.3.1.2 Ash Removal

After harvest, an optional ash removal process was included to understand the costs and benefits of ash removal. This process was based off experimental work performed at Sandia National Laboratories. Ash removal consisted of a water wash process which reduced ash content by 90%, from 75 wt% to 23 wt%. A complete table of process inputs for the ash removal systems is available in Table 8.

Table 8: List of model inputs and outputs for the optional ash removal model

Model Inputs		
Process Inputs		
Ash Reduction	90	wt%
Outlet Slurry Concentration	20	wt%
Reaction Time	24	hours
Filter Press Power Use	1350	kJ m^{-3}

2.3.1.3 Fermentation

A PFD for the fermentation process using solvent recovery is presented in Figure 13. Many of the unit processes are the same as the original model from Phase One, excepting alcohol recovery. Fusel alcohols are now recovered using a polar solvent, ethyl acetate, in a liquid-liquid extraction column. The solvent was then recovered in a distillation column and recycled to the extraction column. Distillation was set to recovery >95% of solvent. Model inputs for the solvent recovery step are available in Table 9.

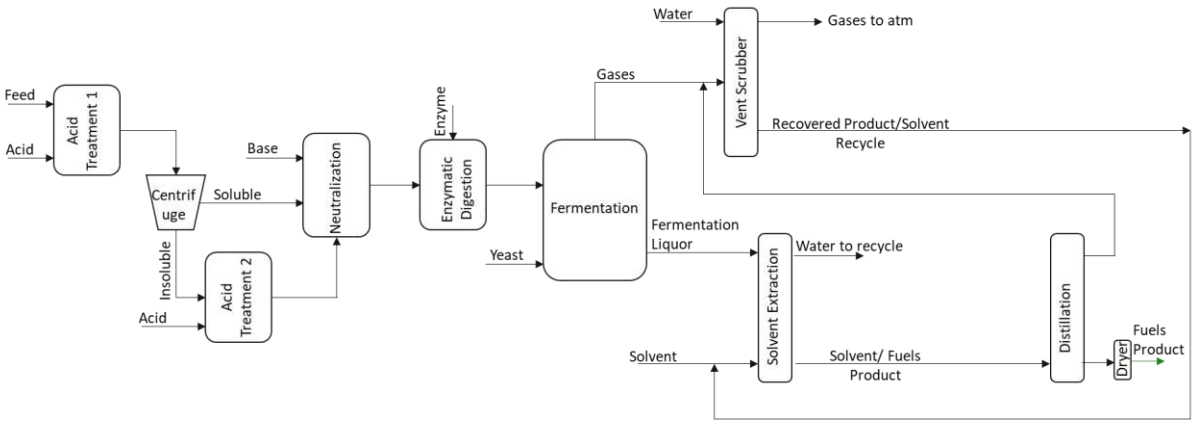

Figure 13: PFD for the fermentation process, including pretreatment through product recovery.

Table 9: Model inputs and outputs for the fermentation conversion process, includes pretreatment, fermentation and product recovery

Model Inputs		
Product Recovery		
Solvent Use	1:5	vol (vol solvent to liquor) $^{-1}$
Extraction Pressure	1	atm
Extraction Temperature	25	
Distillation Pressure	153	mbar
Distillation Temperature	50	°C
Solvent Recovery	95	% by mass
Product purity after Drying	99.5	% by mass

2.3.1.4 Anaerobic Digestion

For AD, the algae were assumed to have a volatile solids (VS) content of 90%. The reaction produced 300 mL CH_4 g VS^{-1}, well within the range of other microalgae anaerobic digestion studies[66–68]. The AD used 0.22 kWh kg total solids^{-1} of heat energy and 0.085 kWh kg total solids^{-1} of electrical energy[11]. The biogas was then burned onsite to produce heat and electricity in the utilities section. Inputs for the AD model can be found in Table 10.

Table 10: Model inputs and outputs for the AD model. Outputs are the ash-reduction case.

Model Inputs		
AD Reaction		
Volatile Solids	90%	wt% of TS
Reaction Temperature	35	°C
Reaction Time	35	days
VS destruction	41%	
Methane Yield	300	mL g VS^{-1}
CH_4:CO_2	2:1	mol CH_4:mol CO_2
AD Heat Requirement	0.22	kWh kg TS^{-1}
AD Electricity Requirement	0.085	kWh kg TS^{-1}
Nutrient Recovery		
% P Recovered in Liquid	50%	
% N Recovered in Liquid	80%	
Solids content of digestate cake	30%	
% N Recovered in cake	20%	
Bioavailable N in cake	40%	
Model Outputs		
Product		
Electricity	16.6	MW
Digestate cake (solids)	98226	tons $year^{-1}$

2.3.1.5 Sensitivity Analysis

A sensitivity analysis was performed to identify which variables would have the greatest impact on the conversion economics. The results from this analysis was used to direct future research and development in areas that will have meaningful impact. To perform the analysis, the variables of interest were varied ±20%, and their effects on the MFSP were documented, results of which were used in a Student's t-test to evaluate which parameters have a significant impact on the overall process economics. Sensitivity analysis focused on the Fermentation + HTL Pathway. A confidence interval of 95% was chosen; and when combined with the degrees of freedom provided a t-critical-ratio. T-ratios

that fall outside of the ± t-critical-ratio are proven to have a significant impact on the process within the confidence interval.

2.3.1.6 Life Cycle Assessment

The LCA was performed using a well-to-wheels system boundary, which includes all emissions from the growth of the algae biomass, processing, distribution, and combustion. Energy and mass consumption was combined with life cycle inventory (LCI) data from Argonne National Labs GREET database to determine the global warming potential of the different processing pathways[69]. Some conversion processes were able to take a displacement credit by exporting electricity or through their fertilizer product. Struvite was assumed to displace di-ammonium phosphate (DAP) on a per kg of phosphorus basis while the bioavailable nitrogen is the digestate cake from the AD case was assumed displace ammonia fertilizer on a per kg of nitrogen basis. A table of LCI data inputs is shown in Table 11.

Table 11: List of LCI's used for the LCA. All data was obtained from GREET[69]

LCA INPUTS		
Life Cycle Inventory Values		
Electricity	0.51	kg CO2 kWh^{-1}
Natural Gas	12.6	kg CO2 $MMBTU^{-1}$
Fuel	16.5	g CO2 MJ $Fuel^{-1}$
Acid	44	g CO2 kg $acid^{-1}$
Base	1280	g CO2 kg $base^{-1}$
Enzyme	2680	g CO2 kg $enzyme^{-1}$
Solvent	4651	g CO2 kg $solvent^{-1}$
Distribution	0.7	g CO2 MJ $Fuel^{-1}$
Ammonia Fertilizer	3161	g CO2 kg N^{-1}
DAP	1661	g CO2 kg P^{-1}

The analysis was performed to find the mass of CO_2 equivalent ($CO_{2\text{-eq}}$) released per MJ of fuel produced. The $CO_{2\text{-eq}}$ is computed based on IPCC 100-year global warming equivalency factors for GHGs of interest. Equivalency factors are used to equate different GHG's based on their total impact (radiative forcing) compared to CO_2 over a given time frame (100 years). This analysis focused on three high

impact greenhouse gases; CO_2, CH_4, and N_2O with global warming equivalency factors of 1, 28, and 265, respectively [70].

2.3.2 Phase Two - Results and Discussion

2.3.2.1 Economic Viability

Four different processing options were evaluated on their ability to produce renewable fuels. A breakdown of the MFSP for each processing option for both the no-ash removal and ash removal scenarios is presented in Figure 14. A summary of total capital investment and operational costs for the four pathways is available in Appendix A 9 - Appendix A 16.

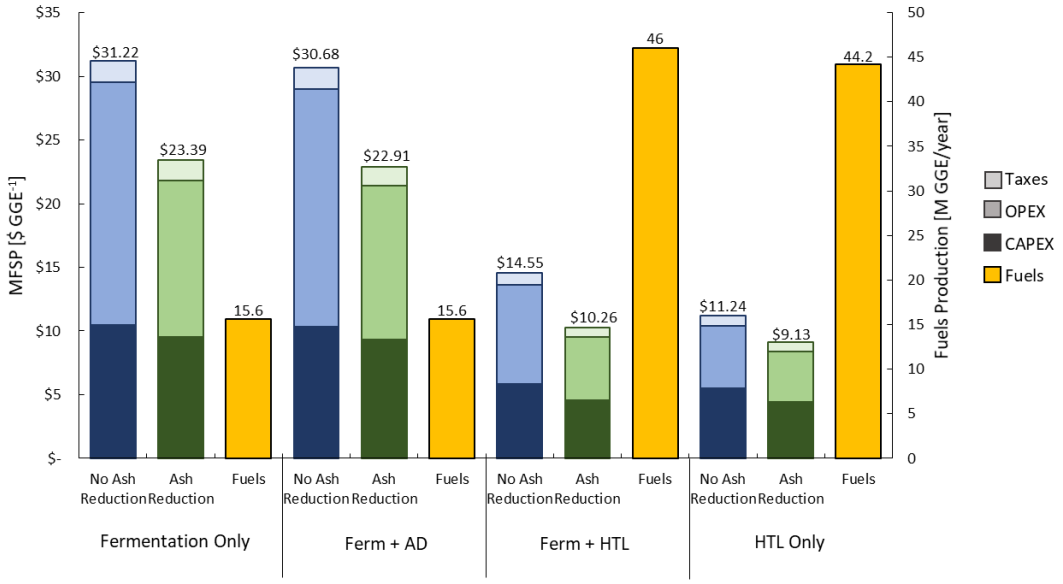

Figure 14: Breakdown of the MFSP for the different integrated conversion cases and the associated fuels production (right hand axis). Each MFSP is broken down to the contributions of the CAPEX, OPEX and taxes.

For all processing options, ash removal has a positive impact and reduced the MFSP. Without ash removal, the incoming algae biomass has an ash content of 75 wt% and when considering the entire feed stream, only 5% of the total feed is available for conversion to fuels. High ash content represents a significant challenge for all conversion pathways as it dramatically increases both the capital and operational requirements. Ash removal reduces associated capital and operational costs by reducing

feed flow rates without affecting fuel production. While the ash removal process reduced ash content from 75wt% to 23wt%, the remaining ash content is still significant. Most ORP algae system produce algae with a low ash content of <10 wt%. Therefore, these conversion systems are still oversized due to ash content compared to ORP based conversion systems. However, further ash removal may be difficult as most of the remaining ash is biogenic and cannot be easily washed off. Another option to reduce ash content is the addition of filters in the AAG system to reduce incoming TSS or strategic seeding of the algae turf. The economics costs and benefits of employing these options should be considered in future work.

The model created herein is an integrated model and includes the capital and operational costs for both the growth and conversion systems. A breakdown of the associated costs for each system divided by type, growth versus conversion is presented in Figure 15. Values shown here are for the pathways which include ash reduction.

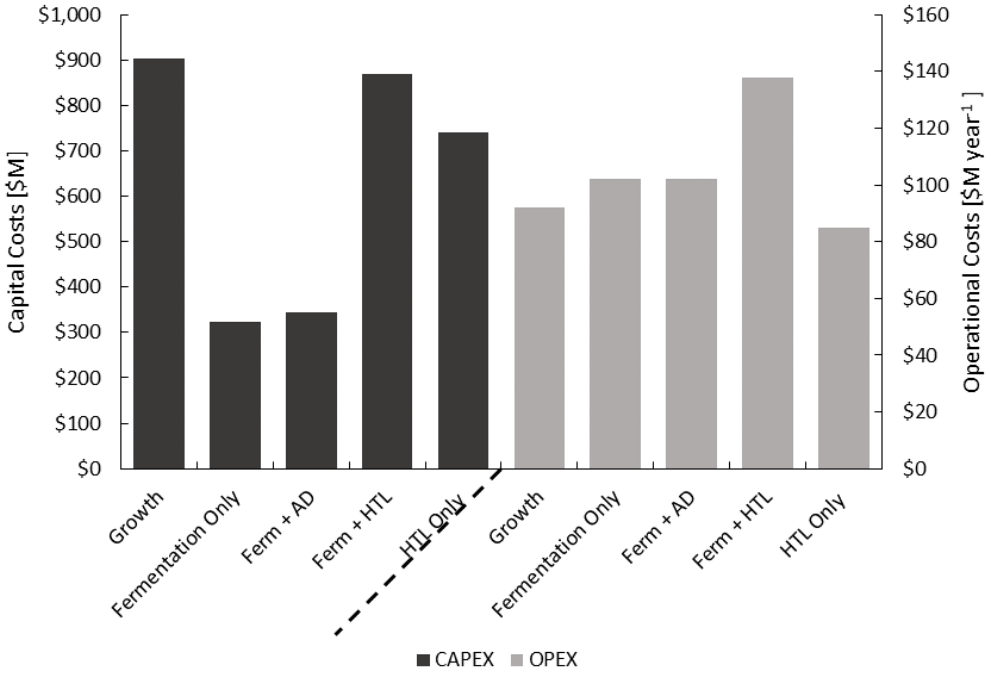

Figure 15: Total CAPEX and annual OPEX for the growth system and the different conversion cases including a pre-processing ash removal step. The growth and conversion systems were sized to produce (growth system) or utilize (conversion system) 1215 AFDW mt of algae biomass per day.

The growth system is responsible for the largest share of capital expenditures with CAPEX costs over $900 M. The main contributors of these costs include the geomembrane liner (31%) and civil works (24%). In the current model, the entire growth area is covered with a geomembrane liner but there may be opportunities to reduce this requirement. ORP designs previously required 100% liner coverage but now require on 5-15% liner coverage[22]. Reducing liner requirements for the AAG systems from 100% to 15% reduced the MFSP by $1.10 GGE^{-1} for the Ferm + HTL and HTL Only cases and $3.15 GGE^{-1} for Fermentation Only and Ferm + AD cases.

One goal of Phase Two was to consider low-cost processing options for the remaining biomass after fermentation. Instead of producing more fuels, AD produces a biogas which is burned on site to produce process heat and electricity. As shown in Figure 15, this system has much lower capital and operational costs than the HTL system. However, the AD system does not make enough electricity to overcome the differences in fuels production, Figure 14. The Ferm + AD system produces 16.6 MW of electricity which is sold to the grid for a total income of $9 M per year from electricity sales. Annual sales required for the Ferm + AD system is $462M. These results imply that HTL captures more of the energy potential for the AAG algae than AD and the increased energy recovery is worth the cost.

The growth system also included significant operational costs ($92M $year^{-1}$) with electricity accounting for 60% of these costs, Figure 16. The AAG system is an open system where water is continually pumped down the long flow ways. Moving these large volumes of water requires significant energy consumption. One opportunity is to employ low energy pumping systems, such as low pressure, low head buoyant piston pumps (US Patent 5131820)[71] which can reduce energy usage by an order of magnitude. Another solution is finding areas with sufficient grade to reduce or eliminate pumping requirements.

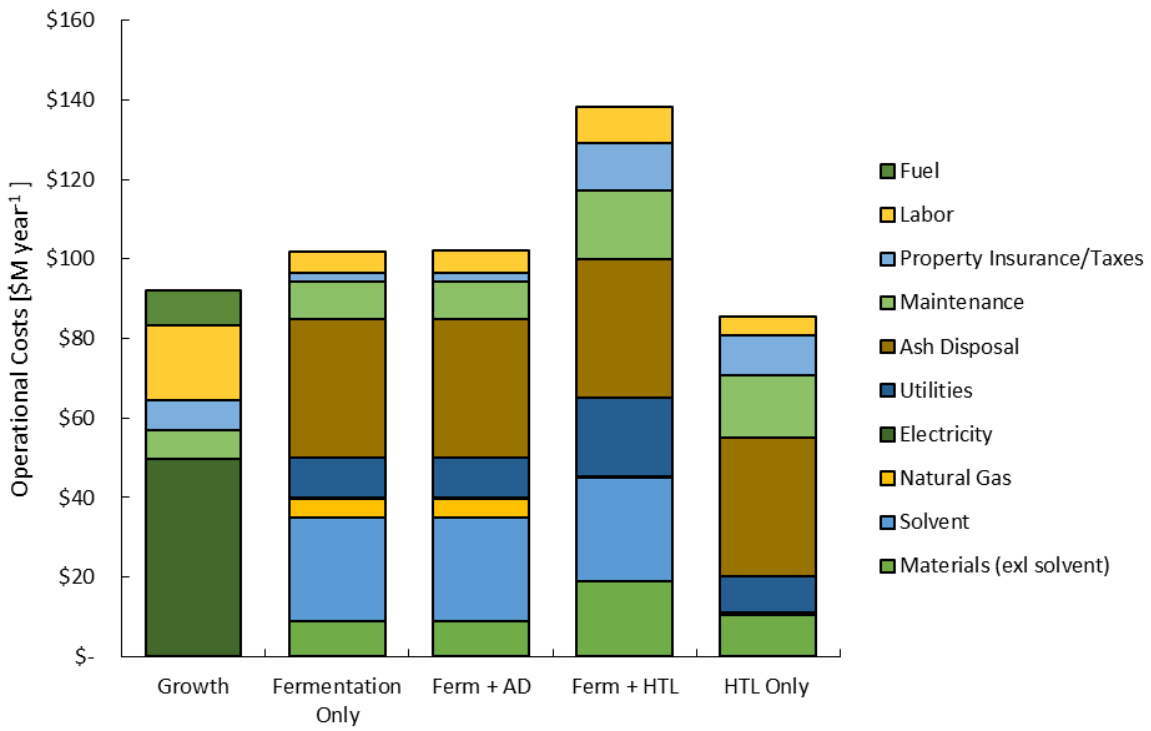

Figure 16: Annual operational costs differentiated by category for the growth system and the different conversion cases

A breakdown of the annual operational costs is presented in Figure 16. For the conversion system, ash disposal accounts for 25-42% of the annual operational costs. Disposal costs are calculated on a mass basis and the high ash content of the AAG system algae directly affects these costs. Current ash disposal assumes disposal at a landfill, but this assumption represents significant uncertainty. Experimentation performed at Sandia National Laboratories shows that algae grown in the AAG system picks up heavy metals such as arsenic. Disposal of potentially hazardous materials may increase ash disposal costs.

Use of solvent recovery instead of distillation to recovery the fusel alcohol products reduced the overall MFSP by \$0.03 GGE^{-1}, and there are still opportunities to improve the solvent recovery process. Currently, there is a 5% loss associated with the solvent use and make up solvent costs over \$26M per year (17-23% of total operational costs). Improving solvent recovery from 95% to 99% reduces the MFSP by \$1.05 GGE^{-1} for the Fermentation Only and Ferm + AD cases and \$0.40 GGE^{-1} for Ferm + HTL case.

Co-products and co-services are another important opportunity for these systems, especially for the growth system and ash. One opportunity for AAG systems in nutrient reduction for nutrient rich waters from non-point sources, explored in Chapter 4 of this work, to prevent or mitigate eutrophication. At a price of \$8 $(kg\ N)^{-1}$ and \$50 $(kg\ P)^{-1}$ the AAG system would have a nutrient removal revenue of \$400 M per year [72] which is more than the current operating costs for both the growth and conversion systems. Future work should concentrate on quantifying the benefits of nutrient removal. If nutrient removal could offset all growth-related operational and capital costs, the MFSP reduces to \$2.34 GGE^{-1} or \$1.05 GGE^{-1} for the Ferm + HTL and HTL Only cases, respectively. In addition to nutrient removal, experimentation has shown that AAG systems also remove heavy metals such as arsenic and lithium opening the prospect for high value metal reclamation or removal. In addition, ash has to the potential to be sold as a co-product instead of being disposed. Any of these opportunities could be incorporated to improve process economics.

2.3.2.2 Sensitivity Analysis

Sensitivity analysis was performed on the Ferm + HTL with ash removal processing case. The results from the analysis are shown in Figure 17. Variables whose t-values lie outside of the t-critical values, shown in vertical dashed lines, are considered to be significant.

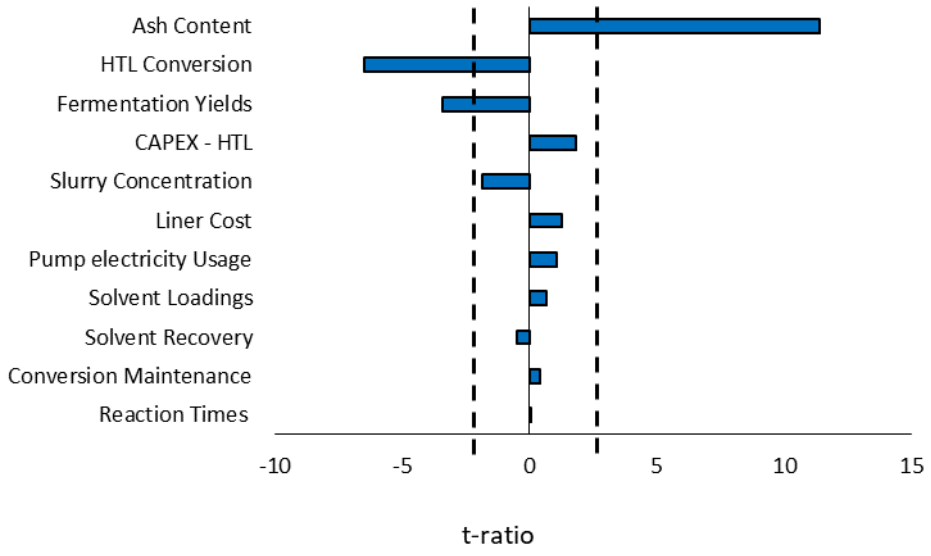

Figure 17: Results from the sensitivity analysis for the Ferm + HTL case with ash removal. Horizontal dashed lines represent the critical t-ratio; variables whose t-ratio is fall outside the critical t-ratio are considered to be significant.

Ash content is shown to be significant variable even with ash removal which results in an ash content of 23 wt%. Ash contributes to capital and operational bloat. In this model, ash is treated as an inert mass flowing through the system, and this inert mass increases water requirements to meet feed slurry specifications. Therefore, high mass flow rates require the system to be oversized, which increases capital equipment sizing, pumping power and heating/cooling requirements compared to a system with much lower ash content. These issues with ash are evident even before incorporating other known impacts of ash on process equipment performance and life. Reduction of ash may be possible through the addition of filters in the growth system, as a significant portion of the ash is made up of debris from the water source, or through operational changes such as strategic seeding of the turf.

Conversion of biomass to fuels through HTL or fermentation are also significant variables. Currently, this model uses a kinetic model based on carbohydrate, lipid, and protein composition to predict biocrude yields from HTL and experimentation should be conducted to validate the yields. Increasing biocrude yields may be possible through catalyst and process optimization. Fermentation

yields should also be validated through experimentation and could be improved through co-culture optimization. Improvements in these yields are potentially possible but may be limited.

2.3.2.3 Life Cycle Assessment

To meet the renewable fuel standard (RFS), renewable fuels may not exceed greenhouse gas (GHG) emissions of 46 g MJ fuel^{-1} or half of the current emissions for petroleum-based fuels (92 g MJ fuel^{-1}) on a per MJ of fuel basis based on a well to wheels system boundary. The results for the well-to-wheels LCA for the different processing cases is presented in Figure 18 with the dashed red line showing the RFS goal with results ranging between 282 - 69 g $CO_{2\text{-eq}}$ MJ fuel^{-1}. All cases include displacement credits for co-products.

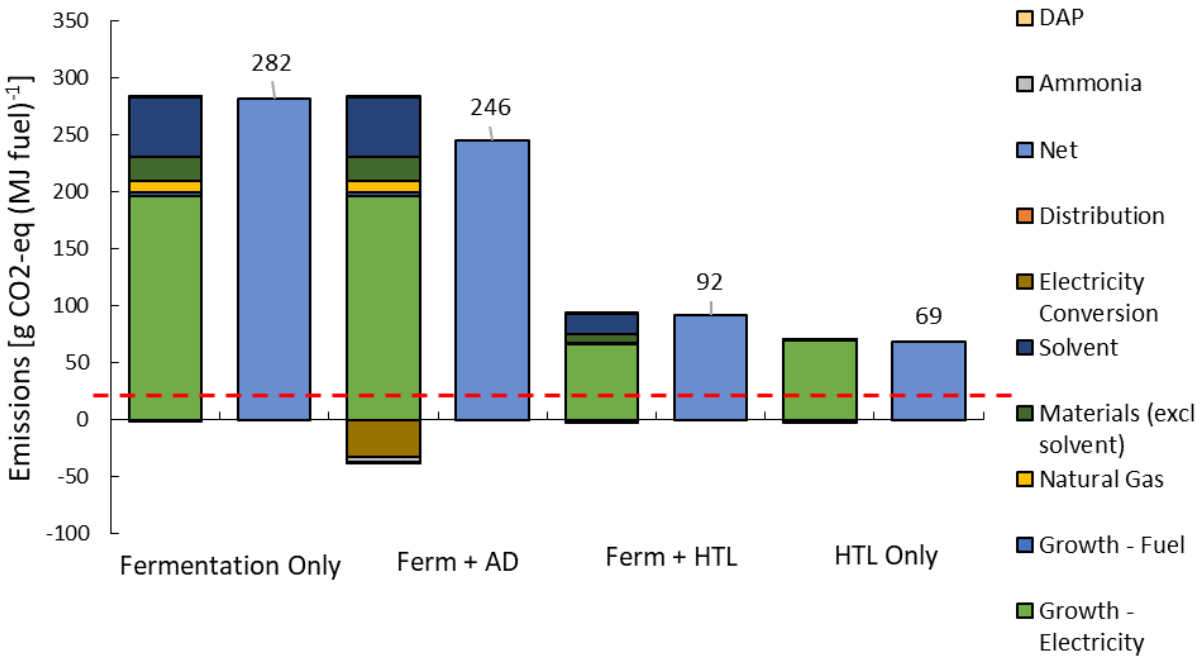

Figure 18: Results from the LCA analysis for the different conversion cases with ash removal. Negative emissions are from displacement credits. The red dashed line indicates the RFS emissions goal with the target being to be below this value.

Currently, none of the processing options can meet the RFS due in large part to the electricity consumption for the growth stage which accounts for 197– 67 g $CO_{2\text{-eq}}$ MJ fuel^{-1}. Similar to the TEA

results, reducing electricity consumption for the growth stage should be one the future area of process optimization. Another option would be considering water remediation as a service or co-product for the AAG system and employing either a displacement credit or a co-product allocation method to reduce the emissions attributed with growing the algae biomass. If these methods could reduce emissions associated with biomass growth by 50%, both the Ferm + HTL and HTL only cases would meet the RFS goal.

Another significant contributor to overall emissions is make-up solvent, which currently accounts for 18-20% of the total emissions for the fermentation-based systems. Increasing solvent recovery is another opportunity for reducing emissions. One trade-off, however, is increased heat requirements for the solvent recovery column. As solvent recovery increases, more heat is required for the column to achieve the desired separations. Emissions based trade-offs should be explored to find the optimal target for solvent recovery.

Two of the fermentation cases, Fermentation Only and Ferm + AD, show very high net emissions per MJ fuel. This is due in large part to low fuels production in these systems and the functional unit chosen for the analysis and not that these systems necessarily produce more emissions overall than the other processes. As mentioned in the economic viability results, these systems produce around one-third of the fuels as the other two processes due to reduced utilization of the biomass. Therefore, for similar net emissions, processes which produce less fuels have higher emissions per MJ of fuel.

2.4 Conclusions

Two phases of research were conducted to ascertain the economic viability and environmental impact of producing renewable fuels from algae grown using an AAG system. In the first phase, two different pathways were considered; the biochemical pathway which utilized a novel fermentation process followed by HTL and the thermal-chemical pathway which was limited to HTL processing. Results showed that biomass costs, high ash content and energy intensive separations were two high

impact areas for improving the system economics. In addition, focus was drawn to capitally and operationally intensive growth and HTL systems. These conclusions drove a second phase of experimentation and analyses. In the second phase, the system boundary was expanded to include the growth system to better understand upstream economics as the first phase fixed a biomass purchase price. An ash removal process, a less energy intensive separations process and an AD process were added to the process model as optional unit process operations. In total, four different processing options were explored and evaluated on their ability to produce economically competitive and environmentally friendly renewable fuels. The MFSP ranged between \$31.22 – \$11.24 GGE^{-1} for systems with no ash removal and between \$23.39 - \$9.13 GGE^{-1} for systems with ash removal.

Ash reduction was found to be beneficial for all conversion technologies. Solvent recovery, a low energy alternative to distillation used for product recovery, was found to reduce energy use but had high economic and environmental costs due to solvent loss. Increasing solvent recovery was found to be beneficial but should be validated experimentally. AD was explored but did not recover enough energy from the remaining biomass to be effective. The Ferm + HTL and HTL only cases show the most potential for producing economically viable fuels as they recovered more energy from the biomass than either Fermentation alone or Ferm + AD.

In Phase Two, three main areas were identified to improve economic viability; ash reduction, improving fuel yields, and co-products or co-services. Even with ash reduction, the biomass entering the bio-refinery has a high ash content which contributes to increased capital and operational costs. Strategic seeding of the turf in the growth system or filters could be used further reduce ash content but would require increased operational costs for the growth system and these trade-offs would need to be quantified. Another opportunity would be co-products or co-services either through conventional products or environmental services, respectively. Ash could be potentially be sold as a filler for concrete, while the AAG system could be employed to remediate nutrient rich water, for high-value metal

reclamation or heavy metal removal. LCA results showed GHG emissions ranging between 69- 282 g $CO_{2\text{-}eq}$ MJ $fuel^{-1}$. Reaching the RFS goal of 46 g MJ $fuel^{-1}$ may be possible through the application of co-product for the Ferm + HTL and HTL Only pathways or increasing fuels yields. Integrating the AAG system as part of an environmental service has the potential to improve both the economic viability and environmental impact of these algae-based renewable fuels. The economic viability of this system is explored in Chapter 4 of this dissertation work.

CHAPTER 3: A CASE STUDY OF SYSTEM BOUNDARIES AND THEIR AFFECT ON SUSTAINABILITY SCIENCES RESULTS USING THE CONVERSION OF DISTILLER'S GRAINS TO RENEWABLE FUELS[2]

3.1 Introduction

The United States' corn ethanol industry is full of controversy [73–75]. To its advantage, corn ethanol represents a mature technology with a long production history as a first-generation alternative biofuel and provides a means for domestic bio-based fuel production [76,77]. However, this process has been widely criticized for its role in the food versus fuel debate and for continuing to have high production costs that are yet to be competitive with conventional fuels, largely due to feed stock costs [73,76,78–81]. Despite these issues, the corn ethanol industry has experienced significant growth and the associated infrastructure has an expected lifetime of multiple decades [76]. Therefore, it is imperative to continue to improve both the economics and sustainability of this process[77,82]. One strategy for achieving these goals is to focus on increased utilization of corn ethanol's largest co-product, distiller's grains with solubles (DGS). DGS consists of the remaining biomass after fermentation and includes fibers, proteins, ash, and unfermented sugars which are typically sold as a protein source for ruminants[48,83–86]. Researchers have proposed a novel second fermentation process to upgrade DGS that results in an increased fuel yield and protein value in an effort to improve ethanol biorefinery economics and sustainability.

Researchers at Sandia National Laboratories have engineered a consortium of *E. coli*-based biocatalyst strains [48] that have been proven to ferment the hydrolyzed sugars and specific amino acids

---

[2] This chapter was published as a manuscript and is reprinted (adapted) with permission from *Conversion of Distiller's Grains to Renewable Fuels and High Value Protein: Integrated Techno-Economic and Life Cycle Assessment*. DeRose, K.; Liu, F.; Davis, R. W.; Simmons, B. A.; Quinn, J. C. *Environmental Science & Technology* **2019** *53*(17). Copyright 2019 American Chemical Society.

available in the DGS into energy products; predominantly composed of a mixture of C4 and C5 alcohols, hereafter referred to as fusel alcohols [48]. Additionally, Lui et al. have verified that fermentation strains preferentially consume the typically high abundance, low value amino acids, producing a protein product that has been enriched with higher value amino acids including valine, proline, alanine, glycine, methionine, cysteine, histidine, and hydroxyproline. While overall protein mass will decrease due to this second fermentation process, it is proposed that the sale of additional fuels and increased value of the upgraded protein product will offset the cost of additional processing with the inherent benefit of increasing overall fuel yields from the starting grain.

The purpose of this study is to evaluate if the upgrade conversion of DGS to protein and fuels adds value for corn ethanol producers through the use of engineering process modeling coupled with TEA and LCA. This type of analysis allows researchers and stakeholders to evaluate the economic potential of this technology while it is still in development based on results from experimental work. This work focuses on identifying the optimal processing pathway by evaluating three different process scenarios, described below. Modularity in foundational engineering process modeling enables a direct comparison of the proposed processes on a consistent system boundary. Results from these scenarios were used to evaluate the economic viability and sustainability metrics of the proposed upgrading facility with recommendations for future research and commercial deployment presented.

Using this process as a case study also presents an interesting opportunity to study the effects of different LCA methodologies. LCA methodology recommends expanding system boundaries and using a displacement method to compute production-related emissions[21]. However, this method may not always be possible due to resource or knowledge (e.g. confidential or proprietary information) constraints. Because the corn-ethanol process is well known, there is an opportunity to explore how employing an expanded or contracted (i.e. around the system being studied) system boundary or different co-product allocation methods affects LCA results.

3.2 Methods

3.2.1 Process Model

A modular engineering process model for the conversion of DGS into fusel alcohols including protein recovery was created and used to capture mass and energy balances for three different production pathways, described below. These balances were used as the foundational inputs for the TEA and LCA studies to evaluate different processing options and the value-add proposition for ethanol producers.

Within the engineering process model, two different processing options for both alcohol recovery and protein recovery were considered. For alcohol recovery, solvent and distillation recovery were considered. For protein recovery, protein concentration and drying to create a high protein content (HPC) product and simple drying to create a low protein (LPC) product were considered. From these processing options, three different pathways were identified; a Base Pathway using solvent extraction and HPC production, a Distillation Pathway using distillation and HPC production and an LPC Pathway using solvent extraction and LPC production. A BFD of the processing pathways including the system boundary delineation is shown in Figure 19. The system boundary included the purchasing of DGS from a co-located corn ethanol facility, processing DGS into fuels and protein products and distribution of products. More detailed PFD's of these processing options are available in Appendix B 1.

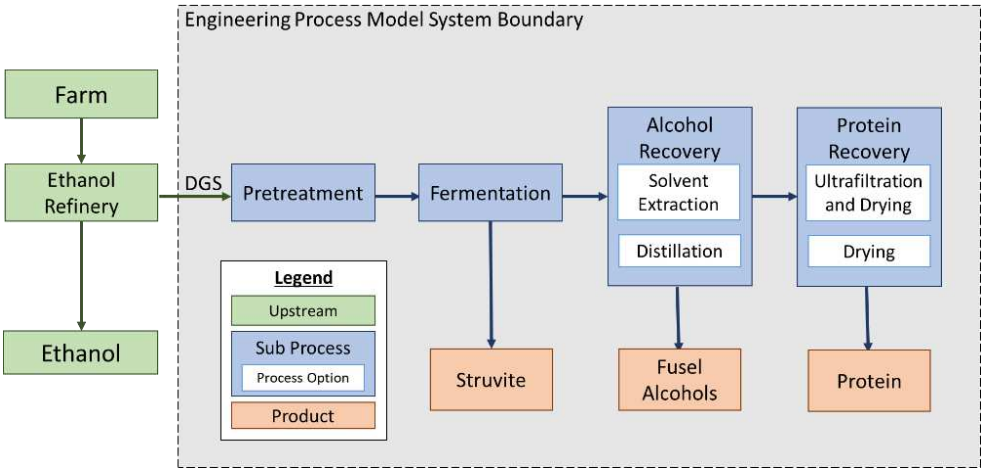

Figure 19: BFD for the DGS upgrading facility. There are two alcohol recovery options including distillation or solvent extraction; and two protein recovery options including ultrafiltration followed by drying and drying.

The process model was constructed in a modular fashion with sub-process models constructed such that different technology pathways could be evaluated while maintaining a consistent system boundary. The performance of the fermentation process models was validated based on laboratory scale experimental data provided by Lui et al., and was modeled in ASPEN Plus[48]. The protein recovery process model was based on the whey protein concentrate production process as described in literature[87,88].

The model assumed the new upgrade facility would be co-located with a corn ethanol facility to reduce costs and eliminate the need for drying, packaging and transporting of the DGS. The bio-refinery was sized to utilize all DGS produced by a 454 M liter per year corn ethanol plant, the most common corn ethanol facility size currently operated in Iowa, USA[89]. Using a conversion of 0.71 kg of DGS per liter of ethanol and 7920 hours of annual plant operation, the DGS feed rate was set to 40,909 kg hr^{-1} of DGS solids [90].

The price of DGS was set at $60 per mt, based on current commodity markets for wet DGS[91]. Biomass composition, provided by Sandia National Laboratories and validated by NJFL, Inc., was reported to be 29% protein, 8% fat, 9.5% insoluble fiber, 4.5% ash and 49% carbohydrates on a dry mass

basis, which is consistent with other results reported in literature [83]. These values were used as the inputs for the process model at the refinery gates. Bio-refinery inputs are shown in Table 12.

Table 12: Bio-refinery model inputs

Model INPUTS		
Feed Conditions		
Feed Rate	40,909	kg day^{-1}
Feed Temperature	20	*C
Feed Pressure	1	atm
Slurry Concentration	35	wt%
Composition		
Carbohydrates	29	wt%
Protein	49	wt%
Lipids	8	wt%
Fiber	9.5	wt%
Ash	4.5	wt%

3.2.1.1 Pretreatment and Fermentation

Prior to fermentation, the DGS were treated with a dilute acid to solubilize and hydrolyze the carbohydrates and proteins into their respective building blocks; monomer sugars and amino acids, respectively. The pH was adjusted to 6 using lime (CaO) after pretreatment. Experimental work showed total solubility of the carbohydrates, proteins and lipids to be 90% ± 10%, 70 ± 10% and 100 ± 10% [g soluble after pretreatment per g total], respectively.

A subsequent enzymatic proteolysis pretreatment step was employed to hydrolyze any remaining non-hydrolyzed proteins, proteolipids, or N-glycans. DGS were treated with a cell-free extract of *Streptomyces gresius* (Pronase ®) at a ratio of 1 gram per liter of total slurry. The enzyme was not produced onsite and was assumed to be purchase for \$1.05 kg^{-1}. Experimental works shows the resulting protein solubility increased to 90 ± 10% [g soluble after pretreatment per g total protein].

Products from pretreatment were assumed to be solubilized carbohydrates, proteins and lipids, water and gypsum ($CaSO_4 \cdot 2H_2O$). The DGS ash and gypsum were assumed to be to be inert masses

flowing through the system with no adverse effects on process equipment or yields. These assumptions would need to be verified with further experimentation. Model inputs for the pretreatment model are presented in Table 13.

Table 13: Inputs for the pretreatment model

Pretreatment		
Treatment Times		
Acid Pretreatment	0.75	hours
2nd Acid Pretreatment	6	hours
Neutralization	5	hours
Digestion	16	hours
Fermentation	54	hours
Material Loadings		
Acid Pretreatment	2	% vol vol^{-1}
Enzyme	0.01	g L^{-1}
Yeast	1	% vol vol^{-1}

The fermentation process modeled was based on experimental work done by Liu et al[48]. This process uses an E. coli consortium to ferment hydrolyzed C5 and C6 carbohydrates and proteins (amino acids) into fusel alcohols. Results from experimentation show a utilization of 31% and 90% of the total solubilized proteins and carbohydrates, respectively. Fusel alcohol yields from fermentation were 39 g of fusel alcohols per 100 g of hydrolyzed carbohydrates and amino acids, yielding a total conversion rate of 24 g of fusel alcohols per 100 g of total DGS [48]. Carbohydrate and amino acid profiles for the DGS hydrolysates before and after fermentation is available Appendix B 2 and Appendix B 3, respectively.

For modeling purposes, fermentation products were limited to fusel alcohols, carbon dioxide (CO_2), hydrogen sulfide (H_2S), ammonia (NH_3), and water (H_2O). To predict fermentation product yields, fusel alcohol yields were set using experimental data with all other yields predicted using an elemental mass balance. Hydrogen sulfide and ammonia yields were based on total liberated sulfur and nitrogen, respectively, while carbon dioxide and water yields were based on remaining carbon and hydrogen balances, respectively. Struvite ($NH_4MgPO_4 \cdot 6H_2O$) was shown to be a by-product of side reactions during

this fermentation process [48]. The hypothesized mechanism for struvite production is magnesium in the ash reacts with liberated nitrogen, phosphorous and water. The struvite was assumed to be recovered in a settling tank and sold as an additional co-product. The proposed model assumes these yields can be maintained at scale; this assumption is reasonable as fermentation represents a mature technology in terms of commercial deployment. Inputs for the fermentation model are presented in Table 14.

Table 14: Inputs for the fermentation model

	Fermentation	
Carbohydrate Utilization	90	% of soluble carbs
Protein Utilization	31.3	% of soluble proteins
Fusel Alcohol Yield	24.0	g Fusel Alcohols (100 g biomass) $^{-1}$
Struvite Yield	0.4	g struvite (100 g biomass) $^{-1}$

3.2.1.2 Alcohol Recovery

The purpose of the alcohol recovery step was to separate the fusel alcohols from the water and remaining biomass. Modularity in the engineering process model supported the evaluation of two different alcohol recovery processes; solvent extraction and distillation.

Solvent extraction was employed by experimenters from Sandia National laboratories, who provided inputs and verification for this method. For this process, the fermentation liquor is fed to the bottom of a ten-stage extraction column. Solvent, ethyl acetate, is added at the top of the extraction column at a ratio of 1:5 volume of solvent to volume of fermentation liquor. After solvent extraction, the fusel alcohols and solvent were sent to a distillation column to recover the solvent. Alcohol recovery from this distillation column was set at 99.5% of total alcohols. The system was assumed to have a 5% solvent loss, as validated from experimental results. This solvent loss is typical of solvent extraction systems[11]. Solvent extraction was considered as part of “Base Pathway”, “Integrated Pathway” (discussed in Section 3.2.2 Techno-Economic Analysis) and the “LPC Pathway”.

Distillation represents a robust technology that is currently used for ethanol recovery in corn ethanol refineries and was therefore also investigated for the feasibility of alcohol recovery. Low boiling alcohol recovery was set to 99.5% recovery by mass in the distillate. Some of the fusel alcohols have boiling points higher than water and were assumed to be lost in the column bottoms, as recovery was found to be uneconomical. The distillate from the first column was sent to a second rectification distillation column. Alcohol recovery from the second distillation column was set at 99% by mass. Distillate from the rectification column was then sent to a molecular sieve dryer for polishing for a final mass purity of 99.5% by mass [kg alcohols per kg total mass^{-1}]. Inputs for the two alcohol recovery models are shown in Table 15. Distillation was considered as part of "Distillation Pathway" for the TEA.

Table 15: Inputs for the two alcohol recovery processes; distillation and solvent extraction

Alcohol Recovery		
Distillation		
1st step FA recovery	99.5	% by mass in distillate
2nd step FA recovery	99	% by mass in distillate
Purity after drying	99.9	% by mass
Solvent Extraction		
Solvent Loading	1:5	vol solvent: vol liquor
Product Recovery from extraction column	97	% by mass
Extraction pressure	1	atm
Extraction temperature	25	°C
Product Recovery from distillation column	99.5	% by mass
Distillation pressure	153	Mbar
Distillation temperature	50	°C
Solvent Recovery	95	% by mass
Purity after drying	99.9	% by mass

3.2.1.3 Protein Recovery

The remaining biomass after alcohol recovery was sent to a protein processing step to recover the protein product. Two different protein recovery strategies were investigated to produce two different products; HPC and LPC. Both of these processes were based on commercial whey protein

recovery processes [87,88]. HPC protein recovery was considered as part of "Base Pathway", "Integrated Pathway" and "Distillation Pathway" for the TEA.

For the HPC product, the insoluble fibers and fats were removed using a centrifuge. Proteins were then concentrated using ultrafiltration with diafiltration. Concentration of the solids in the ultrafiltration unit was set to 25%, a common target used in the whey industry [87]. Sugars and some of the ash were removed by diafiltration washing [87]. Operational costs for the ultrafiltration unit were estimated using information from the San Jose Water Company report on Microfiltration Operating Costs and design information from work performed by Hurst et al. [36,88]. After concentrating the proteins, the product was then dried in a spray dryer to reduce water concentration to 4 wt%. Product loss after drying was set at 20% of the total solids [88]. The spray drier pricing was based on cost curves from work compiled by Hardy [92]. To produce the LPC product, the solids were only dried in a spray dryer to produce a product with 4 wt% water. Inputs for the protein recovery model are displayed in Table 16.

Table 16: Inputs for the protein recovery model

	Protein Recovery	
Centrifuge Outlet Concentration	0.19	Kg L^{-1} solids (lipids and insoluble fibers)
Ultrafiltration Solids Concentration	25x	increase
Diafiltration Removal	60/92.5	% by mass of ash/carbohydrates
Purity after drying	96.2	% by mass solids

3.2.2 Techno-Economic Analysis

The mass and energy outputs from the engineering process models were used as the basis for the economic modeling. Capital costs were estimated based on quotes for similar equipment provided in literature and ASPEN modeling unless otherwise noted using Equations [1] and [2][10]. Additional direct and indirect capital costs were found using information provided in Table 5. Operational costs were estimated based on the energy and mass requirements of the systems combined with cost inputs shown in Table 17.

Table 17: Utility and consumable material costs and co-products selling prices used in the TEA

Model Inputs		
Utility Costs		
Electricity	0.067	$ kWh^{-1} [58]
Natural Gas	5.13	$ $(1000\ scf)^{-1}$ [59]
Feed Unit Costs		
Biomass	60	$ mt^{-1} [91]
Acid	110	$ mt^{-1} [10]
Base	244	$ mt^{-1} [10]
E. coli	50	$ mt^{-1} [60]
Protease	1050	$ mt^{-1} [60]
Solvent	1129	$ mt^{-1}
Co-product Selling Prices		
Fusel Alcohols	3	$ GGE^{-1}
Struvite	455	$ mt^{-1}

For this analysis, the system boundary was drawn around the DGS upgrade facility. This required the facility to have its own independent utilities equipment, storage, office, laboratories and management staff assuming the facility would receive no utilities from the co-located ethanol refinery. All capital equipment was assumed to be purchased new, instead of repurposed or retrofitted. Drawing the system boundary in this way allowed for a clear examination of the costs and benefits accompanying the integration of the upgrade process with existing facilities.

An additional "Integrated" scenario was also considered, where some equipment, infrastructure and personnel are shared between the new facility and existing ethanol facility. This case is not used to evaluate the optimal processing option, but is included to understand the potential economic effects of process integration. Specifically, this scenario leverages the existing drying equipment at the ethanol facility that is currently being used to dry the DGS, reducing capital equipment costs for the protein recovery section and some of the existing home office and utilities. For some utilities, such as compressed air and fire water equipment, the requirement was eliminated for the upgrade facility as the existing equipment should be sufficient. For other equipment, such as boiler, wastewater treatment

and cooling towers, a 50% reduction in capital and operational costs was assumed for the upgrade facility, as there should be some retrofitting or efficiency improvements that can reduce the load required for new equipment and chemicals (e.g. wastewater treatment chemicals). Some personnel requirements were also reduced; 50% reduction for managerial roles, and 20-25% reduction for non-managerial roles. A summary of these changes between the Base Pathway and Integrated Scenario are presented in Table 18.

Table 18: Summary of Input changes for the Integrated Scenario

INPUTS		
CAPEX		
Driers	100	% reduction
Centrifuge	100	% reduction
Home Office	50	% reduction
Wastewater Treatment	50	% reduction
Compressed Air	100	% reduction
Fire Water	100	% reduction
Cooling Towers	50	% reduction
Boilers	50	% reduction
OPEX		
Manager	50	% reduction
Engineers	25	% reduction
Non-managerial labor	20	% reduction
Utilities Treatments	50	% reduction

The TEA used a DCFROR model to estimate the minimum protein selling price (MPSP) required for one kg of upgraded protein product [54]. The DCFROR solves for the minimum selling price of protein necessary to recover all costs over the full operating lifetime of the upgrade facility. The MPSP is of interest for understanding a bare minimum break-even revenue price but does not speak to potential profitability of product streams. The DCFROR model used *N-th* plant assumptions, as outlined by BETO, Appendix A 1 [10,11,54].

Co-products sold from the upgrade facility include the fusel alcohol energy products and struvite. The selling price for the energy products was set at $0.79 per liter of gasoline equivalent

(LGE)$^{-1}$, the target price for energy products set by the DOE[93]. An LGE is defined as the amount of fuel required to provide as much energy as a liter of traditional petroleum-based gasoline; 31.7 MJ L^{-1}. The struvite co-product selling price was set at \$455 mt^{-1} [94,95]. These two co-products represented additional income for the biorefinery.

3.2.2.1 First of a Kind TEA

Preliminary results indicated that the DGS upgrade process may be a viable candidate for commercialization using *N*-th plant economic assumptions. Therefore, a FOAK analysis was also conducted for the Base Pathway to understand near-term economics. For a FOAK facility, capital and operational costs are typically higher than those for a mature technology, Figure 1, and therefore MPSP for FOAK will need to be higher to recover the additional costs. The methodology used herein to estimate the MPSP for the FOAK facility was proposed by the RAND corporation [20]. In this method, capital equipment costs are in inflated using a Cost Growth factor. The equation for the Cost Growth Factor is shown in Equation [3][20]. Operational costs and production are also affected by the technology immaturity and depressed for the first five years of production. This depression in production is estimated using the plant performance metric, Equation [4] [20]. Complete definitions for the equation variables are available in Appendix B 4, with the values used in the analysis presented in Table 19.

$$Cost\ Growth = 1.1219 - 0.00297 \times PCTNEW - 0.02125 \times IMPURITIES - 0.01337 \times COMPLEXITY + 0.00111 \times INCLUSIVENESS - 0.06351 \times PROJECTDEFINITION \quad [3]$$

$$Plant\ Performance = 85.77 - 9.69 \times NEWSTEPS + 0.33 \times BALEQS - 4.12 \times WASTE - 17.91 \times SOLIDS \quad [4]$$

Table 19: Values for variables associated with Equations [3] and [4].

Variable	Value
PCTNEW	27% (47% for LPC pathway)
IMPURITIES	3.5
COMPLEXITY	8 (7 for LPC pathway)
INCLUSIVENESS	33%
PROJECT DEFINITION	2
NEWSTEPS	3 (2 for LPC pathway)
BALEQS	0
WASTE	4
SOLIDS	1

Once the total Cost Growth Factor was calculated, the total capital investment for the FOAK plant (TCI_{FOAK}) could be estimated using from the total capital investment for the *"N-th* plant" in Equation [5] [20]. The Plant Performance factor can then be used to estimate the revenue and costs for the first five years based on the *"N*-th plant" revenue and costs using Equation [6] [20]. These values were then used in the DCFROR analysis to find the MPSP.

$$TCI_{FOAK} = \frac{TCI_{nth}}{Cost\ Growth} \quad [5]$$

$$Cost_{FOAK}(t) = Cost_{nth}(t) \times \frac{(Plant\ Perfomance + 20 \times (t-1))}{100} \quad [6]$$

3.2.3 Protein Market Analysis

To correctly determine economic viability and relative environmental impact, it was necessary to understand the potential protein markets for the high value protein. Protein markets were determined based on two factors; protein digestibility-corrected amino acid score (PDCAAS) and protein content. The PDCAAS is a method for determining the quality of protein and is currently used by both the United States Federal Department of Agriculture and the World Health Organization [96]. This method works by comparing the amount of each essential amino acid with a reference, in this case the amount of that amino acid required for a preschool aged child, Table 20 [96].

Table 20: Table of essential amino acids and the amounts required for a school-aged human child [96]

Amino Acid	Requirement [mg (g crude protein)$^{-1}$]
Isoleucine	28
Leucine	66
Lysine	58
Total Sulfur Amino Acids (Methionine + Cystine)	25
Total Aromatic Amino Acids (Phenylalanine + Tyrosine)	63
Threonine	34
Tryptophan	11
Valine	34
Total	320

The PDCAAS can then be calculated using Equation [7], with scores of greater than 100% truncated to 100% [96]. The overall score given to a specific protein product is based on the limiting amino acid; for example, a protein such as gelatin which contains no tryptophan would receive a score of 0. The highest PDCAAS score is 100, indicating that the protein contains all of the essential amino acids in sufficient amounts over the required amount. An example of a protein with a PDCAAS score of 100 is beef or whey protein.

$$PDCAAS\ [\%] = \frac{mg\ of\ limiting\ amino\ acid\ if\ 1\ g\ of\ test\ protein}{mg\ of\ same\ amino\ acid\ in\ 1\ g\ of\ reference\ protein} \times fecal\ digestibility\ [\%] \qquad [7]$$

For this analysis, the true ileal digestibility of DGS was used instead of the true fecal digestibility, when possible, as there is evidence that this is the better correction factor for determining the quality of the protein [96]. As neither the HPC or LPC products have been tested to determine their digestibility, these percentages were estimated from digestibility of DGS in pigs and cows [85,97]. Cow digestibility was chosen to predict how the upgraded DGS would behave in ruminants, while pigs were chosen to represent monogastric animals. Crude protein digestibility in cows was estimated to be 72%, while ileal digestibility for the different amino acids was found to range between 84 – 95% in pigs [85,97]. While these digestibility scores do not encompass all available protein markets, such as human consumption, they at

least provide some insight. The PDCAAS scores and protein content for the upgraded protein products were 33 for monogastric animals (pigs), 28 for ruminants (cows) and 84% protein by weight for the Base Pathway (HPC protein) and were 30 for monogastric animals (pigs), 28 for ruminants (cows) and 66% protein by weight for the LPC Pathway. The PCDAAS score calculation is shown in Appendix B 5.

To determine which markets the HPC and LPC products would target, protein content and PDCAAS scores for different types of products were assembled, including DGS, soybean meal, corn gluten meal, fish meal, poultry by-product (feather) meal and whey protein. Pricing for the different protein products were based on commodities markets as reported by the United States Department of Agriculture [91]. PDCAAS scores were taken from literature for soy and whey protein [98]. The PDCAAS score for corn gluten, DGS, fish meal and feather meal were calculated based on the amino acid compositions and digestibility as reported in literature [85,99–101]. A complete list of PDCAAS, protein content and commodities pricing for all reference proteins are shown in Appendix B 6.

3.2.4 Life Cycle Assessment

LCA was used to determine the GHG emissions associated with the production of different products; the protein products and energy products (fusel alcohols or ethanol and fusel alcohols). The system boundary was drawn to incorporate all aspects of production from biomass growth to end use, or a well-to-wheels system boundary. A Baseline case was conducted first by expanding the system boundary to include agriculture and ethanol refining and using a displacement method for the co-products per ISO guidelines[21]. However, as this method may not always be feasible for the process under review, since upstream processes may not be as well defined or information as widely and readily available as for corn ethanol production used here. Therefore, a contracted system boundary around the upgrade facility was also considered to understand how different LCA methodologies affect LCA results.

3.2.4.1 Expanded Boundary

The first LCA case considered an expanded system boundary which included upstream agriculture and ethanol production, Figure 20. The total emissions rate for the ethanol production facility and agriculture were estimated through values found in literature. The reported range was 1734 - 2134 g $CO_{2\text{-eq}}$ (L ethanol)$^{-1}$ with an average value of 1974 g $CO_{2\text{-eq}}$ (L ethanol)$^{-1}$ used in this study [69,86,102–104]. Total emissions for the 454 M liter ethanol refinery totaled 897 Gg $CO_{2\text{-eq}}$ year^{-1}.

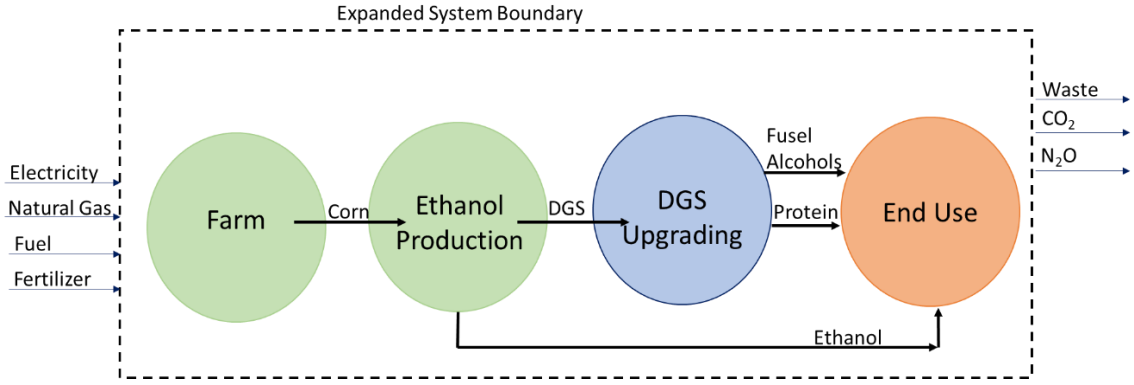

Figure 20: The expanded system boundary for the LCA. This analysis expanded the system boundary from around the DGS Upgrading facility to include the upstream farm and corn-ethanol facility.

The total emissions for the upgrade facility modeled in this study were calculated using the mass and energy balances from the engineering process model. Estimates for the emissions associated with energy production and manufacture of chemicals were taken from GREET [69]. To calculate the total GWP for each component, three different GHG's were examined (CO_2, CH_4 and N_2O) and combined into a CO_2-equivalance ($CO_{2\text{-eq}}$) based on their 100-year global warming potential (1, 28, 265 [g $CO_{2\text{-eq}}$ (g GHG)$^{-1}$], respectively) and summed to provide a total life cycle inventory (LCI) emissions [70]. These LCI's were then multiplied by the upgrade facility's total consumption of various materials and energies to find the total estimated emissions. A list of the LCI's used in presented in Table 21.

Table 21: List of LCI data used in the LCA analysis for the DGS upgrading facility. Co-product credits were given for displacing DAP with struvite on a per kg phosphorus basis, gasoline with fusel alcohols on a per energy basis and corn gluten meal with HCP on a per kg of protein basis. Data was obtained from GREET unless otherwise stated.

LCA INPUTS		
Life Cycle Inventory Values		
Electricity	0.55	kg $CO_{2\text{-eq}}$ kWh^{-1}
Natural Gas	14.59	kg $CO_{2\text{-eq}}$ $MMBTU^{-1}$
Acid	49	g $CO_{2\text{-eq}}$ kg $acid^{-1}$
Base	1294	g $CO_{2\text{-eq}}$ kg $base^{-1}$
Enzyme	2680	g $CO_{2\text{-eq}}$ kg $enzyme^{-1}$
Solvent	4651	g $CO_{2\text{-eq}}$ kg $solvent^{-1}$
DAP	1261	g $CO_{2\text{-eq}}$ kg DAP^{-1}
Gasoline	92	g $CO_{2\text{-eq}}$ MJ $Fuel^{-1}$
Corn Gluten Meal[104]	640	g $CO_{2\text{-eq}}$ kg corn gluten $meal^{-1}$
Aquaculture[105]	265	g $CO_{2\text{-eq}}$ kg $aquaculture^{-1}$
Soybean Meal[106]	820	g $CO_{2\text{-eq}}$ kg soybean $meal^{-1}$
Beef[107]	13,000	g $CO_{2\text{-eq}}$ kg $beef^{-1}$

Next, a displacement method was used to reduce the overall emissions. To employ the ISO 14044 standard displacement method requires LCA results to be generated assuming the system is first a protein production facility. Then the LCA results are generated assuming the system is a fuel production system, with displacement credits calculated for the complementary product. For both cases, struvite was assumed to displace diammonium phosphate (DAP) on a per kg of phosphorous basis. The protein products were assumed to displace corn gluten meal which has a similar PDCAAS score (26) and protein content (60 wt%) as the HPC protein (PDCAAS score of 28 or 33 and protein content of 84 wt%). The fusel alcohol and ethanol products were assumed to be a drop-in replacement for petroleum gasoline, and displaced gasoline on an energy basis. Displacement credits could be calculated using Equations [8]-[10].

$$DAP_{credit} = DAP\ Displaced\left[\frac{kg\ DAP}{year}\right] \times LCI_{DAP}\left[\frac{kg_{CO2-eq}}{kg\ DAP}\right] \quad [8]$$

$$Protein_{credit} = Protein\ Displaced\left[\frac{kg\ protein}{year}\right] \times LCI_{protein}\left[\frac{kg_{CO2-eq}}{kg\ p}\right] \quad [9]$$

$$Energy_{credit} = Gasoline\ Displaced \left[\frac{GGE}{year}\right] \times LCI_{gasoline}\left[\frac{kg_{CO2-eq}}{GGE}\right] \quad [10]$$

The total emissions could then be calculated using Equation [11]. This example equation assumes the primary product was protein and displacement credits could be assumed for the fertilizer (struvite) and energy (fusel alcohol and/or ethanol) products. If a different product was assumed to be the primary product, credits would be taken for the remaining products. The total emissions were then assigned solely to the primary product.

$$Total\ Emissions \left[\frac{kg\ CO_{2-eq}}{year}\right] = Ethanol\ Production\ Emissions + DGS\ Upgrade\ Emissions - DAP_{credit} - Energy_{credit} \quad [11]$$

3.2.4.2 Contracted Boundary

A contracted boundary was also considered with the system boundary drawn around the DGS upgrade system and product end use. There are two complications associated with conducting the LCA in this way; the first is determining the emissions associated with the DGS production and the second assigning emissions to the upgrade products as an equal mass of each are produced.

Quantifying the emissions associated with the DGS production required assigning some burden of the upstream ethanol production emissions to the DGS. In a standard ethanol LCA, a displacement method is used for the DGS product which does not allow for direct quantification of the emissions associated with DGS. Flipping the script and using a displacement method with the DGS as the primary product represents a misguided attempt to determine the emissions that should be allocated to this product stream. To address this issue, this work allocated the ethanol facility and agriculture emissions to the DGS through either an energy or market allocation method, Figure 21, discussed further below.

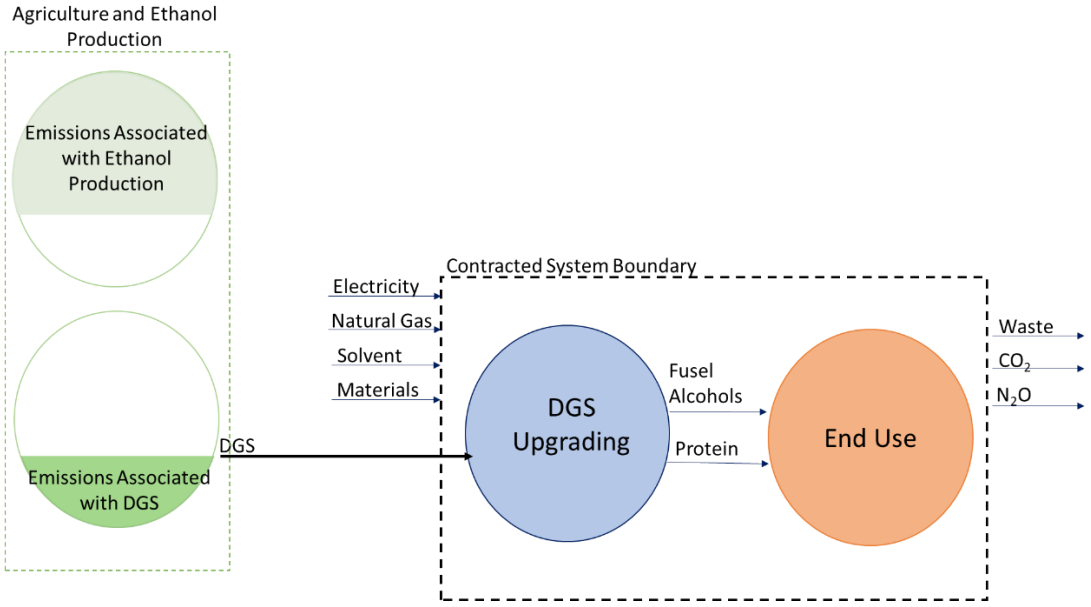

Figure 21: The contracted system boundary for the LCA with the system boundary drawn around the DGS Upgrading facility and product end use. Emissions associated with DGS production were assigned from the upstream ethanol facility through either energy or market allocation methods.

The second complication in this LCA is associated with determining which LCA co-product methodology is appropriate to distribute the upgrade facility emissions between the two main products; displacement, energy allocation and market allocation. In total, six different life cycle scenarios were performed for the contracted system boundary by using displacement, energy and market allocation for two different DGS emissions scenarios, Figure 22.

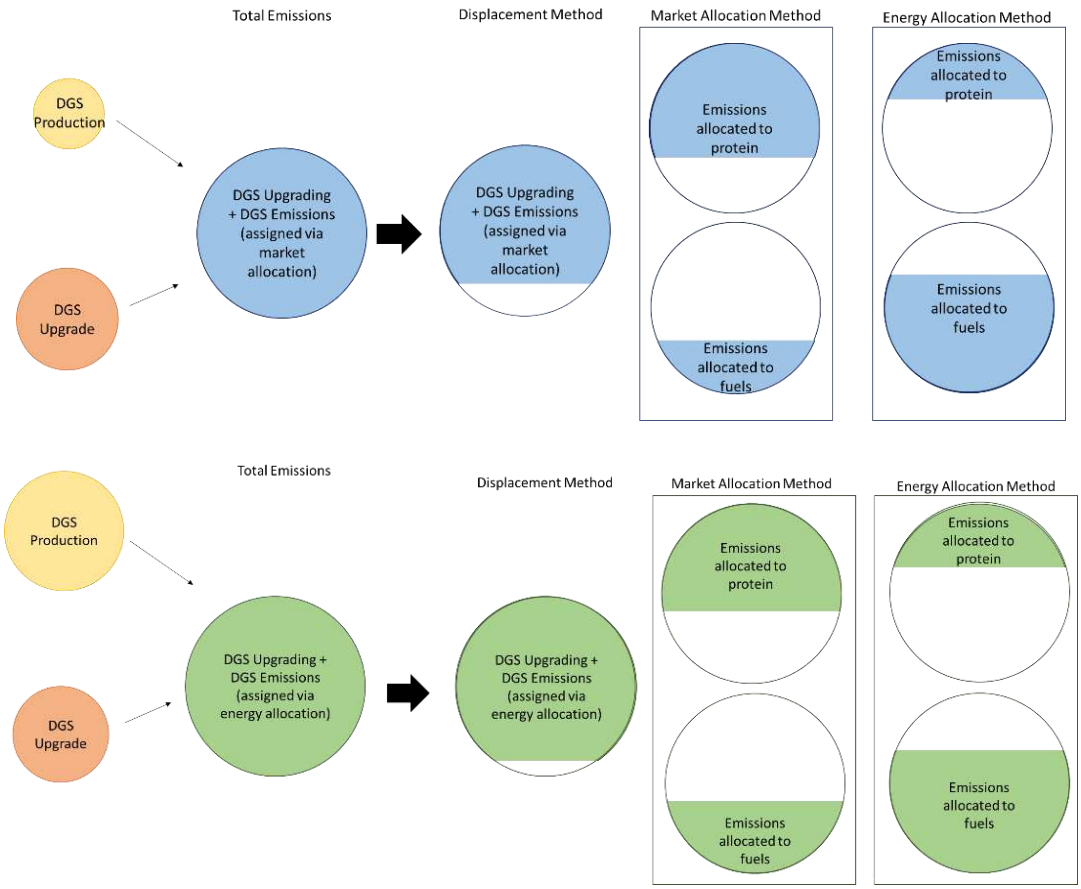

Figure 22: A diagram of all six LCA scenarios. First, DGS related emissions were allocated from the upstream ethanol facility using either market or energy allocation methods. DGS production had a higher emissions burden when using the energy allocation method for the ethanol refinery. Next, total emissions from the DGS Upgrade facility were calculated. Finally, emissions were assigned to the different products from the DGS upgrade facility using either displacement, market allocation or energy allocation methodology.

In the energy allocation method, emissions were allocated based on the energy content of each product. For the energy products, ethanol and fusel alcohols, the energy content was based on the calorific energy values for those products. The metabolic energy was then calculated for the protein product based on its composition of protein, carbohydrates and fats and the associated energy for these constituents; 17 kJ g^{-1} for protein, 16 kJ g^{-1} for carbohydrates and 37 kJ g^{-1} for fats, respectively [108]. An example to find the allocation percentage based on the energy allocation method for fusel alcohols is shown in Equation [12]. Similar logic is followed to find the allocation percentages for the remaining products.

$$\%Fusel\ Alcohols_{energy} = \frac{FA \times ED_{FA}}{[(FA \times ED_{FA}) + (Protein \times ED_{protein})]} \quad [12]$$

Where *FA* is the amount of fusels alcohol produced [kg year^{-1}], ED_{FA} is the energy content of the fusel alcohols [kJ kg^{-1}], *Protein* is the amount of protein produced [kg year^{-1}], and $ED_{Protein}$ is the energy content of the protein [kJ kg^{-1}].

Market allocation was based on the market value for the different products. An example of the percent allocation based on the market method for fusel alcohols is shown in Equation [13] with similar logic employed for the other products.

$$\%Fusel\ Alcohols_{market} = \frac{FA \times Price_{FA}}{[(FA \times Price_{FA}) + +(Protein \times Price_{protein}) + (Struvite \times Price_{struvite})]} \quad [13]$$

Where $Price_{xx}$ is the current market price for the different products [$ kg^{-1}], with $Price_{protein}$ being determined by the MPSP, and *Struvite* is the struvite production [kg year^{-1}].

Results showing the distribution of emissions from the different allocation methods are shown in Table 22.

Table 22: Table of allocation percentages for different upgrade products from the upgrade facility

Products	**Market Allocation**		**Energy Allocation**	
	Price, $ kg^{-1}	Allocation	kJ kg^{-1}	Allocation
Fusel Alcohols	$ 0.98	38%	33159	72%
Feed	$ 1.91	62%	15747	28%
Struvite	$ 0.55	0%	0	0%

The results from the different LCA methodology scenarios were then compared to illustrate the impact of system boundary and allocation criteria on LCA results. The emissions results were also compared to emissions of traditional products to evaluate the technological performance of the DGS

upgrading process. The HPC protein product was compared to traditional protein while energy products were compared to the Renewable Fuel Standard (RFS) goals.

3.2.5 Sensitivity Analysis

A sensitivity analysis was performed to identify high impact areas for further research in the areas of cost and emissions reductions. For this analysis model inputs were varied ± 20% and the resulting change with respect to MPSP. The results were then used in a Student's t-test to determine the t-ratio values for the different variable as the outputs, with ratios t-ratios falling outside the two-tail 95% confidence interval indicating high impact areas.

3.3 Results and Discussion

3.3.1 Techno-Economic Analysis

The TEA results for the different cases are shown in Figure 23 with results broken out for the individual cost components and summed into three main cost categories; capital expenditure (CAPEX), operational costs (OPEX) and taxes. The MPSP was found to be \$1.91 kg-protein^{-1} for the Base Pathway, \$1.94 kg-protein^{-1} for the Distillation Pathway, \$2.48 kg-protein^{-1} for the LPC Pathway and \$1.65 kg-protein^{-1} for the Integrated scenario. Current markets show protein selling prices between \$0.35 - \$2.11 kg^{-1} dependent on protein quality and market opportunity (feed versus food). While comparing the MPSP to market prices for other proteins may not be an absolute indicator of economic viability, it at least provides some insight to the potential viability of the system. In general, there are price differences between minimum selling prices required to cover production costs and actual market selling prices. Market selling prices typically include other related costs (i.e. supply chain, marketing, profit, etc.) which are not included in this TEA. A list of proteins including quality and selling price is located

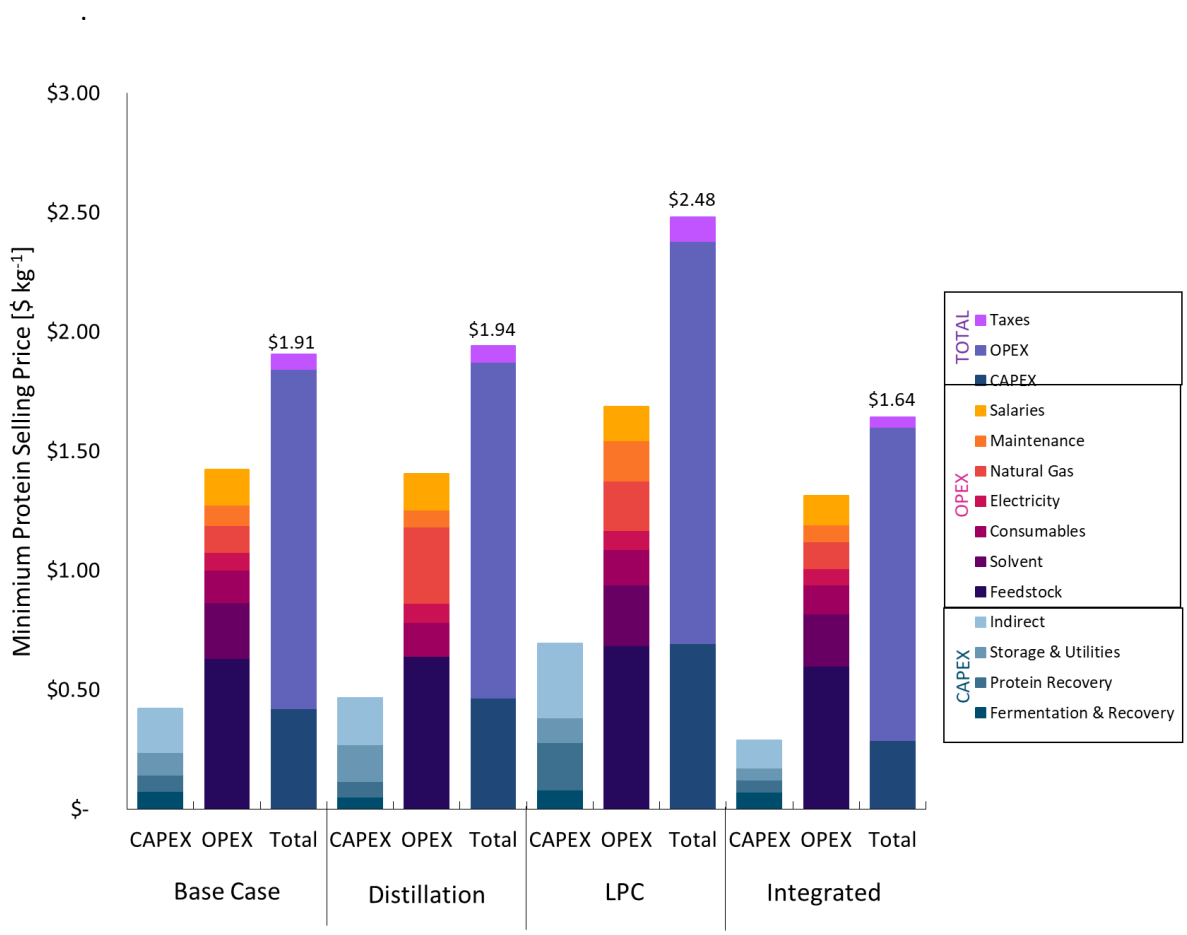

Figure 23: Breakdown of the major economic contributors as a fraction of the MPSP for the three processing pathways and Integrated scenario modeled using "N-th of a kind" assumptions. CAPEX and OPEX were further broken down into their major constituents. Each facility is sized to utilize 982 mt of DGS per day.

The largest cost contributor for the Base Pathway is the operational costs, accounting for 74% of the total MPSP. The greatest cost within OPEX comes from procurement of the feedstock, accounting for 46% of the total annual OPEX and 35% of the total MPSP. A similar trend is seen in the Distillation Pathway and LPC Pathway, with the feedstock accounting for 46% or 42% of the total annual OPEX and 33% or 28% of the total MPSP, for each case respectively. This mimics trends seen in biorefinery TEA's in general; where feedstock represents the largest cost burden. In traditional biofuels processes, feedstock has been shown to represent over 70% of the total MFSP for corn based ethanol, soybean based biodiesel, and sugarcane based ethanol [109]. Similarly, in algal based systems, the feedstock

procurement dominates operational costs [110]. One advantage of this upgrade system is that the feedstock is a waste stream instead of virgin crop, allowing for reduced procurement costs and increased utilization of the original feedstock.

Results were used to identify the optimal processing pathway. TEA indicates the Base Pathway to be the most economically favorable option as it reduces capital and operational cost while maximizing alcohol recovery by employing the optimal alcohol and protein recovery strategies. Additionally, the Base Pathway includes opportunities for process improvement. While distillation is a proven technology for ethanol production systems, the presence of high boilers and higher water content in alcohol-water azeotropic mixtures leads to higher energy requirements making this strategy less feasible for this application. Alcohol recovery is maximized through solvent extraction, as high boilers are not lost leading to higher fuel yields, 78.4 M LGE $year^{-1}$ for solvent recovery compared to 76.5 M LGE $year^{-1}$ for distillation. There is also an opportunity for process improvement by increasing solvent recovery efficiency to reduce make up solvent costs. Optimization of solvent recovery considers the benefit of reduced solvent make-up costs versus the cost of increased recovery in the distillation column. The optimal solvent recovery rate is 98.5%. This optimal rate reduces MPSP by 12% from the original test case to \$1.69 kg-$protein^{-1}$. In addition, solvent extraction reduces the extent of residual alcohols in the protein product. This added benefit was not directly quantifiable in this work but must be considered holistically. These considerations lead to solvent extraction being the optimal choice for alcohol recovery in terms of economic viability.

The Base Pathway was also considered for the Integrated Scenario. By considering this integration with the existing facility, the MPSP is reduced to \$1.65 kg-$protein^{-1}$. Significant savings are seen by reducing protein recovery costs by utilizing existing drying and utilities equipment. These savings also led to reduced indirect capital costs, which are calculated as a percentage of total capital

costs. Similar optimization of the solvent system further reduces the MPSP to $1.42 kg-protein^{-1}. This scenario shows a more optimistic outlook for the process, if these assumptions can be realized.

The TEA also shows the HPC pathway is more economical than the LPC Pathway for protein recovery, with the MPSP for the Base Pathway being 23% lower than the LPC Pathway. While the HPC contains more pieces of processing equipment, e.g. protein concentration equipment, one of the system benefits of this step is bulk water removal. By not removing the water prior to drying in the LPC pathway, the dryers had to be sized to evaporate 4.7 times higher volumes of water, or 29,000 kg hr^{-1} for the Base Pathway compared to 135,000 kg hr^{-1} for the LPC Pathway. This difference in evaporation requirements causes a significant disparity between the two processing pathways with the CAPEX for the LPC pathway 51% higher and the OPEX is 9% more than the Base Pathway. Increased water to the driers also increased the heat energy requirement for this step, which more than offset any potential labor or electricity energy savings that may have been realized by making the process less complicated. These results indicate that a bulk water removal stage may be required for the LPC to reduce the CAPEX and OPEX; or indicates the requirement to integrate with the existing ethanol facilities' drying equipment to negate this cost as shown in the Integrated Scenario.

FOAK analysis performed on the Base Pathway scenario increased the MPSP from $1.91 kg-protein^{-1} to $2.19 kg-protein^{-1}, with a breakdown of the main cost contributors shown in Figure 24. This increase was driven by two changes. First, capital costs for the FOAK facility are 116% higher than for the *N*-th plant facility. In addition, by depressing production in years 1-5, a higher MPSP was required over the lifetime facility to make up for these losses. The higher MPSP also increased the amount of taxes paid over the 30 years, with the NPV of taxes paid increasing by 50% over the *N*-th plant facility.

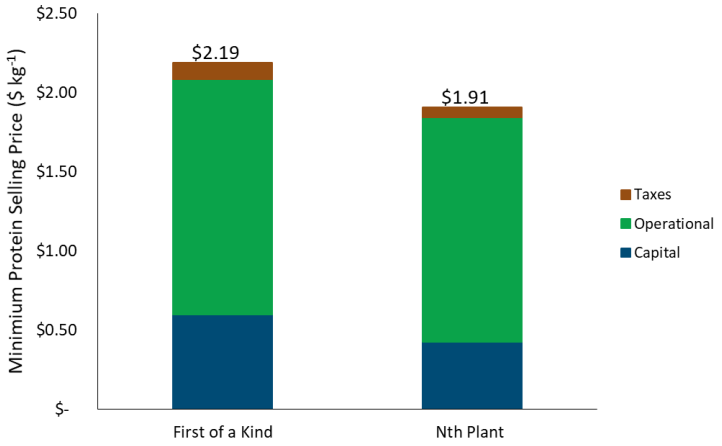

Figure 24: Breakdown of the major cost contributors for the FOAK and N-*th plant facility for the Base Pathway.*

Protein market analysis, Appendix B 6, shows that the HPC was most similar to either corn gluten meal or fish meal, with PDCAAS of 33/28 for the HPC, 26 for corn gluten meal and 38 for fish meal and protein content of 84 wt% for the HPC and 60 wt% for corn gluten meal and fish meal. While corn gluten meal and fish meal have similar protein content and PDCAAS's, the selling prices have wide variability; \$0.55 kg-protein^{-1} for corn gluten meal and \$1.45 kg-protein^{-1} for fish meal. These results indicate that protein content and PDCAAS only make up part of a protein's value. In addition, the PDCAAS is based off requirements for human children and may not be the most appropriate standard when assessing proteins for feed applications. However, TEA and protein market analysis suggest that this DGS upgrade process may be considered as a value-add proposition for ethanol refiners if the protein could be sold in high value markets such as aquaculture, especially as the technology matures and process optimization is integrated. FOAK analysis reinforces the need to target high value protein markets and improve process performance before moving to commercialization.

3.3.2 Life Cycle Assessment

In addition to the economic analyses performed, LCA was completed to estimate emissions associated with the production of the HPC protein product and fusel alcohols. Total emissions for the Base Pathway (solvent recovery and HPC protein recovery) are 200 Gg $CO_{2\text{-eq}}$ year^{-1}. When translated to

emissions burdens per product for the expanded system boundary for the emissions are -0.3 kg $CO_{2\text{-eq}}$ kg-protein^{-1} and 95 g $CO_{2\text{-eq}}$ MJ fuel^{-1} for the protein and fuels products, respectively. When considering the contracted system boundary around the upgrade facility, six different cases were identified for each product, with protein related emissions ranging between 0.5 and 5.6 kg $CO_{2\text{-eq}}$ kg-protein^{-1}, while fuel production related emissions ranged between 42 and 210 g $CO_{2\text{-eq}}$ MJ fuel^{-1}. The breakdown of the associated emissions for the different products, protein and fusel alcohol, for the six cases using the different methods are shown in Figure 25A and B, respectively.

A)

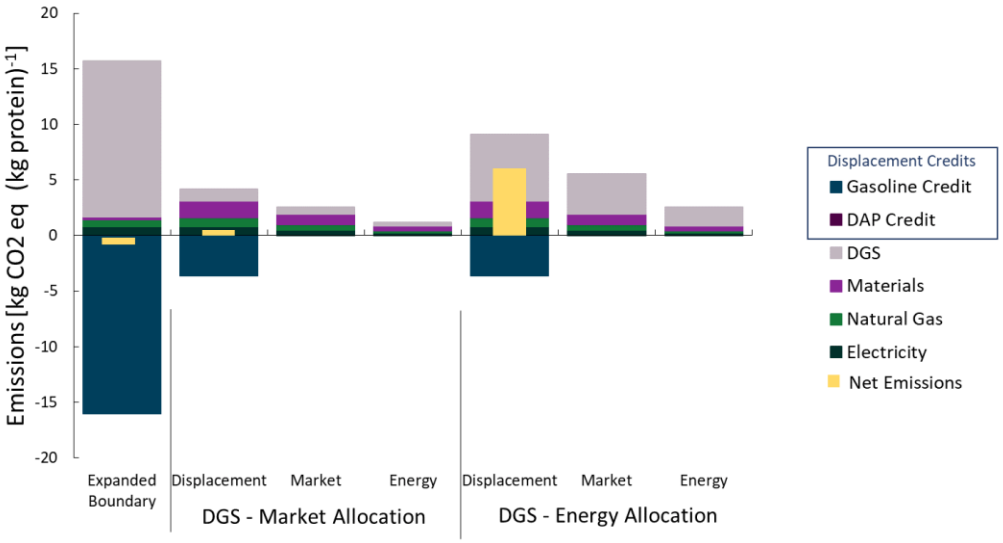

B)

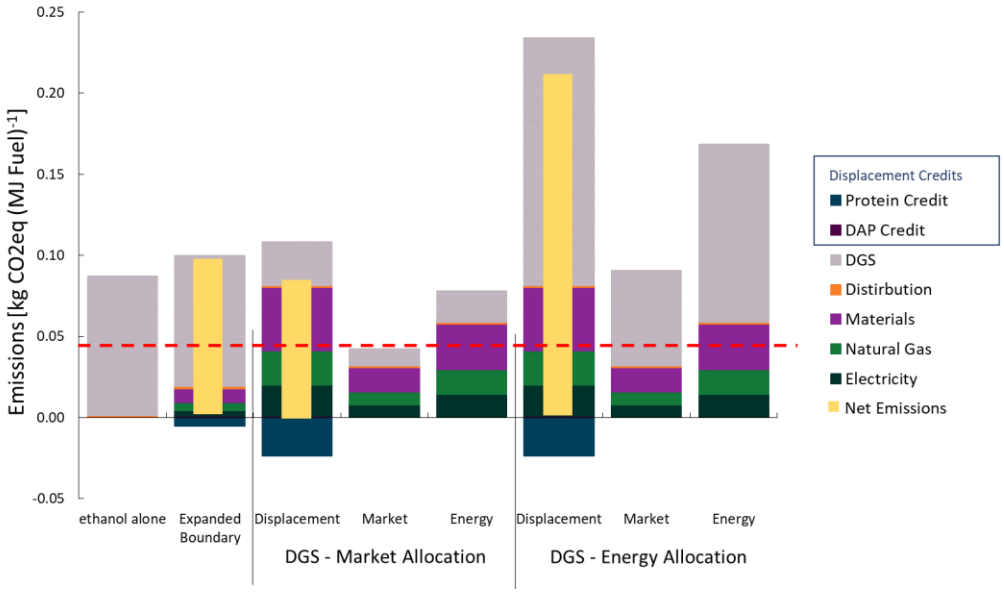

Figure 25 A) Protein-related emissions per kg-protein produced and B) fuels-related emissions per MJ fuel, for a WTW system boundary as calculated using different LCA methodologies; displacement, market allocation and energy allocation. Emissions associated with the production of the DGS feedstock were calculated using either energy or market allocation methods. The results presented are based on the Base Pathway. The red dashed line in Figure B represents the RFS goal.

One of the largest impacts on emissions is associated with DGS production, especially when considering the variance associated with the different allocation methods. When using the energy

allocation method, the DGS production accounts for more emissions than the entire upgrading facility. This highlights how emission intensive the upstream processing is and reinforces the importance of choosing the correct LCA methodology, especially when considering a complex supply chain.

Apart from emissions from DGS production, the largest contributor to the upgrading process emissions are consumable materials, accounting for 47% of the upgrade emissions with solvent production the largest contributor. Increasing the solvent recovery rate from 95% to 96% reduces solvent related emissions by 20% but increased heating emissions by 0.5%. Overall, upgrade emissions are reduced by 3%. As described in the TEA results, the economic optimum solvent recovery rate was 98.5%. At this optimum, the total emissions for the upgrading facility are reduced by 22% to 157 Gg $CO_{2\text{-}eq}$ $year^{-1}$. When looked at from a specific product's emissions, protein related emissions are reduced to -0.3 - 5.1 kg $CO_{2\text{-}eq}$ kg-$protein^{-1}$ and fuel related emissions are reduced to 36 - 193 g $CO_{2\text{-}eq}$ MJ $fuel^{-1}$.

3.3.3 Effects of LCA Co-product Methodology

As described in the LCA methods, two different system boundaries were considered; an expanded system boundary including all upstream processes and a contracted system boundary around the upgrade facility. Both system boundaries have a fixed end point which includes end of life for the products. For the contracted boundary, three different LCA co-product allocation methods were used to determine the emissions related to each product, protein or fuels. Sensitivity to LCA methodology is explored by investigating the effects the of system boundary and methodology strategy on product emissions. Discussed here are the results of each analysis and a comparison of these results across different scenarios.

As seen in Figure 25, both product LCA's were sensitive to system boundary, especially the protein product. In the expanded boundary scenario, even though all of emissions are assigned to the protein product, there are substantial displacement credits for the energy products leading to a negative emissions value for the protein. While this result may be positive for the process LCA, foundational

methodology may be flawed. Protein production is not the impetus for the ethanol production implying that the expanded system boundary is not appropriate for considering protein production related emissions. Care must be taken by LCA practitioners when considering scope and system boundary. For the fuels related pathway, this expanded system boundary was more applicable, as the intent of all processing steps, agriculture through fusel alcohol production, revolve around energy production. In this analysis, we see some increased emissions over the ethanol-alone process due to increased processing, with results of 88 g $CO_{2\text{-eq}}$ MJ $fuel^{-1}$ for ethanol-alone compared to 95 g $CO_{2\text{-eq}}$ MJ $fuel^{-1}$ for the Base pathway. This change in emissions per MJ fuel is due reduced fuels production per GHG emissions in the upgrade facility. In the Base pathway, production related emissions increased by 40%, while fuels production only increased by 29% indicating that the emissions per MJ should increase. Reducing upgrade emissions or increasing fuels production would improve GHG's per MJ fuel.

The LCA's were especially sensitive around the assignment of DGS related emissions, with uniformly higher LCA results seen using the DGS energy allocation method. Table 23 shows the emissions associated with ethanol and DGS production using the two different allocation methods. Using the energy allocation method, approximately 42% of the upfront agriculture and ethanol refining emissions are assigned to the DGS product, creating a significant emissions burden for producing DGS. Using this method may be biasing the LCA results and the underlying logic for employing it may be flawed. The purpose of the upfront processing is to create ethanol, with a DGS as a co-product, and therefore not of equal value to the processor. Therefore, the more appropriate allocation method for the DGS is the market allocation as it better represents the reality of DGS production and intent of the ethanol production process.

Table 23: Table of emissions allocations for ethanol and DGS production. Values shown correspond to a 454M liter ethanol refinery.

	Market Allocation			Energy Allocation		
Products	Price [$ kg^{-1}]	Allocation	GHG Emissions [Gg CO2 $year^{-1}$]	Energy content [kJ kg^{-1}]	Allocation	GHG Emissions [Gg CO2 $year^{-1}$]
Ethanol	$0.75	93%	830	29700	58%	516
DGS	$0.07	7%	66	23560	42%	380

The results were also highly susceptible to co-product displacement credits. For this work, the protein displacement credit was calculated assuming the displacement of corn gluten meal, a protein with relatively low emissions. However, if there is an opportunity to displace a more emissions intensive protein, the value of this credit would increase in terms of LCA emissions. Results could change to be more favorable if the protein displacement credit was increased by choosing to displace a more energy intensive protein. An example of this can be seen in Figure 26. This variable represents a large uncertainty due to its dependence on the type of protein being displaced and highlights the importance of identifying the correct protein displacement markets and displacement ratios when applying this method.

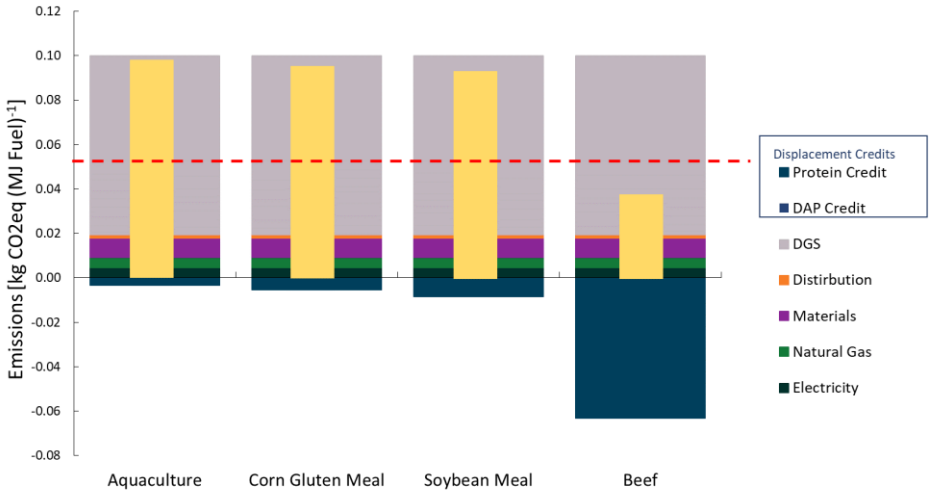

Figure 26: Emissions per MJ fuel when HPC protein is used to displace different proteins. This analysis considered an expanded system boundary and used a displacement method. HPC was assumed to displace either aquaculture, corn gluten meal, soybean meal or beef. Each protein had a different LCI; 0.265 kg $CO_{2\text{-}eq}$ (kg aquaculture)$^{-1}$, 0.64 kg $CO_{2\text{-}eq}$ (kg corn gluten meal)$^{-1}$, 0.82 kg $CO_{2\text{-}eq}$ (kg soybean meal)$^{-1}$, and 13 kg $CO_{2\text{-}eq}$ (kg beef)$^{-1}$. The red dashed line represents the RFS goal for renewable fuels.

To reduce the uncertainty associated with protein markets and displacement credits, co-product allocation methods can be used. These methods, however, bring their own complications. For instance, market allocation uses the current MPSP to allocate emissions within the DGS upgrade facility. But the MPSP does not necessarily represent the market value of the HPC protein. Deviation from the MPSP impacts LCA results when using the market allocation method as shown in Figure 27. As the protein selling price increases, the protein takes a larger share of the process emissions and emissions related to fusel alcohol production are reduced.

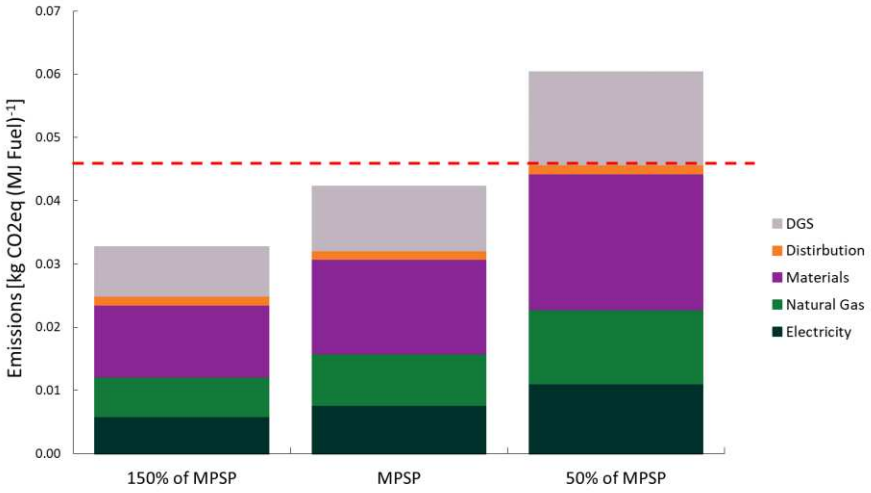

Figure 27: Emissions per MJ of fuel as the protein market price changes from 150% of HPC MPSP, MPSP and 50% of MPSP. The red dashed line represents the RFS goal for renewable fuels. DGS related emissions were assigned through market allocation at the ethanol-refinery.

LCA methodology has a direct effect on a product's ability to meet sustainability metrics. For renewable fuels, one important metric is the Renewable Fuel Standard (RFS) which calls for a 50% reduction of emissions when compared to petroleum-based energy products. For gasoline, well to wheels emissions are approximately 92 g $CO_{2\text{-eq}}$ MJ fuel^{-1} [69], meaning for a renewable fuel to meet the RFS well to wheels emissions would need to be below 46 g $CO_{2\text{-eq}}$ MJ fuel^{-1}. The ability of the fusel alcohols to meet this standard is dependent on the LCA methodology and is only achieved in one of the scenarios, Figure 25B. This result begs the question; should fusel alcohols produced from the upgrade process be considered a renewable fuel as defined by the RFS? Current regulations under the Renewable Fuel Standard are unclear and lack definitive guidance on co-product methodology and system boundary definitions when evaluating renewable fuel LCA's. In addition, with so much discretion left to LCA practitioner, the answer here could be either "yes" or "no" since significant variance exists depending on the chosen methods and system boundary definitions.

The protein emissions were compared to the emissions required to produce one kg of an equivalent protein, however, this comparison proved problematic as the protein displacement credit is

somewhat subjective and represents an area of high uncertainty. Protein related emissions can range from 0.6 kg $CO_{2\text{-eq}}$ (kg-protein)$^{-1}$ for grain-based proteins to over 13 kg $CO_{2\text{-eq}}$ (kg-protein)$^{-1}$ for human-grade protein, such as beef [69,106,107]. Without knowing the correct target protein market, we cannot confidently conclude that these HPC proteins do or do not represent an emissions savings.

From this analysis, we can see how system boundary and LCA methodology can have a significant impact on product related emission and reaffirms the importance of adopting uniform practices within the community, especially when investigating if a product meets certain regulatory goals, such as the RFS. We have also identified the importance of understanding product markets and displacement ratios, as this variable provides great uncertainty for the current state of the model and analysis.

While emissions improvements remain uncertain, there are several other environmental benefits to this upgrade process not captured in the LCA. By producing more fuels from the original grain, we can reduce biofuels-based land requirements reducing food vs fuel and land-use change concerns. The upgraded protein may also help meet increased global protein demands, by providing a product enriched in vital amino acids. Increased utilization of the original feedstock should provide environmental benefits by reducing these burdens.

3.3.4 Sensitivity Analysis

A sensitivity analysis was also performed to identify the high impact variables in terms of process economics. Results for the top 10 model inputs is presented Figure 28A. Variables whose t-ratios fall outside the t-critical range, ± 2.074, are shown to be statistically significant based on a 95% confidence interval. A sensitivity analysis was also performed on the emissions, and the results are shown in Figure 28B with the t-critical ratio for this analysis found to be ± 2.179.

A)

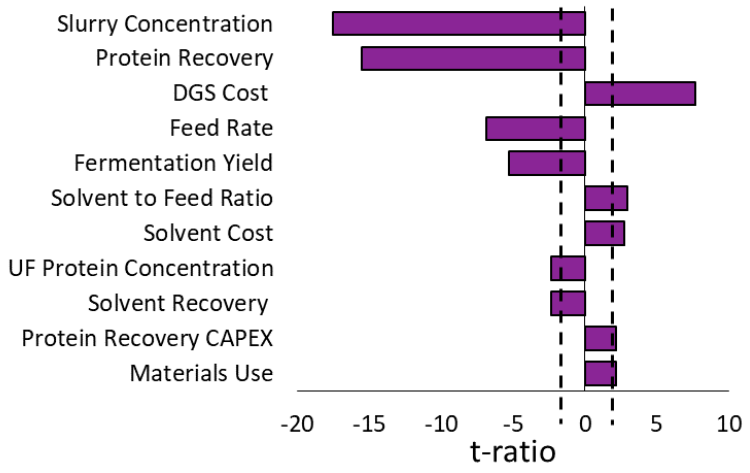

B)

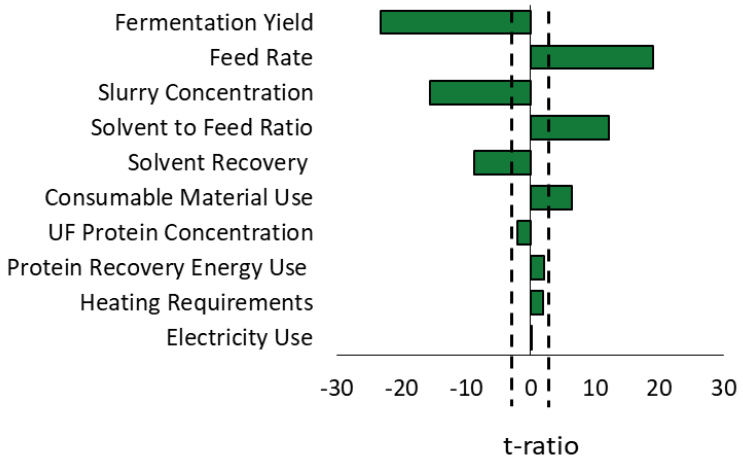

Figure 28: A) Results from the sensitivity analysis for the top 10inputs on the economics model and B) results from the sensitivity analysis for the top 10 variables on the LCA model. Variables whose t-ratios fall outside the t-critical range, indicated by the dashed vertical lines, are considered statistically significant.

Protein recovery, solvent recovery and fermentation yield were shown to be high impact areas for reducing emissions and improving process economics. The variable shown to be the most significant is the incoming slurry concentration. By changing the slurry concentration, the amount of water entering the system is impacted, which directly affects the sizing of the capital equipment and OPEX by modifying the power, heat and consumable materials required. Increasing the slurry concentration by

20% decreases the CAPEX by 7% and OPEX by 11%, reducing the MPSP by 19% to \$1.55 kg-protein^{-1}. Pursuing a lower moisture feedstock will have a systems level impact as the DGS being purchased from the ethanol facility and the additional dewatering would need to happen at the ethanol facility, thereby increasing the purchase price of the DGS. This consequence was explored with the model, and the purchase price of the DGS could increase by 30% before savings from dewatering no longer realized. There may be other issues potentially associated with increasing the solids concentration, such as increased pumping costs or reduced fermentation yields, which were not accounted for in this model. Further, the proximity of the modeled processing facility will have an impact as this work assumes co-location. The investigation of this trade-off represents an opportunity for further investigation.

Protein recovery also represents an area to greatly improve the process. Currently, the model assumes 20% of the total solids entering protein recovery are lost, based on the work from Hurst et al.[88]. However, there may be process opportunities or improvements that have been made in whey processing that would reduce this product loss. Additionally, this assumption assumes uniform product loss across the full spectrum of solids (proteins, sugars, ash, etc.), when it is more likely to see product loss more concentrated to a certain component depending on the reason for the product loss. For example, if product loss is due to volatilization, we'd expect product loss to be concreted to the more volatile component. Therefore, the product-loss variable introduces high uncertainty into the model and indicates a process variable that can be leveraged to improve the model and analysis outcomes.

Feedstock costs are also a significant contributor to the process economics, which is consistent with other bio-refineries [109,110]. Reducing the feedstock costs by 20% reduces annual OPEX by 10%, reducing the MPSP by 13% to 1.67 kg^{-1}. This result also highlights the potential impact that volatile DGS markets could have on the process, as small changes in purchase price will have significant impact on the MPSP. Fermentation yields also improve the MPSP by increasing the amount of fusel alcohol products. As more products are available for sale, a 20% improvement in fermentation yield would

decrease the MPSP by 10% to \$1.71 kg^{-1}. It may be possible to improve these yields by exploring increased carbon utilization by the yeast through genetic engineering or other methods.

When considering the variables with significant impact on the LCA, fermentation yield was found to have the most significant impact on the emissions. The fermentation yield is indicative of carbon utilization during fermentation; therefore, by increasing the amount of carbon converted into fusel alcohols, we increase the amount of carbon sequestered in the fuels as well as improving the yield which is the functional unit. Through this increase in fermentation yield, 20% more carbon was stored in the fuels and allowed for four of the six LCA scenarios to meet the RFS.

Slurry concentration was also found to be statistically significant for reducing overall emissions. By changing slurry concentration, inlet water flow rates are affected, which has a direct impact on heating and power consumption and their corresponding emissions. But again, the additional dewatering step required to increase slurry concentration for the upgrade facility would increase emissions from the upfront ethanol refinery. This in turn would increase overall emissions for the protein product, so it is unclear how much savings could be realized without performing a more in-depth investigation.

Solvent recovery was also shown to have a significant impact on emissions. As previously discussed, increasing solvent recovery decreases emissions associated with consumable materials. While overall emissions were only reduced by 3% overall, the sensitivity analysis indicates this reduction is significant and can be one avenue to reduce overall emissions from the upgrade facility. As previously discussed, improving solvent recovery can have positive impacts on both emissions and economics and should be further explored with more rigor.

One variable not explored here was the impact of protein displacement credits on fuel related emissions. This is because the sensitivity analysis performed was exploring the effects of process variables on the overall emissions of the upgrade facility, not the emissions related to individual

products. The impact of LCA methodology on determining these types of emissions has been discussed in-depth above.

3.4 Conclusion

Three different process options were explored to investigate if the proposed DGS upgrading process could be a value-add proposition for ethanol refiners. The DGS upgrading process was shown to increase fuels production from the refinery by 118% and to increase the PDCAAS score of the end protein product from 22 for DGS to 33 for HPC protein. The preferred pathway process was found to be the combination of solvent extraction for FA recovery and ultrafiltration and drying for protein recovery. TEA results showed that refiners would need to sell the HPC protein product for \$1.91 kg-protein^{-1}, while selling the energy products for \$0.79 LGE^{-1} (\$3.00 GGE^{-1}) to cover production costs. A FOAK analysis was also performed, showing a MPSP of \$2.19 kg-protein^{-1}. Sensitivity analysis results indicate that the MPSP may be reduced by additional dewatering of the DGS product prior to entering the upgrade facility, reducing DGS feedstock costs or increasing fermentation yields.

The addition of the DGS upgrading process may be considered as a value-add proposition if the protein product can be sold in higher value protein markets such as aquaculture. In these higher value protein markets, protein prices are above the MPSP indicating potential profitability. PDCAAS score and protein content indicate that targeting these markets may be possible, but further experimentation to confirm this assumption should be performed before moving forward with implementing this process. Due to this uncertainty, the economic viability of this process remains unknown at this time.

LCA results showed emissions related to fuels production of 42 and 210 g $CO_{2\text{-eq}}$ (MJ fuel)$^{-1}$, with one of the cases showing these energy products meeting the RFS goal. However, the absolute certainty of this result is ambiguous. Using a displacement method and displacing higher emissions proteins changes these results. Therefore, potential protein markets for the HPC protein need to be better understood to increase confidence in LCA results. Using co-product allocation methods removes the

uncertainty associated with protein markets but introduce their own complications. For instance, to use market allocation methods, the market prices of all products need to be well understood. LCA results have large ranges due to the application of different LCA methodologies, indicating the importance and variability of the different methods. These variability issues are also seen to compound when evaluating emissions requires the use of multiple LCA steps. There are two methods for improving LCA are; increased guidance and improving transparency.

While the absolute certainty of value-add is currently unknown, there is evidence to suggest that the DGS upgrading process may improve overall corn-ethanol economics and environmental burdens. This process is still in early stages of development and many areas have been identified to improve process economics and GHG emissions including additional dewatering of the DGS feedstock, increased fermentation yields or optimizing solvent recovery.

CHAPTER 4: CONSEQUENTIAL ECONOMIC ANALYSIS FOR THE ADOPTION OF PROACTIVE HARMFUL ALGAE BLOOM MITIGATION TECHNOLOGIES[3]

4.1 Introduction

Fresh and saltwater bodies around the globe are suffering from overgrowths of marine microorganisms known as Harmful Algae Blooms or "HAB's" [111–116]. Examples in the United States include algal overgrowths of *Karenia brevis* in the Gulf of Mexico, *Microcystis aeruginosa* in the Great Lakes and *Alenandrium catenekka* and *Pseudo-nitzchia* in the Pacific northwest [117–119]. Each year, hundreds of beach recreators and tourists, local communities, and regional ecosystems are negatively impacted by HAB's. The propagation of HAB events is the result of several environmental factors, but the root cause of the events are well established [120–122]. Eutrophication, or nutrient enrichment, of waterways creates a breeding ground for microorganisms [120]. Nutrient reduction has been the long-term goal of most policy plans to prevent or mitigate HAB's [123–125]. These actions have been shown to be successful in the past, as seen in Lake Erie after the signing of the Great Lakes Water Quality Agreement (GLWQA) in 1972 [126–129]. However, changes in the marine ecosystem and nutrient profiles have brought about a return of HAB's to Lake Erie beginning in the mid-1990's [127,128]. The resurgence of HAB events has communities searching for a solution.

As before, policy makers are targeting nutrient reductions to combat HABs, but implementing this strategy is becoming more complicated. In the 1970s, nutrient reduction was accomplished by targeting point source emitters, such as wastewater treatment facilities [129]. Today, the majority of bioavailable nutrients originate from non-point sources, such as agriculture [122,129–131]. Regulation of non-

[3] Parts of this work are currently in review as part of a manuscript to be published: DeRose, K., Davis, R.W., Quinn, J.C. Economic Viability of Proactive Harmful Algae Mitigation Technologies. *Environmental Science & Technology* (In Review). Original copyright for this work will be held by journal publisher.

point source nutrients represents a significant challenge. Instead, policy makers must rely on changes in farming practices to reduce bioavailable nutrient run-off, adoption of which has been slow--with less than one third of farmers adopting new practices [132]. Traditional nutrient reduction technologies present an alternative to achieving this goal but they require extensive capital and operational costs, and it is unclear if technology adoption is economically feasible [133]. Ultimately the economic viability of technology adoption will be dictated by the potential for the reduction of HAB event severity. Many studies have quantified HAB-related economic impacts for Lake Erie, but these studies are general in their approach and do not allow for quantitate assessment of nutrient reduction technologies [134,135].

This study evaluates the economic viability of nutrient reduction technologies as a way to proactively mitigate HABs by determining the costs of implementing nutrient reduction technologies combined with the economic benefits of HAB mitigation using the Western Lake Erie Basin as a case study. A model was created which integrates a nutrient- based HAB growth model with economic damage estimations. Four different technologies were evaluated on their ability to provide cost-effective HAB mitigation; repairing home septic systems, point-source nutrient reduction, lagoon systems and attached algae systems to address non-point source nutrients. Attached algae systems are a novel technology, in which algae is grown in a controlled method proactively removing nutrients before they can collect downstream [43,136]. Economic benefits i.e. reductions in HAB-related losses, and associated technology capital and operational costs are calculated for each solution. The model leverages stochastic modeling for the evaluation of economic impacts of HAB events over a 30-year period. The economic viability of the technology solution is evaluated based on the net present value (NPV) of HAB related losses and technology deployment costs. The model herein considers a single geographic location, the Western Lake Erie Basin, but the methodology and conclusions can be adapted to other locations experiencing HAB events.

4.2 Methods

The modeling architecture is presented in Figure 29 and includes the evaluation of the Business as Usual (BAU) case compared to the adoption of a nutrient (phosphorus) reduction technology. The economic viability of the different pathways is based on the NPV of damages which are based on a dynamic HAB growth model coupled with corresponding economic damages and the costs of technology operation over a 30-year simulation period. Stochastic modeling is used to reduced uncertainty in results.

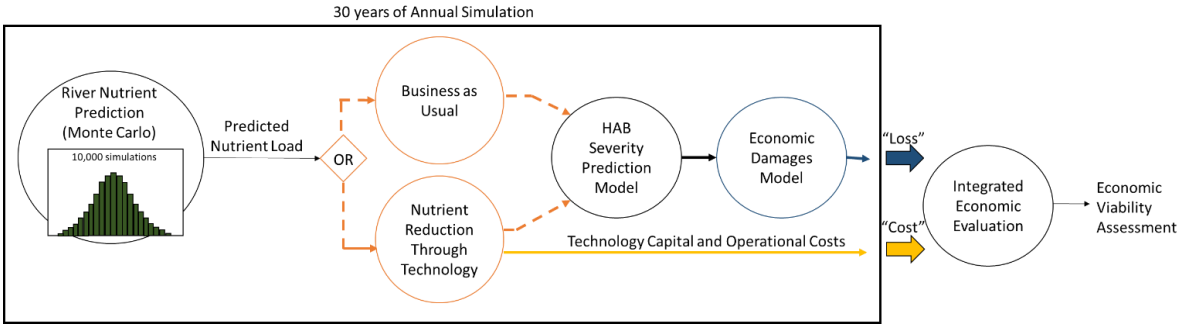

Figure 29: Model flow chart for the prediction of economic losses due to HAB's with and without nutrient reduction technologies. Economic losses can be compared between the BAU case and the nutrient removal technology cases in this study to identify long-term, cost-effective nutrient reduction technologies for HAB mitigation.

4.2.1 Phosphorous Model

For Lake Erie, phosphorous has been identified as the key nutrient contributing to HAB's [129]. HAB severity was modeled using springtime (March-June) bioavailable phosphorus (TBP) loads, July TBP loads and June water temperatures. Estimation of future nutrient loads, used for HAB severity prediction, was done leveraging historical data combined with stochastic modeling. Results from predictive modeling work is shown to be consistent with historical loads through a Chi-Squared Goodness of Fit test (p-value < 0.05).

4.2.1.1 Historical Phosphorous loadings

Historical springtime (March-June) phosphorus loadings were determined based on the methods outlined in Stumpf 2016 and Obenour 2014 [137,138]. First, Any missing TP and DRP concentration data were estimated using linear regression with flow from the closest 20 days of non-missing data [138]. Next, the total phosphorus (TP) and dissolved reactive phosphorus (DRP) flow-weighted mean concentrations (FWMC) were calculated from data collected by Heidelberg University's National Center for Water Quality Research (NCWQR) [139], Equation [14]. To calculate the FWMC, the sample phosphorus load and discharge load were calculated from Equations [15] and [17], where the sample time window was considered to be half the time from the previous sample to the current sample (or from midnight to the current sample) plus half the time from the current sample until the next sample (or from the current sample until midnight). Daily TP, DRP and discharge loads could be calculated for the NCWQR data by summing all of the sample loads that occur for each day, Equations [16] and [18]. Actual daily TP and DRP loadings for the Maumee River were then calculated by multiplying the FWMC by the official river discharge rate as reported by the United States Geological Survey (USGS) at Waterville, OH (Station 04193500) [140], Equation [19]. Springtime TP loads were calculated for years 1982-2018, while %DRP (DRP/TP) was calculated for years 2000-2018 based on recent changes in %DRP trends[129]. Historic water temperatures were found using NASA's Giovanni website, for the southwest section of Lake Erie's western basin (south of 41.914 N and west of 82.741 W) as outlined by Stumpf 2016 [137,141]. Results from the historical data collected and processing are available in Table 24.

$$FWMC_{\ NCWQR}\left[\frac{mg\ P}{L}\right] = \frac{Daily\ Phosphorus\ Load_{\ NCWQR}[\frac{mg\ P}{day}]}{Daily\ River\ Discharge_{\ NCWQR}[\frac{L}{day}]} \quad [14]$$

$$Sample\ Phosphorus\ Load_{NCWQR}\ [mg] = Sample\ River\ Discharge\ \left[\frac{Liter}{hour}\right] \times Sample\ Phosphorus\ Concentration\ \left[\frac{mg\ P}{Liter}\right] \times Sample\ window\ [hours] \quad [15]$$

$$Daily\ Phosphorus\ Load_{NCWQR}[mg] = \sum_{day\ i} Sample\ Phosphorus\ Load_{NCWQR}\ [mg] \quad [16]$$

$$Sample\ Dischage\ Load_{NCWQR}\ [L] = Sample\ River\ Discharge\ \left[\frac{Liter}{hour}\right] \times\ Sample\ window\ [hours] \quad [17]$$

$$Daily\ Discharge_{NCWQR}[L] = \sum_{day\ i} Sample\ Discharge\ Load_{NCWQR}\ [L] \quad [18]$$

$$Daily\ Phosphorus\ Load\ _{actual}\left[\frac{mg}{day}\right] = FWMC\ _{NCWQR}\left[\frac{mg\ P}{L}\right] \times Daily\ River\ Discharge_{USGS}\ [\frac{L}{day}] \quad [19]$$

Where *Sample Phosphorus Load*$_{NCWQR}$ is the calculated phosphorus load (TP or DRP) based on data collected from NCWQR; *Sample River Discharge* is the river discharge rate from the sample collected by NCWQR; *Sample Phosphorus Concentration* is the phosphorus concentration (TP or DRP) from the sample collected by NCWQR; *Sample window* is half the time from the previous sample to the current sample (or from midnight to the current sample) plus half the time from the current sample until the next sample (or from the current sample until midnight); *Daily Phosphorus Load*$_{NCWQR}$ is amount of phosphorus from the Maumee River for a whole day as calculated from data collected by NCWQR *FWMC*$_{NCWQR}$ is the flow weighted mean concentration for a single day based on from data collected by NCWQR; *Daily River Discharge*$_{USGS}$ is the river discharge rate as reported by USGS at station #04193500 Maumee River at Waterville, OH; *Daily Phosphorus Load*$_{actual}$ is the daily calculated phosphorus load (TP or DRP).

The bioavailable fraction of the phosphorus (TBP) loads were calculated using Equations [20]-[23].

$$TP = DRP + TPP \quad [20]$$

$$TBPP = \beta \times TPP \quad [21]$$

$$TBPP_{resid} = (1 - S) \times TBPP \quad [22]$$

$$TBP = DRP + TBPP_{resid} \quad [23]$$

Where *TP* is the total phosphorus load; *DRP* is dissolved reactive phosphorus load; *TPP* is the particulate phosphorus load; *β* is the portion of TPP that is considered bioavailable, value set as 26% [137,142]; *S* is portion of TPP that settles out of the river between Waterville and the Maumee Bay, value set as 70% [137,142]; and $TBPP_{resid}$ is the amount of bioavailable particulate phosphorus that reaches Lake Erie.

Table 24: Table of historical data, including spring (March – June) Maumee river TP loads, July TP loads, %DRP and average June water temperatures.

Year	March - June TP Loads [Metric tons]	July TP Loads [metric tons]	%DRP	June average water temp [°C]
1982	2287	121	12%	
1983	1179	71	11%	
1984	1553	9	11%	
1985	1039	10	3%	
1986	796	361	7%	
1987	240	81	22%	
1988	352	7	9%	
1989	1288	31	8%	
1990	966	325	14%	
1991	705	7	13%	
1992	787	290	10%	
1993	1196	277	14%	
1994	774	26	3%	
1995	880	58	8%	
1996	1273	69	11%	
1997	1293	216	15%	
1998	1291	91	13%	
1999	813	10	13%	
2000	970	49	16%	
2001	488	11	21%	
2002	1222	7	21%	
2003	1373	373	22%	21.9
2004	943	35	20%	21.5
2005	291	20	27%	23.1
2006	573	83	21%	22.5
2007	1013	7	25%	23.3
2008	1293	121	20%	21.7
2009	1358	11	15%	25.3
2010	1283	25	25%	24.3
2011	2311	8	19%	22.8
2012	393	4	16%	22.7
2013	1104	146	22%	21.2
2014	1127	31	26%	23.0
2015	1665	387	26%	19.2
2016	717	9	18%	23.7
2017	1379	434	21%	21.0
2018	1063	22	20%	22.8

4.2.1.2 Predicting future phosphorus loads

Normalcy was added to the springtime TP, July TP and June water temperature data by taking the natural log of these values. The data was then fit to a normal distribution to create the future nutrient prediction model. Goodness of fit was confirmed using a Chi-Squared goodness of fit test (p value <0.05). A triangle distribution was used to predict future % DRP. These models are used as part of the Monte Carlo simulation. Model parameters are shown in Table 25.

Table 25: Phosphorous prediction model parameters

Variable	Model type	Mean	St Deviation (for normal distribution)	Min/Max (for triangle distribution)
Springtime Nutrient Prediction Model				
Ln(Spring TP)	Normal	6.85	0.50	
Ln(July TP)	Normal	3.75	1.45	
Ln(June Temp)	Normal	3.11	0.88	
%DRP	Triangle	21%		15.4%/27%
Nutrient Source Prediction Model				
HSTS load (mt)	Uniform	35 if July loads included, 28 if July loads excluded		
Point Source load (mt)	Uniform	57 if July loads included, 45 if July loads excluded		
Non-point Source	*			

*Non-point source loads were calculated as the difference between total springtime loads predicted in the Phosphorus prediction model and phosphorus loads from HSTS and Point Sources.

Phosphorous Sources

River nutrients originate from a variety of sources and different technologies offer solutions to reducing nutrients depending on the source. The Ohio EPA's Nutrient Mass Balance Study was used to identify nutrient sources and their respective loads, with the results reprinted in the Table 26[143]. The study shows small variations in point-source related nutrient loads, while non-point source loads showed wide variation due to differences in the intensity and frequency of rain events year after year.

Table 26: Annual and springtime (March-June) TP loads by source, reprinted from Ohio EPA's Nutrient Mass Balance Study[143]

	Annual Phosphorus loads [mt year^{-1}]				
Year	2013	2014	2015	2016	2017
HSTS	84	84	84	84	84
Point Source	139.3	142.1	128.6	137.7	129.3
	Springtime Phosphorus loads [mt year^{-1}]				
Year	2013	2014	2015	2016	2017
HSTS*	28	28	28	28	28
Point Source*	46	47	43	46	43
Non-Point Source	1030	1050	1530	656	1293
Total	1104	1125	1601	730	1364

*Phosphorus from HSTS and Point source systems were assumed to be uniform over the year.

For predicating future phosphorous loads based on sources, constant loads were assumed for nutrients originating from home septic systems and point-source facilities. The remainder of the nutrients were assumed to originate from non-point sources. An example of a 30-year simulation of springtime nutrients load, including sources, is shown in Figure 30.

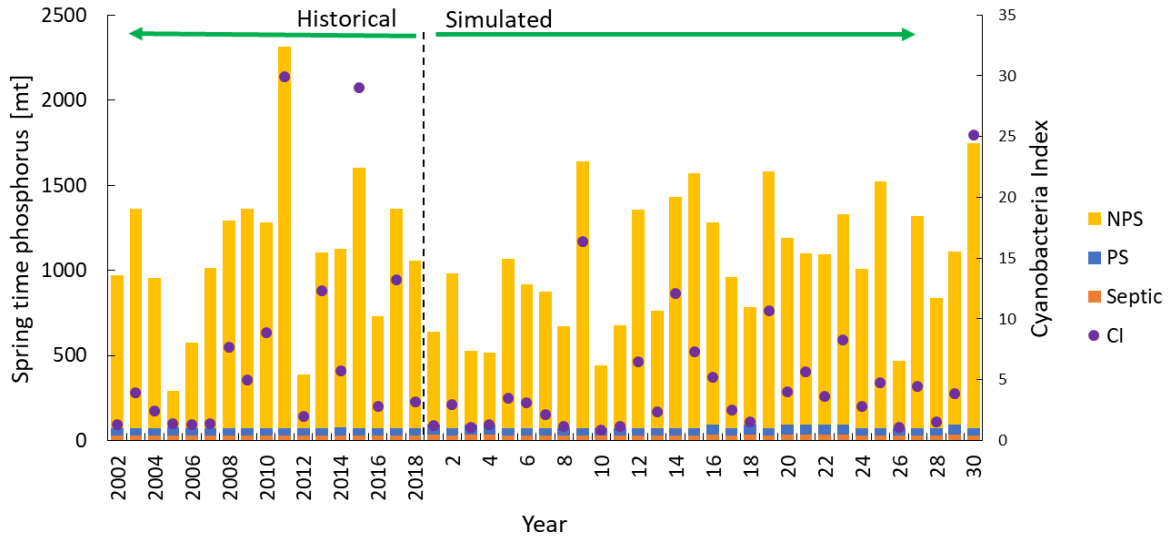

Figure 30: An example of simulated springtime (March – June) Maumee river phosphorous loadings, years 2002 – 2018 are based off historical data and years 1 – 30 are simulated loadings. Includes the breakdown of phosphorous source between septic systems, point source systems and non-point source systems. The right axis shows the actual (years 2002-2018) or predicted (years 1-30) HAB severity, as indicated by the cyanobacteria index.

4.2.2 Nutrient Reduction Technologies

For all nutrient reduction technologies, capital and operational costs were adjusted to 2018 dollars using the Chemical Engineering Price Index and Equation [2][144]. Descriptions below for each technology highlight key performance assumptions with more detailed information including model inputs, phosphorus reductions and costing information is available within each section, while capital and operational costs for each solution are presented in Table 27.

Table 27: Capital and operational costs associated with nutrient reduction solution.

Solution	Capital Costs [$M]	Operational Costs [$M year^{-1}]
Traditional Systems		
Home septic repair	$ 1,169	$ 3
PS - High Level	$ 514	$ 46
PS - Low Level	$ 673	$ 53
Lagoon - Centralized	$ 36,250	$ 3,297
Lagoon - Decentralized	$ 80,880	$ 7,356
Attached Algae Systems		
Centralized - Conservative	$ 1,065	$ 19
Centralized - Optimistic	$ 122	$ 12
Decentralized - Conservative	$ 2,262	$ 51
Decentralized - Optimistic	$ 260	$ 26

4.2.2.1 Point Source Reduction Technologies

Home Septic Systems

Home septic systems are small scale wastewater treatment facilities for individual homes. Intermittent or total system failure leads to nutrients being discharged into the watershed. A total of 117,819 home septic systems are estimated to be in the northwest section of Ohio which may discharge to the Maumee River [145]. Of these systems, 41.5% were estimated to be working, 26.5% were estimated to be failing and 32% were estimating to be discharging[143]. Working systems reduce incoming TP by 80%, while failing and discharging systems reduce incoming TP by 40% and 6%, respectively[143]. Nutrient reduction was accomplished by repairing or replacing failing home septic systems. All discharging

systems were assumed to be replaced, while failing systems were repaired. Within failing systems, 0.1% of systems were assumed to be in critical failure requiring removal and replacement. TP in the effluent was reduced by 50% for repaired systems and 79% for replaced systems[143]. Table 28 presents a table of all inputs used for the home septic system model.

Table 28: Home septic system design criteria, assumptions, and costing information

Design Criteria		
Parameter	Value	Source
Home Septic Systems		
Total # of NW Ohio HSTS	117819	[145]
Current Maumee Watershed HSTS performance		
% Working	41.50%	[143]
% Failing	26.50%	
% Discharging	32%	
% TP reduction based on HSTS performance		
Working	80%	[143]
Failing	40%	
Discharging	6%	
% of TP that is DRP in effluent of failing and discharging systems	85%	[146]
% of TP that is DRP in effluent for working systems	100%	[146]
Costing information		
Repair Cost* [$ system^{-1}]	$ 2,862	[147]
Replacement Cost* [$ system^{-1}]	$ 28,623	
Assumptions:		
% of failing systems that need replacement	0.10%	
% of HSTS systems that fail each year	1%	
Total CAPEX	$ 1,169,348,772	
Total OPEX	$ 3,426,205	
*Converted to 2018 dollars		

Point Source Systems

Two different policy scenarios were considered for nutrient reduction for point-source wastewater treatment facilities (WWTF), a high phosphorous discharge limit (PS-High Limit) with

effluent phosphorous limits of 1 mg TP L^{-1} and a low phosphorous discharge limit (PS-Low Limit) with effluent phosphorous limits of 0.1 mg TP L^{-1}. These limits were then applied to point-source WWTF identified using Appendix C of the 2018 Ohio Domestic Action Plan [148], Appendix C 1. TP concentrations in WWTF effluent were assumed to be constant, such that any fluctuations in TP loads year after year were due to changes in flow rate only providing a constant TP reductions of 5% and 73% for the PS-High and PS-Low Limit scenarios, respectively. Capital and operational costs were found using Equations [24] and [25] and constants in Table 29.

$$Capex\ [\$\ Million] = A\left[\frac{\$Million}{MGD}\right] \times Design\ Flow\ Rate\ [MGD] + B\ [\$Million] \quad [24]$$

$$Opex\left[\frac{\$\ Million}{year}\right] = A\left[\frac{\$Million}{MGD}\right] \times Design\ Flow\ Rate\left[\frac{MGD}{year}\right] + B\left[\frac{\$Million}{year}\right] \quad [25]$$

Table 29: Constants for the CAPEX and OPEX equations for the two point source reduction cases

Scenario	Technology	Capex Equation	Opex Equation	Source
High Limit	3 -stage Activated Sludge + Chemical Addition	A = 1.80 B = 1.88	A = 0.17 B = 0.16	[149]
Low Limit	A/O, fermenter, filter, chemical addition	A = 2.42 B = 1.87	A = 0.18 B = 0.18	[149]

4.2.2.2 Non-point Source Systems

Two different technology options were identified for non-point source nutrient reduction; lagoon systems and attached-algae systems. For both systems we considered either one system located near the mouth of the Maumee River at Lake Erie (hereafter referred to as Centralized systems) or multiple system locations located at 3 different locations along the Maumee which coincide with the USGS sampling stations (hereafter referred to as Decentralized systems. All systems were sized to treat

50% of the Maumee river's average spring flow rate, as estimated from the USGS Stations #04193500, #04183500 and #04192500 [140,150,151], Figure 31.

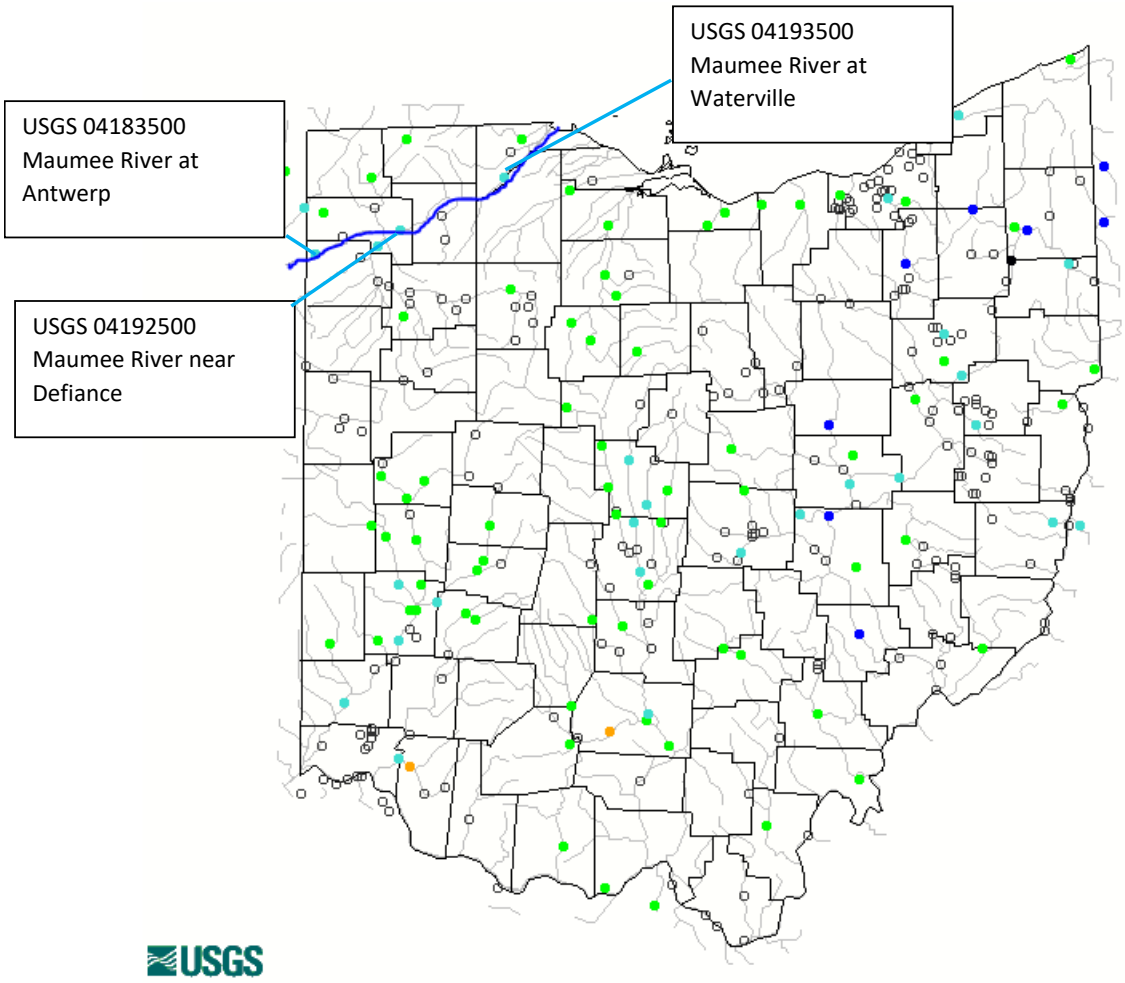

Figure 31: Location of USGS Stations along the Maumee River (traced in blue). Photo taken from USGS website

Lagoon Systems

Constructed wetlands were originally considered for non-point source nutrient reduction, but the target effluent phosphorous levels of these systems (0.5-3 mg TP L^{-1}) exceeded those currently seen in the Maumee river [152]. Historical Maumee River phosphorous concentrations are; max 3.2 mg TP L^{-1}, average 0.28 mg TP L^{-1}, with concentrations exceeding 1 mg TP L^{-1} 1% of the time. Thus, an alternative passive-type nutrient reduction system, lagoons, was selected. In general practice, lagoons are used in

conjunction with wastewater treatment plants for effluent polishing and can by designed to reach effluent concentrations of 0.1 mg TP L^{-1} through chemical addition[149]. Design criteria for the lagoon systems is shown in Table 30. Capital and operational costs for the lagoon systems were estimated using Equations [26] and [27] [149]. Complete system sizing for the centralized and decentralized systems is available in Appendix C 2.

Table 30: Design Criteria for the lagoon systems

Design Criteria			
Parameter	Value	Units	Source
Lagoon depth	7	ft	[153]
Retention time	105	days	[153]
Amount of river water treated	50%	Average springtime flow rate	
% of TP that is DRP in the river	21%		
Land Cost	3370	\$ $acre^{-1}$	[65]
Capex	10.89	\$ $(gallon\text{-}day)^{-1}$	[149]
Opex	2751	\$ MG^{-1}	[149]
Effluent TP concentration	0.1	mg TP L^{-1}	[149]
DRP Reduction	85%		[154,155]

$$Capex\ [Million\ \$] = 10.89\left[\frac{\$Million}{MGD}\right] \times Design\ Flow\ Rate\left[\frac{MG}{day}\right] \quad [26]$$

$$Opex\left[\frac{\$}{year}\right] = 2751\left[\frac{\$}{MG}\right] \times Design\ Flow\ Rate\left[\frac{MG}{day}\right] \times 365\left[\frac{days}{year}\right] \quad [27]$$

Attached-Algae Systems

Attached-algae systems have been shown to be effective for nutrient removal in a variety of conditions, including wastewater, cow manure and river water [136,156–160]. In these systems, nutrient rich waters run over long flow ways which are covered with a substrate (usually a nylon type netting). Native

algae attach to the substrate and grow, removing nutrients from the waterways. Algae is harvested periodically, approximately every 7-10 days. After removal, the algae could potentially be sold as a biofertilizer, used in an anerobic digestor or processed into fuels [161–163].

The attached-algae systems were sized to treat 50% of the river flow of the Maumee River springtime flow rate and reduce incoming TP by 40% [140,150,151]. Two different configurations were considered; 1) a single system located near the mouth of the Maumee River at Lake Erie ("Centralized" systems), and 2) multiple systems deployed at 3 different locations along the Maumee river which coincide with the USGS sampling stations ("Decentralized" systems), Figure 31.

Total algal growth area was calculated by dividing the total desired phosphorous uptake [kg TP day^{-1}] by areal phosphorous uptake by the algae [g TP $(m^2\text{-}day)^{-1}$]. Areal TP uptake was assumed to be a function of linear hydraulic TP load (hydraulic flow rate [L $(min\text{-}linear\ foot)^{-1}$] times TP concentration [mg TP L^{-1}]). Areal phosphorous uptake was shown to have a strong correlation with linear hydraulic phosphorous load in several studies (R^2=0.82), Figure 32A[136,156–160]. The percentage of phosphorous taken up by the algae that is DRP was considered to be a function of DRP/TP ratios in the water, based on strong correlations from previous attached-algae studies (R^2=0.93), Figure 32B [136,156–160]. Data from these historical studies is available in Appendix C 3.

A)

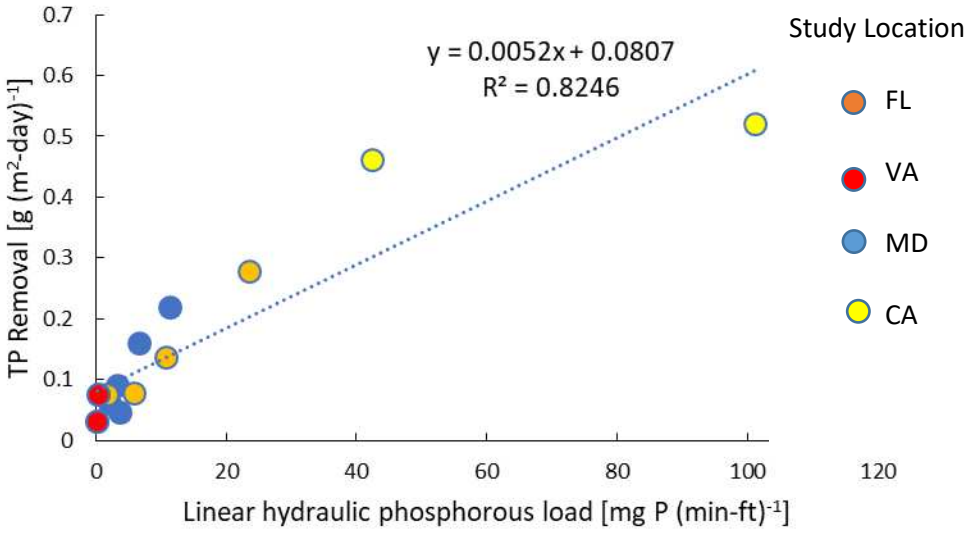

B)

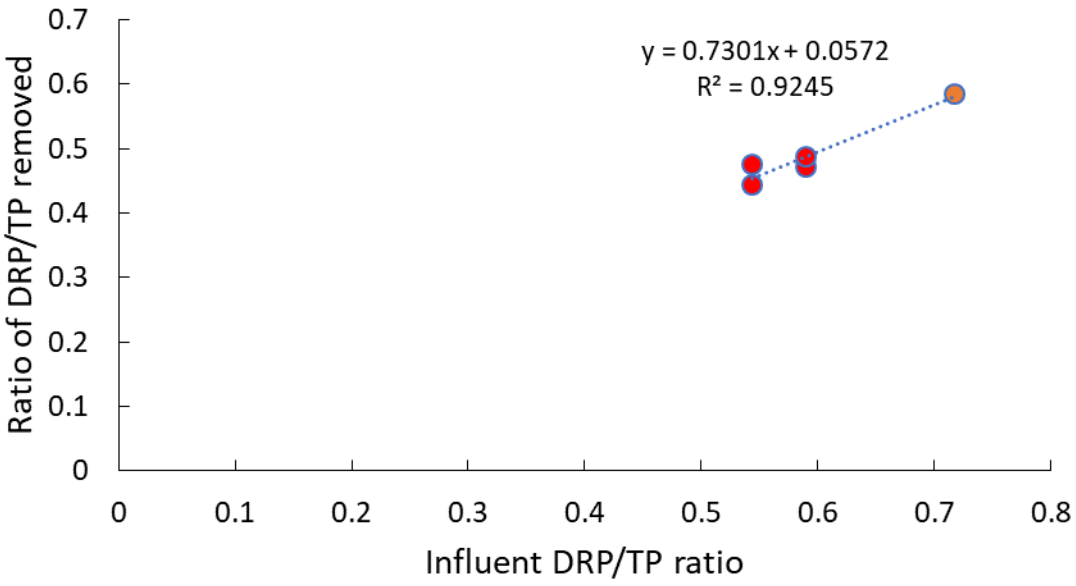

Figure 32:A) Data showing the TP removal as a function of linear hydraulic phosphorus loading from historic attached-algae studies B) Graph of the ratio of DRP/TP removed by the attached algae system as function of influent DRP/TP ratio from historic attached-algae studies

As the attached-algae systems are relatively new and novel, two different costing scenarios for the Centralized and Decentralized systems were considered; a conservative case based off a report by Hydromentia [164] and an optimistic case based on economic assessments for attached-algae systems available in literature and available in Appendix C 4[18,39,62,64]. Design criteria and costing information for the two design cases in available in Table 31.

Table 31: Attached algae system design criteria, assumptions and costing information

Design Criteria			
Parameter	Value	Units	Source
Amount of river water treated	50%	Average springtime flow rate	140,150,151
Required TP Reduction	40%		
Hydraulic Flow Rate	20	Gal (min-ft)$^{-1}$	
# Days running	120	Days (year)$^{-1}$	
Algae productivity	16.6	grams (m^2-day)$^{-1}$	
% of TP that is DRP in the river	21%		
Land Cost	3370	$ acre^{-1}	65
Areal Phosphorous removal	= TPHFL x 0.0052 + 0.0807	grams (m^2-day)$^{-1}$	
% of TP removed that is DRP	=DRP ratio x 0.7301 + 0.0572	%	
Where TPHFL = TP concentration in [mg TP L^{-1}] × hydraulic flow rate [L (min-sec)$^{-1}$], and DRP ratio = the ratio of DRP/TP			
Conservative Costing - CAPEX			
Module Size	12	acres	164
Module Cost	$ 4.64	$ Million module^{-1}	164
Module Cost	$ 387,000	$ acre^{-1}	164
Peripheral Costs	50%	of module costs	164
Land Cost	$ 3,370	$ acre^{-1}	65
Conservative Costing - OPEX			
Operational costs	$ 91,543	$ (module-year)$^{-1}$	164
Pump maintenance	2%	of electrical costs	
Equipment maintenance	2%	of equipment costs	
Equipment costs	10%	of module costs	
Other energy costs	10%	of pumping costs	
Monitoring costs	$ 12,045	$ (module-year)$^{-1}$	
Harvest equip costs	$ 48,181	$ (module-year)$^{-1}$	
Pump energy use	0.006061	Kw gpm^{-1}	
Electrical costs	0.0947	$ kWh^{-1}	
Optimistic Costing - CAPEX			
Growth System	$ 47,446	$ acre^{-1}	Appendix C 4
Harvest Equipment	$ 5,391	$ acre^{-1}	
Optimistic Costing - OPEX			
Labor	$ 1,398	$ acre^{-1}	Appendix C 4
Harvest	$ 646	$ acre^{-1}	
Maintenance	1.6%	[% of capex]	

4.2.3 Algae Bloom Model

While many variables effect HAB formation, duration and intensity, many studies have shown that springtime (March – June) Maumee river TBP loads can be used to effectively predict HAB intensity in Lake Erie's western basin [137,138,165–167]. The HAB prediction model using TBP proposed by Stumpf et al. was used for this study[137], Equation [28]. This model predicts HAB severity using the cumulative cyanobacteria index (CI), where a value of 1 CI equals a biomass mass of 10^{20} cells [137,168]. The model was validated using historic phosphorus loadings and maximum cumulative CI for years 2002-2018 [31]. Validation showed a mean absolute error of 2.6 CI and a mean square error of 6.7 CI^2 over a validation range of 0-30 CI.

$$CI = 0.37 \times 10^{(0.00326 \times \theta)} \quad [28]$$

Where Θ is the TBP loads from March – June, with July loads added for warm Junes (water temperature > 20°C)

The authors acknowledge that phosphorous loads alone cannot predict HAB intensity, however it has been shown to be good indicators of HAB intensity [137,138,165,166]. The goal of this study is to understand the magnitude of potential HAB events and how reducing nutrient loads may reduce HAB severity, thus the authors concluded that this level of prediction was sufficient.

HAB Categories

HAB's were characterized into four categories based on their cumulative CI. These categories were based on NOAA's Western Lake Erie Bloom Severity Index combined with observing differences in HAB related pictures and news headlines. Conversion between NOAA's Western Lake Erie Bloom Severity Index and maximum cumulative CI shown in Appendix C 5.

Table 32 shows the different HAB categories, their corresponding cumulative CI's, water quality descriptions and category delineators.

Table 32: Table of the different HAB categories and the delineation between HAB categories

HAB Category	NOAA's Western Lake Erie Bloom Severity Index	Maximum Cumulative CI	Years	Water Quality	Category delineator
Low	0 - 2	< 2	2002, 2005-2007, 2012	Water is green tinted, with minor scum build up. Photos show people recreating in the water	Based on NOAA severity index.
Mild	2-4	2 ≤ CI < 3.6	2004, 2016, 2018	Water is green tinted, with minor scum build up.	Based on NOAA severity index
Medium	4 – 7	3.6 ≤ CI < 10	2003, 2008-2010, 2014	Water has decided green tint/paint like texture Columns show algae well mixed	The line between Medium and Severe events comes from 3 locations. First in the NOAA Severity index. Second, is photos of the HAB water columns; in 2014 (CI = 5.7), cyanobacteria were shown to be well mixed within the column, while in 2017 (CI = 13.2) the column showed significant scum formation (photos in Appendix C 6). Third, was a look at new articles. In 2010, there were only a few news story [169] found which directly talked about the HAB event. In 2014, news articles focused on the tap water ban in Toldeo, OH. In 2015 (CI = 29.2), there were multiple articles discussing the HAB event in Lake Erie [170–175] and 2017 (CI = 13.2) [176–182], including outside of the region. Therefore, a distinction between the 2014 and 2017 events needed to be drawn, and a CI of 10 was used.
Severe	> 7	> 10	2011, 2013, 2015, 2017	Water is dark green in color, with thick texture. Columns show thick scum layer	

4.2.4 Economic Factors

4.2.4.1 Geographic impacts

For this study, three Ohio counties were considered; Lucas, Ottawa and Erie. To understand geographic spread for each HAB type, the percentage of coastline with local CI > 0.001 was calculated using 10 day-CI composites satellite photos from Stumpf 2016 with an expanded data set provided by Stumpf in a personal communication [137]. A local CI value considers the biomass within one pixel in the satellite image, and a local CI value of 0.001 equals 10^5 cells $(mL)^{-1}$ [137,168]. The average percentage of a county's affected coastline was calculated for each HAB category by considering the average percentage of affected coastline each HAB season, Table 33. The economic damages felt by each county were assumed to be in direct proportion to percentage of affected coastline.

Table 33: Average percentage of each county experiencing a HAB event (local CI > 0.001) for each HAB category

County	Low	Mild	Medium	Severe
Lucas	78%	95%	100%	100%
Ottawa	64%	69%	82%	88%
Erie	40%	42%	42%	65%

4.2.4.2 Real Estate

Lakefront real estate was assumed to incur a loss of 12% due to the presences of HAB's (local CI > 0.001). Average lake front homes were assumed to be evenly distributed along the coast. Indirect losses were also considered and were defined as the difference in values if HABs did occur versus if they did not. Home values were assumed to continue to appreciate at the current real estate growth rates for each county as reported on Zillow, which consolidates information from respective municipal governments [183].

Home values are highly influenced by natural disasters, but these dips in home values typically do not persist long after the negative effects of the event have past [184–186]. For instance, home values

can rebound within a few months after an oil spill is cleaned up [187,188]. One difference with HAB's is that they tend to be annual events. Home values were assumed to have a 2-year memory for HAB events and regain 97% of the lost value with no HAB events over a 2 year period[189,190]. Full inputs for the HAB-related real estate economic damages is available in Appendix C 7.

4.2.4.3 Recreation

For recreational losses, three different types of recreators were evaluated; anglers, beachgoers and non-users, i.e. residents who value clean water. For the beachgoers and anglers, both real and consumer welfare losses were considered. Real losses are dollars not spent in the area due to canceled or replaced trips, where replaced trips were defined as trips where recreators would change their recreation location based on the presence of HAB's. Welfare losses are the reduction in value from the trip/activity felt by the recreator. Growth in the number of recreators was calculated using historical fishing license sales and National Park attendance for anglers and beachgoers, respectively. Full equations for calculating the HAB-related economic losses for all recreator types, as well as detailed model inputs and equations can be found in Appendix C 7 and Appendix C 10, respectively. All economic values were adjusted to 2018 dollars using the Consumer Price Index [191].

Fishing licenses sales decreased by 11% in counties during months that were affected by HABs (local CI > 0.001) [192]. All trips associated with unbought fishing licenses were assumed to be canceled. Approximately 48% of all angling trips occur during the HAB season and have the potential to be replaced[193]. Average coastline CI was used to predict the number of replaced trips Appendix C 8[194].

Five beaches were identified that allow public access to Lake Erie's Western Basin; Maumee Bay, Kelley's Island, East Harbor, Nickel Plate and Lakeview Park. Average local CI for each beach for each HAB category were used to predict replaced trips and welfare losses, Appendix C 9[194,195]. Beach visits were assumed to be uniform over the summer months (May – September).

Non-user based losses were based on a willingness to pay (WTP) for water quality improvements based on the work by Johnston and Thomassin [196]. WTP is tied to the water quality as defined by the water quality ladder [197]. Starting water quality levels of 5, 3, and 1 were set for low/mild, medium and severe blooms, respectively, and water quality level of 7 was set as the desired level [197].

4.2.4.4 Tourism

Tourism has been hypothesized to be the greatest contributors to HAB related economic losses. It is also the least understood economic indicator and represents the greatest uncertainty when estimating losses [134,135,198,199]. Currently, Lake Erie is showing growth in tourism-related spending each year, despite the annual occurrence of HAB's [200,201]. However, many studies continue to show that tourism habits and spending are, or will be, affected by the presence of HABs even if these changes have not been quantified [134,135,202–204]. To address these issues, we considered other industries and natural events to act as corollaries for future HAB events. Full inputs for the HAB related tourism economic damages model is available in Appendix C 7.

Tourism spending and visits were assumed to be uniform over the year, such that 25% of all tourist trips occur during HAB months (mid-July – mid-September) and are susceptible to HAB-related tourism trip reductions. Tourism spending was assumed to grow at a rate of 4.5% per year if no HAB event occurs [200,201]. Tourism reductions were assumed to be in proportion to the percentage of coastline affected by the HAB's (local CI > 0.001), Table 33. For the low and mild HAB's, a 1% reduction in tourism visits was assumed during the HAB susceptible months, equating to a 0.25% reduction in annual tourism spending.

For the Medium HAB events, the more significant reduction in water quality was assumed to have a greater impact on tourist behavior. Reduced water quality for beach towns was assumed to correlate with reduced snow quality for ski areas. This corollary was chosen for several reasons; first, snow and lake-based tourism attract similar types of visitors, with the majority being local or day

trippers, and second, that the quality of the snow/water influences tourist experience. Ski area tourist visits are reduced by 5-25% in low snow years compared to typical years, Appendix C 11[205–208]. For Medium HAB events, tourist visits were assumed to decrease by 11% during the HAB season equating to a 2.5% reduction in tourism spending. Tourism related losses were calculated using Equations [29]-[31].

$$Tourism\ Spending_{t,no\ HABs} = Tousim\ Spending_{\ t-1} \times (\ 1 + Tousim\ Growth) \quad [29]$$

$$Tourism\ Spending_{t,HABs} = \left(1 - HAB\ Tourism\ Reduction_{Mild/Med}\right) \times\ Tousim\ Spending_{\ t} \quad [30]$$

$$Tourism\ Losses_t = \ Tourism\ Spending_{t,no\ HABs} - \ Tourism\ Spending_{t,HABs} \quad [31]$$

Where *Tourism Spending* $_{t,\ No\ HABS}$ is the estimate amount of tourism dollars that would be spent in the area if no HABs occurred in year *t*; *Tourism Spending*$_{t-1}$ is the estimated amount of tourism dollars that would be spent in the area if no HABs occurred in year *t-1*;*Tourism Growth* is the annual percentage growth in tourism spending (4.5%); *Tourism Spending* $_{t,\ HABS\ =\ Med/Mild}$ is the estimate amount of tourism dollars that would be spent in the area if a Low/Mild or Medium HABs occurred in year *t*; *HAB Tourism Reduction*$_{Med/Mild}$ is the amount (percent) tourism dollars are reduced because of a Low/Mild or Medium HAB; *Tourism Losses* $_t$ is the total amount of tourism dollars not spent in the area due to the presence of HABs in year *t.*

Some studies have equated HAB events with oil spills [202,209]. Both events impair the water, negatively affect local wildlife and can produce unpleasant odors. Oil spills are well known to have dramatic effects of local tourism with tourism spending reduced between 1-35% from the previous year's spending, Appendix C 12[188,209,210]. For Severe HAB events, tourism spending was assumed to be reduced by 3.5% from the previous year's total spending, or a 33.7% reduction in tourist visits, Equation [32].

$$Tourism\ Spending_{t,HAB=Severe} = (1 - HAB\ Tourism\ Reduction_{Severe}) \times Tousim\ Spending_{\ t-1} \quad [32]$$

Where

Tourism Spending $_{t,\ HABS\ =\ Severe}$ is the estimate amount of tourism dollars that would be spent in the area if a Severe HABs occurred in year *t*; *HAB Tourism Reduction*$_{Severe}$ is the amount (percent) tourism dollars are reduced from the previous years' spending because of a Severe HAB.

For example, if annual tourism spending is $100k in year 1, we would expect annual tourism spending to be $104.5k in year 2 (growth of 4.5%). If a severe HAB even occurred in year 2, estimated tourism spending would be $96.5k. Therefore, the total loss experienced is $8k. This model assumes tourism spending will rebound after a severe HAB event, such that, in year 3 of this example, tourism spending would be $109.2k (a 4.5% growth from the expected spending if no HAB event had occurred). This is consistent with oil spill impact reports which show tourism spending reaching pre-oil spill predictions. For instance, if tourism spending was predicted to reach $9 million in year 3 before the oil spill, post-oil spill analysis still predict tourism spending will reach $9 million in year 3 [209].

4.2.4.5 Drinking Water

The predominant cyanobacteria species for Lake Erie HAB's are *Microcystis*, which produce a toxin, *Microcystin,* which can cause shortness of breath, nausea/diarrhea, fever, skin irritation and liver damage [211]. Failure to remove these toxins makes water unsafe for drinking or general use, such as in 2014 when the city of Toledo had to issue warnings against using local water due to high *Microcystin* concentrations [212]. Ten drinking water facilities were identified which draw from the western basin of Lake Erie, Appendix C 13. Average local CI for each drinking water intake for different HAB categories were calculated by estimating the average local CI at the facility intake from the satellite images over the HAB season, Appendix C 14. HAB-related losses are associated with additional treatment costs which

are a function of *Microcystin* concentration. Capital costs were assumed to be a function of the highest recorded *Microcystin* concentrations, Appendix C 15, while operational costs were assumed to be a function of the current *Microcystin* concentrations, Appendix C 16[213]. *Microcystin* concentrations were used to calculate required powdered activated carbon (PAC) dosing requirements using Equations [33] - [35]. Full inputs for the HAB-related drinking water economic damages model can be found in Appendix C 7.

$$PAC\ dose_{\ min}\left[\frac{mg}{L}\right] = \frac{[C_i - C_f]}{q} \times 1000 \quad [33]$$

$$q = K_f {C_f}^{1/n} \quad [34]$$

$$PAC\ dose\left[\frac{mg}{L}\right] = PAC\ dose_{\ min}\left[\frac{mg}{L}\right] \times Safety\ Factor \quad [35]$$

Where C_i is the initial *Microcystin* concentration [ug L^{-1}]; C_f is the final *Microcystin* concentration [ug L^{-1}]; *q* is the loading of *Microcystin* on carbon; K_f is the empirical constant for the absorption capacity; *1/n* is the empirical constant for the intensity of absorption.

4.2.5 Economic Analysis

A 30-cash flow for HAB related losses and technology costs was created for the BAU scenario and each technology scenario. The cash-flows were used to predict the NPV of the total economic losses for Lake Erie communities (HAB-related losses plus technology costs) using a discount rate of 3%. Technology-related capital expenditures were paid for by a 20-year loan with an interest rate of 1.7% [214]. All technology solutions were modeled as starting in year 5 to allow time for capital infrastructure to be built with additional inputs presented in Appendix C 7.

4.2.6 Monte Carlo Analysis

A Monte Carlo analysis was performed using 10,000 simulations of predicted phosphorous loads to Lake Erie through the Maumee river. This number of iterations gives 95% confidence that the mean is

within 1% of its real value (i.e. has sufficient convergence) [215]. For each iteration, a random value within each given distribution for TP springtime loads and %DRP were chosen for each year (1-30) of the analysis and a cash-flow of HAB-related and technology costs was created. The average annual NPV of losses was then calculated within each cash flow, and a 90% confidence interval was created for each scenario.

4.2.7 Sensitivity Analysis

A sensitivity analysis was performed on Business as Usual case and all technology cases to identify which variables which have the significant impacts on the model. Each variable was varied individually by +/- 20%, and the Monte-Carlo analysis was reperformed using 5,000 iterations, with the changes to NPV being recorded for each variable change. A Student's t-test was then performed using JMP software to identify which variables are significant based on a 95% confidence interval.

4.2.8 Scenario Analysis

In addition to the distribution-information nutrient scenario outlined above, "Baseline Nutrient", three additional phosphorous scenarios were also considered. The first alternative scenario considers a 40% reduction in TP loads, which reflects current policy targets, "Policy Scenario" [123]. In this scenario, springtime loads are chosen from the initial normal distribution but are reduced by 40% before predicting HAB severity, with the %DRP randomly defined from the triangle distribution. In the second scenario, %DRP increases linearly over time from 21% to 30% (DRP Increasing Scenario). The third scenario looks at %DRP decreasing linearly over time from 21% to 10% (DRP Decreasing Scenario). For both DRP scenarios, total phosphorous is randomly informed from the TP distribution each year.

4.3 Results and Discussion

4.3.1 Baseline Nutrient Scenario Results

Thirty-year cash flows for HAB-related economic losses were created and used to find the NPV of annual economic losses for the BAU and the different technologies outlined. Examples of these 30-year cash flows is available for each scenario in Appendix C 18. Net annual losses for each case from the Monte Carlo analysis were then compared to identify potential long-term economically viable solutions for HAB mitigation. Figure 33A shows a breakdown of the median HAB-related annual losses and technology costs with complete results from the Monte Carlo simulation presented in Figure 33B.

A)

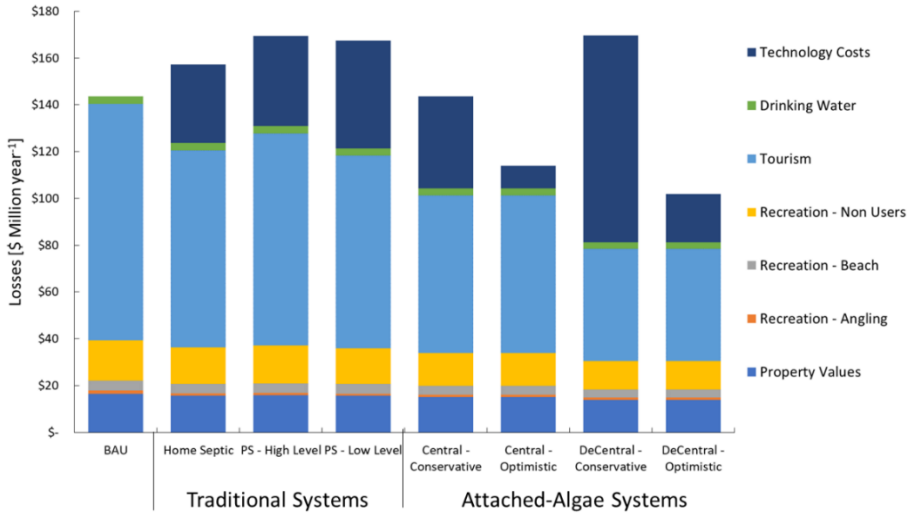

B)

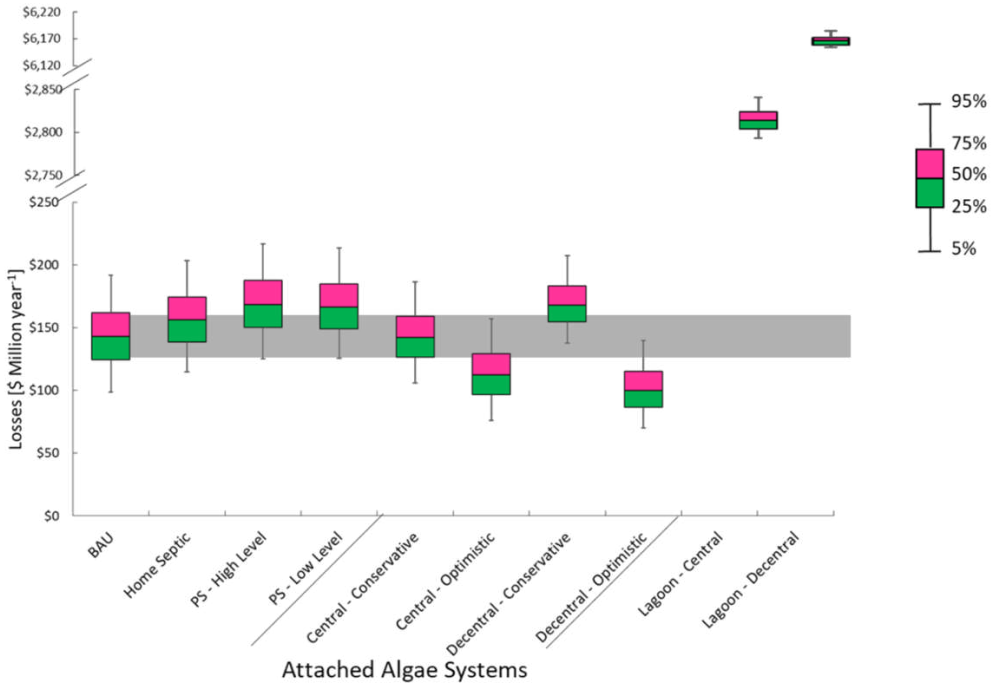

Figure 33: A) Breakdown of the median annual HAB-related losses and technology costs for the BAU and technology cases. Lagoon cases were excluded for brevity but their losses breakdown can be found in Appendix C 17. B) Estimated losses for Lake Erie communities per year due to HAB's for the "Baseline Nutrient" scenario. Reductions in economic losses are predicted for the Attached Algae – Centralized – Optimistic and Attached Algae – Decentralized – Optimistic. The horizontal gray bar shows the 25% - 75% confidence interval for the BAU case.

Results show the BAU case results in a median discounted loss of $142M (standard deviation of $29M) per year. All technology solutions are compared to this scenario. Traditional point-source nutrient reduction technologies do not show a reduction in losses compared to the BAU scenario, indicating that adopting these technologies would not be beneficial for Lake Erie. However, two attached-algae technologies show promise for reducing HAB related losses for Lake Erie communities; Centralized – Optimistic and Decentralized – Optimistic. The majority of HAB-related savings is from the tourism sector, suggesting a reduction of severe and medium HAB events from the BAU case. Decentralized systems reduce direct HAB-related losses more than the Centralized systems by removing more bio-available phosphorus though multiple points of contact between the river and the attached-algae systems, but also require more capital and operational costs. On average, the Decentralized systems removed twice as much bio-available phosphorus as the Centralized attached-algae systems. Results indicate that the increased phosphorus removal is worth the investment, with the Decentralized-Optimistic system showing the lowest annual losses per year, $100M. It is noted, that the technology solutions implemented do not always reduce HAB events from severe.

Reductions in HAB-related losses is considered the economic benefit of the technology. Economic benefits, annual technology's costs, benefit/cost ratio and average TBP reduction for each technology solution are shown in Table 34. Benefit/cost ratios greater than 1 indicate cost-effective HAB mitigation.

Table 34: Average annual cost and HAB related savings (benefits) for the different traditional and attached-algae system cases. Benefit-cost ratios over 1 indicate cost-effective HAB mitigation.

	Benefit [$M year^{-1}]	**Cost [$M year^{-1}]**	**Benefit/Cost**	**TBP Reduction**
Traditional Systems				
Home Septic Repair	$20	$34	0.6	7%
PS – High Limit	$13	$38	0.3	1%
PS – Low Limit	$22	$46	0.5	9%
Lagoon – Central	$69	$2,729	0.0	42%
Lagoon - Decentral	$94	$6,088	0.0	70%
Attached-Algae Systems				
Central - Conservative	$39	$39	1.0	20%
Central - Optimistic	$39	$10	4.1	20%
Decentral - Conservative	$62	$88	0.7	42%
Decentral - Optimistic	$62	$21	3.0	42%

The adoption of traditional nutrient reduction technology for point source systems was not particularly effective. On average, bioavailable nutrients are reduced by 7%, 1% and 9% for the home septic, PS-High and PS-Low systems, respectively, leading to average annual benefits of $20M, $13M and $22M, respectively. These solutions are accompanied with significant capital and operational costs of $34M, $38M and $46M a year over the 30-year analysis. This results in a Benefit/cost ratio of 0.6, 0.3, and 0.5, respectively, which are all well below the target of 1. Most of the bioavailable phosphorus originates from non-point source sources; thus, targeting point source, while more straightforward, is not effective for HAB mitigation. Attached-algae systems show the most potential for cost-effective HAB mitigation, with two of the four modeled systems showing Benefit/Cost ratios > 1. The Centralized-Optimistic system has the greatest benefit/cost ratio, making it to be the most cost-effective phosphorous removal solution investigated.

Attached-algae systems' capacity for cost-effective HAB mitigation is highly dependent on capital costs and phosphorus removal assumptions. Currently, no studies have been conducted to study

nutrient removal using attached-algae systems along the Maumee River, however the areal nutrient removal used in this study is consistent with other studies conducted on impaired waters in other states. Capital costs are also very important. In this study, the attached-algae conservative scenario used capital costs which were 10x higher than those found using the optimistic case. Before implementation, the optimistic costing scheme would need to be verified for large-scale applications. Another benefit of the attached-algae system is the potential revenue stream from the algae biomass, and this opportunity should be explored but is not considered in this study as it was deemed outside the scope. The assumption in this study is the value of the algae grown is equivalent to the required costs for utilization.

4.3.2 *Sensitivity Analysis*

A sensitivity analysis was performed on the Business as Usual case to understand which aspects of the model have the greatest impact on annual HAB related losses, and results are shown in Figure 34. Variables whose t-value lie outside the critical t-value, shown in vertical green lines, are considered significant. Knowing which variables are significant highlights areas with which to improve understanding, reduce model uncertainty through additional research and optimize nutrient reduction technologies. For the Business as Usual case, variables associated with the bioavailability of phosphorus loads and tourism losses were found to be most significant.

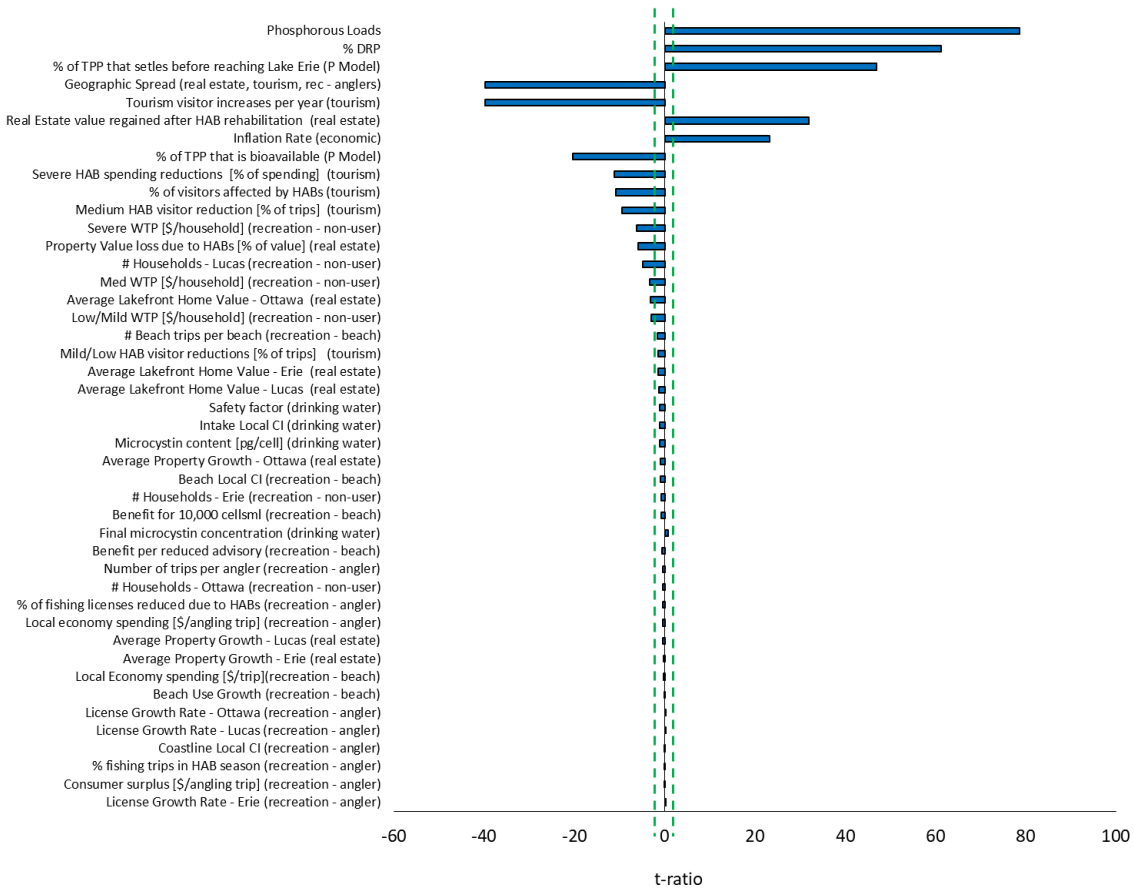

Figure 34: Results from the sensitivity analysis conducted in the BAU case for the Baseline Nutrient scenario. Horizontal lines show the critical t-ratio, variables whose t-ratio fall outside the critical t-ratio are considered significant.

The most significant variables were those than affected TBP loads; TP loads, %DRP and percentage of TPP that settles out of the river before it reaches Lake Erie. TP loads and %DRP Another similar variable is the percentage of TPP that is bioavailable. All of these variables are directly related to the amount of TBP that is available to fuel HAB events and have significant impact on the severity of HAB events each year of analysis. Results from this analysis informed the scenario analysis allowing researchers to understand how affecting phosphorous loads and composition can impact HAB-related losses. It is more difficult to change behaviors associated with TPP settling and bioavailability as these natural phenomena and are most likely out of researcher or policy maker control. In addition, the HAB

prediction model was created with these variables fixed, and its unknown how changing them would affect the prediction power of this model [137].

Tourism is responsible for considerable HAB-related annual losses, making these variables significant in our analysis. As previously stated, it is not well understood how HAB events affect tourism; however, there is a strong consensus in the literature that HAB's either do or will affect tourist behavior. This model used impacts of the other, better known natural events on tourism as corollaries for HAB's. If high beach demand continues or tourists become resilient to HAB's, these corollaries may not be appropriate, which would have significant impact on the analysis conducted herein. More research should be conducted to improve understanding of HAB events on tourist behavior, this economic variable is significant not only in this analysis, but many others [133–135,198].

4.3.3 Scenarios Analysis

A sensitivity analysis was conducted on model variable inputs, with results in the SI. Springtime TP loads and %DRP were found to be the most significant variables and were used to inform the scenario analysis. In the first case, phosphorus levels were reduced by 40% based on an assumed future policy which impacted farming practices. In the last two scenarios, the %DRP was either linearly increased or decreased to understand how changes in phosphorus composition effect the economics of HAB's and potential technologies modeled. Figure 35 A-C below show the results from the Monte Carlo analysis for the economic losses for the different scenarios with a direct comparison to the BAU case from the Baseline Nutrient scenario previously presented.

A)

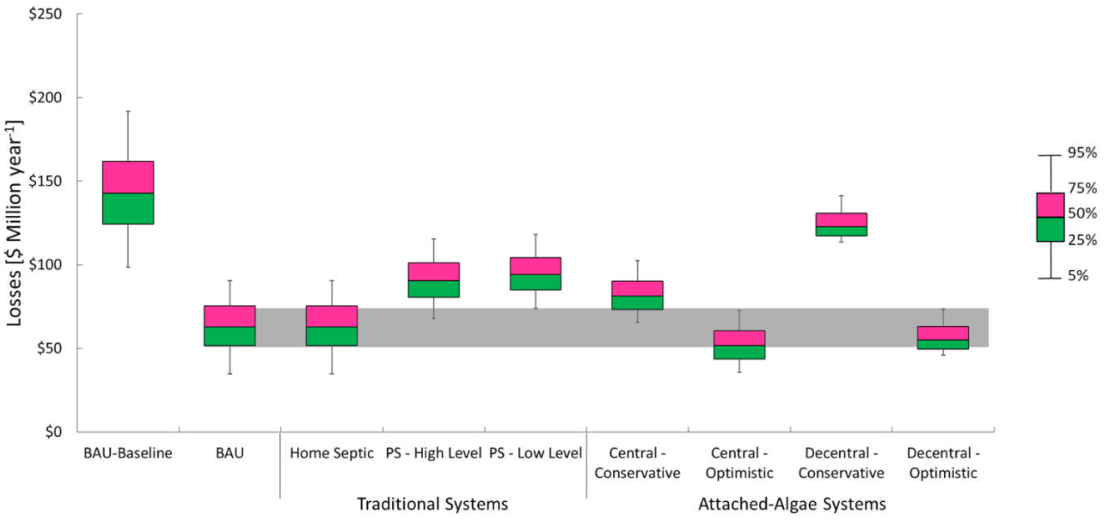
$250
$200
$150
$100
$50
$0
Losses [$ Million year-1]
95%
75%
50%
25%
5%
BAU-Baseline
BAU
Home Septic
PS - High Level
PS - Low Level
Central - Conservative
Central - Optimistic
Decentral - Conservative
Decentral - Optimistic
Traditional Systems
Attached-Algae Systems

B)

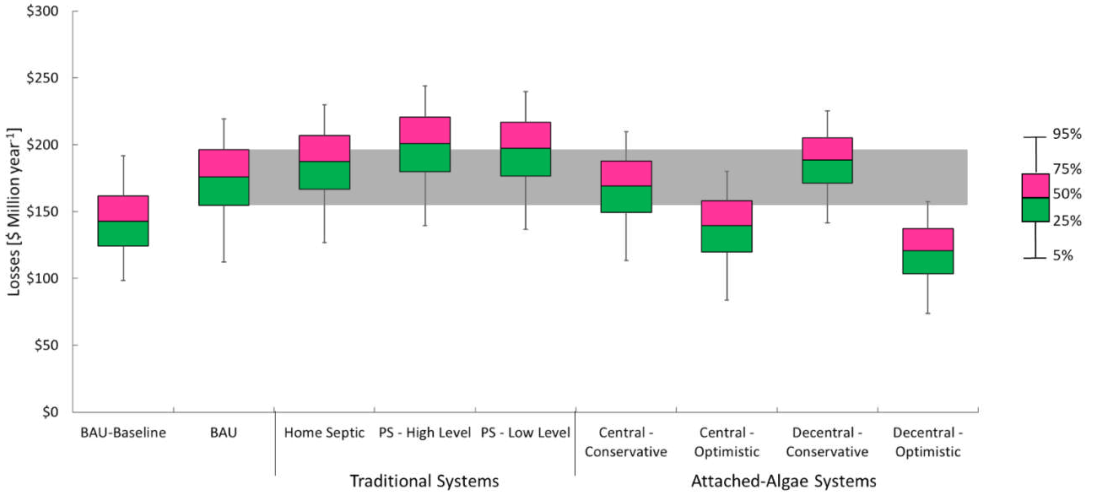
$300
$250
$200
$150
$100
$50
$0
Losses [$ Million year-1]
95%
75%
50%
25%
5%
BAU-Baseline
BAU
Home Septic
PS - High Level
PS - Low Level
Central - Conservative
Central - Optimistic
Decentral - Conservative
Decentral - Optimistic
Traditional Systems
Attached-Algae Systems

C)

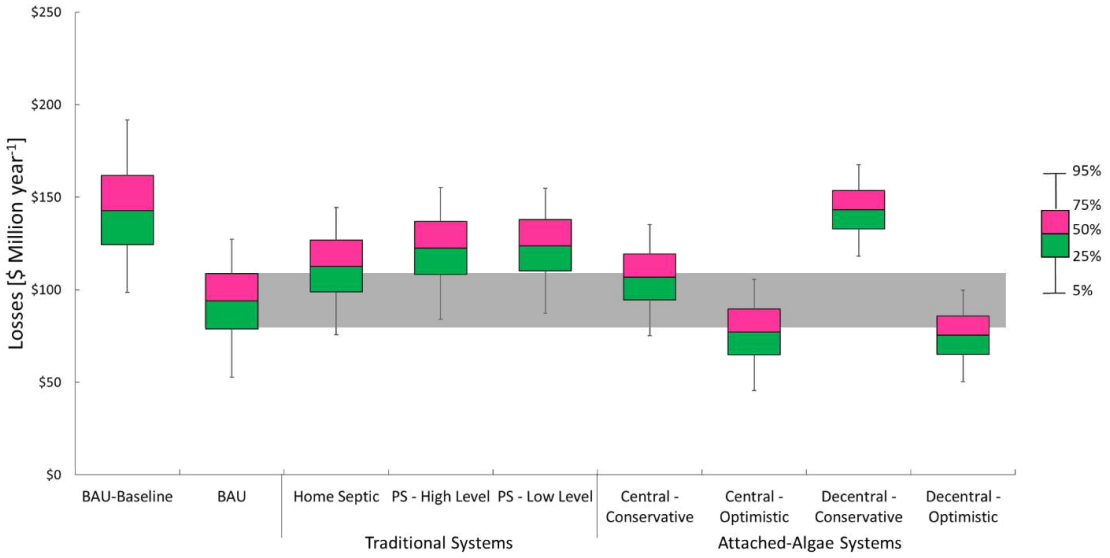

Figure 35: A) Estimated losses for Lake Erie communities per year due to HAB's for the Policy scenario, B) Increasing DRP scenario, and C) Decreasing DRP scenario. The gray horizontal bar shows the 25-75% confidence interval for annual losses for the BAU case for that scenario. All three panels include the BAU result from the Baseline Nutrient scenario for comparison. The lagoon systems were omitted for brevity; with losses over $2B and $6B per year for the centralized and decentralized lagoon systems, respectively, for all scenarios.

Changes in overall phosphorus levels, as shown in the Policy case Figure 35A, has the greatest impact on HAB related economic losses than changes in composition of the phosphorus alone, with average annual HAB-related losses reduced by $78M compared to the Baseline Nutrient scenario. For the DRP scenarios, Figure 35B and Figure 35C, the variance was much smaller. Average BAU HAB-related losses increased by $36M for the Increasing DRP case and decreased by $47M for the Decreasing DRP case.

All scenarios are important when considering how to best use policy to mitigate HAB events. The Policy scenario shows the greatest reduction to annual HAB-related losses. This scenario, however, hinges on significant phosphorus reductions and implementing this strategy would require dramatic changes to agriculture and ranching practices to achieve these results. The Decreasing DRP scenario, while not as effective as the Policy scenario, reduces annual HAB-related losses by 33%. Results of this scenario highlight the importance of targeting changes in phosphorus composition as an effective means

of HAB mitigation. Reducing DRP is also more effective in reducing overall annual HAB-related losses compared to any of the technology solutions investigated in the Baseline Nutrient scenario. Results from the Increasing DRP scenario stress the importance of not increasing DRP loads as the economic damages increase by 125% compared to the Baseline Nutrient scenario.

All scenarios show economic improvements through the implementation of attached-algae systems. The Centralized-Optimistic system reduces annual net losses for all three scenarios, while the Decentralized-Optimistic system reduced annual net losses for the DRP-related scenarios. The point source nutrient reduction technologies, as before, do not have a favorable result economically. These results indicate attached-algae systems have the potential to be beneficial for HAB mitigation, regardless of how phosphorous levels and composition change in the future while traditional technology solutions show limited efficacy.

4.3.4 Limitations

There is much uncertainty when attempting to quantify the economic impacts of natural events such as HAB's. One of the central limitations in this work is the HAB Prediction model. There are many factors which contribute to the formation and severity of HAB's besides eutrophication. For instance, warmer weather and calm winds encourage HAB growth, and yet are not accounted for in this model. HAB categories were used instead of CI to predict economic damages to reduce dependence on the absolute accuracy of the HAB prediction. In this instance, a wide range of phosphorus loads can cause similar HAB events to account of potential differences in other factors such as weather and currents.

This dependence on HAB categories also introduces another limitation of this model, especially for medium and severe events. Currently, economic damages are treated as a step function as the event moves from one HAB category to another, such that very severe events are subject to same losses as borderline severe events. Losses within a category are more likely to be a gradient, with more severe events causing more severe economic losses. Also, each future HAB event should act uniquely, while this

model assumes each HAB event within each category to be the same. Variability of behavior was accounted for by studying historical HAB's and taking averages of past behavior, such as geographic spread and localized CI. However, this HAB data only dates from 2002, so there is limited data to base these averages on. Values used here represent the averages available with current data.

Another limitation of this work lies in uncertainty surrounding future phosphorus loads and composition. Monte Carlo analysis combined with scenario analysis was used to understand how variations in phosphorus loads and composition affect HAB-related economics. The model used for Monte Carlo analysis estimates future loads and composition based on historical data, but this data set is limited and only consists of 36 years of data, and there is not sufficient data available to create a more robust model at this time. Scenario analysis was employed to encompass the most significant model variables and probable future trends.

This work focuses on phosphorous reduction for the Maumee River. The Maumee River is the source of the highest and most concentrated loads of phosphorus for western Lake Erie and is responsible for approximately 50% of all phosphorus entering the lake [129,148]. The model assumes that reducing phosphorous from the Maumee River is sufficient to mitigate HAB events, but this assumption would need to be validated.

HAB-related economic losses for three Ohio counties, Lucas, Ottawa and Erie, for four different economic variables are the basis of this model. These counties represent those most likely to impacted by HAB events in western Lake Erie but is not an exhaustive list. There are also other economic factors, such as commercial fishing and environmental factors which are not included. Therefore, the current model should be considered conservative, as other counties and industries are expected to be affected by HAB events from the area studied.

4.4 Conclusion

HAB's are an annual environmental disruption event for the western Lake Erie basin which produce environmental and economic hardships for the surrounding communities. To mitigate these effects, different nutrient reduction technologies were evaluated on their ability to reduce economic losses. A model was created to quantify the annual HAB-related economic losses over a 30-year period for the various nutrient reduction technologies. Attached algae systems were identified as a potential cost-effective solution for algae bloom mitigation, with average net savings between $12M - $42M per year. Attached algae systems were also effective in reducing economic losses across different nutrient loading scenarios. Addition of a revenue streams for the algae biomass may improve the system and should be explored as part of a holistic approach for HAB mitigation. Scenario analysis indicate reducing the fraction of DRP is an effective method for mitigating HAB's. Overall, attached algae systems show promise to reduce nutrients from non-point sources in a cost-effective manner.

CHAPTER 5: CONCLUSIONS

Engineering-based sustainable solutions offer a method to meet energy, water and food needs for a growing population while reducing environmental and resource burdens. TEA and LCA provide a means to measure economic viability and environmental impacts of these solutions while a technology is still in the research and development phase. These analyses can also be leveraged as part of a feedback loop with experimentalists to improve economic and environmental metrics through targeted, high impact research. The proposed works examine the application of TEA and LCA on two different novel emerging technologies as a part of that feedback loop. In addition, case studies are used to understand the limitations of LCA methodology as well as the development of economic modeling infrastructure that considered economic damages of technology deployment. The latter is the culmination of multiple multi-disciplinary efforts.

First, an algae-to-fuels pathway was examined. Initial research indicated that growth system cost, ash content and energy use were barriers to entry for this application. A second round of research and analysis focused on reducing ash content and examining low energy process alternatives. Results show improved economic viability and reduced environmental impact for this process; however, these conversion processes are still not competitive with conventional fuels or able to meet the RFS standard. Additional areas for targeted research were identified in Phase 2 and will lead to further research and analyses to improve these processes. LCA and TEA are integral in identifying research opportunities and play a key role in creating and adopting sustainable technologies with this system used as a case study to show the impact of this methodology on moving towards a sustainable solution.

The corn-ethanol process was also examined, with the intent of improving process economics and sustainability through the conversion of a waste co-product, DGS, to fuels. This process was shown to potentially improve economics, dependent on economic and protein market assumptions.

Improvement of environmental metrics were found to be more uncertain due to ambiguity in LCA methodology guidance. Co-product allocation methods and system boundary were found to have large effects on the LCA results, showing large variability within the results. From this, we find it is possible to manipulate a product's ability to achieve sustainability goals through strategic application of current LCA methodology, indicating a critical need for improved methodological guidance.

A novel consequential TEA methodology was also developed and applied to identify technology solutions for environmental disruptions such as HAB's. The methodology allowed for the dynamic exploration of the economic consequences of technology adoption to prevent HAB events. Economic benefits and technology costs were quantified for the adoption of four different nutrient reduction technologies for Lake Erie's Western Basin. Attached-algae systems were shown to cost effectively remove nutrients to proactively mitigate the annual HAB events in this area when considering direct and indirect economic impacts. Understanding the costs and benefits of technology adoption helps communities and policy makers make effective investments to prevent or mitigate these events. This methodology could be applied to other HAB affected areas or could adapted for other annual environmental disruptive events.

The research outlined above demonstrates a solid foundation in process modeling and advanced application of sustainability science for emerging technologies, while also being able to manipulate current methodology to new novel purposes.

CHAPTER 6: FUTURE WORK

This dissertation work has explored the application of sustainability sciences to three different technologies; the conversion of algae to renewable fuels, upgrading of DGS to fuels and higher value proteins, and nutrient reduction to pro-actively mitigate HAB's. Results identify the opportunity space of each technology and highlights specific areas for continued research and development such that large-scale implementation can be achieved. Future directions for targeted research and analysis for each technology are outlined below.

6.1 Conversion of algae to fuels

Three main areas were identified to improve the economic viability and reduce environmental impacts of the conversion of AAG algae to fuels; ash reduction, increasing fuel yields, and co-product development. Increased ash reduction may be possible through an additional ash removal process such as the use of filters in the AAG system to reduce TSS or strategic seeding of the algal turf. For all options, the costs and benefits of each system would need to be evaluated through sustainability science. For instance, adding filters in the AAG system may increase energy requirements for the pumping system. This cost would need to be weighed against the benefit of ash reduction through the downstream processing. An advantage of the work performed is the impacts are quantified on a systems level. An additional opportunity shown to drive the sustainability of the system is improving fuel yields. Increasing fuel yields may be possible through either catalyst integration in the HTL system or yeast consortium optimization and/or genetic engineering of the yeast strains in the fermentation system. While research should continue in those areas, the most promising option for this system is addition of co-products or co-services.

Future work should also focus on integrating the AAG system with environmental services and quantifying the impact of these services on renewable fuel economics and environmental impact. One

opportunity may be using AAG systems for pro-active HAB mitigation, explored in Chapter 4 of this dissertation work. Other opportunities for the AAG system are high-value metal reclamation (ex. Lithium) or the removal of hazardous metals (ex. Arsenic) from contaminated water systems. In addition to services, co-products should be explored. Currently, ash from the system is disposed in a landfill but compositional analysis indicates the ash could be used as a filler in construction materials such as concrete. Opportunities for ash co-products should also be explored, verified and incorporated into sustainability analysis.

Research should also be conducted to verify model assumptions. Current modeling work for the fermentation and HTL systems are based on adaptive kinetic models instead of direct experimental results using the AAG system algae. Results have recently been released showing HTL yields for the AAG system algae which should be incorporated into future models. In addition, fermentation experimentation should be conducted on the AAG algae to verify yields and fermentation products.

Lastly, the scalability of AAG needs to be explored. The AAG system has a variety of advantages but the scalability to meet DOE fuel targets has not been fully explored. The scalability of the AAG system is expected to be limited by resources that are very different from traditional algae systems. There is a need to better understand the large-scale potential of the technology integrated geographical information systems (GIS). The work outlined has defined the input requirements and corresponding performance. This could be coupled with data from GIS to better understand specific deployment locations with modeling work used to understand the performance and corresponding impact at scale.

6.2 Upgrading of Distiller's Grains

Economic modeling indicates that the DGS upgrading process may be close to commercialization if the upgraded proteins could be integrated into certain protein markets. Experimentation should be conducted on the upgraded proteins to identify these appropriate markets. PDCAAS and protein content suggest these proteins may be viable as an aquaculture alternative, but this would need to be verified.

The results from this work show the process is near economic viability. Prior to investment, some more detailed analysis needs to be completed. First, a consequential analysis which considers the impacts of DGS upgrading on feed and protein markets. Since DGS are currently used to supplement cattle feed, it is important to understand how removing that feed source would affect cattle and cattle feed markets. A few areas for potential analysis including identifying proteins to displace DGS for cattle feed, understanding the impacts of deferring proteins to different markets, potential land use changes, and effects on beef prices and wider economic impacts. It is also important to understand how this process plays into policy mandates. Currently, ethanol production from corn is capped at 15 billion GGE per year. Development of the proposed system would potentially impact the total yield from the industry. Research needs to explore how this would be viewed in terms of policy. Ethanol is a major constituent of the fusel alcohols mixture so it would be prudent to understand if ethanol production from DGS upgrading as a part of the fusel alcohols would contribute to the current mandated limit. If it does that dramatically changes the commercial viability of the system in the current regulatory environment.

This case study also identified critical limitations in LCA methodology. Through careful applications of different co-product methodologies, LCA's can be biased to generate m results that favor a certain product. These limitations can be overcome through improving guidance on choosing appropriate co-products methods and increasing transparency of LCA methodology within the analysis. Work needs to be dedicated to continuing to clarify and define appropriate methodology for systems that are outside the norm.

6.3 Attached Algae Systems and Harmful Algae Blooms

AAG systems have the potential to cost effectively remove nutrients from nutrient-rich waters to proactively mitigate HAB's. Experimentation needs to be performed locally at the Maumee river to

confirm nutrient removal assumptions used in this model. Economic inputs for the optimistic costing scheme should also be validated for industrial scale AAG systems.

In addition, process and economic optimization should be performed. First, the AAG system used here was sized to treat 50% of the average springtime flow rate and to remove 40% of incoming nutrients; these sizing criteria should be optimized to produce the most cost-effective nutrient reduction. Next, the AAG system should be updated to include revenue streams from the algae biomass or should integrated with a process which utilizes the algae. Some opportunities include AD, fuels production, or fertilizer applications. If fuels production or AD is desired, future research should focus on potential mixing or co-loading of local biomass with the algae feedstock. Cost-sharing between the fuel's producer and local communities may also be possible and should be considered in future scenarios.

In addition, this framework could also be adapted and applied to other waterbodies experiencing HAB's to investigate the economic viability of nutrient reduction technologies for those areas. The Gulf of Mexico is currently experiencing significant HAB events. This area represents a prime opportunity for evaluation. Or the framework could be modified for applications for other preventable environmental disruptions. One such application would be identifying technologies for heavy metal removal in areas affected by heavy metal poisoning. Lastly, continued increased regulation on nutrient discharge limitations represents an additional opportunity for the deployment of AAG systems that needs to be further investigated.

REFERENCES

(1) FAO. The Challenge of Global Agriculture towards 2050. *How to Feed World 2050* **2009**, 1–4.

(2) The United Nations. Water: A Shared Responsibility. World Water Development Report 2. **2006**, p.1-50. https://doi.org/10.7748/nm.21.4.12.s12.

(3) EIA. Annual Energy Outlook. *Energy Inf. Adm. U.S. Dep. Energy* **2008**.

(4) Keeble, B. R. The Brundtland Report: "Our Common Future." *Med. War* **1988**, *4* (1), 17–25. https://doi.org/10.1080/07488008808408783.

(5) U.S. Department of Energy. Bioenergy Technologies Office Strategic Plan. **2016**, 4–5.

(6) Elkington, J. *Cannibals With Forks: The Triple Bottom Line of 21st Century Business*; Captsone, Ed.; Oxford, 1997.

(7) Swanson, R. M.; Satrio, J. a; Brown, R. C.; Platon, A.; Hsu, D. D. Techno-Economic Analysis of Biofuels Production Based on Gasification. *Nrel* **2010**, *89* (November), S11–S19. https://doi.org/10.1016/j.fuel.2010.07.027.

(8) Pfromm, P. H.; Amanor-Boadu, V.; Nelson, R.; Vadlani, P.; Madl, R. Bio-Butanol vs. Bio-Ethanol: A Technical and Economic Assessment for Corn and Switchgrass Fermented by Yeast or Clostridium Acetobutylicum. *Biomass and Bioenergy* **2010**, *34* (4), 515–524. https://doi.org/10.1016/j.biombioe.2009.12.017.

(9) Quinn, J. C.; Davis, R. The Potentials and Challenges of Algae Based Biofuels: A Review of the Techno-Economic, Life Cycle, and Resource Assessment Modeling. *Bioresour. Technol.* **2015**, *184*, 444–452. https://doi.org/10.1016/j.biortech.2014.10.075.

(10) Humbird, D.; Davis, R.; Tao, L.; Kinchin, C.; Hsu, D.; Aden, A.; Schoen, P.; Lukas, J.; Olthof, B.; Worley, M.; Sexton, D.; Dudgeon, D. Process Design and Economics for Biochemical Conversion of Lignocellulosic Biomass to Ethanol. *Renew. Energy* **2011**, *303* (May), 147.

https://doi.org/10.2172/1013269.

(11) Davis, R.; Kinchin, C.; Markham, J.; Tan, E. C. D.; Laurens, L. M. L. Process Design and Economics for the Conversion of Algal Biomass to Biofuels : Algal Biomass Fractionation to Lipid- Products Process Design and Economics for the Conversion of Algal Biomass to Biofuels : Algal Biomass Fractionation to Lipid- and Carbohyd. **2014**, No. September, NREL/TP-5100-62368. https://doi.org/10.2172/1159351.

(12) Jones, S.; Zhu, Y.; Anderson, D.; Hallen, R. T.; Elliott, D. C. Process Design and Economics for the Conversion of Algal Biomass to Hydrocarbons : Whole Algae Hydrothermal Liquefaction and Upgrading. *Pnnl* **2014**, No. March, 1–69. https://doi.org/10.2172/1126336.

(13) Bare, J. C.; Norris, G. a; Pennington, D. W. The Tool for the Reduction and Assessment Impacts. *J. Ind. Ecol.* **2003**, *6* (3), 49–78. https://doi.org/10.1162/108819802766269539.

(14) Bennion, E. P.; Ginosar, D. M.; Moses, J.; Agblevor, F.; Quinn, J. C. Lifecycle Assessment of Microalgae to Biofuel: Comparison of Thermochemical Processing Pathways. *Appl. Energy* **2015**, *154*, 1062–1071. https://doi.org/10.1016/j.apenergy.2014.12.009.

(15) Frank, E. D.; Elgowainy, A.; Han, J.; Wang, Z. Life Cycle Comparison of Hydrothermal Liquefaction and Lipid Extraction Pathways to Renewable Diesel from Algae. *Mitig. Adapt. Strateg. Glob. Chang.* **2013**, *18* (1), 137–158. https://doi.org/10.1007/s11027-012-9395-1.

(16) Jorquera, O.; Kiperstok, A.; Sales, E. A.; Embiruçu, M.; Ghirardi, M. L. Comparative Energy Life-Cycle Analyses of Microalgal Biomass Production in Open Ponds and Photobioreactors. *Bioresour. Technol.* **2010**, *101* (4), 1406–1413. https://doi.org/10.1016/j.biortech.2009.09.038.

(17) United States Congress. Energy Information and Security Act of 2007. **2007**, 310.

(18) Davis, R.; Markham, J.; Kinchin, C.; Grundl, N.; Tan, E. C. D.; Humbird, D. Process Design and Economics for the Production of Algal Biomass: Algal Biomass Production in Open Pond Systems and Processing Through Dewatering for Downstream Conversion. *Natl. Renew. Energy Lab.* **2016**,

No. February, 128. https://doi.org/10.2172/1239893.

(19) Lynd, L.; Larson, E. Mature Technology. 2003. https://doi.org/10.16309/j.cnki.issn.1007-1776.2003.03.004.

(20) Merrow, E. W.; Phillips, K. E.; Myers, C. W. *Understanding Cost Growth and Performance Shortfalls in Pioneer Process Plants*; 1981.

(21) ISO_14040-2006 (1).Pdf.

(22) Davis, R.; Markham, J.; Kinchin, C.; Grundl, N.; Tan, E. C. D.; Humbird, D.; Davis, R.; Markham, J.; Kinchin, C.; Grundl, N.; Tan, E. C. D.; Humbird, D. Process Design and Economics for the Production of Algal Biomass : Algal Biomass Production in Open Pond Systems and Processing Through Dewatering for Downstream Conversion Process Design and Economics for the Production of Algal Biomass : Algal Biomass P. **2016**, No. February.

(23) Quinn, J. C.; Smith, T. G.; Downes, C. M.; Quinn, C. Microalgae to Biofuels Lifecycle Assessment - Multiple Pathway Evaluation. *Algal Res.* **2014**, *4* (1), 116–122. https://doi.org/10.1016/j.algal.2013.11.002.

(24) Molina Grima, E.; Belarbi, E. H.; Acién Fernández, F. G.; Robles Medina, A.; Chisti, Y. Recovery of Microalgal Biomass and Metabolites: Process Options and Economics. *Biotechnol. Adv.* **2003**, *20* (7–8), 491–515. https://doi.org/10.1016/S0734-9750(02)00050-2.

(25) Barlow, J.; Sims, R. C.; Quinn, J. C. Techno-Economic and Life-Cycle Assessment of an Attached Growth Algal Biorefinery. *Bioresour. Technol.* **2016**, *220*, 360–368. https://doi.org/10.1016/j.biortech.2016.08.091.

(26) Richardson, J. W.; Johnson, M. D.; Zhang, X.; Zemke, P.; Chen, W.; Hu, Q. A Financial Assessment of Two Alternative Cultivation Systems and Their Contributions to Algae Biofuel Economic Viability. *Algal Res.* **2014**, *4* (1), 96–104. https://doi.org/10.1016/j.algal.2013.12.003.

(27) Mata, T. M.; Martins, A. A.; Caetano, N. S. Microalgae for Biodiesel Production and Other

Applications: A Review. *Renew. Sustain. Energy Rev.* **2010**, *14* (1), 217–232. https://doi.org/10.1016/j.rser.2009.07.020.

(28) Campbell, M. N. Biodiesel : Algae as a Renewable Source for Liquid Fuel. *Guelph Eng. J.* **2008**, No. 1, 2–7. https://doi.org/1916-1107.

(29) Rawat, I.; Ranjith Kumar, R.; Mutanda, T.; Bux, F. Biodiesel from Microalgae: A Critical Evaluation from Laboratory to Large Scale Production. *Appl. Energy* **2013**, *103*, 444–467. https://doi.org/10.1016/j.apenergy.2012.10.004.

(30) Miao, X.; Wu, Q. Biodiesel Production from Heterotrophic Microalgal Oil. *Bioresour. Technol.* **2006**, *97* (6), 841–846. https://doi.org/10.1016/j.biortech.2005.04.008.

(31) Norsker, N. H.; Barbosa, M. J.; Vermuë, M. H.; Wijffels, R. H. Microalgal Production - A Close Look at the Economics. *Biotechnol. Adv.* **2011**, *29* (1), 24–27. https://doi.org/10.1016/j.biotechadv.2010.08.005.

(32) Richardson, J. W.; Johnson, M. D.; Outlaw, J. L. Economic Comparison of Open Pond Raceways to Photo Bio-Reactors for Profitable Production of Algae for Transportation Fuels in the Southwest. *Algal Res.* **2012**, *1* (1), 93–100. https://doi.org/10.1016/j.algal.2012.04.001.

(33) Moody, J. W.; McGinty, C. M.; Quinn, J. C. Global Evaluation of Biofuel Potential from Microalgae. *Proc. Natl. Acad. Sci.* **2014**, *111* (23), 8691–8696. https://doi.org/10.1073/pnas.1321652111.

(34) Pate, R.; Klise, G.; Wu, B. Resource Demand Implications for US Algae Biofuels Production Scale-Up. *Appl. Energy* **2011**, *88* (10), 3377–3388. https://doi.org/10.1016/j.apenergy.2011.04.023.

(35) Quinn, J. C.; Catton, K. B.; Johnson, S.; Bradley, T. H. Geographical Assessment of Microalgae Biofuels Potential Incorporating Resource Availability. *Bioenergy Res.* **2013**, *6* (2), 591–600. https://doi.org/10.1007/s12155-012-9277-0.

(36) Rogers, J. N.; Rosenberg, J. N.; Guzman, B. J.; Oh, V. H.; Mimbela, L. E.; Ghassemi, A.; Betenbaugh, M. J.; Oyler, G. A.; Donohue, M. D. A Critical Analysis of Paddlewheel-Driven Raceway Ponds for

Algal Biofuel Production at Commercial Scales. *Algal Res.* **2014**, *4* (1), 76–88. https://doi.org/10.1016/j.algal.2013.11.007.

(37) Harun, R.; Davidson, M.; Doyle, M.; Gopiraj, R.; Danquah, M.; Forde, G. Technoeconomic Analysis of an Integrated Microalgae Photobioreactor, Biodiesel and Biogas Production Facility. *Biomass and Bioenergy* **2011**, *35* (1), 741–747. https://doi.org/10.1016/j.biombioe.2010.10.007.

(38) Slade, R.; Bauen, A. Micro-Algae Cultivation for Biofuels: Cost, Energy Balance, Environmental Impacts and Future Prospects. *Biomass and Bioenergy* **2013**, *53* (0), 29–38. https://doi.org/10.1016/j.biombioe.2012.12.019.

(39) Hoffman, J.; Pate, R. C.; Drennen, T.; Quinn, J. C. Techno-Economic Assessment of Open Microalgae Production Systems. *Algal Res.* **2017**, *23*, 51–57. https://doi.org/10.1016/j.algal.2017.01.005.

(40) Higgins, B. . T. .; Kendall, A. Life Cycle Environmental and Cost Impacts of Using an Algal Turf Scrubber to Treat Dairy Wastewater . ATS Wastewater Characteristics ATS Systems Reduce Pollutant Concentrations through Biological Means and Through. *J. Ind. Ecol.* **2012**, *1*, 1–12.

(41) Wang, B.; Li, Y.; Wu, N.; Lan, C. Q. CO2 Bio-Mitigation Using Microalgae. *Appl. Microbiol. Biotechnol.* **2008**, *79* (5), 707–718. https://doi.org/10.1007/s00253-008-1518-y.

(42) Gudin, C.; Therpenier, C. Bioconversion of Solar Energy into Organic Chemicals by Microalgae. *Adv. Biotechnol. Processes* **1986**, *6*, 73–110.

(43) Adey, W. H.; Kangas, P. C.; Mulbry, W. Algal Turf Scrubbing: Cleaning Surface Waters with Solar Energy While Producing a Biofuel. *Bioscience* **2011**, *61* (6), 434–441. https://doi.org/10.1525/bio.2011.61.6.5.

(44) Brennan, L.; Owende, P. Biofuels from Microalgae-A Review of Technologies for Production, Processing, and Extractions of Biofuels and Co-Products. *Renew. Sustain. Energy Rev.* **2010**, *14* (2), 557–577. https://doi.org/10.1016/j.rser.2009.10.009.

(45) Davis, R.; Fishman, D.; Frank, E. D.; Wigmosta, M. S.; Authors, C.; Aden, A.; Coleman, A. M.; Pienkos, P. T.; Skaggs, R. J.; Venteris, E. R.; Wang, M. Q. Renewable Diesel from Algal Lipids : An Integrated Baseline for Cost , Emissions , and Resource Potential from a Harmonized Model. No. June 2012.

(46) Jones, C. D.; Sharifi, A.; Andrew, R. M.; Smith, P.; Kraxner, F.; Nakicenovic, N.; Fuss, S.; Yamagata, Y.; Jackson, R. B.; Canadell, J. G.; Ciais, P.; Peters, G. P.; Raupach, M. R.; Le Quéré, C.; Tavoni, M. Betting on Negative Emissions. *Nat. Clim. Chang.* **2014**, *4* (10), 850–853. https://doi.org/10.1038/nclimate2392.

(47) Primus, F. J.; Goldenberg, M. D.; Hills, S. United States Patent (19). **1991**, No. 19. https://doi.org/10.1016/j.(73).

(48) Liu, F.; Wu, W.; Tran-Gyamfi, M. B.; Jaryenneh, J. D.; Zhuang, X.; Davis, R. W. Bioconversion of Distillers' Grains Hydrolysates to Advanced Biofuels by an Escherichia Coli Co-Culture. *Microb. Cell Fact.* **2017**, *16* (1), 1–14. https://doi.org/10.1186/s12934-017-0804-8.

(49) Kim, N.-J.; Li, H.; Jung, K.; Chang, H. N.; Lee, P. C. Ethanol Production from Marine Algal Hydrolysates Using Escherichia Coli KO11. *Bioresour. Technol.* **2011**, *102* (16), 7466–7469. https://doi.org/https://doi.org/10.1016/j.biortech.2011.04.071.

(50) USDA. The Economic Feasibility of Ethanol Production from Sugar in the United States. **2006**, No. July.

(51) Lane, P.; Davis, R. W.; Hewson, J.; Siccardi, A.; Kipp, P.; Truscott, S.; Wyatt, N.; Lane, T. Nutrient Recycling for Sustained Algal Production. In *Algal Biomass Summit*; 2014.

(52) Valdez, P. J.; Tocco, V. J.; Savage, P. E. A General Kinetic Model for the Hydrothermal Liquefaction of Microalgae. *Bioresour. Technol.* **2014**, *163*, 123–127. https://doi.org/10.1016/j.biortech.2014.04.013.

(53) Sheehan, J. D.; Savage, P. E. Modeling the Effects of Microalga Biochemical Content on the

Kinetics and Biocrude Yields from Hydrothermal Liquefaction. *Bioresour. Technol.* **2017**, *239*, 144–150. https://doi.org/10.1016/j.biortech.2017.05.013.

(54) Short, W.; Packey, D. J.; Holt, T. A Manual for the Economic Evaluation of Energy Efficiency and Renewable Energy Technologies. **1995**, No. March. https://doi.org/10.2172/35391.

(55) Saydah, B. *Optimized Co-Processing of Algae Bio-Crude through a Petroleum Refinery*; 2014.

(56) Beal, C. M.; Gerber, L. N.; Sills, D. L.; Huntley, M. E.; Machesky, S. C.; Walsh, M. J.; Tester, J. W.; Archibald, I.; Granados, J.; Greene, C. H. Algal Biofuel Production for Fuels and Feed in a 100-Ha Facility: A Comprehensive Techno-Economic Analysis and Life Cycle Assessment. *Algal Res.* **2015**, *10*, 266–279. https://doi.org/10.1016/j.algal.2015.04.017.

(57) Towler, G.; Sinnott, R. *Chemical Engineering Design: Principles, Practice, and Economics of Plant and Process Design*; Butterworth-Heinemann: Oxford, 2008.

(58) Administration, U. S. E. I. Average Price of Electricity to Ultimate Customers https://www.eia.gov/electricity/annual/html/epa_02_04.html.

(59) Administration, U. S. E. I. United States Natural Gas Industrial Price https://www.eia.gov/dnav/ng/hist/n3035us3a.htm.

(60) De Mill, C. Integrated Life Cycle and Techno-Economic Assessment of the Conversion of High Productivity, Low Lipid Algae to Renewable Fuels, Utah State University, 2016.

(61) Hoffman, J.; Hoffman, J. Techno-Economic Assessment of Micro-Algae Production Systems By. **2016**.

(62) Pizarro, C.; Mulbry, W.; Blersch, D.; Kangas, P. An Economic Assessment of Algal Turf Scrubber Technology for Treatment of Dairy Manure Effluent. *Ecol. Eng.* **2006**, *26* (4), 321–327. https://doi.org/10.1016/j.ecoleng.2005.12.009.

(63) Ray, N. E.; Terlizzi, D. E.; Kangas, P. C. Nitrogen and Phosphorus Removal by the Algal Turf Scrubber at an Oyster Aquaculture Facility. *Ecol. Eng.* **2015**, *78*, 27–32.

https://doi.org/10.1016/j.ecoleng.2014.04.028.

(64) Kangas, P.; Mulbry, W. Nutrient Removal from Agricultural Drainage Water Using Algal Turf Scrubbers and Solar Power. *Bioresour. Technol.* **2014**, *152*, 484–489. https://doi.org/10.1016/j.biortech.2013.11.027.

(65) USDA - NASS. Land Values 2019 Summary. **2019**, No. August.

(66) GOLUEKE, C. G.; OSWALD, W. J.; GOTAAS, H. B. Anaerobic Digestion of Algae. *Appl. Microbiol.* **1957**, *5* (1), 47–55. https://doi.org/10.1128/aem.5.1.47-55.1957.

(67) Samson, R.; LeDuy, A. Biogas Production from Anaerobic Digestion Of. *Biotechnol. Bioeng.* **1982**, *XXIV*, 1979–1924.

(68) Ward, A. J.; Lewis, D. M.; Green, F. B. Anaerobic Digestion of Algae Biomass: A Review. *Algal Res.* **2014**, *5* (1), 204–214. https://doi.org/10.1016/j.algal.2014.02.001.

(69) Elgowainy, A., Dieffenthaler, D., Sokolov, V., Sabbisetti, R., Cooney, C., Anjum, A. GREET. Argonne National Laboratory 2017.

(70) Core Writing Team, R. K. P. and L. A. M. (eds. . *Climate Change 2014: Synthesis Report. Contribution of Working Groups I, II and III to the Fifth Assessment Report of the Intergovernmental Panel on Climate Change*; Geneva, Switzerland, 2014.

(71) Jensen, K. R. LOW PRESSURE, LOW HEAD BUOYANT PISTON PUMP FOR WATER PURIFICATION. 5131820, 1992.

(72) Davis, R. W.; Laboratories, S. N.; Ca, C. A. S. N. L.; Pate, R.; Laboratories, N.; Nm, N. M. S. N. L.; Wu, B.; Ca, S. N. L.; Drennen, T.; Nm, S. N. L. Updated Project Status and Feasibility Assessment of Polyculture Algal Turf to Fuels Project Goal : Investigate the Feasibility for Polyculture Algal Turf as a Promising Path to Algal Biofuels • New Paradigm Not Focused on Monoculture , Lipids , and PBRs .

(73) Keyzer, M. A.; Merbis, M. D.; Voortman, R. L. Notes and Communications: The Biofuel

Controversy. *Economist* **2008**, *156* (4), 507–527. https://doi.org/10.1007/s10645-008-9098-x.

(74) Luchansky, M. S.; Monks, J. Supply and Demand Elasticities in the U.S. Ethanol Fuel Market. *Energy Econ.* **2009**, *31* (3), 403–410. https://doi.org/10.1016/j.eneco.2008.12.005.

(75) Yang, Y.; Bae, J.; Kim, J.; Suh, S. Replacing Gasoline with Corn Ethanol Results in Significant Environmental Problem-Shifting. *Environ. Sci. Technol.* **2012**, *46* (7), 3671–3678. https://doi.org/10.1021/es203641p.

(76) Peplow, M. Cellulosic Ethanol Fights for Life. *Nature* **2014**, *507* (March), 4–5.

(77) Farrell, A. E.; Plevin, R. J.; Turner, B. T.; Jones, A. t.; O'Hare, M.; Kammen, D. M. Ethanol Can Contribute to Energy and Environmental Goals. *Science (80-.).* **2006**, *311* (January), 506–509.

(78) Pimentel, D.; Patzek, T. W. Ethanol Production Using Corn, Switchgrass, and Wood; Biodiesel Production Using Soybean and Sunflower. *Food, Energy, Soc. Third Ed.* **2007**, *14* (1), 311–332. https://doi.org/10.1201/9781420046687.

(79) Administration, U. S. E. I. Factors Affecting Gasoline Prices.

(80) Irwin, S. The Profitability of Ethanol Production in 2016. *farmdoc Dly.* **2017**, *7* (18).

(81) Luchansky, M. S.; Monks, J. Supply and Demand Elasticities in the U.S. Ethanol Fuel Market. *Energy Econ.* **2009**, *31* (3), 403–410. https://doi.org/10.1016/j.eneco.2008.12.005.

(82) Tiffany, D. G. Economic and Environmental Impacts of Ethanol Production From. *Fed. Reserv. Bank St. Louis Reg. Econ. Dev.* **2009**, *5* (1), 42–58.

(83) Liu, K. Chemical Composition of Distillers Grains , a Review. **2011**, 1508–1526. https://doi.org/10.1021/jf103512z.

(84) Arora, S.; Arora, S.; Wu, M.; Wu, M.; Wang, M.; Wang, M. Update of Distillers Grains Displacement Ratios for Corn Ethanol Life-Cycle Analysis. *Contract* **2008**, No. September. https://doi.org/10.2172/1004867.

(85) Adeola, O.; Ragland, D. Comparative Ileal Amino Acid Digestibility of Distillers' Grains for Growing

Pigs. *Anim. Nutr.* **2016**, *2* (4), 262–266. https://doi.org/10.1016/j.aninu.2016.07.008.

(86) Edwards, K.; Anex, C. R. P. Co-Product Allocation in Life Cycle Assessment: A Case Study Extended Abstract 2009-645-AWMA. *Analysis* **2009**, No. 651.

(87) Pak, T. Dairy Processing Handbook - Whey Processing https://dairyprocessinghandbook.com/chapter/whey-processing.

(88) Hurst, S.; Aplin, R.; Barbano, D. M. Whey Powder and Whey Protein Concentrate Production Technology, Costs and Profitability. *Cornell Progr. Dairy Mark. Policy* **1990**, No. April, 1–51.

(89) Association, I. R. F. Iowa Ethanol Biorefineries https://iowarfa.org/ethanol-center/ethanol-biorefineries/.

(90) Rendleman, C. M.; Shapouri, H. New Technologies in Ethanol Production. *Semin. Ser.* **2007**, *Report Num* (14), 30. https://doi.org/Agricultural Economic Report Number 842.

(91) Agriculture, U. S. D. of. National Weekly Feedstuff Wholesale Prices https://www.ams.usda.gov/mnreports/ms_gr852.txt.

(92) Hardy, W. L. COSTS, Process and Construction Spray Drying Costs. *Ind. Eng. Chem.* **1955**, *47* (10), 73A-74A. https://doi.org/10.1021/ie50550a008.

(93) Energy, O. of E. E. and R. Energy Department Announces $11.3 Million Available for Mega-Bio: Bioproducts to Enable Biofuels https://www.energy.gov/eere/bioenergy/articles/energy-department-announces-113-million-available-mega-bio-bioproducts.

(94) Li, B.; Boiarkina, I.; Yu, W.; Huang, H. M.; Munir, T.; Wang, G. Q.; Young, B. R. Phosphorous Recovery through Struvite Crystallization: Challenges for Future Design. *Sci. Total Environ.* **2019**, *648*, 1244–1256.

(95) Molinos-Senante, M.; Hernández-Sancho, F.; Sala-Garrido, R.; Garrido-Baserba, M. Economic Feasibility Study for Phosphorus Recovery Processes. *Ambio* **2011**, *40* (4), 408–416. https://doi.org/10.1007/s13280-010-0101-9.

(96) Reeds, P.; Schaafsma, G.; Tomé, D.; Young, V. Criteria and Significance of Dietary Protein Sources in Humans. Summary of the Workshop with Recommendations. *J. Nutr.* **2000**, *130* (7), 1874S-6S. https://doi.org/10.1093/jn/130.7.1874S.

(97) Julien, C.; Petit, H. V.; Gervais, R.; Chouinard, P. Y.; Hassanat, F.; Benchaar, C.; Massé, D. I. Effects of Increasing Amounts of Corn Dried Distillers Grains with Solubles in Dairy Cow Diets on Methane Production, Ruminal Fermentation, Digestion, N Balance, and Milk Production. *J. Dairy Sci.* **2013**, *96* (4), 2413–2427. https://doi.org/10.3168/jds.2012-6037.

(98) Hoffman, J. R.; Falvo, M. J. Protein - Which Is Best? *J. Sport. Sci. Med.* **2004**, *3* (3), 118–130. https://doi.org/10.1016/j.compstruct.2011.11.030.

(99) Feedipedia. Corn Gluten Meal. *Anim. Feed Resour. Inf. Syst.* **2016**, No. Dm, 1–3.

(100) Montoya Martinez, C.; Nolasco Soria, H.; Carrillo Farnes, O.; Civera Cerecedo, R.; Alvarez Gonzalez, C.; Vega Villasante, F. Chemical Score of Different Protein Sources to Four Macrobrachium Species. *Lat. Am. J. Aquat. Res.* **2016**, *44* (4), 835–844. https://doi.org/10.3856/vol44-issue4-fulltext-19.

(101) Cruz-Suárez, L. E.; Nieto-López, M.; Guajardo-Barbosa, C.; Tapia-Salazar, M.; Scholz, U.; Ricque-Marie, D. Replacement of Fish Meal with Poultry By-Product Meal in Practical Diets for Litopenaeus Vannamei, and Digestibility of the Tested Ingredients and Diets. *Aquaculture* **2007**, *272* (1–4), 466–476. https://doi.org/10.1016/j.aquaculture.2007.04.084.

(102) Wang, M.; Wu, M.; Huo, H. Life-Cycle Energy and Greenhouse Gas Emission Impacts of Different Corn Ethanol Plant Types. **2007**. https://doi.org/10.1088/1748-9326/2/2/024001.

(103) Wang, M.; Han, J.; Dunn, J. B.; Cai, H. Well-to-Wheels Energy Use and Greenhouse Gas Emissions of Ethanol from Corn , Sugarcane and Cellulosic Biomass for US Use. https://doi.org/10.1088/1748-9326/7/4/045905.

(104) Marland, G.; Turhollow, A. F. CO2emissions from the Production and Combustion of Fuel Ethanol

from Corn. *Energy* **1991**, *16* (11–12), 1307–1316. https://doi.org/10.1016/0360-5442(91)90004-6.

(105) Fréon, P.; Durand, H.; Avadí, A.; Huaranca, S.; Orozco Moreyra, R. Life Cycle Assessment of Three Peruvian Fishmeal Plants: Toward a Cleaner Production. *J. Clean. Prod.* **2017**, *145*, 50–63. https://doi.org/10.1016/j.jclepro.2017.01.036.

(106) Dalgaard, R.; Schmidt, J.; Halberg, N.; Christensen, P.; Thrane, M.; Pengue, W. A. LCA for Food Products LCA for Food Products (Subject Editor : Niels Jungbluth) Case Study LCA of Soybean Meal. **2008**, *10* (7), 240–254.

(107) Beauchemin, K. A.; Henry Janzen, H.; Little, S. M.; McAllister, T. A.; McGinn, S. M. Life Cycle Assessment of Greenhouse Gas Emissions from Beef Production in Western Canada: A Case Study. *Agric. Syst.* **2010**, *103* (6), 371–379. https://doi.org/10.1016/j.agsy.2010.03.008.

(108) Nations, F. and A. O. of the U. *Food Energy - Methods of Analysis and Conversion Factors*; 2003.

(109) Ling, T.; Aden, A. The Economics of Current and Future Biofuels. In *Biofuels*; Tomes, D., Lakshmanan, P., Songstad, D., Eds.; Springer: New York, NY, 2011.

(110) Cruce, J.; Quinn, J. C. Economic Viability of Multiple Algal Biorefining Pathways and the Impact of Public Policies. *Appl. Energy* **2019**, *233–234* (1), 735–746.

(111) O'Neil, J. M.; Davis, T. W.; Burford, M. A.; Gobler, C. J. The Rise of Harmful Cyanobacteria Blooms: The Potential Roles of Eutrophication and Climate Change. *Harmful Algae* **2012**, *14*, 313–334. https://doi.org/10.1016/j.hal.2011.10.027.

(112) Pick, F. R. Blooming Algae: A Canadian Perspective on the Rise of Toxic Cyanobacteria. *Can. J. Fish. Aquat. Sci.* **2016**, *73* (7), 1149–1158. https://doi.org/10.1139/cjfas-2015-0470.

(113) Wang, J.; Wu, J. Occurrence and Potential Risks of Harmful Algal Blooms in the East China Sea. *Sci. Total Environ.* **2009**, *407* (13), 4012–4021. https://doi.org/10.1016/j.scitotenv.2009.02.040.

(114) Al Shehhi, M. R.; Gherboudj, I.; Ghedira, H. An Overview of Historical Harmful Algae Blooms

Outbreaks in the Arabian Seas. *Mar. Pollut. Bull.* **2014**, *86* (1–2), 314–324. https://doi.org/10.1016/j.marpolbul.2014.06.048.

(115) Hernández-Becerril, D. U.; Alonso-Rodríguez, R.; Álvarez-Góngora, C.; Barón-Campis, S. A.; Ceballos-Corona, G.; Herrera-Silveira, J.; Castillo, M. E. M. Del; Juárez-Ruíz, N.; Merino-Virgilio, F.; Morales-Blake, A.; Ochoa, J. L.; Orellana-Cepeda, E.; Ramírez-Camarena, C.; Rodríguez-Salvador, R. Toxic and Harmful Marine Phytoplankton and Microalgae (HABs) in Mexican Coasts. *J. Environ. Sci. Heal. - Part A Toxic/Hazardous Subst. Environ. Eng.* **2007**, *42* (10), 1349–1363. https://doi.org/10.1080/10934520701480219.

(116) Lewitus, A. J.; Horner, R. A.; Caron, D. A.; Garcia-Mendoza, E.; Hickey, B. M.; Hunter, M.; Huppert, D. D.; Kudela, R. M.; Langlois, G. W.; Largier, J. L.; Lessard, E. J.; RaLonde, R.; Jack Rensel, J. E.; Strutton, P. G.; Trainer, V. L.; Tweddle, J. F. Harmful Algal Blooms along the North American West Coast Region: History, Trends, Causes, and Impacts. *Harmful Algae* **2012**, *19*, 133–159. https://doi.org/10.1016/j.hal.2012.06.009.

(117) Administration, N. O. and A. Gulf of Mexico/Florida: Harmful Algal Blooms.

(118) Administration, N. O. and A. Great Lakes: Harmful Algal Blooms.

(119) Administration, N. O. and A. West Coast/Alaska: Harmful Algae Blooms https://oceanservice.noaa.gov/hazards/hab/west-coast.html (accessed Jan 4, 2020).

(120) Chislock, M. F., Doster, E., Zitomer, R. A. & Wilson, A. E. Eutrophication: Causes, Consequences, and Controls in Aquatic Ecosystems. *Nat. Educ. Knowl.* **2013**, *4* (4), 10. https://doi.org/10.1002/j.1551-8833.1969.tb03755.x.

(121) Sellner, K. G.; Doucette, G. J.; Kirkpatrick, G. J. Harmful Algal Blooms: Causes, Impacts and Detection. *J. Ind. Microbiol. Biotechnol.* **2003**, *30* (7), 383–406. https://doi.org/10.1007/s10295-003-0074-9.

(122) Smith, D. R.; King, K. W.; Williams, M. R. What Is Causing the Harmful Algal Blooms in Lake Erie? *J.*

Soil Water Conserv. **2015**, *70* (2), 27A-29A. https://doi.org/10.2489/jswc.70.2.27A.

(123) Ohio, S. of. Domestic Action Plan 1.0. **2018**, No. February, 0–56.

(124) Deq, O.; Algal, H. Oregon DEQ Harmful Algal Bloom (HAB) Strategy. Appendix D. **2011**, No. June.

(125) Ontario Ministry of the Environment and Climate Change. *Canada-Ontario Lake Erie Action Plan: Partnering on Achieving Phosphorus Loading Reductions to Lake Erie from Canadian Sources*; 2018.

(126) Makarewicz, J. C.; Bertram, P. Evidence for the Restoration of the Lake Erie Ecosystem. *J. Great Lakes Res.* **1993**, *19* (2), 197. https://doi.org/10.1016/S0380-1330(93)71209-5.

(127) Kane, D. D.; Conroy, J. D.; Peter Richards, R.; Baker, D. B.; Culver, D. A. Re-Eutrophication of Lake Erie: Correlations between Tributary Nutrient Loads and Phytoplankton Biomass. *J. Great Lakes Res.* **2014**, *40* (3), 496–501. https://doi.org/10.1016/j.jglr.2014.04.004.

(128) Scavia, D.; David Allan, J.; Arend, K. K.; Bartell, S.; Beletsky, D.; Bosch, N. S.; Brandt, S. B.; Briland, R. D.; Daloğlu, I.; DePinto, J. V.; Dolan, D. M.; Evans, M. A.; Farmer, T. M.; Goto, D.; Han, H.; Höök, T. O.; Knight, R.; Ludsin, S. A.; Mason, D.; Michalak, A. M.; Peter Richards, R.; Roberts, J. J.; Rucinski, D. K.; Rutherford, E.; Schwab, D. J.; Sesterhenn, T. M.; Zhang, H.; Zhou, Y. Assessing and Addressing the Re-Eutrophication of Lake Erie: Central Basin Hypoxia. *J. Great Lakes Res.* **2014**, *40* (2), 226–246. https://doi.org/10.1016/j.jglr.2014.02.004.

(129) US EPA. Ohio Lake Erie Phosphorus Task Force Final Report. *Ohio EPA* **2010**, 109.

(130) Richards, R. P.; Baker, D. B.; Crumrine, J. P.; Stearns, A. M.; Erie, L. Unusually Large Loads in 2007 from the Maumee and Sandusky Rivers , Tributaries to Lake Erie Raisin. **2010**, *65* (6), 450–462. https://doi.org/10.2489/jswc.65.6.450.

(131) Joosse, P. J.; Baker, D. B. Context for Re-Evaluating Agricultural Source Phosphorus Loadings to the Great Lakes. *Can. J. Soil Sci.* **2011**, *91* (3), 317–327. https://doi.org/10.4141/cjss10005.

(132) Fussell, K.; Hesse, G.; Johnson, L.; King, K.; Labarge, G.; Martin, J.; Reutter, J.; Wilson, R.; Winslow,

C. Summary of Findings and Strategies to Move toward a 40% Phosphorus Reduction: A White Paper. **2017**, OHSU-EXT-1545.

(133) May 2015 General Abbreviations and Acronyms. **2015**, No. May.

(134) Smith, R. B.; Bass, B.; Sawyer, D.; Depew, D.; Watson, S. B. Estimating the Economic Costs of Algal Blooms in the Canadian Lake Erie Basin. *Harmful Algae* **2019**, *87* (June), 101624. https://doi.org/10.1016/j.hal.2019.101624.

(135) Bingham, M.; Sinha, S. K.; Lupi, F. Economic Benefits of Reducing Harmful Algal Blooms in Lake Erie. *Environ. Consult. Technol. Inc.* **2015**, 66.

(136) Craggs, R. J.; Adey, W. H.; Jenson, K. R.; St. John, M. S.; Green, F. B.; Oswald, W. J. Phosphorus Remocal from Wastewater Using an Algal Turf Scrubber. *Water Sci. Technol.* **1996**, *33* (7), 191–198.

(137) Stumpf, R. P.; Johnson, L. T.; Wynne, T. T.; Baker, D. B. Forecasting Annual Cyanobacterial Bloom Biomass to Inform Management Decisions in Lake Erie. *J. Great Lakes Res.* **2016**, *42* (6), 1174–1183. https://doi.org/10.1016/j.jglr.2016.08.006.

(138) Obenour, D. R.; Gronewold, A. D.; Stow, C. A.; Scavia, D. Using a Bayesian Hierarchical Model to Improve Lake Erie Cyanobacterial Bloom Forecasts. *J. Am. Water Resour. Assoc.* **2014**, *50* (10), 7847–7860. https://doi.org/10.1111/j.1752-1688.1969.tb04897.x.

(139) Baker, D. B. Tributary Data Download https://ncwqr.org/monitoring/data/.

(140) USGS. Site Map for Ohio. USGS 04193500 Maumee River at Waterville, OH https://waterdata.usgs.gov/nwis/inventory?agency_code=USGS&site_no=04193500.

(141) NASA. Giovanni https://giovanni.sci.gsfc.nasa.gov/giovanni/ (accessed Jan 4, 2020).

(142) Baker, D. B.; Confesor, R.; Ewing, D. E.; Johnson, L. T.; Kramer, J. W.; Merryfield, B. J. Phosphorus Loading to Lake Erie from the Maumee, Sandusky and Cuyahoga Rivers: The Importance of Bioavailability. *J. Great Lakes Res.* **2014**, *40* (3), 502–517.

https://doi.org/10.1016/j.jglr.2014.05.001.

(143) Ohio EPA. Nutrient Mass Balance Study for Ohio's Major Rivers. **2018**, 83.

(144) Magazine, C. E. Chemical Engineering Magazine Plant Cost Index.

(145) Health, O. D. of. *Ohio ' s Sewage Treatment System Rules How Is Sewage Treated across the State ?*

(146) Lombardo, P. Phosphorus Geochemistry in Septic Tanks, Soil Absorption Systems, and Groundwater. **2006**, 87.

(147) U.S. EPA. Decentralized Systems Technology Fact Sheet Septic System Tank. *United States Environ. Prot. Agency Off. Water Washington, D.C. EPA* **2000**, 1–4.

(148) Commission, L. E. Ohio Domestic Action Plan https://lakeerie.ohio.gov/LakeEriePlanning/OhioDomesticActionPlan2018.aspx (accessed Aug 10, 2019).

(149) Ohio Environmental Protection Agency by Tetra Tech. Cost Estimate of Phosphorus Removal At Wastewater Treatment Plants. **2013**, 1–49.

(150) USGS. Site Map for Ohio. USGS 04183500 Maumee River at Antwerp, OH https://waterdata.usgs.gov/nwis/inventory?agency_code=USGS&site_no=04183500.

(151) USGS. Site Map for Ohio. USGS 04192500 Maumee River at Definance, OH https://waterdata.usgs.gov/nwis/inventory?agency_code=USGS&site_no=04192500.

(152) United States Environmental Protection Agency. Free Water Surface Wetlands. *Environ. Prot. Agency* **2000**, 1–8. https://doi.org/EPA 832-F-00-024.

(153) Manual, W. P.; Section, C. Design Criteria ; Wastewater Treatment Lagoons. **2003**, *1049* (614).

(154) Omoike, A. I.; VanLoon, G. W. Removal of Phosphorus and Organic Matter Removal by Alum during Wastewater Treatment. *Water Res.* **1999**, *33* (17), 3617–3627. https://doi.org/https://doi.org/10.1016/S0043-1354(99)00075-5.

(155) Engel, W. T.; Schwing, T. *Field Report of Nutrient Control in a Multicell Lagoon*; 1980.

(156) Mulbry, W.; Kondrad, S.; Pizarro, C.; Kebede-Westhead, E. Treatment of Dairy Manure Effluent Using Freshwater Algae: Algal Productivity and Recovery of Manure Nutrients Using Pilot-Scale Algal Turf Scrubbers. *Bioresour. Technol.* **2008**, *99* (17), 8137–8142. https://doi.org/10.1016/j.biortech.2008.03.073.

(157) Adey, W. H.; Laughinghouse, H. D.; Miller, J. B.; Hayek, L. A. C.; Thompson, J. G.; Bertman, S.; Hampel, K.; Puvanendran, S. Algal Turf Scrubber (ATS) Floways on the Great Wicomico River, Chesapeake Bay: Productivity, Algal Community Structure, Substrate and Chemistry1. *J. Phycol.* **2013**, *49* (3), 489–501. https://doi.org/10.1111/jpy.12056.

(158) Adey, W. H.; Kangas, P. C.; Mulbry, W. Algal Turf Scrubbing: Cleaning Surface Waters with Solar Energy While Producing a Biofuel. *Bioscience* **2011**, *61* (6), 434–441. https://doi.org/10.1525/bio.2011.61.6.5.

(159) Mulbry, W.; Kangas, P.; Kondrad, S. Toward Scrubbing the Bay: Nutrient Removal Using Small Algal Turf Scrubbers on Chesapeake Bay Tributaries. *Ecol. Eng.* **2010**, *36* (4), 536–541. https://doi.org/10.1016/j.ecoleng.2009.11.026.

(160) Florida, S.; Management, W. S-154 Pilot Single Stage Algal Turf Scrubber ® (ATS ™) Final Report Table of Contents. *Contract* **2005**, No. C.

(161) DeRose, K.; DeMill, C.; Davis, R. W.; Quinn, J. C. Integrated Techno Economic and Life Cycle Assessment of the Conversion of High Productivity, Low Lipid Algae to Renewable Fuels. *Algal Res.* **2019**, *38* (January), 101412. https://doi.org/10.1016/j.algal.2019.101412.

(162) Wp, R. (17) (PDF) Macro-Economics of Algae Products.

(163) Gimondo, J. The Horticultural Potential of Wastewater-Grown Algae Fertilizers. **2018**, 136.

(164) HydroMentia Inc. Preliminary Engineering Assessment for a Comprehensive Algal Turf Scrubber (ATS) Based Nutrient Control Program for the Suwannee River in Florida. **2006**.

(165) Stumpf, R. P.; Wynne, T. T.; Baker, D. B.; Fahnenstiel, G. L. Interannual Variability of Cyanobacterial Blooms in Lake Erie. *PLoS One* **2012**, *7* (8). https://doi.org/10.1371/journal.pone.0042444.

(166) Bertani, I.; Obenour, D. R.; Steger, C. E.; Stow, C. A.; Gronewold, A. D.; Scavia, D. Probabilistically Assessing the Role of Nutrient Loading in Harmful Algal Bloom Formation in Western Lake Erie. *J. Great Lakes Res.* **2016**, *42* (6), 1184–1192. https://doi.org/10.1016/j.jglr.2016.04.002.

(167) Verhamme, E. M.; Redder, T. M.; Schlea, D. A.; Grush, J.; Bratton, J. F.; Depinto, J. V. Development of the Western Lake Erie Ecosystem Model (WLEEM): Application to Connect Phosphorus Loads to Cyanobacteria Biomass. *J. Great Lakes Res.* **2016**, *42* (6), 1193–1205. https://doi.org/10.1016/j.jglr.2016.09.006.

(168) Wynne, T. T.; Stumpf, R. P.; Tomlinson, M. C.; Dyble, J. Characterizing a Cyanobacterial Bloom in Western Lake Erie Using Satellite Imagery and Meteorological Data. *Limnol. Oceanogr.* **2010**, *55* (5), 2025–2036. https://doi.org/10.4319/lo.2010.55.5.2025.

(169) St. Claiif, J. Attack of the Blue-Green Algae. *WKSU*. 2010.

(170) Geiling, N. Lake Erie's Enormous Algae Bloom Is Back. *ThinkProgress*. 2015.

(171) Fritz, A. Lake Erie Is in the Midst of yet Another Dangerous, Disgusting Algae Outbreak. *The Washington Post*. August 7, 2015.

(172) Henry, T. Toxic Algae Struggles Leave Toledo's Reputation Hanging in the Balance. *The Toledo Blade*. August 2, 2015.

(173) Henry, T. Scientists: Algae Not Just Toledo Problem. *The Toledo Blade*. 2015.

(174) Glaser, S. Should Swimming Be Banned When Lake Erie Water Is Unsafe? Toxic Algae Policies Differ across Ohio (Photos). *Cleveland.com*. August 24, 2015.

(175) Gertz, E. J. A Living Carpet of Green Slime Expands Across Lake Erie. *TakePart*. August 23, 2015.

(176) Wright, P. Hundreds of Miles of Potentially Toxic Algae Chokes the Western Basin of Lake Erie

Again. *Weather Channel*. 2017.

(177) Kozlowski, K.; Steinberg, S. Spread of Lake Erie Algae Raises Alarm across Region. *The Detroit News*. September 28, 2017.

(178) Metcalfe, J. Lake Erie Gets Legendarily Slimed, Again. *CityLab*. October 5, 2017.

(179) Gorder, P. F. Algal Blooms Cost Ohio Homeowners $152 Million over Six Years. *Science News*. August 17, 2017.

(180) McCarty, J. F. Harmful Algal Blooms Continue to Plague Lake Erie, Threaten Drinking Water, Fish, Pets. *Cleveland.com*. August 30, 2017.

(181) Patel, J. K.; Parshina-Kottas, Y. Miles of Algae Covering Lake Erie. *The New York Times*. October 3, 2017.

(182) Hobson, J. Algae Bloom Covers 700 Square Miles Of Lake Erie. *WBUR*. October 5, 2017.

(183) Zillow www.zillow.com.

(184) Michael, H.; Boyle, K.; Bouchard, R. Water Quality Affects Property Prices: A Case Study of Selected Maine Lakes. *Maine Agric. For. Exp. Stn. Misc. Rep. 398* **1996**, No. February, 18.

(185) Freybote, J.; Fruits, E. Perceived Environmental Risk, Media, and Residential Sales Price. *J. Real Estate Res.* **2015**, *37* (2), 217–243.

(186) Stetler, K. M.; Venn, T. J.; Calkin, D. E. The Effects of Wildfire and Environmental Amenities on Property Values in Northwest Montana, USA. *Ecol. Econ.* **2010**, *69* (11), 2233–2243. https://doi.org/10.1016/j.ecolecon.2010.06.009.

(187) Roddewig, R. J.; Brigden, C. T.; Baxendale, A. S. A Pipeline Spill Revisited : How Long Do Impacts on Home Prices Last ? **2018**, 23–47.

(188) Siegel, C.; Caudill, S. B.; Mixon, F. G. Clear Skies, Dark Waters: The Gulf Oil Spill and the Price of Coastal Condominiums in Alabama. *Econ. Bus. Lett.* **2013**, *2* (2), 42. https://doi.org/10.17811/ebl.2.2.2013.42-53.

(189) Baron, A.; Zhang, W.; Irwin, E. Estimating the Capitalization Effects of Harmful Algal Bloom Incidence, Intensity and Duration? A Repeated Sales Model of Lake Erie Lakefront Property Values. In *2016 Agricultural & Applied Economics Association Annual Meeting*; 2016; pp 0–40.

(190) Kashian, R.; Eiswerth, M. E.; Skidmore, M. Lake Rehabilitation and the Value of Shoreline Real Estate: Evidence from Delavan, Wisconsin. *Rev. Reg. Stud.* **2006**, *36* (2), 221–238.

(191) Statistics, U. S. B. of L. Consumer Price Index https://www.bls.gov/cpi/tables/supplemental-files/home.htm.

(192) Wolf, D.; Georgic, W.; Klaiber, H. A. Reeling in the Damages: Harmful Algal Blooms' Impact on Lake Erie's Recreational Fishing Industry. *J. Environ. Manage.* **2017**, *199*, 148–157. https://doi.org/10.1016/j.jenvman.2017.05.031.

(193) Sohngen, B.; Zhang, W.; Bruskotter, J.; Sheldon, B. Results from a 2014 Survey of Lake Erie Anglers Results from a 2014 Survey of Lake Erie Anglers. **2015**.

(194) Wolf, D.; Chen, W.; Gopalakrishnan, S.; Haab, T.; Klaiber, H. A. The Impacts of Harmful Algal Blooms and E. Coli on Recreational Behavior in Lake Erie. *Land Econ.* **2019**, *95* (4), 455–472.

(195) Murray, C.; Sohngen, B.; Pendleton, L. Valuing Water Quality Advisories and Beach Amenities in the Great Lakes. *Water Resour. Res.* **2001**, *37* (10), 2583–2590. https://doi.org/10.1029/2001WR000409.

(196) Johnston, R. J.; Thomassin, P. J. Willingness to Pay for Water Quality Improvements in the United States and Canada: Considering Possibilities for International Meta-Analysis and Benefit Transfer. *Agric. Resour. Econ. Rev.* **2010**, *39* (1), 114–131. https://doi.org/10.1017/S1068280500001866.

(197) Mitchell, R. C.; Carson, R. T. An Experiment in Determining Willingness to Pay for National Water Quality Improvments. *EPA Rep.* **1981**, 1–81.

(198) Dodds, W. K.; Bouska, W. W.; Eitzmann, J. L.; Pilger, T. J.; Pitts, K. L.; Riley, A. J.; Schloesser, J. T.; Thornbrugh, D. J. Eutrophication of U. S. Freshwaters: Analysis of Potential Economic Damages.

Environ. Sci. Technol. **2009**, *43* (1), 12–19. https://doi.org/10.1021/es801217q.

(199) Larkin, S. L.; Adams, C. M. Harmful Algal Blooms and Coastal Business: Economic Consequences in Florida. *Soc. Nat. Resour.* **2007**, *20* (9), 849–859. https://doi.org/10.1080/08941920601171683.

(200) Islands, O. L. E. S. and. Research https://www.shoresandislands.com/media/research.

(201) Ohio, T. *Plan to Win: Tourism Ohio Strategic Plan 2015-2018*; 2018. https://doi.org/10.1057/9780230374898.

(202) July, E.; Agency, S.; Management, W. *Tourism and Recreation Industries in the Baltic Sea Area How Are They Affected by the State of the Marine Tourism and Recreation Industries in the Baltic Sea Area – How Are They Affected by the State of The*; 2011; Vol. 46.

(203) Dodds, W. K.; Bouska, W. W.; Eitzmann, J. L.; Pilger, T. J.; Pitts, K. L.; Riley, A. J.; Schloesser, J. T.; Thornbrugh, D. J. Eutrophication of U. S. Freshwaters: Analysis of Potential Economic Damages. *Environ. Sci. Technol.* **2009**, *43* (1), 12–19. https://doi.org/10.1021/es801217q.

(204) Anthony, R.; Sharara, M. A.; Runge, T. M.; Anex, R. P. Life Cycle Comparison of Petroleum- and Bio-Based Paper Binder from Distillers Grains (DG). *Ind. Crops Prod.* **2017**, *96*, 1–7. https://doi.org/10.1016/j.indcrop.2016.11.014.

(205) Töglhofer, C.; Eigner, F.; Prettenthaler, F. Impacts of Snow Conditions on Tourism Demand in Austrian Ski Areas. *Clim. Res.* **2011**, *46* (1), 1–14. https://doi.org/10.3354/cr00939.

(206) Dawson, J.; Scott, D.; Mcboyle, G. Climate Change Analogue Analysis of Ski Tourism in the Northeastern USA. *Clim. Res.* **2009**, *39* (1), 1–9. https://doi.org/10.3354/cr00793.

(207) Hamilton, L.; Brown, C.; Keim, B. D. Ski Areas, Weather and Climate: Time Series Models for New England Case Studies Lawrence. *Int. J. Climatol.* **2007**, *27*, 2113–2124. https://doi.org/10.1002/joc.

(208) Shih, C.; Nicholls, S.; Holecek, D. F. Impact of Weather on Downhill Ski Lift Ticket Sales. *J. Travel Res.* **2009**, *47* (3), 359–372. https://doi.org/10.1177/0047287508321207.

(209) Oxford Economics. Potential Impact of the Gulf Oil Spill on Tourism. *Prep. US Travel Assoc.* **2010**, 1–27.

(210) Garza-Gil, M. D.; Prada-Blanco, A.; Vázquez-Rodríguez, M. X. Estimating the Short-Term Economic Damages from the Prestige Oil Spill in the Galician Fisheries and Tourism. *Ecol. Econ.* **2006**, *58* (4), 842–849. https://doi.org/10.1016/j.ecolecon.2005.09.009.

(211) Chorus, I.; Bartram, J. *Toxic Cyanobacteria in Water : A Guide to Their Public Health Consequences , Monitoring and Management*; 1999.

(212) Fitzsimmons, E. Tap Water Ban for Toledo Residents. *The New York Times*. 2014.

(213) Najm, I. N.; Snoeyink, V. L.; Jr, B. W. L.; Jeffrey, Q. Using Powdered Activated Carbon: A Critical Review. *J. Am. Water Works Assoc.* **1991**, *83* (1), 65–76.

(214) US EPA. Clean Water State Revolving Fund (CWSRF) https://www.epa.gov/cwsrf/clean-water-state-revolving-fund-cwsrf-reports.

(215) Morgan, M.; Henrion, M. *Uncertainty: A Guide to Dealing with Uncertainty in Quantitative Risk and Policy Analysis*; 1990.

(216) Hung, Y.-T.; Britz, T.; van Schalkwyk, C. Treatment of Dairy Processing Wastewaters. *Waste Treat. Food Process. Ind.* **2005**, No. c, 1–28. https://doi.org/10.1201/9781420037128.ch1.

(217) Adey, W.; Luckett, C.; Jensen, K. Phosphorus Removal from Natural Waters. *Restoration Ecology*. 1993.

(218) Oceanic and Atmospheric Administration, N. Harmful Algal Blooms in Lake Erie - Experimental and Operational HAB Bulletin Archive https://www.glerl.noaa.gov/res/HABs_and_Hypoxia/lakeErieHABArchive/.

(219) Erickson, Jim; Kitchens, C. Lake Erie Algal Blooms 'Seeded' Internally by Overwintering Cells in Lake-Bottom Sediments. *University of Michigan News*.

(220) Frankel, T.; Ghanbari, H. The Toxin That Shut off Toledo's Water? The Feds Don't Make You Test

for It. *The Washington Post2*. 2014.

(221) Wolf, D.; Klaiber, H. A. Bloom and Bust: Toxic Algae's Impact on Nearby Property Values. *Ecol. Econ.* **2017**, *135*, 209–221. https://doi.org/10.1016/j.ecolecon.2016.12.007.

(222) Resources, O. D. of N. Historical License Information http://wildlife.ohiodnr.gov/licenses-and-permits/historical-license-information.

(223) Sohngen, B.; Lichtkoppler, F.; Bielen, M. TB-039 Value of Day on Beach.Pdf. Ohio Sea Grant College Program 1999.

(224) Murray, B. C.; Economics, D.; Lichtkoppler, F.; Specialist, D.; Grant, O. S.; Program, E.; Bielen, M.; Agent, E.; Oceanic, N.; Reutter, J. M.; Ricker, K. T.; Coordinator, C. The Economics of Lake Erie Beaches. *Time* 1–2.

(225) Palm-Forster, L. H.; Lupi, F.; Chen, M. Valuing Lake Erie Beaches Using Value and Function Transfers. *Agric. Resour. Econ. Rev.* **2016**, *45* (2), 270–292. https://doi.org/10.1017/age.2016.15.

(226) Murray, B. C.; Sohngen, B. FS-082 The Economics of Lake Erie Beaches 1998 Lake Erie Beach User Survey Results. **1998**.

(227) Service, U. S. N. P. Visitation Numbers https://www.nps.gov/aboutus/visitation-numbers.htm.

(228) Bureau, U. C. Quick Facts https://www.census.gov/quickfacts/fact/table/US/PST045219 (accessed Jan 2, 2019).

(229) Section, O.; Committee, T. Draft White Paper on Cyanotoxin Treatment. **2015**, 1–15.

(230) Office, L.; June, T. The Impact of the BP Oil Spill on Visitor Spending in Louisiana: Revised Estimates Based on Data through 2010 Q4 The Impact of the BP Oil Spill on Visitor Spending in Louisiana. **2011**, No. June.

(231) McDowell Group. An Assessment of the Impact of the Exxon Valdez Oil Spill on The Alaska Tourism Industry Phase I: Initial Assessment. **1990**, 1–96.

Appendix A

Appendix A 1: "Nth" Plant Assumptions as Provided by BETO used for economic assessment [10–12,22]

Assumption	Value	
Internal Rate of Return	10%	
Plant Financing Debt	60 %	of Total Capital Cost
Plant Financing Equity	40%	of Total Capital Cost
Plant Life	30	years
Income Tax Rate	35%	
Interest Rate for Debt Financing	8%	annual
Loan Term	10	years
Working Capital Cost	5%	of Capital Cost (Excluding Land)
Depreciation Schedule	7	years MACRS[1] schedule
Plant Salvage Value	None	
Startup Time	6	months
Startup Capacity	50%	

[1]*Modified Accelerated Cost Recovery System*

Appendix A 2: Total Capital investment for the Biochemical Pathway

Biochemical Pathway

Process Area			**Purchased Cost**	**Installed Cost**
Area 100: Pretreatment			$ 91,000,000	$ 160,000,000
Area 200: Fermentation			$ 17,000,000	$ 28,000,000
Area 300: Product Recovery			$ 27,000,000	$ 62,000,000
Area 400: Hydrothermal Liquefaction			$ 267,000,000	$ 539,000,000
Area 600: Utilities			$ 6,000,000	$ 12,000,000
Area 700: Storage			$ 3,000,000	$ 6,000,000
Totals				**$ 807,000,000**
Warehouse	4.0%	of ISBL		$ 31,600,000
Site Development	9.0%	of ISBL		$ 71,100,000
Additional Piping	4.5%	of ISBL		$ 35,600,000
Total Direct Costs (TDC)				**$ 945,300,000**
Indirect Costs - Conversion				
Prorateable expenses	10.0%	of TDC		$ 94,600,000
Field expenses	10.0%	of TDC		$ 94,600,000
Home office & construction fees	20.0%	of TDC		$ 189,100,000
Project contingency	10.0%	of TDC		$ 94,600,000
Other costs (start-up, permits, etc.)	10.0%	of TDC		$ 94,600,000
Total Indirect Costs				**$ 567,500,000**
Fixed Capital Investment (FCI)				**$ 1,512,800,000**
Land				$ 1,900,000
Working capital	5.0%			$ 75,700,000
Total Capital Investment				**$ 1,590,400,000**

Appendix A 3: Total Capital investment for the Thermal-Chemical Pathway

Thermal-Chemical Pathway

Process Area			**Purchased Cost**	**Installed Cost**
Area 400: Hydrothermal Liquefaction			$ 267,000,000	$ 539,000,000
Area 600: Utilities			$ 6,000,000	$ 12,000,000
Area 700: Storage			$ 3,000,000	$ 6,000,000
Totals				**$ 557,000,000**
Warehouse	4.0%	of ISBL		$ 21,560,000
Site Development	9.0%	of ISBL		$ 48,510,000
Additional Piping	4.5%	of ISBL		$ 24,255,000
Total Direct Costs (TDC)				**$ 651,325,000**
Indirect Costs - Conversion				
Prorateable expenses	10.0%	of TDC		$ 65,200,000
Field expenses	10.0%	of TDC		$ 65,200,000
Home office & construction fees	20.0%	of TDC		$ 130,300,000
Project contingency	10.0%	of TDC		$ 65,200,000
Other costs (start-up, permits, etc.)	10.0%	of TDC		$ 65,200,000
Total Indirect Costs				**$ 391,100,000**
Fixed Capital Investment (FCI)				**$ 1,042,425,000**
Land				$ 6,000,000
Working capital	5.0%			$ 52,200,000
Total Capital Investment				**$ 1,100,625,000**

Appendix A 4: Operational costs for the biochemical pathway

OPEX		
Variable		
Biomass	$	206,500,000
Materials	$	41,000,000
Electricity	$	10,200,000
Natural Gas	$	39,300,000
Catalyst	$	11,000,000
TOTAL - Variable	$	308,000,000
Fixed		
Labor	$	24,400,000
Maintenance	$	24,000,000
TOTAL - Fixed	$	48,400,000
TOTAL	**$**	**356,400,000**

Appendix A 5: Operational costs for the Thermal-Chemical pathway

OPEX		
Variable		
Biomass	$	206,500,000
Electricity	$	7,800,000
Natural Gas	$	19,400,000
Catalyst	$	11,700,000
TOTAL - Variable	$	245,400,000
Fixed		
Labor	$	15,100,000
Maintenance	$	17,100,000
TOTAL - Fixed	$	32,200,000
TOTAL	**$**	**277,600,000**

Appendix A 6: Detailed BFD's for the algae conversion processes; A) Fermentation Only, B) Fermentation + AD, 3) Fermentation + HTL and 4) HTL Only

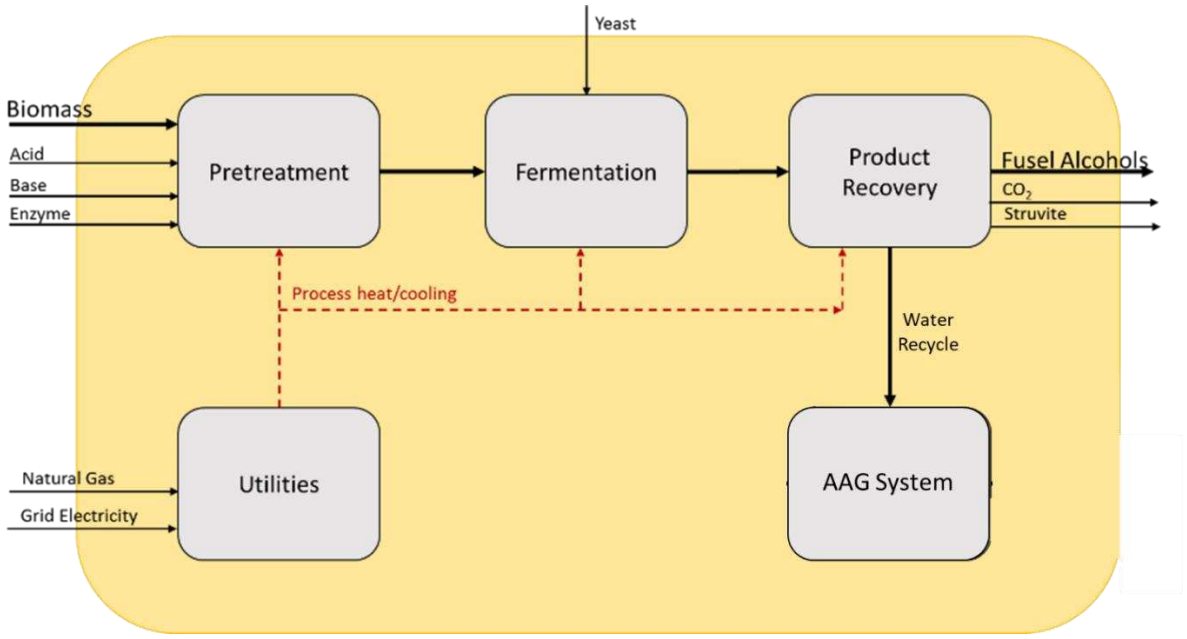

A)

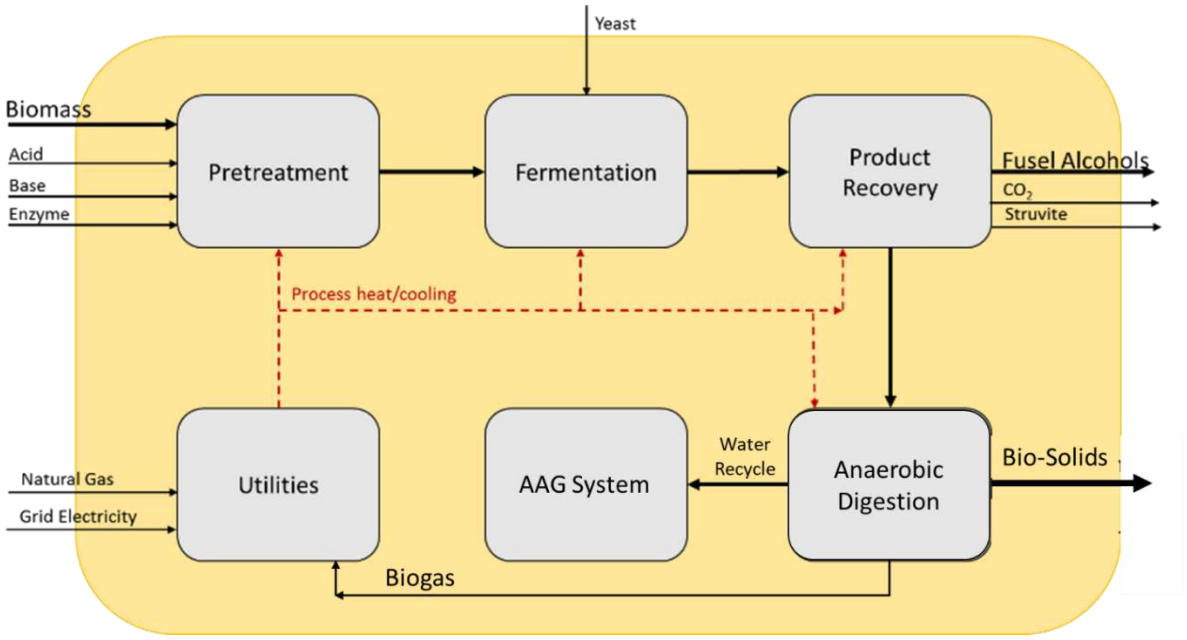

B)

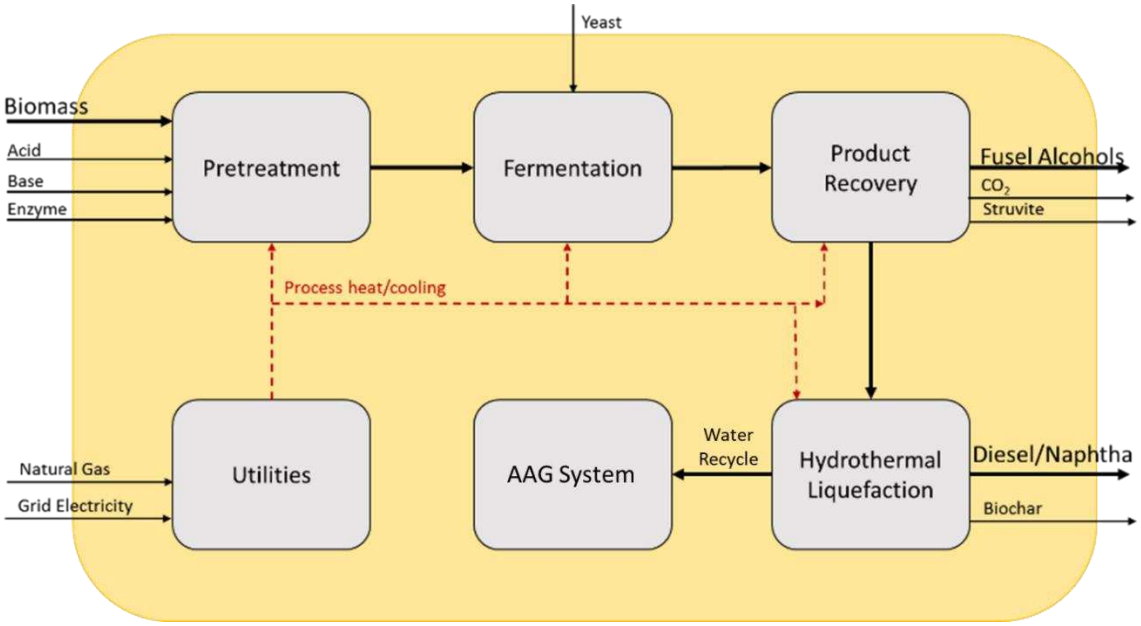
Yeast
Biomass
Acid
Base
Enzyme
Pretreatment
Fermentation
Product Recovery
Fusel Alcohols
CO_2
Struvite
Process heat/cooling
Natural Gas
Grid Electricity
Utilities
AAG System
Water Recycle
Hydrothermal Liquefaction
Diesel/Naphtha
Biochar

C)

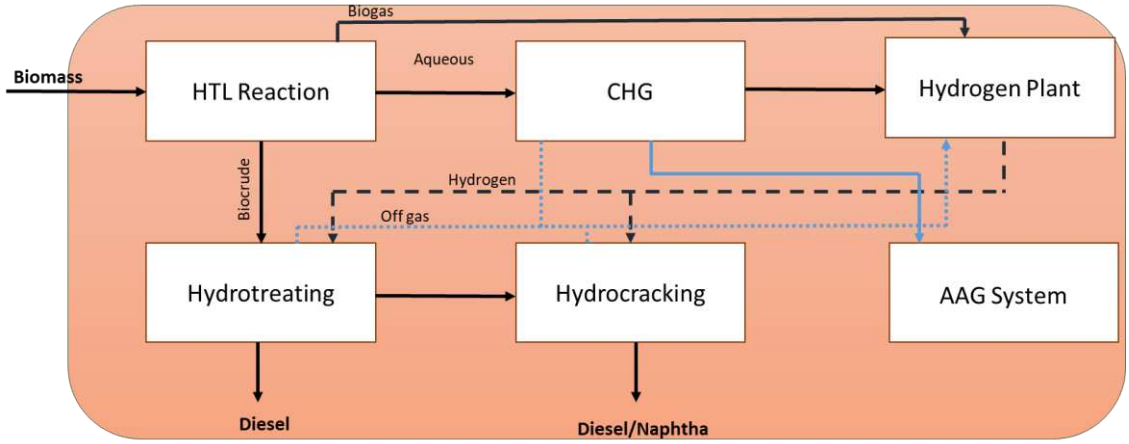
Biogas
Biomass
HTL Reaction
Aqueous
CHG
Hydrogen Plant
Biocrude
Hydrogen
Off gas
Hydrotreating
Hydrocracking
AAG System
Diesel
Diesel/Naphtha

D)

Appendix A 7: AAG Algae carbohydrate hydrolysate profile

Component	Chemical Formula	Mass %
Mannitol*	$C_6H_{14}O_6$	53
Glucose*	$C_6H_{12}O_6$	23
Mannose	$C_6H_{12}O_6$	12
Galactose	$C_6H_{12}O_6$	6
Xylose*	$C_5H_{10}O_5$	3
Fucose	$C_6H_{12}O_5$	3

*Considered fermentable

Appendix A 8: AAG Algae protein hydrolysate profile

Amino Acid	Chemical Formula	Mass %
Glutamic Acid	$C_5H_9O_4N$	16
Aspartic Acid	$C_4H_7O_4N$	13.5
Leucine	$C_6H_{13}O_2N$	8
Proline	$C_5H_9O_2N$	5.5
Alanine	$C_3H_7O_2N$	7.5
Valine	$C_5H_{11}O_2N$	7
Arginine	$C_6H_{14}O_4N_2$	7.5
Lysine	$C_6H_{14}O_2N_2$	5.5
Phenylalanine	$C_9H_{11}O_2N$	5.5
Isoleucine	$C_6H_{13}O_2N$	4.7
Glycine	$C_2H_5O_2N$	7
Threonine	$C_4H_9O_3N$	5
Serine	$C_3H_7O_3N$	2.8
Tyrosine	$C_9H_{11}O_3N$	2
Histidine	$C_6H_9O_2N_3$	2.5

Appendix A 9: Total Capital investment for the Ferm Only with ash removal Pathway in Phase Two

Fermentation Only

Process Area			Purchased Cost	Installed Cost
Area ATS 000: Civil Works			$ 186,900,000	$ 186,900,000
Area ATS 100: Growth System			$ 383,500,000	$ 383,500,000
Area ATS 300: Harvest System			$ 73,200,000	$ 73,200,000
Area ATS 400: Ash Removal			$ 12,700,000	$ 21,200,000
Area 100: Pretreatment			$ 26,200,000	$ 44,900,000
Area 200: Fermentation			$ 2,600,000	$ 4,400,000
Area 300: Product Recovery			$ 8,200,000	$ 17,300,000
Area 400: Hydrothermal Liquefaction			$ -	$ -
Area 500: Wastewater Treatment			$ -	$ -
Area 600: Utilities			$ 51,300,000	$ 91,600,000
Area 700: Storage			$ 3,100,000	$ 5,300,000
Area 800: Anaerobic Digestion			$ -	$ -
Totals			**$ 747,700,000**	**$ 828,300,000**
Warehouse	4.0%	of ISBL		$ 9,000,000
Site Development	9.0%	of ISBL		$ 8,000,000
Additional Piping	4.5%	of ISBL		$ 4,000,000
Total Direct Costs (TDC)				**$ 849,300,000**
Indirect Costs - Growth				
Prorateable expenses	4.0%	of TDC		$ 26,000,000
Field expenses	4.5%	of TDC		$ 29,300,000
Home office & construction fees	10.3%	of TDC		$ 66,900,000
Project contingency	10.0%	of TDC		$ 65,000,000
Other costs (start-up, permits, etc.)	2.6%	of TDC		$ 16,900,000
Indirect Costs - Conversion				
Prorateable expenses	10.0%	of TDC		$ 17,600,000
Field expenses	10.0%	of TDC		$ 17,600,000
Home office & construction fees	20.0%	of TDC		$ 35,100,000
Project contingency	10.0%	of TDC		$ 17,600,000
Other costs (start-up, permits, etc.)	10.0%	of TDC		$ 17,600,000
Total Indirect Costs				**$ 309,600,000**
Fixed Capital Investment (FCI)				**$ 1,158,900,000**
Land				$ 60,700,000
Working capital	5.0%			$ 58,000,000
Total Capital Investment				**$ 1,277,600,000**

Appendix A 10: Total Capital investment for the Ferm + AD with ash removal Pathway in Phase Two

Ferm + AD

Process Area			Purchased Cost	Installed Cost
Area ATS 000: Civil Works			$ 186,900,000	$ 186,900,000
Area ATS 100: Growth System			$ 383,500,000	$ 383,500,000
Area ATS 300: Harvest System			$ 73,200,000	$ 73,200,000
Area ATS 400: Ash Removal			$ 12,700,000	$ 21,200,000
Area 100: Pretreatment			$ 26,200,000	$ 44,900,000
Area 200: Fermentation			$ 2,600,000	$ 4,400,000
Area 300: Product Recovery			$ 8,200,000	$ 17,300,000
Area 400: Hydrothermal Liquefaction			$ -	$ -
Area 500: Wastewater Treatment			$ -	$ -
Area 600: Utilities			$ 46,800,000	$ 83,500,000
Area 700: Storage			$ 3,100,000	$ 5,300,000
Area 800: Anaerobic Digestion			$ 18,700,000	$ 19,900,000
Totals			**$ 761,900,000**	**$ 840,100,000**
Warehouse	4.0%	of ISBL		$ 9,000,000
Site Development	9.0%	of ISBL		$ 8,000,000
Additional Piping	4.5%	of ISBL		$ 4,000,000
Total Direct Costs (TDC)				**$ 861,100,000**
Indirect Costs - Growth				
Prorateable expenses	4.0%	of TDC		$ 26,000,000
Field expenses	4.5%	of TDC		$ 29,300,000
Home office & construction fees	10.3%	of TDC		$ 66,900,000
Project contingency	10.0%	of TDC		$ 65,000,000
Other costs (start-up, permits, etc.)	2.6%	of TDC		$ 16,900,000
Indirect Costs - Conversion				
Prorateable expenses	10.0%	of TDC		$ 18,800,000
Field expenses	10.0%	of TDC		$ 18,800,000
Home office & construction fees	20.0%	of TDC		$ 37,500,000
Project contingency	10.0%	of TDC		$ 18,800,000
Other costs (start-up, permits, etc.)	10.0%	of TDC		$ 18,800,000
Total Indirect Costs				**$ 316,800,000**
Fixed Capital Investment (FCI)				**$ 1,177,900,000**
Land				$ 61,600,000
Working capital	5.0%			$ 58,900,000
Total Capital Investment				**$ 1,298,400,000**

Appendix A 11: Total Capital investment for the Ferm + HTL with ash removal Pathway in Phase Two

Ferm + HTL

Process Area			Purchased Cost	Installed Cost
Area ATS 000: Civil Works			$ 186,900,000	$ 186,900,000
Area ATS 100: Growth System			$ 383,500,000	$ 383,500,000
Area ATS 300: Harvest System			$ 73,200,000	$ 73,200,000
Area ATS 400: Ash Removal			$ 12,700,000	$ 21,200,000
Area 100: Pretreatment			$ 26,200,000	$ 44,900,000
Area 200: Fermentation			$ 2,600,000	$ 4,400,000
Area 300: Product Recovery			$ 8,200,000	$ 17,300,000
Area 400: Hydrothermal Liquefaction			$ 140,000,000	$ 274,000,000
Area 500: Wastewater Treatment			$ -	$ -
Area 600: Utilities			$ 51,300,000	$ 91,600,000
Area 700: Storage			$ 5,200,000	$ 11,300,000
Area 800: Anaerobic Digestion			$ -	$ -
Totals			**$ 889,800,000**	**$ 1,108,300,000**
Warehouse	4.0%	of ISBL		$ 20,000,000
Site Development	9.0%	of ISBL		$ 32,600,000
Additional Piping	4.5%	of ISBL		$ 16,300,000
Total Direct Costs (TDC)				**$ 1,177,200,000**
Indirect Costs - Growth				
Prorateable expenses	4.0%	of TDC		$ 26,000,000
Field expenses	4.5%	of TDC		$ 29,300,000
Home office & construction fees	10.3%	of TDC		$ 66,900,000
Project contingency	10.0%	of TDC		$ 65,000,000
Other costs (start-up, permits, etc.)	2.6%	of TDC		$ 16,900,000
Indirect Costs - Conversion				
Prorateable expenses	10.0%	of TDC		$ 49,300,000
Field expenses	10.0%	of TDC		$ 49,300,000
Home office & construction fees	20.0%	of TDC		$ 98,500,000
Project contingency	10.0%	of TDC		$ 49,300,000
Other costs (start-up, permits, etc.)	10.0%	of TDC		$ 49,300,000
Total Indirect Costs				**$ 499,800,000**
Fixed Capital Investment (FCI)				**$ 1,677,000,000**
Land				$ 62,500,000
Working capital	5.0%			$ 83,900,000
Total Capital Investment				**$ 1,823,400,000**

Appendix A 12: Total Capital investment for the HTL Only with ash removal Pathway in Phase Two

HTL Only

Process Area		Purchased Cost	Installed Cost
Area ATS 000: Civil Works		$ 186,900,000	$ 186,900,000
Area ATS 100: Growth System		$ 383,500,000	$ 383,500,000
Area ATS 300: Harvest System		$ 73,200,000	$ 73,200,000
Area ATS 400: Ash Removal		$ 12,700,000	$ 21,200,000
Area 100: Pretreatment		$ -	$ -
Area 200: Fermentation		$ -	$ -
Area 300: Product Recovery		$ -	$ -
Area 400: Hydrothermal Liquefaction		$ 147,100,000	$ 286,200,000
Area 500: Wastewater Treatment		$ -	$ -
Area 600: Utilities		$ 46,500,000	$ 83,000,000
Area 700: Storage		$ 2,600,000	$ 7,700,000
Area 800: Anaerobic Digestion		$ -	$ -
Totals		**$ 852,500,000**	**$ 1,041,700,000**
Warehouse	4.0%	of ISBL	$ 17,800,000
Site Development	9.0%	of ISBL	$ 27,700,000
Additional Piping	4.5%	of ISBL	$ 13,900,000
Total Direct Costs (TDC)			**$ 1,101,100,000**
Indirect Costs - Growth			
Prorateable expenses	4.0%	of TDC	$ 26,000,000
Field expenses	4.5%	of TDC	$ 29,300,000
Home office & construction fees	10.3%	of TDC	$ 66,900,000
Project contingency	10.0%	of TDC	$ 65,000,000
Other costs (start-up, permits, etc.)	2.6%	of TDC	$ 16,900,000
Indirect Costs - Conversion			
Prorateable expenses	10.0%	of TDC	$ 41,900,000
Field expenses	10.0%	of TDC	$ 41,900,000
Home office & construction fees	20.0%	of TDC	$ 83,700,000
Project contingency	10.0%	of TDC	$ 41,900,000
Other costs (start-up, permits, etc.)	10.0%	of TDC	$ 41,900,000
Total Indirect Costs			**$ 455,400,000**
Fixed Capital Investment (FCI)			**$ 1,556,500,000**
Land			$ 60,700,000
Working capital	5.0%		$ 77,900,000
Total Capital Investment			**$ 1,695,100,000**

Appendix A 13: Operational costs for the Fermentation Only with ash removal Pathway in Phase Two

OPEX	
Variable	
Materials	$ 35,000,000
Natural Gas	$ 4,700,000
Electricity	$ 50,100,000
Fuel	$ 8,600,000
Utilities	$ 10,100,000
Ash Disposal	$ 34,800,000
TOTAL - Variable	$ 143,300,000
Fixed	
Labor	$ 24,300,000
Maintenance	$ 16,800,000
Property Taxes	$ 9,800,000
TOTAL - Fixed	$ 50,900,000
TOTAL	**$ 194,200,000**

Appendix A 14: Operational costs for the Ferm + AD with ash removal Pathway in Phase Two

OPEX	
Variable	
Materials	$ 35,000,000
Natural Gas	$ 4,700,000
Electricity	$ 50,100,000
Fuel	$ 8,600,000
Utilities	$ 10,100,000
Ash Disposal	$ 34,800,000
TOTAL - Variable	$ 143,300,000
Fixed	
Labor	$ 24,800,000
Maintenance	$ 16,800,000
Property Taxes	$ 9,800,000
TOTAL - Fixed	$ 51,400,000
TOTAL	**$ 194,700,000**

Appendix A 15: Operational costs for the Ferm + HTL with ash removal Pathway in Phase Two

OPEX	
Variable	
Materials	$ 44,890,000
Natural Gas	$ 200,000
Electricity	$ 50,100,000
Fuel	$ 8,600,000
Utilities	$ 19,600,000
Ash Disposal	$ 34,800,000
TOTAL - Variable	$ 158,190,000
Fixed	
Labor	$28,100,000
Maintenance	$25,000,000
Property Taxes	$19,400,000
TOTAL - Fixed	$ 72,500,000
TOTAL	**$ 230,690,000**

Appendix A 16: Operational costs for the HTL Only with ash removal Pathway in Phase Two

OPEX	
Variable	
Materials	$ 10,510,000
Natural Gas	$ 100,000
Electricity	$ 50,100,000
Fuel	$ 8,600,000
Utilities	$ 9,200,000
Ash Disposal	$ 34,800,000
TOTAL - Variable	$ 113,310,000
Fixed	
Labor	$23,800,000
Maintenance	$23,300,000
Property Taxes	$17,500,000
TOTAL - Fixed	$ 64,600,000
TOTAL	**$ 177,910,000**

Appendix A 17: Compositional analysis of AAG ash. Data provided by Sandia National Laboratories.

Component	Wt%
Oxygen	45
Silica	27.4
Aluminum	6.8
Iron	4.9
Calcium	2.2
Magnesium	1.7
Other	11.9

Appendix B

Appendix B 1: PFD's for the three different processing options for converting DGS into fuels and higher value protein products. A) PFD for the Base Pathway which includes solvent recovery for alcohol recovery and protein concentration via ultrafiltration. B) PFD for the Distillation Case which includes distillation for alcohol recovery and protein concentration via ultrafiltration. C) PFD for the LPC Case which includes solvent recovery for alcohol recovery and no protein concentration via ultrafiltration

A)

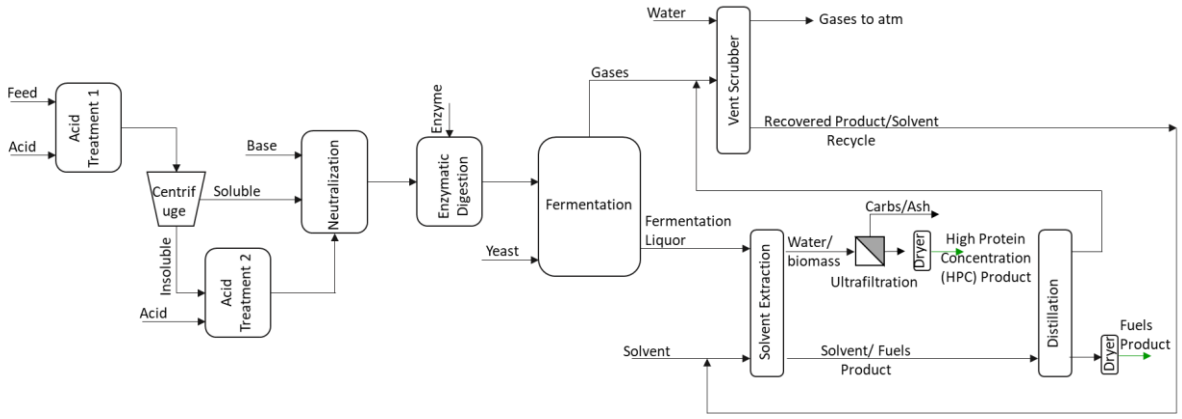

B)

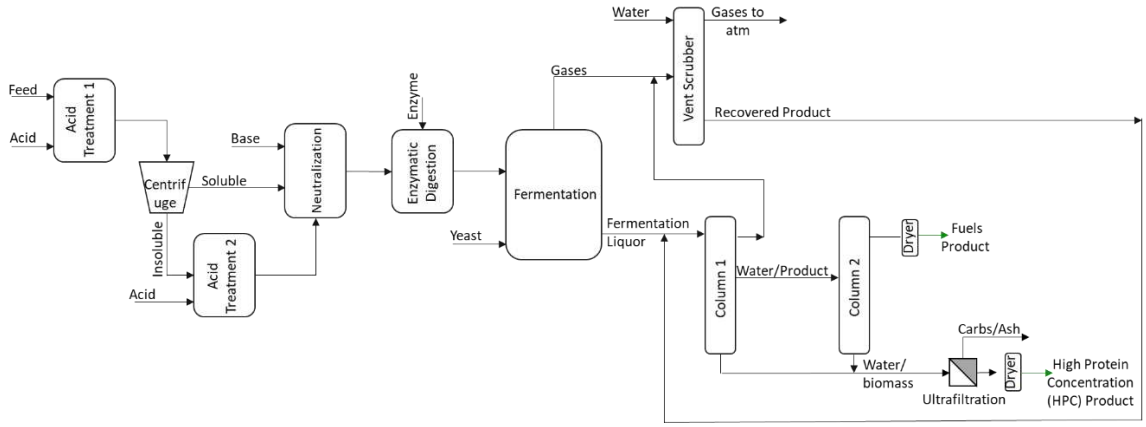

C)

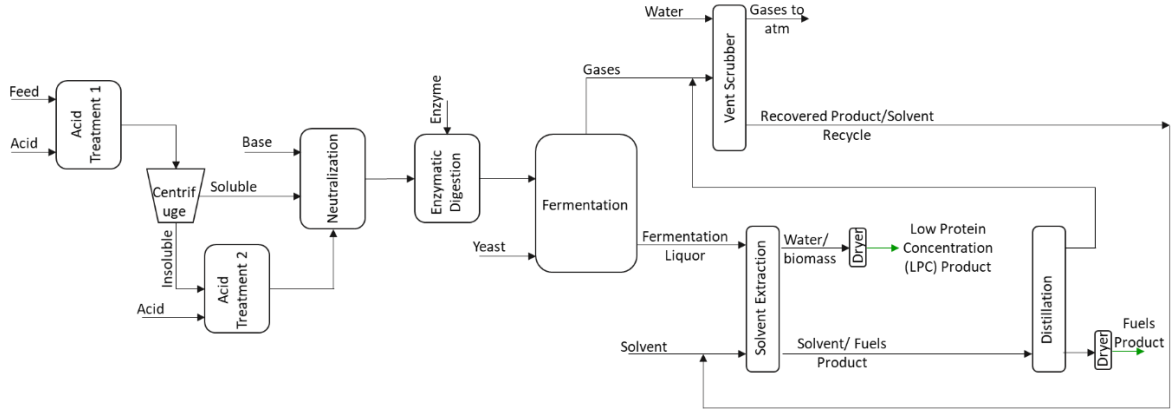
Feed
Acid
Acid Treatment 1
Centrif uge
Soluble
Insoluble
Acid
Acid Treatment 2
Base
Neutralization
Enzyme
Enzymatic Digestion
Yeast
Fermentation
Gases
Water
Vent Scrubber
Gases to atm
Recovered Product/Solvent Recycle
Fermentation Liquor
Solvent
Solvent Extraction
Water/ biomass
Dryer
Low Protein Concentration (LPC) Product
Solvent/ Fuels Product
Distillation
Dryer
Fuels Product

Appendix B 2: Carbohydrate hydrolysate profiles before and after fermentation. Data was provided by Sandia National Laboratories.

		Mass Composition	
Component	**Chemical Formula**	**Before Fermentation**	**After Fermentation**
Glucose	$C_6H_{12}O_6$	26%	
Arabinose	$C_5H_{10}O_5$	30%	
Xylose	$C_5H_{10}O_5$	44%	100%
Average Composition		**$C_{5.2}H_{10.5}O_{5.2}$**	**$C_5H_{10}O_5$**

Appendix B 3: Amino acid hydrolysate profiles before and after fermentation. Data was provided by Sandia National Laboratories.

		Mass Composition (wt%)	
Component	**Chemical Formula**	**Before Fermentation**	**After Fermentation**
Methionine	$C_5H_{11}O_2NS$	1.8	2.2
Cystine	$C_6H_{12}O_4N_2S_2$	1.8	2.2
Lysine	$C_6H_{14}O_2N_2$	4.1	2.2
Phenylalanine	$C_9H_{11}O_2N$	4.1	3.0
Leucine	$C_6H_{13}O_2N$	9.2	3.0
Isoleucine	$C_6H_{13}O_2N$	4.6	1.5
Threonine	$C_4H_9O_3N$	5.5	2.2
Valine	$C_5H_{11}O_2N$	6.0	20.7
Histidine	$C_6H_9O_2N_3$	3.2	4.4
Arginine	$C_6H_{14}O_4N_2$	4.6	3.0
Glycine	$C_2H_5O_2N$	5.0	5.2
Aspartic Acid	$C_4H_7O_4N$	7.8	6.7
Serine	$C_3H_7O_3N$	6.0	2.2
Glutamic Acid	$C_5H_9O_4N$	13.3	14.8
Proline	$C_5H_9O_2N$	8.7	11.1
Hydroxyproline	$C_5H_9O_3N$	0.5	0.7
Alanine	$C_3H_7O_2N$	7.3	8.1
Tyrosine	$C_9H_{11}O_3N$	4.6	6.0
Tryptophan	$C_{11}H_{12}O_2N_2$	1.4	0.7
Taurine	$C_2H_7O_3NS$	0.5	0
Average Composition		$\mathbf{C_{7.5}H_{15}O_4N_2S_{0.0625}}$	$\mathbf{C_{7.2}H_{14}O_{3.75}N_2S_{0.0625}}$

Appendix B 4: Explanation of FOAK methodology variables used in Equations [3] and [4]

The variables for Equation [3] are defined as follows:

PCTNEW (0 to 100%): The percentage cost of novel use equipment as a percentage of total cost. For this analysis, it was assumed that the protein recovery process would be a novel and not yet commercially proven for this application.

IMPURITIES (0 to 5): This variable is indicative of the chance for issues in the processing facility due to impurities. These issues include damage to equipment from corrosion, handling of solids or waste products, and wastewater treatment. A value of 0 indicates there are no potential complications expected from impurities, while a value of 5 means these impurities were a source of significant difficulties during early stage process design [20]. Due to the production of hydrogen sulfide from fermentation and possible complications from wastewater treatment [216], a value of 3.5 was assigned.

COMPLEXITY (0+): This variable is count of the number of continuously linked process steps in the process facility. For the upgrading facility, there were 8 linked processes; pretreatment, fermentation, extraction or distillation, molecular sieve drying, scrubbing, centrifugation, ultrafiltration and drying.

INCLUSIVENESS (0 to 100%): This variable accounts for mis-estimation and includes three categories: land purchase cost, initial inventory costs including parts, materials and catalysts, and pre-operating personnel costs. If the costs of each category were investigated and including in the initial capital investment calculation, that category receives a score of 0. If it was not included or was not rigorously investigated, that category receives a score of 1. The inclusiveness variable is calculated as shown in Equation [36].

$$\text{INCLUSIVENESS } [\%] = \frac{\text{Total calculated category score}}{\text{Total number of categories}} \qquad [36]$$

For this analysis, land costs and pre-operating personnel costs were included, giving both categories a score of 0. Initial inventory costs were not included, so this category was awarded a score of 1. The overall INCLUSIVENESS variable was found to be 33%.

PROJECT DEFINITION (2 to 8): This variable is a measure of process development stage. As this process in still in the Exploratory/Predevelopment phase; that is, most process information is from small scale laboratory experiments and/or literature, this variable received a value of 2.

The variables for Equation [4] are defined as follows:

NEWSTEPS (0+): This is number of new, not commercially proven process steps. For this process, the steps associated with protein concentration and recovery were chosen as new steps, since they have not been commercially proven for this type of feedstock. These steps include centrifugation, ultrafiltration and drying.

BALEQS (0 to 100): The value represents the percentage of the heat and mass balances that are based on current plant data from similar processes. Since this process is novel, a value of 0 was chosen.

WASTE (0 to 5): This variable is indicative of the complexity of dealing with possible waste streams. A value of 0 indicates no waste stream complexities, while a value of 5 indicates significant waste stream challenges. A value of 4 was chosen for waste, since hydrogen sulfide or other sulfur containing compounds are expected from fermentation, and there are significant issues associated with the treatment of dairy waste [216]. Since this process is modeled after whey protein recovery, it was assumed that similar wastewater issues may arise with this process as well.

SOLIDS (0 or 1): If solids are present, this variable is given a value of 1. Solids are expected in this process, so a value of 1 was used.

Appendix B 5: PCDAAS calculation for the HPC and LPC products

		HPC Protein				**LPC Protein**			
		Monogastric		**Ruminant**		**Monogastric**		**Ruminant**	
Amino Acid	Required [mg g^{-1}]	Illeal Digestibility [%]	PCDAAS [%]	Fecal Digestibility [%]	PCDAAS [%]	Illeal Digestibility [%]	PCDAAS [%]	Fecal Digestibility [%]	PCDAAS [%]
Isoleucine	28	92.1	49	72	38	87.6	46	72	38
Leucine	66	94.8	43	72	32	91.6	41	72	32
Lysine	58	87.1	33	72	28	78.1	30	72	28
Methionine + Cystine	25	92.6	100	72	100	89.4	100	72	100
Phenylalanine + Tyrosine	63	78.4	100	72	100	90.1	100	72	100
Threonine	34	88.4	58	72	47	84.5	55	72	47
Tryptophan	11	90.0	61	72	48	89.3	60	72	48
Valine	35	91.1	100	72	100	86.6	100	72	100
Histidine	19	92.0	100	72	100	87.9	100	72	100
Scoring Criteria									
Protein Content [%]			84%		84%		67%		67%
PCDAAS			33		28		30		28

Appendix B 6: PCDAAS score, protein content as weight percentage, and market price for different protein products.

Protein Products	PCDAAS [%]	Protein Content [%]	Cost [$/kg]
Feather Meal	19	80%	$ 0.50
DGS	22	35%	$ 0.07
Corn Gluten	26	60%	$ 0.55
Fish Meal	38	60%	$ 1.45
Soybean Meal	100	48%	$ 0.35
Whey Protein	100	95%	$ 2.11
HPC	33 (monogastric)/ 28 (ruminants)	84%	$ 1.91
LPC	30 (monogastric)/ 28 (ruminants)	66%	$ 2.48

Appendix C

Appendix C 1: List of point source systems including flow rates and phosphorus loads feeding into the Maumee River for the year 2016 [123]

Permit Name	Design Flow (gal day^{-1})	Actual Annual Flow (Million Gal)	[TP] (mg L^{-1})	TP Load (kg yr^{-1})	TP Load with High Level (kg $year^{-1}$)	TP Load with Low Level (kg $year^{-1}$)
Toledo Bay View Park WWTP	130,000,000	23,089	0.48	41,952	41,952	8,740
Lucas Co WRRF	22,500,000	5,590	0.74	15,659	15,659	2,116
Findlay WPCF	15,000,000	3,766	0.73	10,407	10,407	1,426
Lima WWTP	18,500,000	4,812	0.5	9,107	9,107	1,821
Campbell Soup Supply Co LLC	10,000,000	1,470	0.915	5,092	5,092	557
PCS Nitrogen Ohio LP	3,740,000	1,118	1.135	4,803	4,232	423
Perrysburg WWTP	5,400,000	1,840	0.59	4,109	4,109	696
Elida WWTP	500,000	187	3.115	2,207	709	71
New Bremen WWTP	900,000	244	2.192	2,024	923	92
Montpelier WWTP[A]	1,000,000	326	1.59	1,960	1,233	123
Shawnee No 2 WWTP	2,000,000	774	0.6	1,758	1,758	293
Van Wert WWTP	4,000,000	990	0.37	1,386	1,386	375
Napoleon WWTP	2,500,000	603	0.585	1,334	1,334	228
Ada WWTP[B]	2,000,000	298	1.13	1,273	1,127	113
Columbus Grove WWTP	820,000	194	1.68	1,237	736	74
Paulding WWTP	710,000	254	1.235	1,185	960	96
Weston WWTP	280,000	97	2.78	1,022	368	37

Defiance WWTP	6,000,000	1,046	0.25	990	990	396
Delta WWTP	725,000	158	1.655	987	596	60
Lima Refinery	5,490,000	1,572	0.16	952	952	595
St Mary's City WWTP	3,000,000	665	0.37	932	932	252
Hicksville WWTP[C]	4,000,000	376	0.62	884	884	143
Ottawa WWTP	3,000,000	456	0.495	855	855	173
Wapakoneta WWTP	4,000,000	855	0.25	809	809	324
Antwerp WWTP	330,000	86	2.43	789	325	32
American-Bath WWTP	1,500,000	404	0.5	765	765	153
Delphos WWTP	3,830,000	358	0.56	759	759	136
Archbold WWTP	2,500,000	474	0.415	745	745	179
Edgerton WWTP	300,000	120	1.6	726	454	45
Cooper Farms Cooked Meats Van Wert	147,945	54	3.27	669	205	20
TOTAL P Loads (mt)				**117,377***	**110,361**	**19,788**

* Total Phosphorus loads for this year were reported to be 134,513 kg, indicating that not all sources were including in this list. We assumed any system not included here would not be affected by policy changes, i.e. that the 17.14 mt currently emitted by these unnamed systems will always be emitted.

% P reduction, High Limit = 1 – (110,361 + 17,136)/ 134,513 = 5%

% P reduction, Low Limit = 1 – (19,788 + 17,136)/ 134,513 = 73%

Appendix C 2: Detailed sizing of the centralized and decentralized lagoon systems

Centralized System				
Parameter	**Units**			
Lagoon Location		Waterville		
River Flow Rate	[MGD]	6566		
Treated Flow Rate	[MGD]	3283		
Wetted area	[acres]	151131		
Average TP concentration	[mg TP L^{-1}]	0.28		
Average TP into Lagoon	[kg TP day^{-1}]	3493		
Average DRP into Lagoon	[kg DRP day^{-1}]	734		
Land Cost	[$ Million]	$509		
Equipment CAPEX	[$ Million]	$35,740		
Total CAPEX (equipment + land)	[$ Million]	$36,250		
OPEX	[$ Million $year^{-1}$]	$3,297		
Average TP in effluent	[kg TP day^{-1}]	1243		
Average DRP in effluent	[kg DRP day^{-1}]	110		
Decentralized System				
Parameter	**Units**			
Lagoon Location		Antwerp	Defiance	Waterville
River Flow Rate	[MGD]	2400	5684	6566
Treated Flow Rate	[MGD]	1200	2842	3283
Wetted area	[acres]	55250	130823	151131
Average TP concentration	[mg TP L^{-1}]	0.62	0.20*	0.14*
Average TP into Lagoon	[kg TP day^{-1}]	2803	2147	1784
Average DRP into Lagoon	[kg DRP day^{-1}]	589	447	293
Land Cost	[$ Million]	$186	$441	$509
Equipment CAPEX	[$ Million]	$13,066	$30,938	$35,740
Total CAPEX (equipment + land)	[$ Million]	$13,252	$31,379	$36,250
OPEX	[$ Million $year^{-1}$]	$1,205	$2,854	$3,297
Average TP in effluent	[kg TP day^{-1}]	454	1076	1243
Average DRP in effluent	[kg DRP day^{-1}]	88	67	44

Study	Location	Water type	Hydraulic Loading [gal (min-ft)$^{-1}$]	Algae productivity [g (m2-day)$^{-1}$]	Influent TP [mg L^{-1}]	TP Removal [g (m2-day)$^{-1}$]	Influent DRP [mg L^{-1}]	DRP Removal [g (m2-day)$^{-1}$]	% of TP removed that is DRP
Craggs, et al[136]	CA	Wastewater effluent	7.65	24.47	3.5	0.52			
			3.75	19.73	3	0.46			
Mulbry, et al[156]	MD	Dairy manure effluent	7.49	8.3	0.08	0.06			
			7.49	11	0.12	0.09			
			7.49	18.2	0.24	0.16			
			7.49	25.1	0.4	0.22			
Adey, et al[217]	FL	River	9.07	21.16	0.05	0.08	0.038	0.04	59%
Mulbry, et al[159]	MD		4.43	21.4	0.23	0.05			
Hydromentia[160]	FL	River	4.7	11.67	0.33	0.07			
			8.5	11.86	0.33	0.13			
			18.8	14.18	0.33	0.25			
Adey, et al[157]	VA	River	5.02	15.4	0.02	0.03	0.0095	0.01	47%
			5.02	15.4	0.02	0.03	0.0095	0.02	49%
			5.02	15.4	0.03	0.07	0.015	0.04	48%
			5.02	15.4	0.03	0.08	0.015	0.03	44%

Appendix C 4: List of studies used to inform optimistic CAPEX costing information

CAPEX									
Paper	**Resource**	**Grading/ civil works [$ acre^{-1}]**	**Liner /Netting [$ acre^{-1}]**	**Piping [$ acre^{-1}]**	**Electrical [$ acre^{-1}]**	**Pumps [$/acre]**	**Misc. [% of growth capital]**	**Total CAPEX [$ acre^{-1}]**	**Harvesting equipment [$ acre^{-1}]**
NREL - Leidos	[18]	$11,430		$ 8,547	$ 1,442	$ 3,046	31%	$ 32,146	
NREL - Micro	[18]	$ 2,265	$ 18,710	$ 8,444	$ 2,986	$ 3,046	31%	$ 46,583	
NREL - Harris	[18]	$ 8,238	$18,710	$ 10,297	$ 1,442	$ 3,046	31%	$ 54,837	
NREL - GAI	[18]	$ 9,370	$29,628	$ 8,238		$ 3,046	31%	$ 66,071	
Pizarro	[62]	$21,318	$ 20,325		$ 1,820	$ 4,396	15%	$ 55,038	$ 9,381
Kangas	[64]	$16,047	$ 19,360	$ 4,302		$ 3,270	15%	$ 49,426	
Hoffman	[39]	$ 1,917	$ 23,679	$ 1,866		$ 557		$ 28,020	$ 1,400
							Average	**$ 47,446**	**$ 5,391**

All costing information has been updated to 2018 $.

All costing information has been updated to 2018 $.

OPEX				
Paper	**Resource**	**Labor [$ (acre-year)$^{-1}$]**	**Maintenance [% of capex]**	**Harvest [$ (acre-year)$^{-1}$]**
NREL - Leidos	[18]	$ 1,438	0.5%	
NREL - Microbio	[18]	$ 1,438	0.5%	
NREL - Harris	[18]	$ 1,438	0.5%	
NREL - GAI	[18]	$ 1,438	0.5%	
Pizarro	[62]	$ 2,950	5%	$ 624
Kangas	[64]	$ 673		
Hoffman	[39]	$ 410	1%	$ 668
	Average	**$ 1,398**	**1.6%**	**$ 646**

Appendix C 5: Conversion between NOAA's Western Lake Erie Bloom Severity Index and maximum cumulative CI. Maximum cumulative CI was reported by Stumpf et al (2015)[137] and the Western Lake Erie Bloom Severity Index was reported by NOAA in their Lake Erie HAB reports[218].

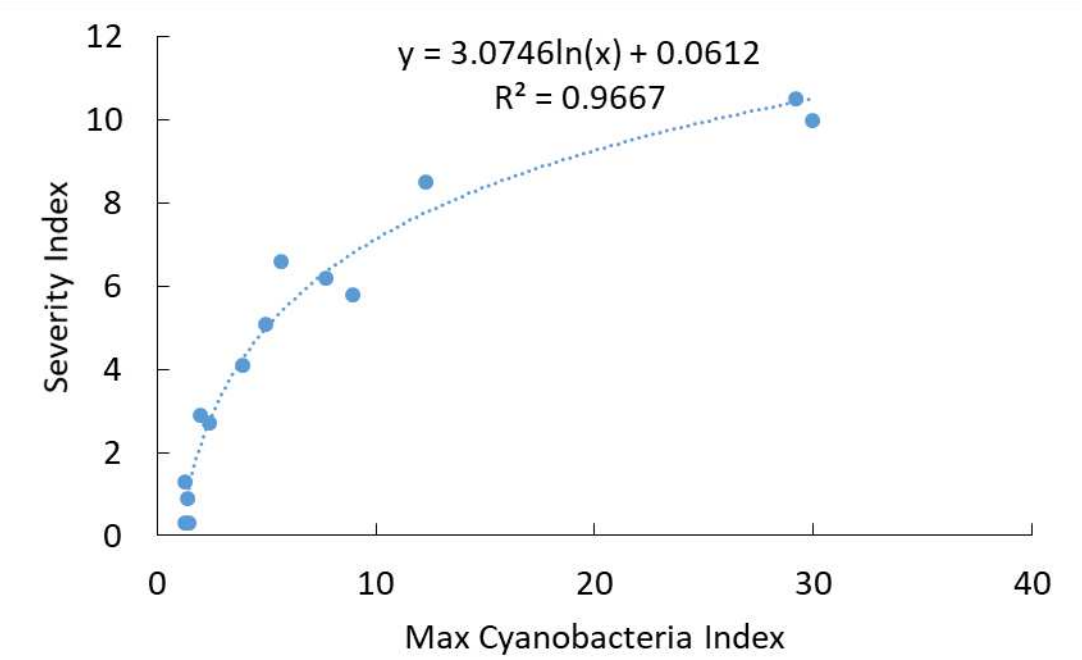

Year	Max CI	NOAA Severity Index[218]
2002	1.27	0.3
2003	3.92	4.1
2004	2.39	2.7
2005	1.43	0.3
2006	1.27	1.3
2007	1.39	0.9
2008	7.71	6.2
2009	4.99	5.1
2010	8.93	5.8
2011	29.94	10
2012	1.96	2.9
2013	12.28	8.5
2014	5.65	6.6
2015	29.2	10.5
2016	2.8*	3.2
2017	13.2*	8
2018	3.2*	3.6

**Calculated based on the NOAA severity index and were not used to calibrate the model*

Appendix C 6: Photos of water columns of Medium and Severe HAB's

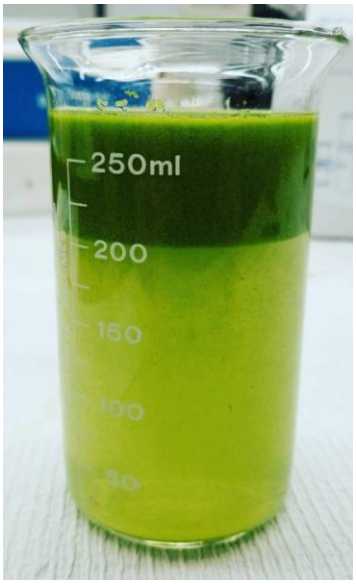

Photo of a water column during the 2017 Severe HAB event (Max CI = 13.2, NOAA Severity Index = 8)[219]

Photo of a water column during the 2014 Medium HAB event (Max CI = 5.65, NOAA Severity Index = 6.6)[220]: Table of model inputs for the HAB-related economic damages model

Appendix C 7: Table of inputs for the economic damages model

Parameter	Value	Units	Source	Notes
Property Values				
Lake Erie average lakefront home values				
County				
Lucas	$498,512,998		135	
Ottawa	$1,174,342,313			
Erie	$805,320,313			
Property value loss due to HABs	11.53%	of total value	221	Range 11 – 17%, with lakefront homes losing 22%
Value Regained after HAB rehabilitation	97%	of total value	190	
Average property value growth				
Lucas	2.3%		183	
Ottawa	2.8%			
Erie	1.7%			
Recreation				
Angling				
Number trips per angler	17.6	Trips (angler-season) $^{-1}$	193	
License cost	$19	$ license^{-1}	222	
Local Economy spending	$95	$ trip^{-1}	193	
Consumer surplus	$14.81	$ trip^{-1}	193	
% of license sales reduced due to HABs	11%		192	
% of licenses bought during HAB season	22.4%		192	
% fishing trips in HAB season	48%		193	
Angler consumer welfare coefficient	$0.52	$ (10^5 cells)$^{-1}$	194	
Angler choice logit coefficient	-0.0126		194	
Average fishing license sales growth				
Lucas	-4%		222	Based on years 1995-2018
Ottawa	-4.9%			
Erie	-3.1%			
Beachgoers				
# Beach trips per beach	154286		195,223–225	varies between 123023 - 269253

Beach trips per person	15		226	
Benefit per reduced advisory	$2.61	$ (advisory-trip)$^{-1}$	195	Assumed max of 1 advisory per HAB season
Beachgoer choice logit coefficient	-0.01		194	
Beachgoer consumer welfare coefficient for algae	$0.05	$ (10^5 cells)$^{-1}$	194	
Local Economy spending	$39.11	$ (trip)$^{-1}$	226	
Annual Beach Use Growth	0.8%		227	No actual data on Ohio beach use as admission is free
Non-Users				
WTP - Lucas - Low/Mild	$50.42	$ household^{-1}	196	
WTP - Lucas - Med	$199.43	$ household^{-1}		
WTP - Lucas - Severe	$282.90	$ household^{-1}		
WTP - Ottawa - Low/Mild	$51.30	$ household^{-1}		
WTP - Ottawa - Med	$121.52	$ household^{-1}		
WTP - Ottawa - Severe	$287.85	$ household^{-1}		
WTP - Erie - Low/Mild	$50.84	$ household^{-1}		
WTP - Erie - Med	$120.44	$ household^{-1}		
WTP - Erie - Severe	$285.30	$ household^{-1}		
Starting WQL – Low/Mild	5			
Starting WQL – Med	3			
Starting WQL – Severe	2			
Desired WQL	7			
# Households – Lucas County	179,065		228	
# Households – Ottawa County	17,691			
# Households – Erie County	31,301			
Tourism				
Tourism visitor increases	4.5%		200,201	Average value. Tourism Ohio shows 3.5% annual growth, Lake Erie Shores and Islands reports 5.5% growth for Ottawa and Erie counties
Visitor type				
Day	80%		135	

Overnight - friends	4%			
Overnight - hotel	16%			
Visitor spending/day				
Day	$ 62.02	$ day^{-1}	135	
Overnight - friends	$358.43	$ day^{-1}		
Overnight - hotel	$513.91	$ day^{-1}		
Average Spending per visitor per day	$226.18	$ day^{-1}		
% of visitors affected by HABs	25%			Assumed visits were uniformly distributed, with the HAB season lasting from mid-July – mid-Oct
Severe HAB spending reductions	3.5%	Reduced spending from previous year		
Medium HAB visitor reduction	11%	Reduced visits from expected		
Mild HAB visitor reductions	1%	Reduced visits from expected		
Starting Tourism Spending				
Lucas	1,980	$M year^{-1}	135	
Ottawa	496	$M year^{-1}		
Erie	1,980	$M year^{-1}		
Drinking Water				
Microcystic conversion	0.20	ug (100,000 cells)$^{-1}$	211	
Safety Factor	3		229	
Final microcystin concentration	0.3	ug L^{-1}	229	
Empirical constant for the absorption capacity (K_f)	6309		229	
Empirical constant for the intensity of absorption (*1/n*)	0.56		229	
Operational costs	varies		213	Based on PAC dosing requirements and facility size
Economics				
Discount Rate	3%			
Loan Terms - Interest	1.7%		214	
Loan Terms - # Years	20			
Solution Start time	5			

Appendix C 8: Table of the average local CI for the coastline of each county for each HAB type

	County		
	Lucas	Ottawa	Erie
Low	0.0021	0.0007	0.0007
Mild	0.0017	0.0007	0.0007
Med	0.0034	0.0012	0.0007
Severe	0.0031	0.0017	0.0010

Appendix C 9: Table of the average local CI for each beach with public access to Western Lake Erie for each HAB category

	BEACH						
	Maumee	Kelley's Island	East Harbor	Nickel Plate	Lakeview	Huntington Beach	Edgewater
Low	0.007	0.001	0.004	0.002	0.005	0.000	0.000
Mild	0.009	0.003	0.003	0.004	0.003	0.000	0.000
Medium	0.015	0.003	0.005	0.007	0.006	0.002	0.002
Severe	0.023	0.006	0.012	0.016	0.005	0.009	0.003

Appendix C 10: Equations for calculating recreation-based economic damages from HAB's

Estimating baseline fishing license sales in year t for county i

$$Fishing\ License\ Sales_{t,i} = Fishing\ License\ Sales_{t-1,i} \times (1 + Fishing\ License\ Growth\ Rate_{i})$$

Estimating fishing licenses not sold due to HAB's in year t for county i

$$Fishing\ License\ Lost_{t,i} = Fishing\ License\ Sales_{t,i} \times HAB\ License\ Sales \times HAB\ License\ Reduction$$

Where

HAB License Sales is the proportion of fishing licenses sold during the HAB season

HAB License Reduction is the reduction is fishing license sales due to HAB's

Estimating the number of trips not taken due to reduced fishing license sales

$$Reduced\ trips_t = \sum_{i=1}^{3} Fishing\ License\ Lost_{t,i} \times Angler\ Trips$$

Where

Angler trips is the average number of trips each angler takes per year

Estimating the economic losses due to reduced fishing license sales

$$HAB\ Losses_{angler,license,t} = Reduced\ trips_t \times \left(Real\ Benefit_{angler} + Welfare\ Benefit_{angler}\right) + \sum_{i=1}^{3} Fishing\ License\ Lost_{t,i} \times Cost\ fishing\ license$$

Where

Real Benefit$_{angler}$ is the average spent in the local economy per angler

Welfare Benefit$_{angler}$ is the average consumer welfare benefit for each angler trip

Estimate the number of trips taken in Western Basin of Lake Erie during the HAB season

$$WBLE\ Trips_{t,i} = \left(Fishing\ License\ Sales_{t,i} - Fishing\ License\ Lost_{t,i}\right) \times Angler\ Trips \times WBLE$$

Where

WBLE is the proportion of angling trips occurring in the western basin of Lake Erie during the HAB season

Estimating the probability an angler will change location due to HAB's

$$\Pr(A, X) = \frac{e^{B_{angler}\, X}}{(1 + e^{B_{angler}\, X})}$$

Where

Pr(A, X) is the probability an angler will choose spot A with an algae cell concentration of *X*

B_{angler} is the logit coefficient for angler's

X is the concentration of algae cells [10^5 cells mL^{-1}]

Estimating the number of anglers who change locations due to HAB's

$$Trips\ changed_{angler,t,i} = WBLE\ Trips_{t,i} \times \frac{\Pr(A, 0) - \Pr(A, algae\ cells_t)}{2}$$

Where

Pr(A, 0) is the probability of choosing site A if no algae is present

Pr(A, algae cells) is the probability of choosing site A if algae is present at concentration *algae cells* [10^5 cells mL^{-1}]

Estimating the economic losses due to trips that were changed

$$HAB\ Losses_{angler,trips\ changed,t,i} = Trips\ changed_{angler,t,i} \times Real\ Benefit_{\ angler}$$

Estimating the consumer benefit loss due to the presence of HAB's

$$HAB\ Losses_{angler,welfare,t}$$

$$= \left(WBLE\ Trips_{t,i} - \ Trips\ changed_{angler,t}, i\right) \times Welfare\ Coeff_{\ anglers}$$

$$\times\ Algae\ Cells_i$$

Where

Welfare Coeff$_{anglers}$ is the amount of consumer welfare lost per 10,000 cells mL^{-1}

Algae cells$_i$ is the average coastline concentration of algae for county i [10^5 cells mL^{-1}]

Estimating the total economic losses due to HAB's for recreational anglers

$$HAB\ Losses_{rec-anglers,t}$$

$$= \sum_{i=1}^{3} HAB\ Losses_{angler,license,t,i} + \ HAB\ Losses_{angler,trips\ changed,t,i}$$

$$+ \ HAB\ Losses_{angler,welfare,t,i}$$

Estimating baseline number of beach trips in year t for beach j

$$Beach\ trips_{\ t,j} = Beach\ trips_{\ t-1,j} \times (1 + Beach\ trip\ growth\ rate)$$

Estimating number of HAB affected beach trips in year t for beach j

$$HAB\ Beach\ trips_{\ t,j} = Beach\ trips_{\ t,j} \times \frac{HAB\ Length_{t,j}}{Beach\ season}$$

Where

HAB Beach trips$_{t,j}$ is the number of beach trips affected by HAB's in year t for beach j

HAB length$_{t,j}$ is the number of days a beach has a local CI > 0.001 in year t for beach j

Estimating the probability a beachgoer will change location due to HAB's

$$\Pr(A, X) = \frac{e^{B_{beach}\,X}}{(1 + e^{B_{beach}\,X})}$$

Where

Pr(A, X) is the probability a beachgoer will choose spot A with an algae cell concentration of *X*

B_{beach} is the logit coefficient for beachgoers

X is the concentration of algae cells [10^5 cells mL^{-1}]

Estimating the number of anglers who change locations due to HAB's

$$Trips\ changed_{beach,j,t} = HAB\ Beach\ trips_{\ t,j} \times \frac{\Pr(A, 0) - \Pr(A, algae\ cells_{j,t})}{2}$$

Where

Pr(A, 0) is the probability of choosing site A if no algae is present

Pr(A, algae cells) is the probability of choosing site A if algae is present at concentration *algae cells* [10^5 cells mL^{-1}] for beach j

Estimating the economic losses due to trips that were changed in year t for beach j

$$HAB\ Losses_{beach,trips\ changed,j,t} = Trips\ changed_{beach,j,t} \times Real\ Benefit_{\ beach}$$

Where

Real Benefit$_{angler}$ is the average spent in the local economy per beachgoer

Estimating the consumer benefit loss due to HAB based beach advisory in year t at beach j

$$HAB\ Losses_{beach,w\ adv,j,t} = \left(HAB\ Beach\ trips_{\ t,j} - Trips\ changed_{beach,j,t}\right) \times Welfare\ Coeff_{\ beach,adv.} \times Number\ of\ advisories_{t,j}$$

Where

Welfare Coeff$_{beach,\ adv.}$ is the welfare loss coefficient for each beach advisory

Number of advisories$_{t,j}$ is the number of HAB related beach advisories for beach j in year t

Estimating the consumer benefit loss due to the presence of HAB's in year t at beach j

$$HAB\ Losses_{beach,w\ HAB,j,t} = \left(HAB\ Beach\ trips_{\ t,j} - Trips\ changed_{beach,j,t}\right) \times Welfare\ Coeff_{\ beach,HAB.} \times Algae\ cells_{j,t}$$

Where

Welfare Coeff$_{beach,\ HAB.}$ amount of consumer welfare lost per 10,000 cells mL^{-1}

Algae cells$_{t,j}$ is the concentration of algae for beach j in year t [10,000 cells mL^{-1}]

Estimating the total economic losses due to HAB's for recreational beachgoers

$$HAB\ Losses_{rec-beach,t} = \sum_{j=1}^{5}(HAB\ Losses_{beach,trips\ changed,j,t} + HAB\ Losses_{beach,w\ adv,j,t} + HAB\ Losses_{beach,w\ HAB,j,t})$$

Appendix C 11: Tourism related studies for snow/ski resorts

Author	Study	Subject	Findings	Source
Snow/Ski Related Studies				
Dawson, J., Scott, D., McBoyle, G.	Climate change analogue analysis of ski tourism in the northeastern USA	Historic warm winters (98-99 and 01-02) were used as climate change analogue for future ski seasons	Number of resort visits was down 10.8% and 11.6% during the 98-99 and 01-02 warm winters, respectively. For Lake Erie, a reduction of 10.8% and 11.6% of all trips during the HAB season reduced tourism spending by **2.7%** and **2.9%**, respectively.	[206]
Vail Resorts	Vail Resorts Reports Certain Ski Season Metrics for the Season-to-Date Period Ended April 22, 2012	Ski seasons metrics for Vail Resorts for the 2011-2012 ski season	Colorado resorts were down 8.9% in visits, Tahoe resorts (excluding Kirkwood) down 24.2% in visits. For Lake Erie, a reduction of 8.9% of all trips during the HAB season reduced tourism spending by **2.2%.**	
Hamilton, L., Brown, C., Keim, B.D.	Ski areas, weather and climate: time series model for New England Case Studies	Weather effects, including the "backyard effect" i.e. conditions of nearby towns, on ski resort visits was examined for ski resorts in New England	Looking at Figure 5, average attendance for Gunnison and Cannon ski resorts was 175k and 110k visitors, respectively. Low snow years (estimated by snow cover in nearby towns) showed reductions in ski attendance between 5 – 25%. This study implies changes in nearby-town snow cover is more likely to affect day-trippers. For Lake Erie, a reduction in 5-25% of day trippers during the HAB season reduced tourism spending between **1 – 3.5%**.	[207]
Töglhofer, C., Eigner, F., Prettenthaler, F.	Impacts of snow conditions on tourism demand in Austrian ski areas	This study considers how changes in snow conditions affect overnight stays for Austrian ski resorts	A one standard deviation in snow conditions reduces overnight visitors by 0.6-1.9%. For Lake Erie, a reduction in 0.6% - 1.9% of overnight trips during the HAB season reduced tourism spending between **0.1–0.2%**. This study only considers overnight visits	[205]

Appendix C 12: Tourism related studies for oil spills

Author	Study	Subject	Findings	Source
Oil spill related studies				
Garza-Gil, M. D., Prada-Blanco, A., Vazquez-Rodriquez, M. X.	Estimating the short-term economic damages from the *Prestige* oil spill in the Galician fisheries and tourism	Examines the impact of the Prestige oil spill on tourism (spill location northern Spain, spill occurred November 2002).	Tourism spending was down **7.3%**, the number of overnight tourists was down 8% after the oil spill. For Lake Erie, an 8% reduction overnight trips during the HAB season reduced tourism spending by **3.6%** (does not include day-trippers) *.	[210]
Tourism Economics	The Impact of the BP Oil Spill on Visitor Spending in Louisiana: Revised estimates based on data through 2010 Q4	Examines the impacts of the BP Oil spill on tourism in Louisiana (spill occurred April 2010)	Leisure/tourism spending reduced by **3%** compared to the baseline forecast.	[230]
Oxford Economics	Potential Impact of the Gulf Oil Spill on Tourism	Examines how different events (oil spills, pandemics, hurricanes, terrorism, etc.) effect tourism	The Peak Impact vs Duration graph shows oil spill/HAB related tourism reductions between **1-11%** for shorter events (events lasting less than 10 months). These values indicate the % reduced spending from the previous year*.	[209]
McDowell Group	An Assessment of the Impact of the Exxon Valdez Oil Spill on The Alaska Tourism Industry	Impact of the Exxon Valdez oil spill on Alaskan tourism. Spill occurred March 1989	Visitor spending decreased by **8%** and **35%** from the previous year for the two major spill-affected areas*.	[231]

*These studies all indicate that there was no "tourism growth" from the previous year, so losses were based on the previous year's spending.

Appendix C 13: List of drinking water treatment facilities which draw from the Lake Erie western basin including design size, highest recorded Microcystin concentration in the inlet and the required PAC dosage for that Microcystin concentration

	Size [MGD]	Highest Microcystin in inlet [ug L^{-1}]	Highest required dose [mg L^{-1}]
Toledo	75	9.69	112
Oregon City	16	50	108
Carroll	0.5	50	61
Marble Head	0.2	3.8	74
Kelley's Island	0.7	5.88	49
Put in Bay	0.2	4.09	75
Sandusky	5.7	2.5	65
Huron	1.5	4.624	103
Vermillion	2.3	1.01	33
Lorain	17.2	0.615	18

Appendix C 14: Average local CI at the drinking water treatment inlet for the different HAB categories

Water treatment facility	Low	Mild	Medium	Severe
Toledo	0.0009	0.0013	0.0023	0.0025
Oregon	0.0014	0.0020	0.0036	0.0033
Carrol Water	0.0004	0.0005	0.0014	0.0021
Marblehead	0.0004	0.0006	0.0010	0.0012
Kelley's Island	0.0016	0.0014	0.0023	0.0010
Put in Bay	0.0005	0.0005	0.0012	0.0012
Sandusky	0.0003	0.0004	0.0006	0.0011
Huron	0.0002	0.0002	0.0006	0.0010
Vermillion	0.0004	0.0003	0.0003	0.0004
Lorain	0.0006	0.0005	0.0004	0.0004

Appendix C 15: Annual drinking water treatment costs due to equipment purchase, operation and maintenance. These values remained constant over the course of the analysis and were based on the required PAC dosage for the highest historical Microcystin concentration. Data is reprinted from Najm et al. and updated to 2018$.

Annual Costs from Feed Equipment + O&M[213]					
	PAC Dosing				
Drinking water treatment facility design size [MGD]	5 mg L^{-1}	10 mg L^{-1}	25 mg L^{-1}	50 mg L^{-1}	75 mg L^{-1}
0.1	$3,557	$3,574	$3,624	$3,959	$4,344
0.5	$4,051	$4,386	$5,281	$6,804	$7,809
1	$5,474	$6,118	$7,892	$9,918	$11,684
2.5	$8,528	$10,052	$13,090	$18,630	$23,736
5	$12,646	$14,672	$21,225	$31,486	$39,303
10	$18,773	$22,798	$35,587	$48,702	$61,917
15	$23,568	$30,615	$46,434	$64,947	$80,832
25	$33,971	$44,232	$62,905	$89,243	$113,598
50	$53,740	$66,855	$98,751	$144,146	$189,258
75	$72,513	$90,875	$133,911	$200,062	$254,966
100	$81,987	$103,438	$159,278	$232,142	$292,770
150	$114,653	$143,761	$223,840	$312,221	$417,023

Appendix C 16: Annual drinking water treatment costs for the purchase of PAC. These values are dependent on required PAC dose Data is reprinted from Najm et al. and updated to 2018$.

Annual Costs from the purchase of PAC[213]					
	PAC Dosing				
Drinking water treatment facility design size [MGD]	5 mg L^{-1}	10 mg L^{-1}	25 mg L^{-1}	50 mg L^{-1}	75 mg L^{-1}
0.1	$713	$1,428	$3,569	$7,136	$10,704
0.5	$3,569	$7,136	$17,840	$35,680	$53,521
1	$7,136	$14,272	$35,680	$71,361	$107,067
2.5	$17,840	$35,680	$89,201	$178,402	$267,652
5	$35,680	$71,361	$178,402	$356,879	$535,304
10	$71,361	$142,747	$356,879	$713,732	$1,070,610
15	$107,067	$214,108	$535,304	$1,070,610	$1,605,915
25	$178,428	$356,879	$892,161	$1,784,341	$2,676,500
50	$356,879	$713,732	$1,784,341	$3,568,683	$5,322,896
75	$535,304	$1,070,610	$2,676,500	$5,354,699	$8,029,551
100	$713,732	$1,427,464	$3,568,683	$7,137,368	$10,706,051
150	$1,070,610	$2,141,196	$5,353,026	$10,706,051	$16,059,103

Appendix C 17: Breakdown of the median annual HAB-related losses and technology costs for the lagoon cases

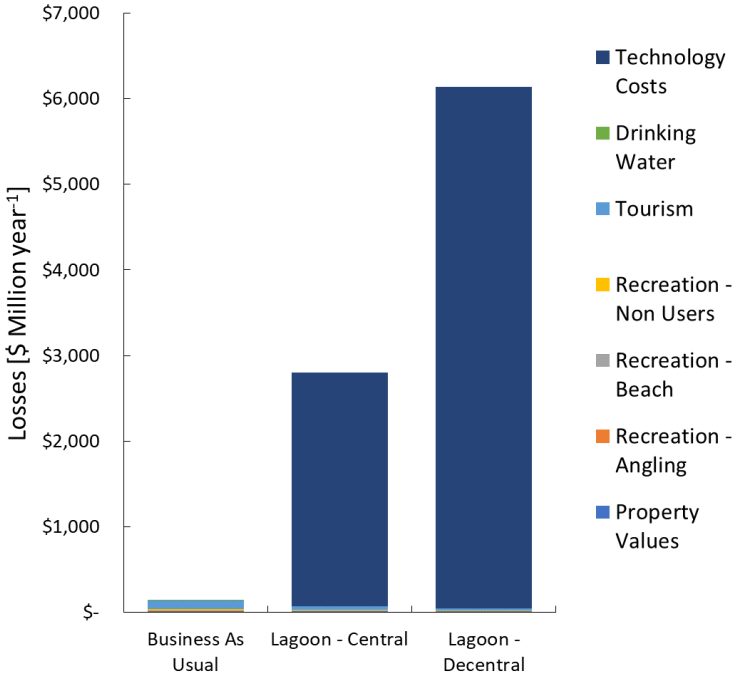

Appendix C 18: Example 30-year cash flows for the Business as Usual and technology cases

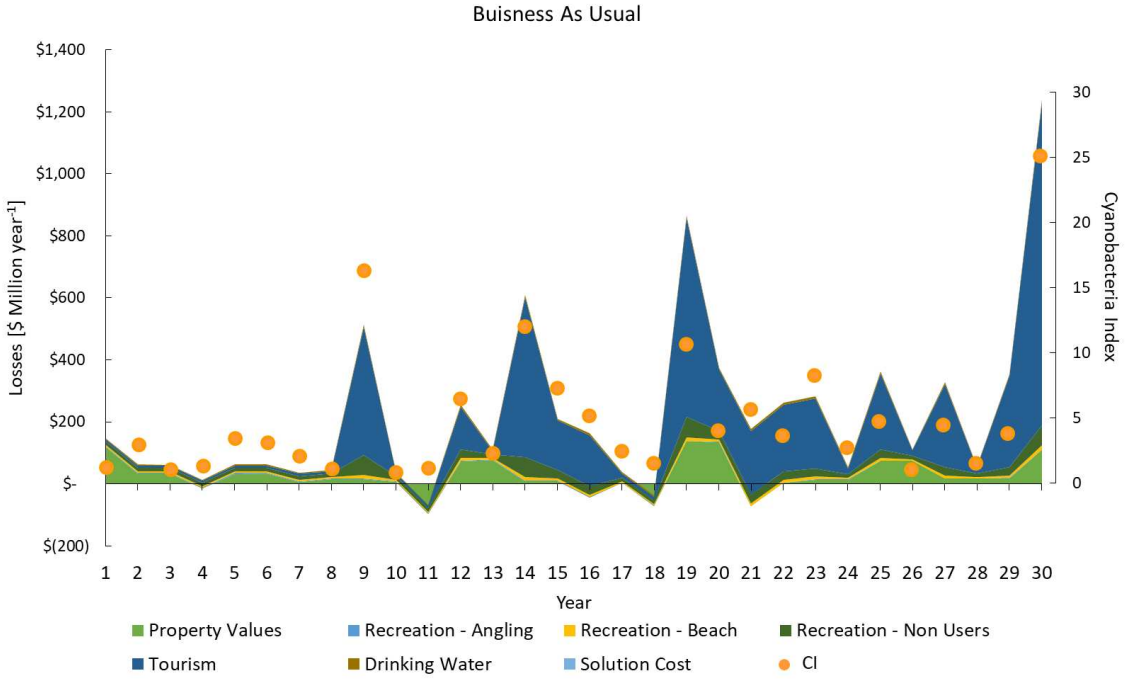

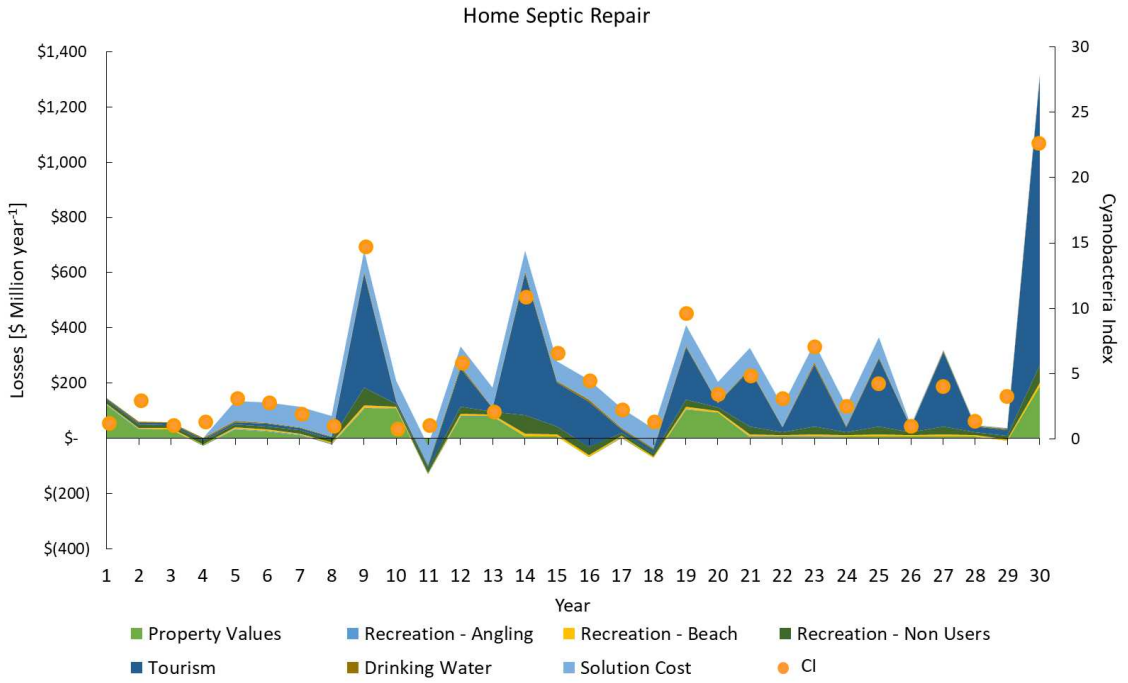

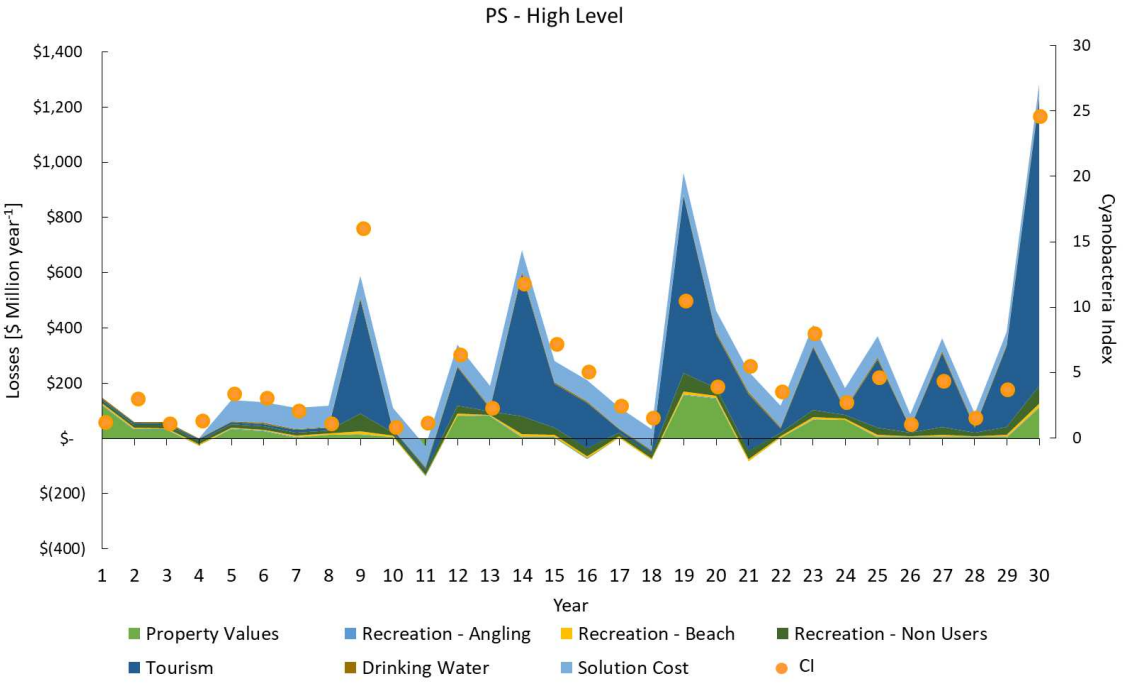
PS - High Level
Losses [$ Million year-1]
$1,400
$1,200
$1,000
$800
$600
$400
$200
$-
$(200)
$(400)
Cyanobacteria Index
30
25
20
15
10
5
0
1 2 3 4 5 6 7 8 9 10 11 12 13 14 15 16 17 18 19 20 21 22 23 24 25 26 27 28 29 30
Year
Property Values
Recreation - Angling
Recreation - Beach
Recreation - Non Users
Tourism
Drinking Water
Solution Cost
CI

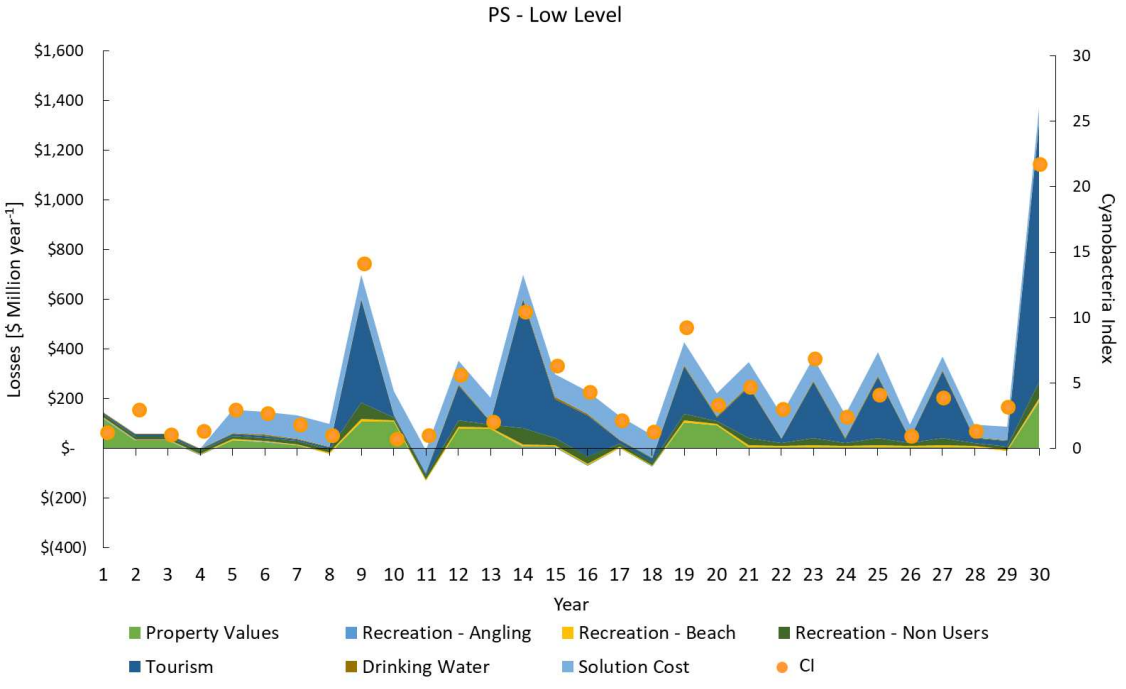
PS - Low Level
Losses [$ Million year-1]
$1,600
$1,400
$1,200
$1,000
$800
$600
$400
$200
$-
$(200)
$(400)
Cyanobacteria Index
30
25
20
15
10
5
0
1 2 3 4 5 6 7 8 9 10 11 12 13 14 15 16 17 18 19 20 21 22 23 24 25 26 27 28 29 30
Year
Property Values
Recreation - Angling
Recreation - Beach
Recreation - Non Users
Tourism
Drinking Water
Solution Cost
CI

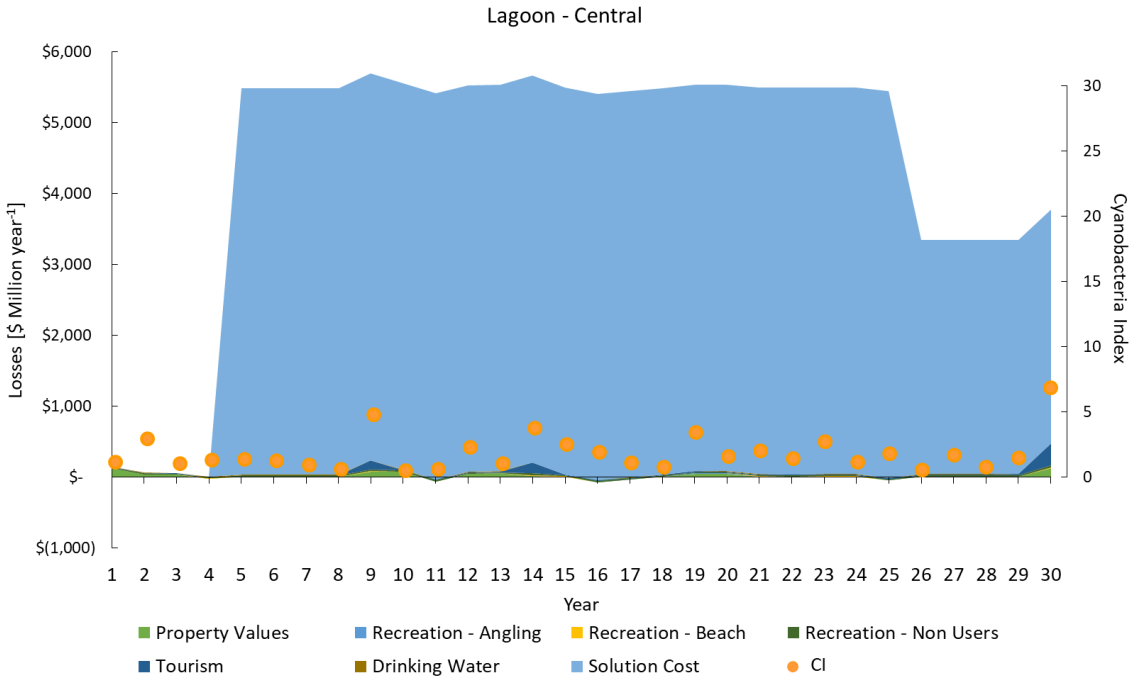
Lagoon - Central
$6,000
$5,000
$4,000
$3,000
$2,000
$1,000
$-
$(1,000)
Losses [$ Million year-1]
30
25
20
15
10
5
0
Cyanobacteria Index
1 2 3 4 5 6 7 8 9 10 11 12 13 14 15 16 17 18 19 20 21 22 23 24 25 26 27 28 29 30
Year
Property Values
Recreation - Angling
Recreation - Beach
Recreation - Non Users
Tourism
Drinking Water
Solution Cost
CI

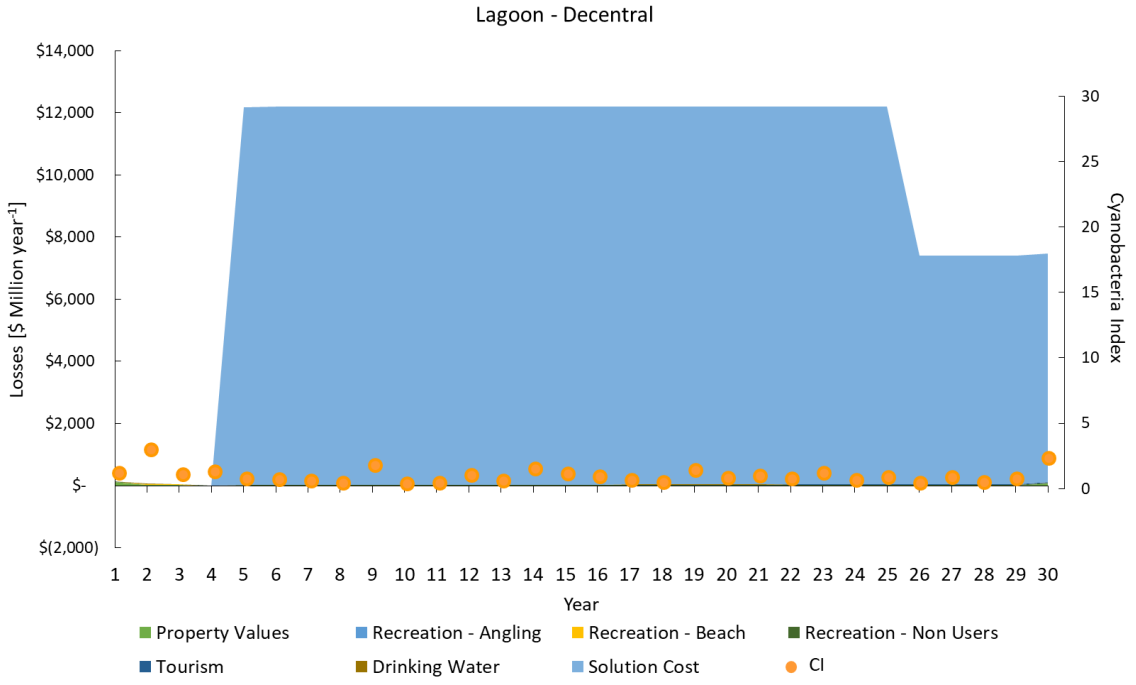
Lagoon - Decentral
$14,000
$12,000
$10,000
$8,000
$6,000
$4,000
$2,000
$-
$(2,000)
Losses [$ Million year-1]
30
25
20
15
10
5
0
Cyanobacteria Index
1 2 3 4 5 6 7 8 9 10 11 12 13 14 15 16 17 18 19 20 21 22 23 24 25 26 27 28 29 30
Year
Property Values
Recreation - Angling
Recreation - Beach
Recreation - Non Users
Tourism
Drinking Water
Solution Cost
CI

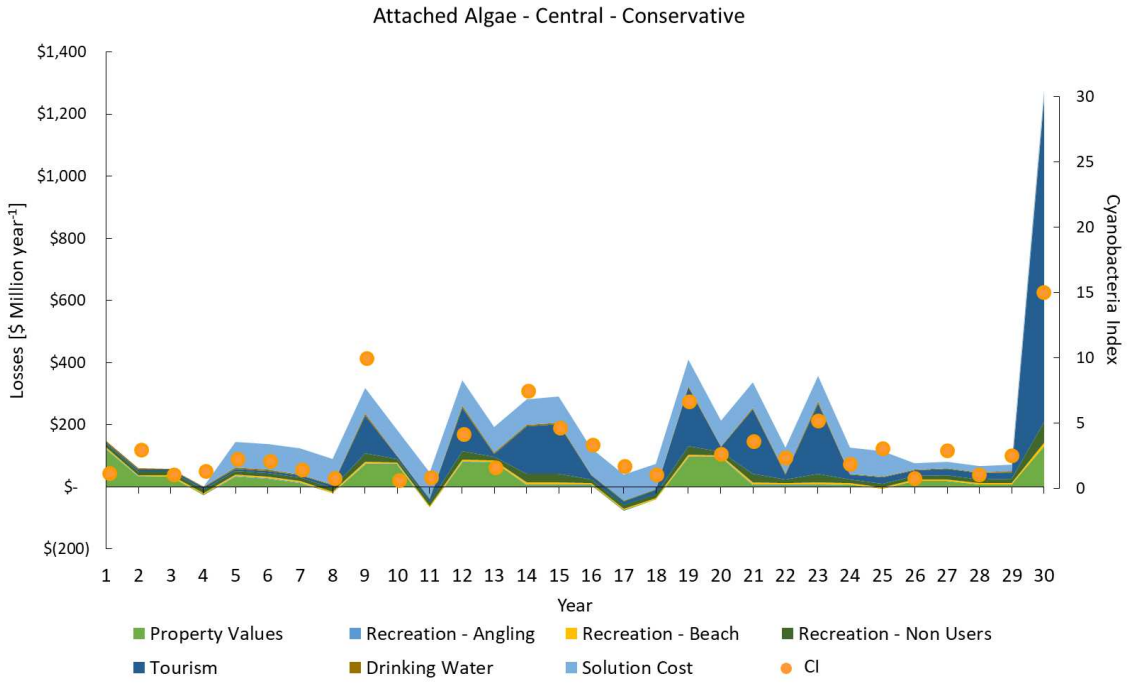
Attached Algae - Central - Conservative
Losses [$ Million year-1]
$1,400
$1,200
$1,000
$800
$600
$400
$200
$-
$(200)
Cyanobacteria Index
30
25
20
15
10
5
0
1 2 3 4 5 6 7 8 9 10 11 12 13 14 15 16 17 18 19 20 21 22 23 24 25 26 27 28 29 30
Year
Property Values
Recreation - Angling
Recreation - Beach
Recreation - Non Users
Tourism
Drinking Water
Solution Cost
CI

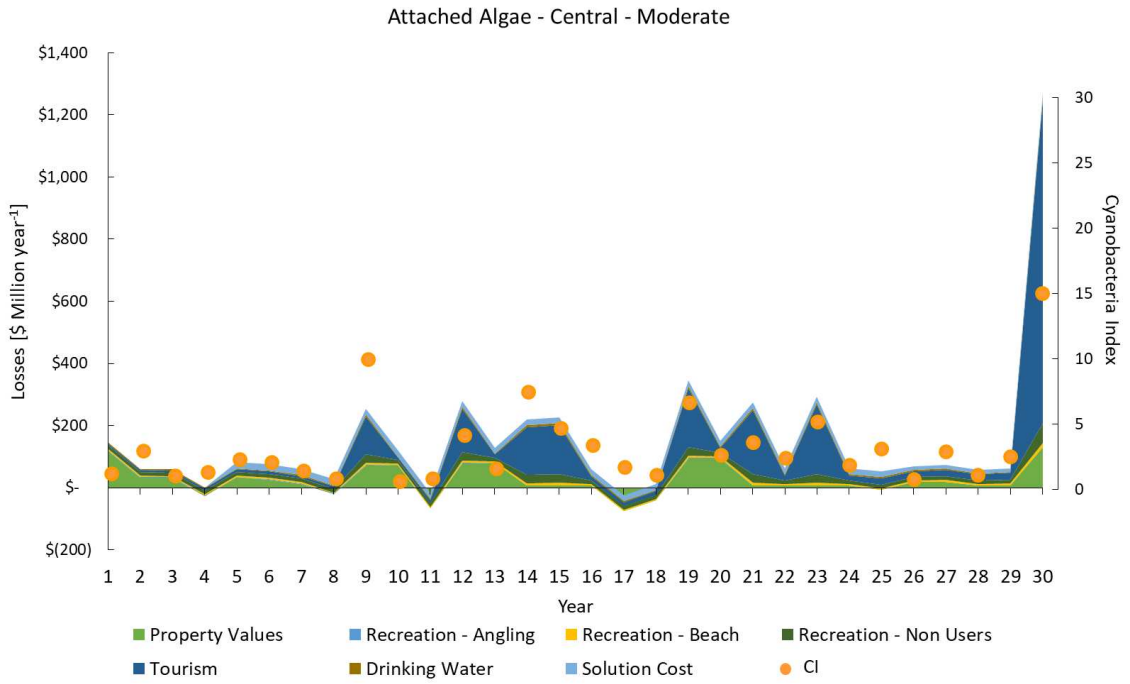
Attached Algae - Central - Moderate
Losses [$ Million year-1]
$1,400
$1,200
$1,000
$800
$600
$400
$200
$-
$(200)
Cyanobacteria Index
30
25
20
15
10
5
0
1 2 3 4 5 6 7 8 9 10 11 12 13 14 15 16 17 18 19 20 21 22 23 24 25 26 27 28 29 30
Year
Property Values
Recreation - Angling
Recreation - Beach
Recreation - Non Users
Tourism
Drinking Water
Solution Cost
CI

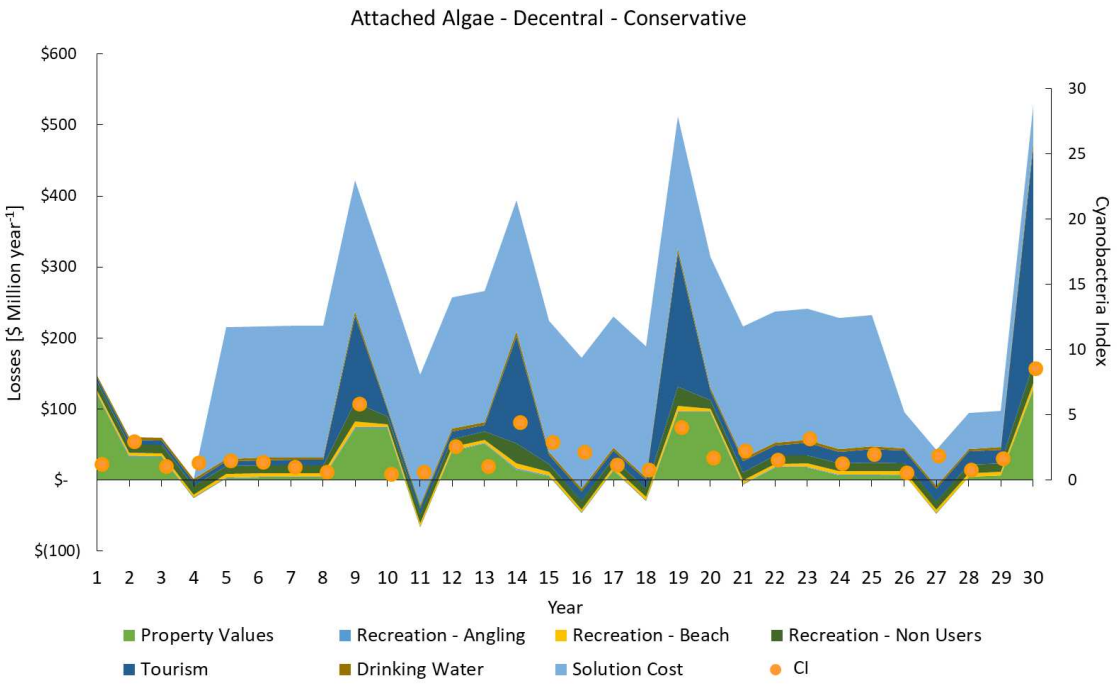
Attached Algae - Decentral - Conservative
$600
$500
$400
$300
$200
$100
$-
$(100)
Losses [$ Million year-1]
30
25
20
15
10
5
0
Cyanobacteria Index
1 2 3 4 5 6 7 8 9 10 11 12 13 14 15 16 17 18 19 20 21 22 23 24 25 26 27 28 29 30
Year
Property Values
Recreation - Angling
Recreation - Beach
Recreation - Non Users
Tourism
Drinking Water
Solution Cost
CI

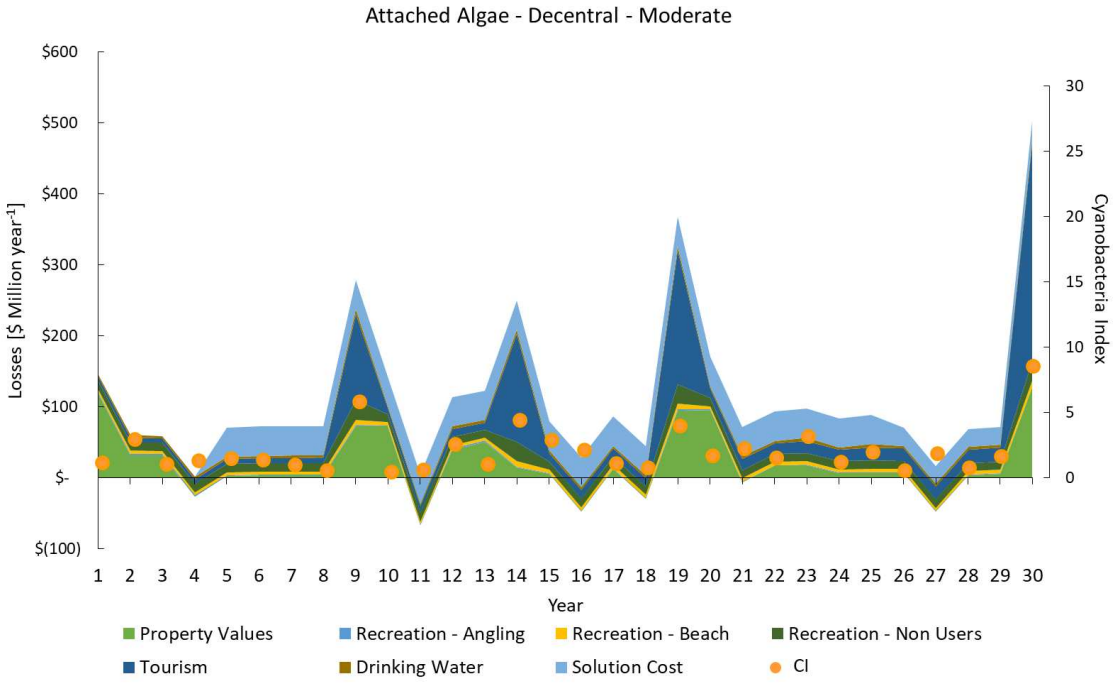
Attached Algae - Decentral - Moderate
$600
$500
$400
$300
$200
$100
$-
$(100)
Losses [$ Million year-1]
30
25
20
15
10
5
0
Cyanobacteria Index
1 2 3 4 5 6 7 8 9 10 11 12 13 14 15 16 17 18 19 20 21 22 23 24 25 26 27 28 29 30
Year
Property Values
Recreation - Angling
Recreation - Beach
Recreation - Non Users
Tourism
Drinking Water
Solution Cost
CI